

Cover Page



Universiteit Leiden



The handle <http://hdl.handle.net/1887/26945> holds various files of this Leiden University dissertation

Author: Snelder, Nelleke

Title: Towards predictive cardiovascular safety : a systems pharmacology approach

Issue Date: 2014-06-25

**Towards predictive cardiovascular safety -
a systems pharmacology approach**

Nelleke Snelder

The publication of this thesis was financially supported by LAP&P Consultants BV, Leiden,
The Netherlands

Lay-out and printing by Ridderprint BV, Ridderkerk

© 2014. Copyright by N. Snelder

**Towards predictive cardiovascular safety -
a systems pharmacology approach**

Proefschrift

ter verkrijging van
de graad van Doctor aan de Universiteit Leiden,
op gezag van Rector Magnificus prof.mr. C.J.J.M. Stolker,
volgens besluit van het College voor Promoties
te verdedigen op woensdag 25 juni 2014
klokke 12.30 uur

door

Nelleke Snelder

geboren te Rotterdam
in 1980

Promotiecommissie

Promotoren:

Prof. Dr. M. Danhof

Prof. Dr. D.R. Stanski

Co-Promotor:

Dr. B.A. Ploeger

Overige leden:

Prof. Dr. A.H.J. Danser, Erasmus Universiteit Rotterdam

Prof. Dr. P.H. van der Graaf

Prof. Dr. J. Burggraaf

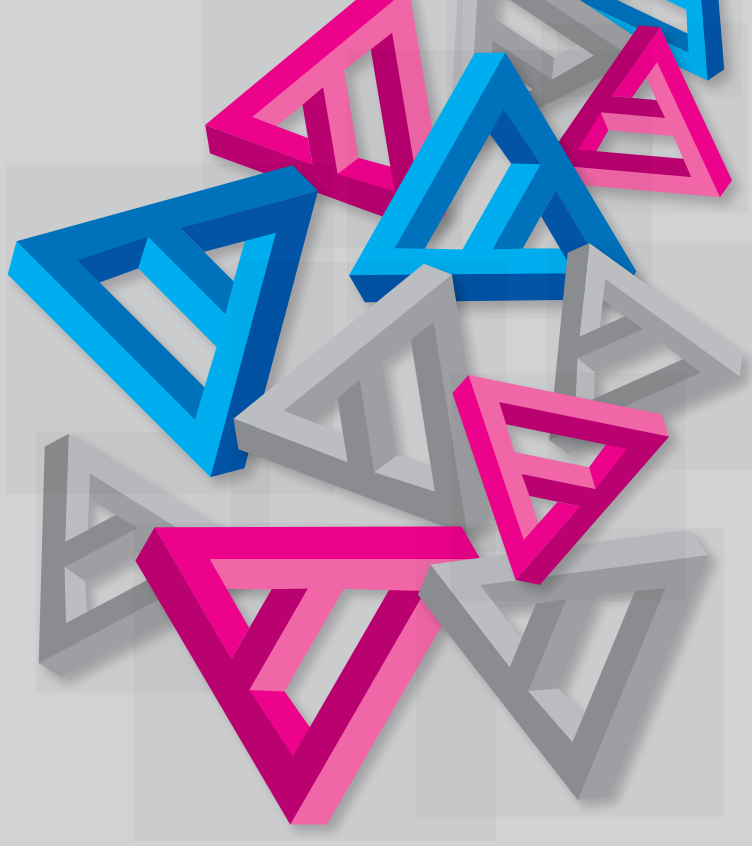
Prof. Dr. T. Hankemeier

Prof. Dr. B. van de Water

... The End is in the Beginning, and now we go on ...
A. van der Veen according to S. Becket

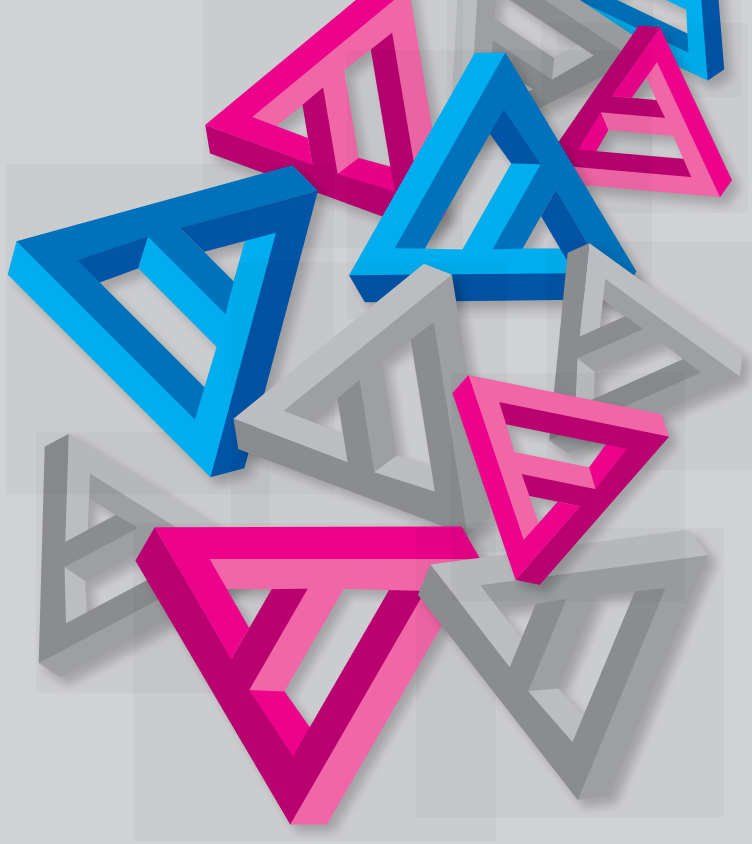
Table of contents

Section I	General introduction	
1.	A systems pharmacology approach for predicting drug-induced changes in hemodynamic variables	11
2.	Scope and outline of the investigations	31
Section II	Development of a systems pharmacology model to characterize drug effects on the CVS	
3.	PKPD modeling of the interrelationship between mean arterial blood pressure, cardiac output and total peripheral resistance in conscious rats	39
4.	Drug effects on the cardiovascular system in conscious rats – separating cardiac output into heart rate and stroke volume using PKPD modeling	69
Section III	Application of the developed systems pharmacology model to S1P receptor agonists	
5.	Translational pharmacokinetic modeling of fingolimod as a paradigm compound subject to sphingosine kinase-mediated phosphorylation	105
6.	Characterization and prediction of cardiovascular effects of fingolimod and siponimod using a systems pharmacology modeling approach	131
Section IV	Summary, conclusions & perspectives	
7.	A systems pharmacology approach to the prediction of cardiovascular side effects in man - Summary, conclusions & perspectives	169
	Samenvatting in het Nederlands	193
	Nawoord	205
	List of Publications	207
	Curriculum Vitae	208



SECTION I

General introduction



CHAPTER 1

A systems pharmacology approach for predicting drug-induced changes in hemodynamic variables

Persistent elevation of blood pressure (BP) is a risk factor for heart failure and is a leading cause of cardiovascular disease (Graham *et al.*, 2007). Clinically, hypertension is defined as BP higher than 140/90 mmHg, (i.e. a systolic pressure higher than 140 mmHg and a diastolic pressure higher than 90 mmHg), and affects 44.2 and 27.6 % of the European and American population in the age range of 35 to 64 years, respectively (Wolf-maier *et al.*, 2003). The most common form of hypertension is primary hypertension (also called essential hypertension), of which by definition, the cause is unknown. This complicates the treatment and has led to a “trial and error” treatment strategy based on predefined first-, second- and third-line therapy (Royal College of Physicians, Management of hypertension in adults in primary care. NICE Clinical Guideline 18, 2006). The prevalence of secondary hypertension, i.e. hypertension with an identifiable underlying cause, is much lower. Although in only 5% of the hypertensive patients the cause of hypertension is known, the absolute number of patients affected by secondary hypertension is still high. Secondary hypertension can be caused by various diseases including endocrine and kidney diseases and cancer (Grossman and Messerli, 2012). However, it can also be caused as a side effect of drugs that are prescribed for non-cardiovascular indications, (Sager *et al.*, 2013). This is still an unappreciated cause of secondary hypertension even though a myriad of drugs have been reported to induce a transient or sustained increase in BP, including non-steroidal anti-inflammatory drugs and analgesics, anti-anginogenic therapies that inhibit vascular endothelial growth factor signaling, antidepressant agents, steroids and sex hormones (Grossman and Messerli, 2012). For these specific drug classes the mechanisms of action (MoA) underlying the undesired effects on BP have been elucidated. However, in drug development cardiovascular safety issues occur frequently with novel compounds (Sager *et al.*, 2013). The MoA underlying these undesired BP effects is often not fully understood. This is a major drawback since a quantitative understanding of the pharmacological effects of (novel) drugs on BP control is pivotal from a drug safety point of view. In addition, although clinically hypertension is defined by a clear cut-off value, i.e. BP higher than 140/90 mmHg, it should be noted that the risk of cardiovascular events continuously increases with increased BP levels. Even changes in BP as small as 3 mmHg can have a relatively large influence in certain patient populations (Sager *et al.*, 2013; EMEA, 2004). This underscores the importance of detecting and understanding undesired BP effects of novel compounds.

This thesis focuses on identification of the MoA of drugs with an undesired effect on BP. Moreover, it describes how the magnitude and dynamics of drug effects on the cardiovascular system (CVS) in man can be predicted from pre-clinical investigations, which is important as this determines the benefit-risk ratio of novel drugs. In this chapter, the physiology of the CVS is described first. Thereafter, it is discussed how the parameters of

the CVS can be monitored. Subsequently, the current status with regard to the assessment of drug-induced changes in BP during drug development is reviewed. Finally, the use of systems pharmacology modeling to provide a quantitative understanding of the pharmacological effects of (novel) drugs on the CVS to improve the prediction of the magnitude of the hemodynamic effects in humans is discussed. Although this chapter focuses on undesired effects of drug on BP it should be realized that many of the principles that are discussed are also relevant for drugs with desired effects on BP. However, this is beyond the scope of this chapter.

Physiology of the CVS

The primary function of the CVS, which consists of the heart, blood, and blood vessels and includes the pulmonary and systemic circulation, is the rapid convective transport of oxygen, glucose, amino acids, fatty acids, vitamins and water to the tissues and the rapid washout of metabolic waste products such as carbon dioxide, urea and creatinine (Levick, 2003).

Hemodynamics

The blood flow through the systemic circulation (hemodynamics) is governed by physical laws. Under steady flow conditions, the flow is proportional to the pressure difference between the inlet and outlet pressure (Equation 1) (Levick, 2003).

$$\dot{Q} = K \cdot (P_1 - P_2) \quad (1)$$

In this equation, Q represents the flow, K represents the hydraulic conductance, and P_1 and P_2 represent the inlet and outlet pressure, respectively. As resistance (R) is the reverse of conductance, i.e. $1/K$, the basic law of flow can be re-written into Darcy's law of flow, which is similar to Ohm's law for fluid flow (Equation 2).

$$\dot{Q} = \frac{P_1 - P_2}{R} \quad (2)$$

It indicates that resistance equals the difference in pressure needed to drive one unit of flow in steady state, i.e. mmHg per mL/min. In the CVS, flow through the entire systemic circulation equals the cardiac output (CO). The pressure difference is mean arterial pressure (MAP) minus central venous pressure (CVP) and resistance is called total peripheral

resistance (TPR). Therefore, when applying Darcy's law to the CVS, equation 2 translates into Equation 3.

$$CO = \frac{MAP - CVP}{TPR} \quad (3)$$

Since CVP is much smaller than MAP, this equation can be simplified (Equation 4).

$$CO = \frac{MAP}{TPR} \quad (4)$$

In addition, CO equals the volume of blood ejected by one ventricle per unit of time. It is the product of stroke volume (SV) and heart rate (HR) (Equation 5).

$$CO = HR \cdot SV \quad (5)$$

Mean Arterial Pressure (MAP) = Total Peripheral Resistance (TPR) x Cardiac Output (CO)

Cardiac Output (CO) = Heart Rate (HR) x Stroke Volume (SV)

Figure 1: Equations to characterize the hemodynamics of the CVS

In conclusion, the hemodynamics of the CVS are characterized by two equations (Figure 1).

It should be noted that arterial pressure is pulsatile, because the heart ejects blood intermittently. Between successive ejections the systemic arterial pressure decays from a peak of ~120 mmHg to a trough of ~80 mmHg. The pulsatile character of arterial pressure is not captured by these equations. However, this is deemed irrelevant as this thesis focuses on drug effects on MAP.

Blood pressure regulation

The mechanisms of BP regulation by the CVS have been carefully characterized, and the homeostatic principles of the CVS are thoroughly understood. Briefly, MAP is maintained within narrow limits by various regulatory feedback systems which control BP on different time scales (Figure 2). The baroreceptor reflex system is primarily responsible for short term BP regulation at the time scale of seconds. Other systems that regulate BP within seconds include the chemoreceptor reflex and the ischemic response. In addition, several hormonal systems including the renin-angiotensin-aldosterone system (RAAS) (indicated by “Capillary” in Figure 2), and some minor systems, control blood pressure within at

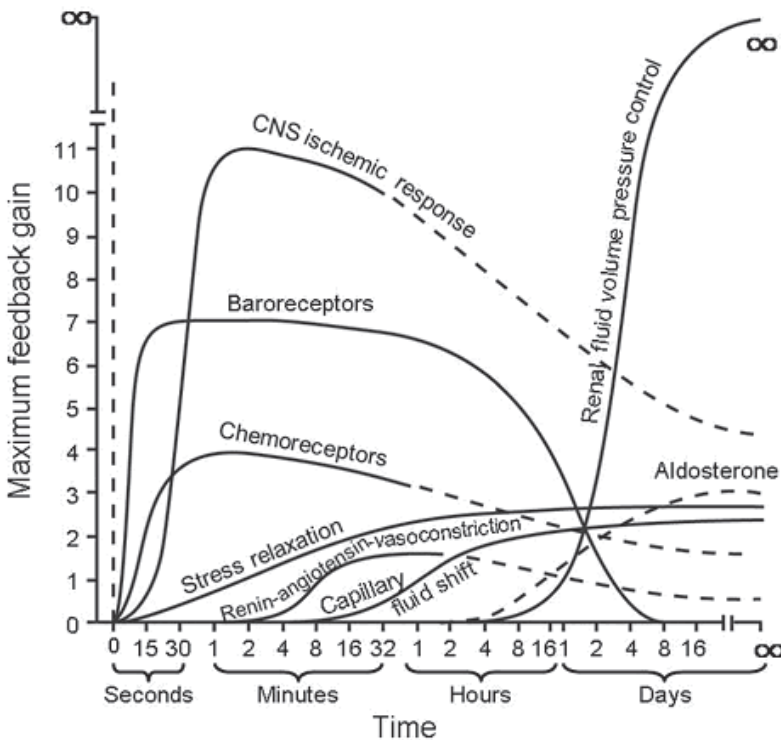


Figure 2: Blood pressure control. Degree of activation, expressed in terms of feedback gain at optimal pressure, of different pressure control mechanisms after a sudden change in arterial pressure. CNS, central nervous system (Okumura and Cheng, 2012)

a time scale of minutes. Finally, the kidney-fluid volume system is responsible for long term BP regulation and affects blood pressure within hours or days (Okumura and Cheng,

2012). In this chapter, first, the baroreflex system and, subsequently, the RAAS will be discussed in more detail.

The baroreceptor reflex system regulates HR and TPR and, thereby, MAP through the sympathetic and parasympathetic nervous system. Baroreceptors are stretch-sensitive mechanoreceptors, which are present in the vena cavae, carotid sinuses and aortic arch. When MAP rises, the carotid and aortic sinuses are distended resulting in stretch and, subsequently, activation of the baroreceptors. Active baroreceptors fire action potentials more frequently than inactive baroreceptors. The greater the stretch the more rapidly baroreceptors fire action potentials. These action potentials are relayed to the brainstem. Baroreceptor activation results in inhibition of the sympathetic nervous system and activation of the parasympathetic nervous system. The sympathetic and parasympathetic branches of the autonomic nervous system have opposing effects on MAP. Sympathetic activation leads to an elevation of TPR and CO via increased contractility of the heart and increased heart rate and, thus, to increased MAP. Conversely, parasympathetic activation leads to decreased CO via a decrease in HR and, thus, to decreased MAP. By coupling sympathetic inhibition and parasympathetic activation, the baroreflex maximizes MAP reduction (Levick, 2003). In a similar manner, sympathetic activation with parasympathetic inhibition allows the baroreflex to elevate MAP.

The RAAS regulates blood volume. If blood volume increases the venous return of blood to the heart increases, resulting in increased SV, CO and MAP. The blood volume is regulated through changes in MAP. Briefly, a decrease in MAP promotes the release of the hormone renin from the kidney into the blood. Renin promotes the production of angiotensin I from angiotensinogen. Subsequently, angiotensin I is converted into angiotensin II by angiotensin converting enzyme (ACE). Angiotensin II constricts blood vessels and promotes renal salt and water retention by direct intrarenal actions and by stimulating and by stimulating the release of aldosterone (Cleophas, 1998). Aldosterone acts on the distal tubules and collecting ducts of the nephron, increasing reabsorption of ions and water in the kidney. This causes the conservation of sodium, secretion of potassium, increase in water retention, and increase in MAP.

Drug effects on the cardiovascular system

The cardiovascular system can be influenced by drugs through a variety of different, and often complex, mechanisms. However, basically, most compounds directly influence HR, SV and/or TPR as elucidated for a selection of commonly applied cardiovascular drugs in Table 1. Due to the different feedback mechanisms that regulate the CVS the direct effect

Table 1: A selection of commonly applied cardiovascular drugs and their mechanism of action (this thesis).

Compound	Class	Mechanism of action	Effect
amiloride	diuretic	Diuretics cause blood volume contraction and lower venous pressure, which decreases cardiac filling and, by the Frank-Starling mechanism, decreases ventricular stroke volume (Levick, 2003).	SV
amlodipine	calcium channel blocker	Amlodipine is a dihydropyridine that blocks voltage gated calcium channels and selectively inhibits Ca^{2+} influx into vascular smooth muscle cells. Calcium antagonists act by decreasing total peripheral resistance to lower arterial pressure. As a consequence, reflex tachycardia, increased cardiac output, and increased plasma catecholamine and plasma renin activity are commonly seen, particularly with the initial dose and with short-acting dihydropyridines (Michalewicz <i>et al.</i> , 1997; Perez-Reyes <i>et al.</i> , 2009).	TPR
atropine	M2 receptor antagonist	Muscarinic (M2) receptor antagonist (MRA) is an agent that blocks the activity of the muscarinic acetylcholine receptor. It causes tachycardia by blocking vagal effects on the sinoatrial node. Acetylcholine hyperpolarizes the sinoatrial node which is overcome by MRA and thus increases the heart rate	HR
enalapril	angiotensin-converting enzyme (ACE) inhibitor	ACE inhibitors competitively inhibit angiotensin I-converting enzyme, preventing the conversion of angiotensin I to angiotensin II, a potent vasoconstrictor that also stimulates release of aldosterone. Decreased levels of angiotensin II lead to decreased total peripheral resistance that is unassociated with reflex stimulation of the heart (Frohlich, 1989). In addition, aldosterone acts on the distal tubules and collecting ducts of the nephron, the functional unit of the kidney. Decreased levels of aldosterone, cause the depletion of sodium, conservation of potassium, decreased water retention, and decreased blood pressure	TPR and SV
fasudil	rho-kinase inhibitor	Rho-kinase inhibits myosin light chain phosphatase activity and plays a key role in Ca^{2+} sensitization and hypercontraction of vascular smooth muscle cells. Rho-kinase inhibitors decrease total peripheral resistance (Masumoto <i>et al.</i> , 2001).	TPR
HCTZ	diuretic	See amiloride	SV
prazosin	selective α_1 adrenergic receptor blocker	Prazosin is a quinazoline derivative that is a specific and selective competitive antagonist of α_1 adrenoceptors on vascular smooth muscle cells. Prazosin reduces BP by reducing elevated peripheral resistance and has little effect on cardiac function (Reid <i>et al.</i> , 1987).	TPR
propranolol	β -adrenergic receptor blocker	Propranolol is a non-selective beta blocker. It antagonizes the action of norepinephrine and epinephrine at all β -adrenergic receptors. Propranolol decreases cardiac output and heart rate with a reflex rise in total peripheral resistance (Ebadi <i>et al.</i> , 2008).	HR

of compounds are translated into differential effects on the other variables of the CVS, i.e. MAP, CO, HR, SV and TPR (this thesis). For example, fasudil is a calcium channel blocker, which decreases TPR through smooth muscle cell contraction (direct effect). Since MAP equals the product of TPR and CO, MAP is also decreased. As a result of the different

feedback mechanisms regulating the CVS HR, SV and CO are increased after administration of fasudil (indirect effect).

Monitoring the variables of the cardiovascular system

Detection of drug-induced changes in the hemodynamics may be influenced by the frequency and type of cardiovascular measurements during a study (Sager *et al.*, 2013). As mentioned in the section “Physiology”, the hemodynamics of the CVS are characterized by five basic variables, i.e. MAP, HR, CO, SV and TPR. In experimental and clinical pharmacology measuring MAP and HR is common practice. However, measuring CO, SV and TPR is not due to a lack of a perfect ‘gold’ standard measuring technique as detailed further in this section. Moreover, most measurement techniques require invasive instrumentation procedures, which limits the applicability of these techniques. Nevertheless measuring CO is important, because when MAP, HR and CO are measured SV and TPR can be derived using Equations 4 and 5. This provides a full understanding of drug effects on all variables of the CVS instead of on only two, i.e. MAP and HR. Moreover, since drug effects on CO and TPR may be much larger than anticipated from the observed responses on MAP and HR, measuring CO provides powerful information to detect patho-physiological conditions. In this section, it is first discussed how MAP and HR can be measured in conscious animals and in humans. Subsequently, it is discussed how CO can be measured.

Despite the fact that MAP is one of the most commonly measured hemodynamic parameters throughout drug development, there is no uniformly agreed methodology for how MAP should be measured (Sager *et al.*, 2013). Typically, in preclinical research, dedicated telemetry studies are performed to evaluate acute effects of drugs in conscious rats, dogs or nonhuman primates. In these studies, MAP and HR are usually continuously recorded using indwelling catheters (Sager *et al.*, 2013). Since MAP and HR are continuously recorded over several days this provides information for detecting 1) the diurnal profile, 2) direct and delayed drug effects and 3) short and long term effects on MAP and HR. In addition, another noninvasive technique to measure MAP is available, i.e. oscillometric tail cuff with jackets, but this technique requires further refinement to improve system sensitivity to detect smaller changes in MAP (Ward *et al.*, 2012, Sager *et al.*, 2013). In human, MAP is measured noninvasively using manual or digital sphygmomanometers (blood pressure meters) or by ambulatory blood pressure monitoring (ABPM) and HR can be measured by ABPM, electrocardiograph (ECG) or pulse oximeters. The information obtained on changes in MAP and HR by ABPM is comparable to the information obtained from telemetry studies in conscious animal. Therefore, ABPM measurements are uniquely suited to detect the dynamics of drug effects on MAP and HR. In addition, the variability in measurements is much smaller with ABPM as compared to measurements from sphyg-

momanometers. Especially when MAP and HR are measured in the clinic the variation in MAP and HR measurements can be very large, e.g. because of the white-coat effect (i.e. a transient elevation in MAP that does not appear to be linked to target organ damage or prognosis, but to the anxiety or stress that can be experienced during a visit to a physician). This should be taken into account when assessing drug-induced changes in the CVS. Although measuring CO could provide a better understanding of underlying pathophysiological processes, this has not been integrated into daily practice due to difficulties associated with invasive instrumentation procedures in both animal and human (Vincent *et al.*, 2011; Doursout *et al.*, 2001). In conscious and freely moving rats, CO can be measured with a variety of techniques (Doursout *et al.*, 2001), including the Fick method, thermodilution, microsphere detection, impedance cardiography, transit ultrasound and electromagnetic flowmetry (Tsuchiya *et al.*, 1978; Gotshall *et al.*, 1987). Only the last method allows immediate observation of phasic aortic flow patterns and has been used to estimate cardiac function indirectly by means of derivatives of phasic aortic signals (deWildt and Sangster, 1983). Another method of interest for measurement of blood flow is the use of pulsed Doppler flow probes. This method is based on the direct relationship between blood velocity and volume flow. This method of measuring CO has not been used in many species. However, it has been claimed that these measurements are accurate in rats (Gardiner *et al.*, 1990). In human, the pulmonary artery catheter, also called Swan-Ganzkatheter, has long been considered optimal for hemodynamic monitoring, allowing for the almost continuous, simultaneous recording of pulmonary artery and cardiac filling pressures, cardiac output and oxygen saturation. However, the technique is invasive. Moreover, there is increasing evidence that this method is neither accurate nor effective in guiding therapy (Vincent *et al.*, 2011). There are many different monitoring systems available ranging from the highly invasive pulmonary artery catheter to the completely non-invasive bioimpedance/bioreactance, CO₂ rebreathing and echocardiography and echo-Doppler techniques. In general, variability in CO measurements is large. Classifying them according to how accurate or precise they are is difficult, in part because of the lack of a perfect 'gold' standard for comparison (Vincent *et al.*, 2011). Most devices have been evaluated by comparing their results with those obtained by intermittent thermodilution from the pulmonary artery catheter as the reference, although this technique has its own limitations and may not represent the gold standard best. The bioimpedance/bioreactance technique has been used for physiological studies in healthy individuals (Marque *et al.*, 2009). This technique has the advantage that it allows continuous recording of CO. However, further investigation is required to investigate if this technique is reliable in critically ill patients (Vincent *et al.*, 2011).

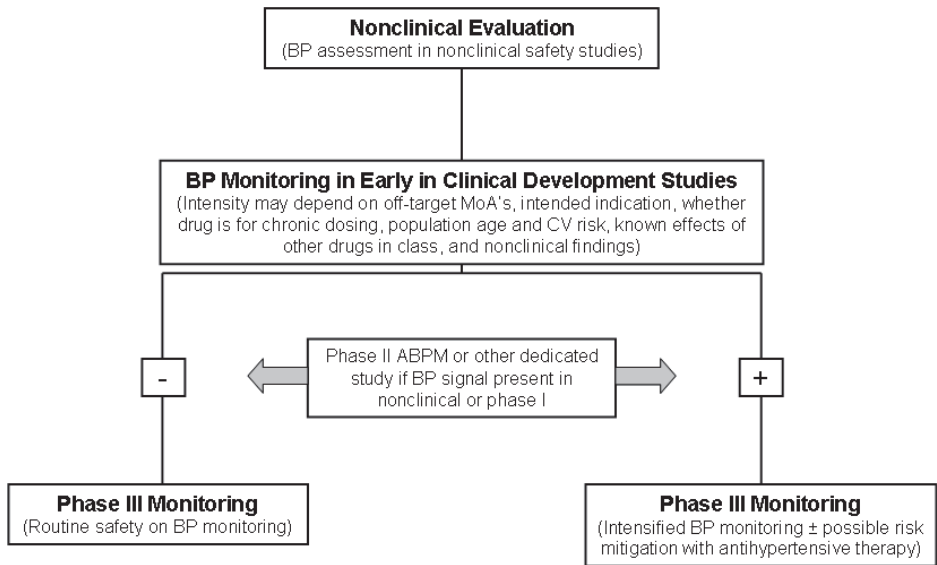


Figure 3: MAP Assessment Development process (Sager et al., 2013)

Assessment of drug effects on the CVS in drug-development

In general, drug effects on MAP are assessed in all phases of the drug-development process (Figure 3). In preclinical development, safety studies are performed ranging from *in vitro* assays to fully integrated *in vivo* animal models (Sager et al., 2013). The translation of these effects from preclinical to clinical development is often not fully understood and it is under debate whether preclinical studies are predictive for clinical studies. A recent meta-analysis comparing the effects of small molecules on diastolic BP measured in conscious dog telemetry studies and the single-ascending dose phase of first-in-human studies suggest that a 5% change in diastolic BP in dog telemetry studies would provide for 37% sensitivity (probability of dog correctly identifying a positive phase I outcome) and 60% specificity (probability of correctly identifying negative phase I outcome) (Sager et al., 2013). As the physiology of the CVS is comparable between species (Schmidt-Nielsen, 1995) it is plausible that drug effects on the CVS are comparable between species too, albeit that there may be quantitative differences resulting from differences in size and function. Therefore, in cases where at first site the drug effect observed in animals seems to be not predictive for human, this may be explained by an incomprehensive understanding of the translation (the system differences). Another explanation may be that the interpretation of the results is not adequate, e.g. because of the lack of uniformity in the nonclinical approaches and the variability in the MAP measurements in clinical development (section “Monitoring the parameters of the CVS”). Therefore, an integrative

approach to data interpretation would appear most desirable (section “Modelling the CVS”).

Although undesired cardiovascular drug effects are usually detected in preclinical studies, the clinical relevance of these effects often only becomes apparent in the clinical development when drug effects are evaluated in healthy volunteers and/or in the target population. The clinical relevance of drug-induced cardiovascular effects is determined by many factors, such as the benefit-risk profile, treatment indication and duration of treatment and the cardiovascular risk of the target population. The clinical evaluation of drug effects on MAP involves multiple considerations, which are usually based on the presumed MoA underlying the undesired effects on MAP (Figure 3). However, in contrast to the detailed understanding of the physiologic regulation of MAP, the mechanisms underlying the effects on MAP of compounds with a novel MoA are often less clear. This is a major drawback since a quantitative understanding of the pharmacological effects of (novel) drugs on MAP control is pivotal with regard to safety, the prediction of the magnitude of hemodynamic effects in human and the adequate assessment during clinical development. For example, if intensified MAP monitoring in phase III studies is required to investigate possible risk mitigation with antihypertensive therapy it is pivotal to understand the MoA of the compound in order to adequately reverse an adverse effect on MAP (Sager *et al.*, 2013). This underscores the importance of understanding these effects early in preclinical development since this could improve the anticipation of the magnitude of hemodynamic effects in humans.

Modelling the CVS

Pharmacometrics is the scientific discipline that uses mathematical models based on biology, pharmacology, physiology, and disease for *in vivo* quantification of drugs effects. Models in pharmacometrics can be differentiated by their area of application, for example “pharmacokinetic-pharmacodynamic (PKPD) models”, “disease models”, “trial execution model” or any combination of these (Zhang *et al.*, 2008). In this section, the focus is on PKPD modeling. The primary objective of PKPD modeling is to identify key properties of a drug *in vivo*, which allows the characterization and prediction of the time course of drug effects under physiological and pathological conditions. A pharmacokinetic (PK) model characterizes the time-course of the drug concentration and a pharmacodynamic (PD) model characterizes the relationship between exposure and pharmacological effect. PKPD modeling is applied in all stages of drug development and has proven to be a useful tool to support decision making in the key steps of drug development process (Breimer and Danhof, 1997). Within this context, PKPD modeling constitutes the theoretical basis for

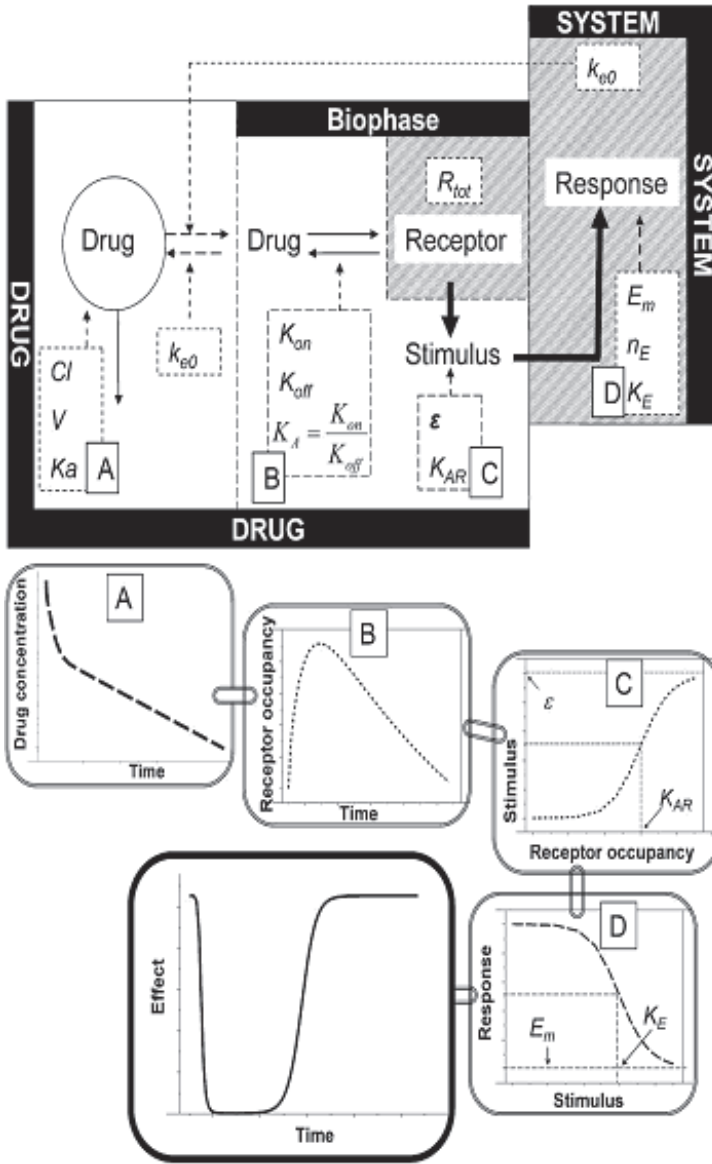


Figure 4: Processes in the causal chain between drug administration and the change in response over time, including the pharmacokinetics of a drug (process A), target site distribution and receptor (target) binding kinetics (process B), receptor activation (process C) and transduction (process D). These processes are characterized by receptor theory models incorporated in mechanism-based PK-PD models (Ploeger *et al.*, 2009).

the selection of drug candidates, lead optimization, and the optimization of early proof-of-concept clinical trials on the basis of information from preclinical studies (Danhof *et al.*, 2007; Danhof *et al.*, 2008). PKPD modeling has developed from an empirical and descriptive approach into a scientific discipline based on the (patho-) physiological mechanisms behind PKPD relationships. As a result PKPD models range from purely empirical models, i.e. descriptive models to mechanism-based and systems pharmacology models with an increasing level of complexity an increasing level of predictive power. Mechanism-based models differ from empirical models in that they quantitatively characterize specific processes in the causal chain between drug administration and effect. A key element of mechanism-based modelling is the explicit distinction between parameters to describe drug-specific properties and biological system-specific properties. Drug-specific parameters (i.e., receptor affinity, intrinsic efficacy) describe the interaction between the drug and the biological system in terms of target affinity and target activation, whereas system-specific parameters describe the functioning of the biological system (Figure 4). The explicit distinction between drug-specific parameters and biological system-specific parameters is crucial to the prediction of *in vivo* drug effects (Danhof *et al.*, 2007; Ploeger *et al.*, 2009). Therefore, mechanism-based PKPD models have much improved properties for extrapolation and prediction as compared to empirical models. Systems pharmacology models attempt to inject biological realism to bring molecular or cellular detail closer to high-level, functional behavior (Vicini and van der Graaf, 2013). Where mechanism-based models focus on pathways, the level of complexity in systems pharmacology is increased further by focusing on networks and the interaction between different components of the network. This can be on different levels in the biological system ranging the organ level to the cellular level. Focusing on networks instead of pathways has the advantage that drug effects on interrelationships between the components of a network, i.e. different pathways, can be characterized and predicted.

Systems biology is an approach to understanding biological processes as integrated systems instead of as isolated parts. The influence of systems biology has often been at a very fundamental (cellular or subcellular) biological scale, difficult to mechanistically link to higher-order tissue or organ systems. The Guyton and Coleman, which describes the physiology of the CVS in great detail model (Guyton *et al.*, 1972), represents an example of a systems biology model (Figure 5). This model is a systems model of the human circulatory physiology, capable of simulating a variety of experimental conditions and contains a number of linked subsystems related to the circulation and its neuroendocrine control. The complete model consists of separate modules, each of which characterizes a separate part of the physiological subsystem. The “Circulation Dynamics” part is the primary system, to which other modules/blocks are connected. The other modules characterize

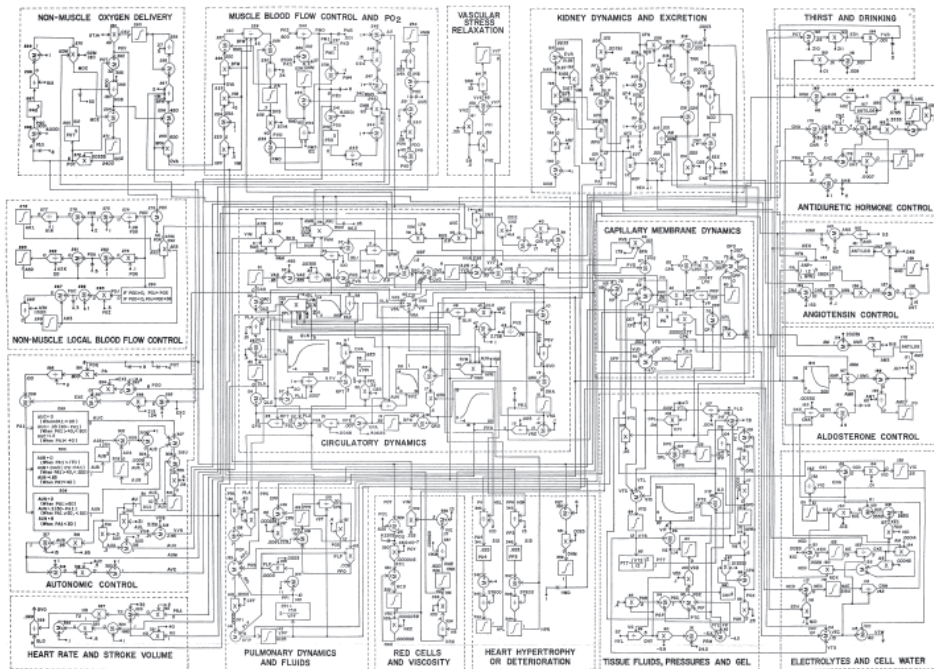


Figure 5: A systems analysis diagram for the full Guyton model describing circulation regulation (CellML, 2008)

the dynamics of the kidney, electrolytes and cellular water, thirst and drinking, hormone regulation, autonomic regulation, cardiovascular system etc., and these feed back on the central circulation model. The Guyton model has provided the scientific basis for the understanding of long-term BP control (Montani and Van Vliet, 2009).

Typically, systems biology is not concerned about therapeutic intervention; rather, deep study of targets and pathways is its focus. In that respect systems biology models differ from PKPD models, which aim to characterize drug effects. Next to this obvious difference, these models also differ in the level of detail included in the model and in the model selection criteria and the criteria for parameter identification. In PKPD modelling a data driven, top-down approach is followed starting at a parsimonious descriptive level and subsequently adding more complexity to better understand the system. These models are developed and selected by finding a middle ground between the model's complexity and its descriptive power. Such middle ground can be based on statistical principles (e.g., balancing number of parameters and goodness of data fitting). The driver is invariably parsimony — in other words, selection of a model whose complexity is “just right” (least complex with the fewest parameters), given the data. On the other hand, systems biology models are inherently complete and fully mechanistic and one follows a bottom-up approach, starting from the level of molecular pathways (Ploeger *et al.*, 2009). In systems

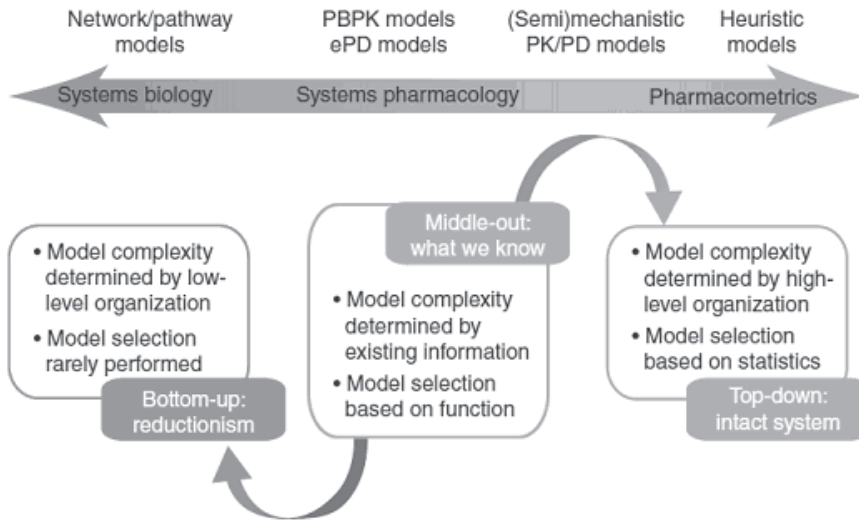


Figure 6: A graphical summary of bottom-up, middle-out, and top-down approaches to model development and their relationship to various model types currently applied in drug discovery and development. In bottom-up approaches, low-level information determines the model, and this often remains conceptual. In top-down approaches, high-level organization and information determine interpretative models. In middle-out approaches, the driving force is available information, and models are selected and built on the basis of functional behavior. In this framework, systems pharmacology can be regarded as an approach to integrate the desirable features of the various model types spanning the spectrum between systems biology and pharmacometrics (Vicini and van der Graaf, 2013).

biology, model selection is rarely performed. Systems pharmacology provides a middle-out approach. As discussed earlier the level of detail in the model is increased further as compared to mechanistic models as networks instead of pathways are characterized in a quantitative manner on different levels in the biological system ranging the organ level to the cellular level. Thereby, the level of detail included in these models middles the level of detail in systems biology models and empirical models. Next to the statistical criteria for model selection, systems pharmacology models are selected based on their function (Figure 6).

Although in many therapeutic areas PKPD modeling has evolved from empirical modeling to mechanistic or systems pharmacology modeling, with examples in diverse areas such as central nervous system disease (Geerts *et al.*, 2013), osteoporosis (Post *et al.*, 2013; Peterson and Riggs, 2012), endometriosis (Riggs *et al.*, 2012) and safety (Lippert *et al.*, 2012), PKPD modeling did not exceed the stage of empirical modeling in the area of cardiovascular disease. For several antihypertensive drugs, no clear relationship be-

tween drug concentration and its effect on MAP has been reported (Gomez *et al.*, 1989; MacGregor *et al.*, 1983; Hansson *et al.*, 1974). This is probably the result of initial studies in which relatively high doses were administered with exposures in the upper part of the sigmoid concentration–response curve, resulting in effects all close to the maximum response (van Rijn-Bikker *et al.*, 2013). Furthermore, the description of the concentration–effect relationship for antihypertensive drugs is often confounded by a failure to collect sufficient pharmacodynamic data, a failure to identify and account for the fact that the MAP-lowering effect develops over a number of weeks, and a failure to account for circadian variability in the diurnal MAP profile (Meredith, 1997). On the other hand, the concentration–effect relationship for angiotensin converting enzyme inhibitors, calcium antagonists and alpha blockers have been successfully established (Bellissant and Giudicelli, 1998; Bellissant and Giudicelli, 2001; Donnelly, 1989; Donnelly *et al.*, 1988; Donnelly *et al.*, 1993). These models may be classified as empirical models. To date no mechanism-based, mechanistic or systems pharmacology models exist that provide an integrated description of the effects of drugs on the CVS except for a model that was postulated by Francheteau *et al.* (Francheteau *et al.*, 1993). This model provides a description of the effect of dihydropyridine drugs on the relationship between MAP, CO and TPR. However, as several key model parameters of the Francheteau model were not identifiable this is not a truly mechanism-based model in the sense that drug- and system-specific properties were distinguished. The fact that no systems pharmacology models are available to characterize drug effects on the CVS is a major drawback since these models are uniquely suited to provide a quantitative understanding of the pharmacological effects of (novel) drugs on the CVS, which is pivotal with regard to drug safety. Moreover, understanding these effects early in preclinical development could improve the anticipation of the magnitude of hemodynamic effects in humans.

References

- Bellissant E, Giudicelli JF (1998). Pharmacokinetic-pharmacodynamic model relating zibicoprilat plasma concentrations to brachial and femoral haemodynamic effects in normotensive volunteers. *Br J Clin Pharmacol.*, 46, 383-393.
- Bellissant E, Giudicelli JF (2001). Pharmacokinetic-pharmacodynamic model for perindoprilat regional haemodynamic effects in healthy volunteers and in congestive heart failure patients. *Br J Clin Pharmacol.*, 52, 25-33.
- Breimer DD, Danhof M (1997). Relevance of the application of pharmacokinetic-pharmacodynamic modelling concepts in drug development. The "wooden shoe" paradigm. *Clin Pharmacokinet.*, 32, 259-267.
- CellML (2008). "<http://models.cellml.org/exposure/f97a5eb092b12f4f0f32ac51ee20d20e>"
- Cleophas TJ (1998). Mechanisms offsetting the beneficial effects of antihypertensive drugs: a problem increasingly considered but incompletely understood. *Am J Ther.*, 5, 413-419.
- Danhof M, de Jongh J, De Lange EC, Della Pasqua O, Ploeger BA, Voskuyl RA (2007). Mechanism-based pharmacokinetic-pharmacodynamic modeling: biophase distribution, receptor theory, and dynamical systems analysis. *Annu Rev Pharmacol Toxicol.*, 47, 357-400.
- Danhof M, de Lange EC, Della Pasqua OE, Ploeger BA, Voskuyl RA (2008). Mechanism-based pharmacokinetic-pharmacodynamic (PK-PD) modeling in translational drug research. *Trends Pharmacol Sci.*, 29, 186-191.
- de Wildt DJ, Sangster B (1983). An evaluation of derived aortic flow parameters as indices of myocardial contractility in rats. *J Pharmacol Methods.*, 10, 55-64.
- Donnelly R, Elliott HL, Meredith PA, Howie CA, Reid JL (1993). The pharmacodynamics and pharmacokinetics of the combination of nifedipine and doxazosin. *Eur J Clin Pharmacol.*, 44, 279-282.
- Donnelly R, Elliott HL, Meredith PA, Kelman AW, Reid JL (1988). Nifedipine: individual responses and concentration-effect relationships. *Hypertension.*, 12, 443-449.
- Donnelly R, Elliott HL, Meredith PA, Reid JL (1989). Concentration-effect relationships and individual responses to doxazosin in essential hypertension. *Br J Clin Pharmacol.*, 28, 517-526.
- Doursout MF, Wouters P, Kashimoto S, Hartley CJ, Rabinovitz R, Chelly JE (2001). Measurement of cardiac function in conscious rats. *Ultrasound Med Biol.*, 27, 195-202.
- Ebadi M (2008). *Desk Reference of Clinical Pharmacology*. Taylor & Francis Group: Boca Raton Florida (book).
- EMA (2004). «EMA guideline: note for guidance on clinical investigation of medicinal products in the treatment of hypertension.» CPMP/EWP/238/95 Rev. 2.
- Francheteau P, Steimer JL, Merdjan H, Guerret M & Dubray C (1993). A mathematical model for dynamics of cardiovascular drug action: application to intravenous dihydropyridines in healthy volunteers. *J Pharmacokinet Biopharm.*, 21, 489-514.
- Frohlich ED (1989). Angiotensin converting enzyme inhibitors. Present and future. *Hypertension.*, 13, 1125-30.
- Gardiner SM, Compton AM, Bennett T, Hartley CJ (1990). Can pulsed Doppler technique measure changes in aortic blood flow in conscious rats? *Am J Physiol.*, 259, H448-456.
- Geerts H, Spiros A, Roberts P, Carr R (2013). Quantitative systems pharmacology as an extension of PK/PD modeling in CNS research and development. *J Pharmacokinet Pharmacodyn.*, 40, 257-265.
- Gomez HJ, Cirillo VJ, Sromovsky JA, Otterbein ES, Shaw WC, Rush JE *et al.* (1989). Lisinopril dose-response relationship in essential hypertension. *Br J Clin Pharmacol.*, 28, 415-420.
- Gotshall RW, Breay-Pilcher JC, Boelcskevsky BD (1987). Cardiac output in adult and neonatal rats utilizing impedance cardiography. *Am J Physiol.*, 253, H1298-304.
- Graham I, Atar D, Borch-Johnsen K, Boysen G, Burell G, Cifkova R *et al.* (2007). European guidelines on cardiovascular disease prevention in clinical practice: executive summary. Fourth Joint Task Force of the European Society of Cardiology and other societies on cardiovascular disease prevention in clinical practice (constituted by representatives of nine societies and by invited experts). *Eur J Cardiovasc Prev Rehabil.*, 14, E1-40.

- Grossman E, Messerli FH (2012). Drug-induced hypertension: an unappreciated cause of secondary hypertension. *Am J Med.*, 125, 14-22
- Guyton AC, Coleman TG, Granger HJ (1972). Circulation: overall regulation. *Annu Rev Physiol.*, 34, 13-46.
- Hansson L, Zweifler AJ, Julius S, Ellis CN (1974). Propranolol therapy in essential hypertension. Observations on predictability of therapeutic response. *Int J Clin Pharmacol.*, 10, 79-89.
- Levick JR (2003). An introduction to cardiovascular physiology.
- Lippert J, Brosch M, von Kampen O, Meyer M, Siegmund HU, Schafmayer C *et al.* (2012). A mechanistic, model-based approach to safety assessment in clinical development. *CPT Pharmacometrics Syst Pharmacol.*, 1:e13., 10.1038/psp.2012.14.
- MacGregor GA, Banks RA, Markandu ND, Bayliss J, Roulston J (1983). Lack of effect of beta-blocker on flat dose response to thiazide in hypertension: efficacy of low dose thiazide combined with beta-blocker. *Br Med J (Clin Res Ed)*. 286, 1535-1538.
- Marque S, Cariou A, Chiche JD, Squara P (2009). Comparison between Flotrac-Vigileo and Bioreactance, a totally noninvasive method for cardiac output monitoring. *Crit Care.*, 13, R73.
- Masumoto A, Hirooka Y, Shimokawa H, Hironaga K, Setoguchi S, Takeshita A (2001). Possible involvement of Rho-kinase in the pathogenesis of hypertension in humans. *Hypertension*. 38, 1307-1310.
- Meredith PA (1997). Clinical relevance of optimal pharmacokinetics in the treatment of hypertension. *J Hypertens Suppl.*, 15, S27-31.
- Michalewicz L, Messerli FH (1997). Cardiac effects of calcium antagonists in systemic hypertension. *Am J Cardiol.*, 79, 39-46; discussion 47-48.
- Montani JP, Van Vliet BN (2009). Understanding the contribution of Guyton's large circulatory model to long-term control of arterial pressure. *Exp Physiol.*, 94, 382-388.
- Okumura K, Cheng XW (2012). Characteristics of blood pressure profiles and vascular dysfunction. *Hypertens Res.*, 35, 23-24.
- Perez-Reyes E, Van Deusen AL, Vitko I (2009). Molecular pharmacology of human Cav3.2 T-type Ca²⁺ channels: block by antihypertensives, antiarrhythmics, and their analogs. *J Pharmacol Exp Ther.*, 328, 621-627.
- Peterson MC, Riggs MM (2012). Predicting nonlinear changes in bone mineral density over time using a multiscale systems pharmacology model. *CPT Pharmacometrics Syst Pharmacol.*, 1:e14., 10.1038/psp.2012.15.
- Ploeger BA, van der Graaf PH, Danhof M (2009). Incorporating receptor theory in mechanism-based pharmacokinetic-pharmacodynamic (PK-PD) modeling. *Drug Metab Pharmacokinet.*, 24, 3-15.
- Post TM, Schmidt S, Peletier LA, de Greef R, Kerbusch T, Danhof M (2013). Application of a mechanism-based disease systems model for osteoporosis to clinical data. *J Pharmacokinet Pharmacodyn.*, 40, 143-156.
- Reid JL, Elliott HL, Vincent J, Meredith PA (1987). Clinical pharmacology of selective alpha blockers. Hemodynamics and effects on lipid levels. *Am J Med.*, 82, 15-20.
- Riggs MM, Bennetts M, van der Graaf PH, Martin SW (2012). Integrated pharmacometrics and systems pharmacology model-based analyses to guide GnRH receptor modulator development for management of endometriosis. *CPT Pharmacometrics Syst Pharmacol.*, 1:e11. 10.1038/psp.2012.10.
- Sager P, Heilbraun J, Turner JR, Gintant G, Geiger MJ, Kowey PR *et al.* (2013). Assessment of drug-induced increases in blood pressure during drug development: report from the Cardiac Safety Research Consortium. *Am Heart J.*, 165, 477-488.
- Schmidt-Nielsen K (1995). Why is animal size so important?. Cambridge.
- Tsuchiya M, Ferrone RA, Walsh GM, Frohlich ED (1978). Regional blood flows measured in conscious rats by combined Fick and microsphere methods. *Am J Physiol.*, 235, H357-60.
- van Rijn-Bikker PC, Ackaert O, Snelder N, van Hest RM, Ploeger BA, Koopmans RP *et al.* (2013). Pharmacokinetic-pharmacodynamic modeling of the antihypertensive effect of eprosartan in Black and White hypertensive patients. *Clin Pharmacokinet.*, 52, 793-803.
- Vicini P, van der Graaf PH (2013). Systems pharmacology for drug discovery and development: paradigm

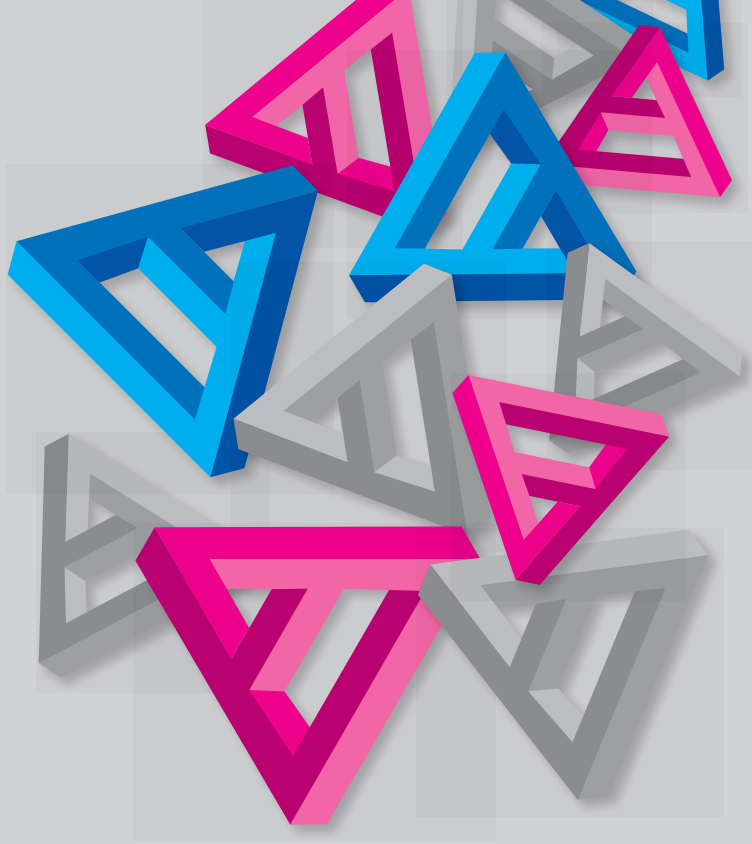
shift or flash in the pan? *Clin Pharmacol Ther.*, 93, 379-381.

Vincent JL, Rhodes A, Perel A, Martin GS, Della Rocca G, Vallet B *et al.* (2011). Clinical review: Update on hemodynamic monitoring--a consensus of 16. *Crit Care.*, 15, 229.

Ward G, Milliken P, Patel B, McMahon N (2012). Comparison of non-invasive and implanted telemetric measurement of blood pressure and electrocardiogram in conscious beagle dogs. *J Pharmacol Toxicol Methods.*, 66, 106-113.

Wolf-Maier K, Cooper RS, Banegas JR, Giampaoli S, Hense HW, Joffres M *et al.* (2003). Hypertension prevalence and blood pressure levels in 6 European countries, Canada, and the United States. *Jama.*, 289, 2363-2369.

Zhang L, Pfister M, Meibohm B (2008). Concepts and challenges in quantitative pharmacology and model-based drug development. *Aaps J.*, 10, 552-559.



CHAPTER 2

Scope and outline of the investigations

Scope

In general, cardiovascular safety issues in drug development occur often (Sager *et al.*, 2013). In this context, an adequate understanding of the cardiovascular system (CVS) which regulates blood pressure in both preclinical species and human is pivotal to efficiently anticipate clinical effects of drugs on blood pressure in man. The development of such a translational PKPD model for the cardiovascular system requires a mechanistic understanding of blood pressure regulation (Ploeger *et al.*, 2009; Danhof *et al.*, 2007). The physiological principles of the CVS including BP regulation are well established and the homeostatic principles of the CVS are thoroughly understood. Briefly, mean arterial pressure (MAP) equals the product of cardiac output (CO) and total peripheral resistance (TPR) and CO equals the product of heart rate (HR) and stroke volume (SV) (Levick, 2003). However, drug effects on this interrelationship have not been analyzed in a mechanism-based and quantitative manner.

The objectives of the investigations described in this thesis were 1) to establish a systems pharmacology model to characterize the effects of drugs with different MoA's on the interrelationship between BP, TPR, CO, HR and SV in a quantitative manner and 2) to apply the model to the quantification of the cardiovascular effect of the sphingosine 1-phosphate (S1P) receptor modulator fingolimod on the CVS.

Outline

In **section I** an overview is presented of the analysis on drug effects on CVS (**Chapter 1**). First, the physiology of the CVS is described. Thereafter, it is discussed how the variables of the CVS can be monitored and, the assessment of drug-induced changes in BP during drug development is reviewed. Finally, the use of systems pharmacology modeling to provide a quantitative understanding of the pharmacological effects of (novel) drugs on the CVS early in preclinical development for the prediction of drug effects in humans is discussed. In **section II**, a systems pharmacology model is proposed to characterize the CVS in normotensive and hypertensive rats. As a first step a systems pharmacology model was developed that describes in a strictly quantitative manner the interrelationship between BP, CO and TPR (Snelder *et al.*, 2013). It is shown that this model can describe the pharmacological effects of cardiovascular drugs in hypertensive rats and can be applied to elucidate that MoA of novel compounds using MAP and CO measurements (**Chapter 3**). Subsequently, this model was extended by parsing CO into HR and SV (**Chapter 4**). This extension was deemed important as it facilitates the elucidation of the MoA of cardiovascular drug effects using MAP and HR measurements only. In other words no CO measurements are required, which is beneficial as measuring CO is invasive and technically demanding.

Moreover, differences in BP regulation between normotensive and hypertensive rats were quantified, which is important since it is anticipated that effects observed in normotensive rats may be more representative for hemodynamic side effects in normotensive persons. To develop these system pharmacology models, rigorous preclinical experiments were designed measuring, MAP, HR and CO during the on- and offset phases of the drug effects when challenging the hemodynamic system with a training set of cardiovascular drugs with well described, but different mechanisms of action.

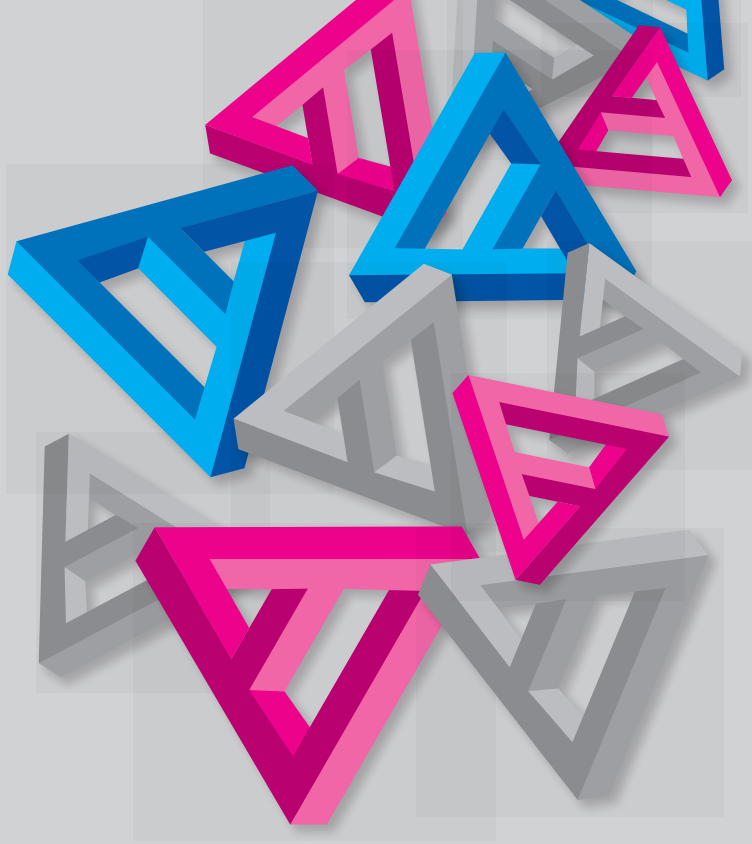
In **Section III**, the system-specific model to characterize drug effects on the interrelationship between MAP, CO, HR, SV and TPR (**Chapter 4**) was applied to characterize the cardiovascular effects of S1P receptor agonists (Kappos *et al.*, 2006; Kappos *et al.*, 2010; Selmaj *et al.*, 2013; Gergely *et al.*, 2012) using fingolimod as a paradigm compound, as a basis for the prediction of its effects in humans. Fingolimod exerts its pharmacological effect through its active metabolite fingolimod-phosphate (fingolimod-P), which is formed by the enzyme sphingosine kinase (S1PHK) (Billich *et al.*, 2003; Kihara and Igarashi, 2008; Kharel *et al.*, 2005). First, a semi-mechanistic population PK model for the inter-conversion of S1PHK substrates and their respective phosphates in rats and humans was presented. Specific aim of this study was to investigate whether the rate of phosphorylation in blood platelets constitutes a basis for interspecies scaling using fingolimod as a paradigm compound (**Chapter 5**). In this model, differences in the rate of phosphorylation in blood, estimated from *ex vivo* inter-conversion measurements in platelets, partly explain the differences in exposure between rats and humans. It is demonstrated that in addition, differences in pre-systemic phosphorylation should also be taken into account. Subsequently, the in **Chapter 4** developed systems pharmacology model and the in **Chapter 5** developed PK model for fingolimod and fingolimod-P in rat was applied to obtain a quantitative understanding of the mechanisms leading to cardiovascular effects following the administration of fingolimod in normotensive and hypertensive rats (**Chapter 6**). To this end, the systems pharmacology model (**Chapter 4**) was integrated with expressions to describe S1P receptor binding kinetics, internalization and sensitization. This enabled the application of the model to the prediction of the effect of siponimod, a S1P receptor agonist with different receptor subtype selectivity, on MAP and HR in rat.

In **Section IV**, the next steps towards characterization and prediction of cardiovascular drug effects in human are discussed (**Chapter 7**). In this chapter, the results of the presented

research are summarized. In addition, the future perspectives are presented. An ultimate application of the developed systems pharmacology model would be the anticipation of the clinical response based on preclinical data for newly developed compounds and, more specifically, for S1P receptor agonists, i.e. follow-up compounds of fingolimod. First, the translation of the systems pharmacology model is discussed. Thereafter, the translation of the effect of S1P receptor agonists is addressed.

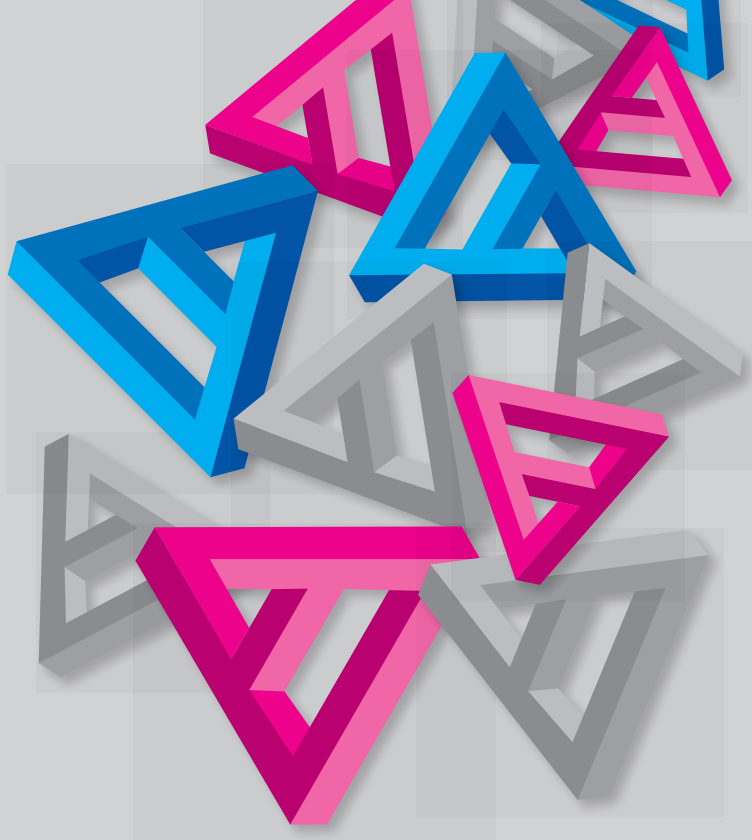
References

- Billich A, Bornancin F, Devay P, Mechtcheriakova D, Urtz N, Baumruker T (2003). Phosphorylation of the immunomodulatory drug FTY720 by sphingosine kinases. *J Biol Chem.*, 278, 47408-47415.
- Danhof M, de Jongh J, De Lange EC, Della Pasqua O, Ploeger BA, Voskuyl RA (2007). Mechanism-based pharmacokinetic-pharmacodynamic modeling: biophase distribution, receptor theory, and dynamical systems analysis. *Annu Rev Pharmacol Toxicol.*, 47, 357-400.
- Gergely P, Nuesslein-Hildesheim B, Guerini D, Brinkmann V, Traebert M, Bruns C, et al. (2012). The selective sphingosine 1-phosphate receptor modulator BAF312 redirects lymphocyte distribution and has species-specific effects on heart rate. *Br J Pharmacol.*, 167, 1035-1047.
- Kappos L, Antel J, Comi G, Montalban X, O'Connor P, Polman CH, et al. (2006). Oral fingolimod (FTY720) for relapsing multiple sclerosis. *N Engl J Med.*, 355, 1124-1140.
- Kappos L, Radue EW, O'Connor P, Polman C, Hohlfeld R, Calabresi P, et al. (2010). A placebo-controlled trial of oral fingolimod in relapsing multiple sclerosis. *N Engl J Med.*, 362, 387-401.
- Kharel Y, Lee S, Snyder AH, Sheasley-O'neill S L, Morris MA, Setiady Y, et al. (2005). Sphingosine kinase 2 is required for modulation of lymphocyte traffic by FTY720. *J Biol Chem.*, 280, 36865-36872.
- Kihara A, Igarashi Y (2008). Production and release of sphingosine 1-phosphate and the phosphorylated form of the immunomodulator FTY720. *Biochim Biophys Acta.*, 1781, 496-502.
- Levick JR (2003). An introduction to cardiovascular physiology.
- Ploeger BA, van der Graaf PH, Danhof M (2009). Incorporating receptor theory in mechanism-based pharmacokinetic-pharmacodynamic (PK-PD) modeling. *Drug Metab Pharmacokinet.*, 24, 3-15.
- Sager P, Heilbraun J, Turner JR, Gintant G, Geiger MJ, Kowey PR, et al. (2013). Assessment of drug-induced increases in blood pressure during drug development: report from the Cardiac Safety Research Consortium. *Am Heart J.*, 165, 477-488.
- Selmaj K, Li DK, Hartung HP, Hemmer B, Kappos L, Freedman MS, et al. (2013). Siponimod for patients with relapsing-remitting multiple sclerosis (BOLD): an adaptive, dose-ranging, randomised, phase 2 study. *Lancet Neurol.*, 12, 756-767.
- Snelder N, Ploeger BA, Luttringer O, Rigel DF, Webb RL, Feldman D, et al. (2013). PKPD modeling of the interrelationship between mean arterial blood pressure, cardiac output and total peripheral resistance in conscious rats. *Br J Pharmacol.*, 169, 1510-1524.



SECTION II

Development of a systems pharmacology model to characterize drug effects on the CVS



CHAPTER 3

PKPD modeling of the interrelationship between mean arterial blood pressure, cardiac output and total peripheral resistance in conscious rats

N. Snelder, B.A. Ploeger, O. Luttringer, D.F. Rigel, R.L. Webb, D. Feldman, F. Fu, M. Beil, L. Jin, D.R. Stanski and M. Danhof

British Journal of Pharmacology, 2013; 169(7): 1510-1524.

Summary

Background and purpose | The homeostatic control of arterial blood pressure is well understood with changes in blood pressure (BP) resulting from changes in cardiac output (CO) and/or total peripheral resistance (TPR). Drug effects on this interrelationship have not been analyzed in a mechanism-based and quantitative manner. This is important since it may constitute a basis for the prediction of drug effects on BP. This investigation aimed to describe, in a mechanism-based and quantitative manner, the effects of drugs with different mechanisms of action (MoA) on the interrelationship between BP, CO and TPR.

Experimental approach | The cardiovascular effects of 6 drugs with diverse MoA's, (amlodipine, fasudil, enalapril, propranolol, hydrochlorothiazide and prazosin) were characterized in spontaneously hypertensive rats. The rats were chronically instrumented with ascending aortic flow probes and/or aortic catheters/radiotransmitters for continuous recording of CO and/or BP. Data were analyzed in conjunction with independent information on the time course of drug concentration using a mechanism-based PKPD modeling approach.

Key results | By simultaneous analysis of the effects of 6 different compounds, the dynamics of the interrelationship between BP, CO and TPR, were quantified. System-specific parameters could be distinguished from drug-specific parameters indicating that the developed model is drug-independent.

Conclusions and Implications | A system-specific model characterizing the interrelationship between BP, CO and TPR has been obtained, which can be used to quantify and predict cardiovascular drug effects and to elucidate the MoA for novel compounds. Ultimately, the proposed PKPD model may allow prediction of BP effects in humans based on preclinical data.

Introduction

Persistent elevation of blood pressure (BP) is a risk factor for heart failure and is a leading cause of cardiovascular disease (Graham *et al.*, 2007). This risk continuously increases with the level of BP. Even small changes in BP, i.e. 10-20 mmHg, can have a relatively large influence (EMEA, 2004). BP regulation by the cardiovascular system (CVS) is well characterized, and the homeostatic principles of the CVS are thoroughly understood. Briefly, mean arterial pressure (MAP) equals the product of cardiac output (CO) and total peripheral resistance (TPR). This relationship has been well established for many years and is based on Ohm's Law, when applied to fluid flow. MAP is maintained within narrow limits by various regulatory feedback systems such as the renin-angiotensin-aldosterone system (RAAS) and the baroreflex system (Cleophas, 1998). In contrast to the detailed understanding of the physiologic regulation of BP, the mechanisms underlying the desired or undesired drug effects on BP are often less clear. This is a major drawback since a quantitative understanding of the pharmacological effects of (novel) drugs on BP control is pivotal with regard to drug efficacy and safety. Moreover, understanding these effects early in preclinical development could improve the anticipation of the magnitude of hemodynamic effects in humans.

To date no models exist that provide an integrated description of the effects of drugs on the interrelationship between MAP, CO and TPR. A mechanism-based pharmacokinetic-pharmacodynamic (PKPD) modeling approach is uniquely suited to provide quantitative insights in drug effects on the CVS since it clearly distinguishes drug-specific properties from system-specific properties (Danhof *et al.*, 2007; Ploeger *et al.*, 2009). This separation enables prediction and extrapolation of treatment effects to later stages of development using a translational modeling approach and, thereby, facilitating the drug development process and supporting compound selection (Danhof *et al.*, 2007).

Following the concepts proposed by Van Der Graaf *et al.* (1999) and Van Schaick *et al.* (1997), we hypothesize that by challenging the CVS with a variety of compounds the rate and feedback parameters of the CVS can be quantified and a clear distinction can be made between drug- and system- specific parameters that govern the pharmacological effect. A crucial factor is that the 'training set' of selected compounds acts on the same system, but with different target sites and time courses of effect. We have selected a training set of six antihypertensive compounds with different, but well described, effects on CO and/or TPR: enalapril, fasudil, amlodipine, prazosin, propranolol and hydrochlorothiazide (HCTZ) to challenge the CVS. The first four compounds have their primary effect on TPR; whereas the last two compounds have their primary effect on CO (Cleophas, 1998; Masumoto *et al.*, 2001; Ram *et al.*, 1981). An overview of the MoA of these compounds can be found

in Table 1. Besides an adequate selection of compounds, another important aspect of the experimental design is the selection of endpoints to monitor the drug effects on the CVS. Measuring BP is common practice, but it represents a ‘secondary’ pharmacodynamic parameter, as BP depends on both CO and TPR. At present, measuring CO has not been integrated into daily practice due to difficulties associated with invasive instrumentation procedures (Doursout *et al.*, 2001). Still, from a mechanistic point of view these data are pivotal for a quantitative understanding of the dynamics of the system, especially since, due to the homeostatic feedback mechanisms, the effects on the underlying parameters CO and TPR may be much larger than the effects on BP (Brands *et al.*, 2000). Finally, monitoring BP during the onset and offset of the drug effects provides the information

Table 1: Selected compounds to challenge the CVS with the aim of distinguishing system- from drug-specific parameters and their mechanism of action.

Compound	Class	Mechanism of action	Primary effect
enalapril	angiotensin-converting enzyme (ACE) inhibitor	ACE inhibitors competitively inhibit angiotensin I-converting enzyme, preventing the conversion of angiotensin I to angiotensin II, a potent vasoconstrictor that also stimulates release of aldosterone. Decreased levels of angiotensin II lead to decreased total peripheral resistance that is unassociated with reflex stimulation of the heart (Frohlich, 1989).	TPR
fasudil	rho-kinase inhibitor	Rho-kinase inhibits myosin light chain phosphatase activity and plays a key role in Ca ²⁺ sensitization and hypercontraction of vascular smooth muscle cells. Rho-kinase inhibitors decrease total peripheral resistance (Masumoto <i>et al.</i> , 2001).	TPR
amlodipine	calcium channel blocker	Amlodipine is a dihydropyridine that blocks voltage gated calcium channels and selectively inhibits Ca ²⁺ influx into vascular smooth muscle cells. Calcium antagonists act by decreasing total peripheral resistance to lower arterial pressure. As a consequence, reflex tachycardia, increased cardiac output, and increased plasma catecholamine and plasma renin activity are commonly seen, particularly with the initial dose and with short-acting dihydropyridines (Michalewicz and Messlerli, 1998; Perez-Reyes <i>et al.</i> , 2009)	TPR
prazosin	selective α_1 adrenergic receptor blocker	Prazosin is a quinazoline derivative that is a specific and selective competitive antagonist of α_1 adrenoceptors on vascular smooth muscle cells. Prazosin reduces BP by reducing elevated peripheral resistance and has little effect on cardiac function (Reid <i>et al.</i> , 1987).	TPR
propranolol	β -adrenergic receptor blocker	Propranolol is a non-selective beta blocker. It antagonizes the action of norepinephrine and epinephrine at all β -adrenergic receptors. Propranolol decreases cardiac output and heart rate with a reflex rise in total peripheral resistance (Ebadi, 2008).	CO
HCTZ	diuretic	Diuretics cause blood volume contraction and lower venous pressure, which decreases cardiac filling and, by the Frank-Starling mechanism, decreases ventricular stroke volume (Levick, 2003).	CO

needed to quantify the parameters of a dynamical system as this information can only be derived when the system is not in equilibrium. The offset phase can be especially informative as it provides information on the question if, and how fast, the system returns to its initial state.

In this investigation, we describe the development of a mechanism-based PKPD model that integrates a quantitative description of the physiology of the interrelationship between BP, CO and TPR and the pharmacological effects of cardiovascular drugs using data from preclinical experiments with a training set of six antihypertensive drugs. Ultimately, this quantitative pharmacology model may be used to predict clinical responses to novel pharmacologic agents.

Methods

Animals

Experiments were conducted on male, spontaneously hypertensive rats (SHR) (Taconic Farms, Germantown, NY) in accordance with approved Novartis Animal Care and Use Committee protocols and the Guide for the Care and Use of Laboratory Animals. At the time of study, rats' ages ranged from 21-45 wk and body weights ranged from 269-490 gram. Rats were housed on a 12-h light/dark cycle (light: 6 am to 6 pm) and were provided normal chow (Harlan Teklad 8604; Indianapolis, IN) and water ad libitum. The total number of rats used was 12 (10 in Study 1 and 2 in Study 2). All studies involving animals are reported in accordance with the ARRIVE guidelines for the reporting of experiments involving animals (Kilkenny et al., 2010; McGrath et al., 2010).

Experimental Procedures

The effects of a training set of compounds were obtained in two studies. In Study 1, detailed profiles of the time-course of the effects on MAP and HR were obtained after repeated dosing. In Study 2, information on the effect on MAP and CO was obtained following a single administration of a range of different doses. The combined information from both studies was crucial to the identification of the system-specific model characterizing the interrelationship between MAP, CO and TPR.

For the recording of BP (Study 1), a sterile gel-filled catheter/radiotransmitter (PA-C40, Data Sciences International, St. Paul, MN) was surgically implanted under isoflurane anesthesia into a femoral artery (catheter tip residing in the lower abdominal aorta) and a

subcutaneous pocket or directly into the abdominal aorta. Arterial BP was recorded for 15 sec every 10 min as detailed previously (Bazil *et al.*, 1993).

For BP and CO measurement (Study 2), rats were surgically instrumented with both an ascending aortic flow probe and a femoral arterial catheter/radiotransmitter (Figure 1). Rats were anesthetized with isoflurane, tracheally intubated, and artificially ventilated. A pre-calibrated 2.5 mm or 3.0 mm transit-time volumetric flow probe (2.5PS or 3PS, Transonic Systems Inc., Ithaca, NY) was placed around the ascending aorta via an incision at the right second intercostal space. The flow probe connector was tunneled subcutaneously to the mid-scapular region, where it was attached to the skin by a cutaneous button. The ribs were approximated with sutures, the chest was evacuated of air, and the chest wound closed in layers. Ketoprofen and penicillin G were administered for analgesia and infection prophylaxis. The rat was extubated and allowed to recover for approximately two weeks. Thereafter, the catheter/radiotransmitter was implanted as described above.

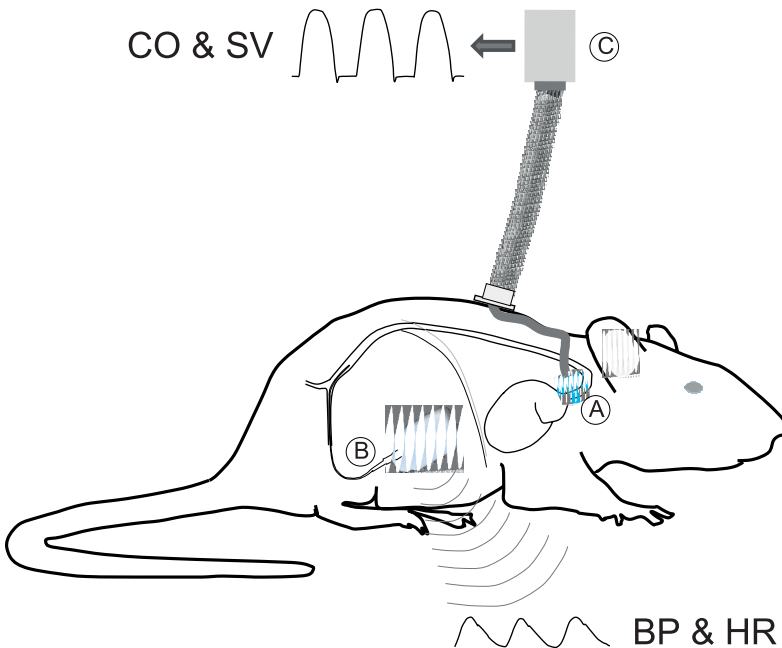


Figure 1: Experimental animal instrumentation. Rats in Study 2 were surgically instrumented with both an ascending aortic flow probe (A) and a femoral arterial catheter/radiotransmitter (B). CO was measured by connecting the flow probe to the flow meter via a cable and electrical swivel (C), which allowed the animal to remain fully ambulatory. MAP, heart rate, stroke volume, CO, and TPR were derived for all beats averaged over consecutive 2-min intervals.

Table 2: Study overview

Study	Measures	Study designs	Compound	Dose	Number of rats
1 Multiple dosing study	MAP	Days -1 - 0 : baseline (not included in analysis)	enalapril	30 mg/kg p.o	5
		Day 1 : baseline	fasudil	30 mg/kg p.o	5
		Days 2 - 3 : vehicle	amlodipine	10 mg/kg p.o	5
		Days 4 - 9 : active treatment (once daily) Days 10 - 15: washout	propranolol	1 mg/mL in drinking water	5
2 Single administrations of different doses on separate days	MAP, CO (and TPR)	Day 1: vehicle	amlodipine	0.3, 1, 3, 10 mg/kg p.o.	2
		Days 2-5: a different dose each day	prazosin	0.04, 0.2, 1, and 5 mg/kg p.o.	2
			HCTZ	0.1, 0.3, 1, 3 mg/kg p.o.	2

In Study 2, rats were used repeatedly for up to 6 months with sufficient washout between consecutive experiments. For continuously recording of cardiac output, a tether cable was attached to the flow probe connector and a flow meter (Model T402, Transonic Systems) via an electrical swivel (Dragonfly Research & Development, Ridgeley, WV). The digitized flow and telemetered pressure signals were analyzed by a Ponemah data acquisition system (Data Sciences International). MAP, heart rate, stroke volume, CO, and TPR were derived for all beats averaged over consecutive 2-min intervals.

Experimental design

Two different studies were conducted (Table 2). In Study 1, rats were treated once daily for 6 days with a single dose of drug (enalapril, fasudil, amlodipine or propranolol); SHR, n=5/drug. In Study 2, rats received single administrations of 4 different doses of each drug (amlodipine, prazosin or HCTZ) on 4 separate days.

In Study 1, rats were telemetered and after 2 weeks recovery, received 1 week of daily, oral dosing of saline (dosing training), then baseline data were collected during 3 days of no treatment. Subsequently, rats were treated with vehicle for 2 days prior to active treatment with active drug, which was administered once daily for 6 days at 11.00 am. Thereafter, washout data were collected during 6 days.

In Study 2, flow cables were connected to the flow probes by 7:00 am and disconnected after 5:00 pm. Baseline data were collected between 8:00 am and 10:00 am each day. Rats were dosed at 10:00 am and all data were continued to be collected until 5:00 pm. Thereafter, only MAP and HR data were captured until the flow probes were reconnected the next morning.

Compounds

In Study 1, enalapril maleate (Sigma-Aldrich, St. Louis, MO, USA, E6888), fasudil mono HCl (LC Laboratories, Woburn, MAF-4660), and amlodipine besylate (Lek pharmaceuticals d.d., Verovskova, Ljubljana, Slovenia) were formulated for administration at 5 ml/kg by oral gavage. (\pm)-Propranolol HCl (Sigma-Aldrich, P0884) was dissolved in drinking water at 1 mg/mL. Enalapril maleate, fasudil and amlodipine were homogenized in 0.5% methylcellulose (MC) (Fisher Scientific, Pittsburgh, PA).

In Study 2, prazosin HCl (Sigma-Aldrich, P7791), amlodipine besylate, and HCTZ (H2910, Sigma-Aldrich) were formulated for administration at 2 ml/kg by oral gavage. Prazosin and amlodipine were homogenized in 0.5% MC whereas HCTZ was dissolved in NaOH and diluted with filtered water (vehicle was water adjusted to pH 11).

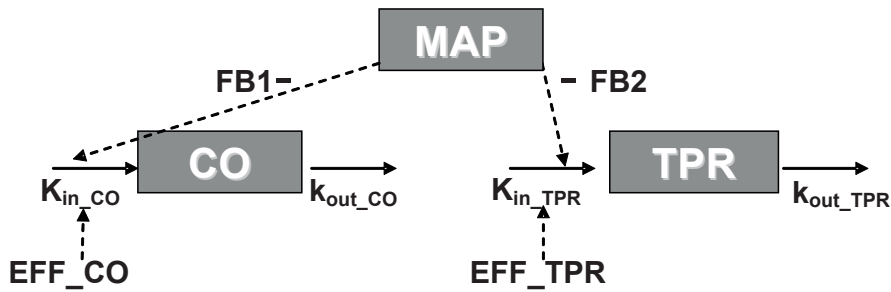


Figure 2: Cardiovascular model to describe the change in mean arterial BP after administration of different compounds acting on cardiac output (CO) and total peripheral resistance (TPR). MAP equals the product of CO and TPR ($\text{MAP}=\text{CO}\cdot\text{TPR}$). Effects on CO and TPR are described by two linked turnover equations. When MAP increases as a result of a stimulating effect on CO or TPR, the values of CO and TPR will decrease as a result of the action of the different feedback mechanisms regulating the CVS. The magnitude of feedback on CO and TPR is represented by *FB1* and *FB2*. $K_{\text{in_CO}}$ and $K_{\text{in_TPR}}$ represent the zero-order production rate constants of CO and TPR and $k_{\text{out_CO}}$ and $k_{\text{out_TPR}}$ represent the first-order dissipation rate constants of CO and TPR.

Data analysis

The interrelationship between MAP, CO and TPR is expressed in the formula: $\text{MAP}=\text{CO}\cdot\text{TPR}$ (Levick, 2003). On the basis of this relationship a model was developed to describe the time course of the effects on MAP, CO and TPR (Figure 2). The model was defined by two linked turnover equations involving CO and TPR (Equation 1). Turnover models are also called indirect response models and can be used to describe hysteresis, i.e. the delay between a perturbation and a response (Dayneka *et al.*, 1993). Examples of applications of this type of model can be found in the modeling of the homeostatic features of the release of endogenous compounds such as hormones or proteins (Gabrielsson and Weiner, 2000), or in the modeling of pharmacological responses such as drug-induced hypothermia (Zuideveld *et al.*, 2001).

$$\begin{aligned} \frac{d\text{CO}}{dt} &= K_{\text{in_CO}} \cdot (1 - \text{FB1} \cdot \text{MAP}) - k_{\text{out_CO}} \cdot \text{CO} \\ \frac{d\text{TPR}}{dt} &= K_{\text{in_TPR}} \cdot (1 - \text{FB2} \cdot \text{MAP}) - k_{\text{out_TPR}} \cdot \text{TPR} \end{aligned} \quad (1)$$

$$\text{MAP} = \text{CO} \cdot \text{TPR}$$

In these equations, $K_{\text{in_CO}}$ and $K_{\text{in_TPR}}$ represent the zero-order production rate constants and $k_{\text{out_CO}}$ and $k_{\text{out_TPR}}$ represent the first-order dissipation rate constants of CO and TPR respectively. These hypothetical production and dissipation rate constants reflect the rate of change in CO and TPR. *FB1* and *FB2* are constants representing the magnitude of the

negative feedback of MAP on CO and TPR. Following the criteria for statistical significance as specified in the section “Computation”, linear relationships between MAP and the production rate constants of CO and TPR were the most parsimonious relationships that captured the feedback mechanism adequately.

Initially, the circadian rhythm in BP was described as the sum of a maximum of 10 harmonics with different periods (Equation 2). The number of cosine functions was systematically reduced following the criteria for statistical significance (section “Computation”).

$$\text{MAP} = \text{CO} \cdot \text{TPR} + \sum_{n=1}^{10} \text{amp}_n \cdot \cos\left(\frac{n \cdot 2\pi \cdot (t + \text{hor})}{24}\right) \quad (2)$$

In this equation, *amp* represents the amplitude, *t* the time and *hor* the horizontal displacement over time. From a mechanistic point of view it is expected that the circadian rhythm in BP is a result of a circadian rhythm in CO and/or TPR as these are the primary drivers of MAP. However, as no 24 h measurements could be obtained for CO and TPR, the circadian rhythm was included in the model on MAP. Before pharmacological intervention (at baseline), MAP oscillates around its baseline value, which equals the product of the baseline values of CO and TPR (*BSL_CO* and *BSL_TPR*).

Before pharmacological intervention, the system is in steady state, or dynamic equilibrium in mathematical terminology, denoting that MAP, CO and TPR do not change over time and are equal to their baseline values. As is common practice for turnover models (Dayneka *et al.*, 1993) steady state conditions are described by the following equations (Equation 3) in which K_{in} is expressed in terms of *BSL* and k_{out} .

$$K_{in_CO} = \frac{-k_{out_CO} \cdot \text{BSL_CO}}{-1 + \text{FB1} \cdot \text{BSL_CO} \cdot \text{BSL_TPR}} \quad (3)$$

$$K_{in_TPR} = \frac{k_{out_TPR} \cdot (K_{in_CO} \cdot \text{FB1} \cdot \text{BSL_TPR} + k_{out_CO}) \cdot \text{BSL_TPR}}{K_{in_CO} \cdot \text{FB1} \cdot \text{BSL_TPR} + k_{out_CO} - \text{FB2} \cdot K_{in_CO} \cdot \text{BSL_TPR}}$$

In the experiments, TPR was derived (Equation 1) from the directly measured MAP and CO. In contrast, in the modeling, the baseline values of MAP (*BSL_MAP*) and *BSL_TPR* were estimated and *BSL_CO* was derived from these parameters for reasons of model stability. The system was functionally characterized by challenging the CVS with six different drugs with different mechanisms of action. Drug effects (*EFF*) were assumed to influence the production rates of either CO or TPR according to Equation 4.

$$\begin{aligned}\frac{dCO}{dt} &= K_{in_CO} \cdot (1 - FB1 \cdot MAP - EFF) - k_{out_CO} \cdot CO \\ \frac{dTPR}{dt} &= K_{in_TPR} \cdot (1 - FB2 \cdot MAP - EFF) - k_{out_TPR} \cdot TPR\end{aligned}\quad (4)$$

During pharmacological intervention TPR and CO can be calculated using Equation 5, where TPR_{ss} and CO_{ss} represent TPR and CO at steady state.

$$\begin{aligned}a &= k_{out_TPR} \cdot K_{in_CO} \cdot FB1 \\ b &= K_{in_TPR} \cdot K_{in_CO} \cdot FB2 + k_{out_TPR} \cdot k_{out_CO} + K_{in_TPR} \cdot K_{in_CO} \cdot FB1 \cdot (EFF - 1) \\ c &= K_{in_TPR} \cdot k_{out_CO} \cdot (EFF - 1) \\ TPR_{ss} &= \frac{(-b + \sqrt{b^2 - 4 \cdot a \cdot c})}{2 \cdot a} \\ CO_{ss} &= \frac{K_{in_CO}}{K_{in_CO} \cdot FB1 \cdot TPR_{ss} + k_{out_CO}}\end{aligned}\quad (5)$$

Linear, E_{max} and Sigmoid E_{max} models were evaluated to describe the drug effects on CO or TPR. The effects of all compounds were best described by E_{max} models (Equation 6):

$$EFF = \frac{E_{max} \cdot C(t)}{EC_{50} + C(t)}\quad (6)$$

In this equation, E_{max} and EC_{50} represent the maximum effect and the concentration resulting in a half-maximal effect, respectively, and C equals the drug concentration in plasma, which varies with time. Using the time course of the drug plasma concentrations, i.e., the pharmacokinetics (PK), rather than the dose or exposure, as a predictor for the pharmacodynamics (PD) has the advantage that it enables a better description of the time course of the drug effect. As the PK was not measured in these experiments, predicted plasma concentration *versus* time profiles were derived from the literature (Table 3). However, experimental conditions and formulations were different in these literature studies as compared to the experiments described in this paper. Therefore, for some compounds, PK parameters, e.g. the absorption rate, were estimated based on the known other PK parameters and the effect on BP (Table 3). In that case, PK and PD parameters were estimated simultaneously.

Table 3: Specification of the PK models to describe the pharmacokinetics of the six selected compounds, enalapril, fasudil, amlodipine, prazosin, propranolol and HCTZ to challenge the CVS. The PK models were based on literature models. The adjustments required to account for the differences in experimental conditions and formulations in these literature studies as compared to the experiments described in this paper are described in the “Comments” column.

Compound	PK model	Literature model	Comments	Species
enalapril	2-compartmental model with Michaelis-Menten elimination	(Lin <i>et al.</i> , 1988)	Data read out from the manuscript and a 2-compartmental model with Michaelis-Menten elimination was optimized in NONMEM	Sprague-Dawley rats
fasudil	1-compartmental model	(Ikegaki <i>et al.</i> , 2001): Non-compartmental analysis	K_a and lag-time were derived from the reported half-life, AUC and C_{max} using Berkeley Madonna	Wistar-Kyoto rats
amlodipine	1-compartmental model	(Stopher <i>et al.</i> , 1988): Non-compartmental analysis	K_a was derived from the reported half-life, V_d , F and T_{max} using Berkeley Madonna	Sprague-Dawley rats
prazosin	1-compartmental model	(Hamilton <i>et al.</i> , 1985): 1-compartmental model	CL , V_d ; scaled to rat using allometric scaling. K_a was estimated	New Zealand white rabbits
propranolol	3-compartmental model	(van Steeg <i>et al.</i> , 2010) 3-compartmental model	Absorption described as an infusion with a fixed duration of 24 h. K_a was estimated	Wistar-Kyoto rats
HCTZ	1-compartmental model	(Asdaq and Inamdar, 2009): 1-compartmental model	Reported: K_e , K_a , V_d , AUC $\rightarrow F$ was calculated from these parameters	Wistar-Kyoto rats

CL: clearance

V_d : distribution volume

K_e : elimination rate

K_a : absorption rate

F : bioavailability

Assumptions

The PK and PD models were based on the assumptions described in Table 4.

Table 4: Model assumptions

No.	Assumption	Clarification
1	Compounds selectively influence either CO or TPR.	Although some compounds may have a combined mechanism of action, i.e., have an effect on both CO and TPR, it was assumed that only including the direct/primary effect was sufficient for identifying the system. Therefore, any changes observed in the other parameters were assumed to be a result of the feedback (indirect/secondary effect).
2	All compounds influence the production rates of CO or TPR rather than the dissipation rates.	This assumption is based on the MoA of the selected compounds (Table 1).
3	For compounds for which the maximum effect was not observed, complete inhibition (i.e., $E_{max} = 1$) was assumed at infinite concentrations to ensure identification of the EC_{50} parameter.	To evaluate the validity of this assumption, the influence of different values of the E_{max} (i.e. $E_{max} = 0.8$) on the estimates of the system parameters was tested. This was done for one of the compounds (amlodipine).
4	The PK do not differ between rat strains and can be scaled between rabbit and rat on the basis of an allometric function (West <i>et al.</i> 1999; Anderson and Holford, 2009).	Although published information on the PK of all selected compounds was available, the PK was often evaluated in different rat strains and, for prazosin, even in a different species (rabbit).

3

Influence of the selection of compounds on the system-parameters

An adequate selection of compounds to challenge the functioning of the CVS was thought to be pivotal to successfully quantify the parameters of the CVS model. The compounds were selected to have different mechanisms and durations of action as this provides the maximum power to identify the model i.e. to distinguish system- and drug-specific parameters. Furthermore, we expected that a combined analysis of data from the six compounds would enable accurate and precise quantification of all system-parameters. To determine whether the obtained model is truly system specific, the influence of selectively omitting the data of one of the six compounds on the values of the system parameters was examined. If omission of these data does not lead to significant changes in these parameter estimates, this indicates that the model is truly drug-independent. In this analysis, the estimates of the system parameters obtained with these six sub-models were compared with those of the model based on all compounds.

System properties

Simulations were performed to investigate if the profiles of the time-course of the drug effect on MAP, CO and TPR are different for compounds with an influence on either CO or TPR. The typical profiles of MAP, CO and TPR *versus* time and of CO *versus* TPR are referred to as signature profiles. Pertinent differences in signature profiles for compounds with either an effect on CO or TPR indicate whether the drug-independent model can be applied to investigate the site of action (CO or TPR) of new compounds with an unknown MoA on BP. The responses on CO, TPR and MAP were simulated after triggering the model by enhancing TPR or inhibiting CO. The stimulation and inhibition functions were analyzed for a hypothetical constant rate infusion during 100 h to ensure that the drug effect is in steady state.

Computation

The data from Studies 1 and 2 were simultaneously analyzed using the non-linear mixed-effects modeling approach implemented in NONMEM (version 7.1.0; Icon Development Solutions, Ellicott City, Maryland, USA). The models were compiled using Digital Fortran (version 6.6C3, Compaq Computer Corporation, Houston, Texas) and executed on a PC equipped with an AMD Athlon 64 processor 3200+ under Windows XP. The results from the NONMEM analysis were subsequently analyzed using the statistical software package S-Plus for Windows (version 6.2 Professional, Insightful Corp., Seattle, USA). The simulations were carried out using Berkeley Madonna (version 8.3.5, Berkeley Madonna Inc., University of California). Parameters were estimated using the first order conditional estimation method with interaction between the two levels of stochastic effects (FOCE interaction). Random effects were included as exponential terms reflecting lognormal distributions of model parameters. The residual variability was explored with proportional and additive error models. Goodness-of-fit was determined using the minimum value of the objective function defined as minus twice the log-likelihood. For nested models, a decrease of 10.8 points in the objective function (MVOF) (corresponding to $p < 0.001$ in a chi-squared distribution) by adding an additional parameter was considered significant. The goodness-of fit was also investigated by visual inspection of the plots of individual predictions and the diagnostic plots of (weighted) residuals. In addition, a visual predictive check was performed in which the median and the 90% inter-quantile range of data simulated with the developed model were plotted together with the observations.

Results

Model development

The CVS model as expressed by Equations 1 - 6 and graphically represented in Figure 2 was used to simultaneously analyze the data from Studies 1 and 2. To characterize the circadian variation in the baseline, the amplitudes of 5 harmonics of the circadian rhythm could be quantified. $Amp_{1,}$ $amp_{3,}$ $amp_{4,}$ $amp_{5,}$ and $amp_{7,}$ were estimated to be 3.17, -2.03, 1.15, 1.63 and 1.28 mmHg, respectively. $Amp_{2,}$ $amp_{6,}$ $amp_{8,}$ $amp_{9,}$ and $amp_{10,}$ were fixed to 0 implying that these harmonics did not contribute to the circadian rhythm. In Study 1, BSL_MAP was allowed to vary between individual rats (inter-individual variability (IIV)). Study 2 provided information to estimate IIV on both BSL_MAP and BSL_TPR . The residual errors of MAP and TPR were best described by additive residual error models, whereas the residual error of CO was best described by a proportional error model. The dissipation rate of CO (k_{out_CO}) was found to be very high and could not be estimated with good precision. Therefore, this parameter was fixed to a high value (99 1/h) prior to estimating the other model parameters. The effects of all compounds were best described by E_{max} models. However, for amlodipine, fasudil, enalapril and HCTZ it was not possible to identify both drug effect parameters, E_{max} and EC_{50} , independently and with good precision. This was due to the fact that the maximum effect was not observed. Therefore, E_{max} was fixed to 1 for these compounds assuming that complete inhibition of K_{in} can be reached for infinite concentrations. For these compounds the drug effects could have also been described with a linear concentration-effect relationship. However, these models were not applicable as the inhibition of K_{in} exceeded 100% during parameter optimization. In addition, adding a sigmoidicity parameter to the E_{max} models did not result in an improvement in the goodness of fit for all compounds.

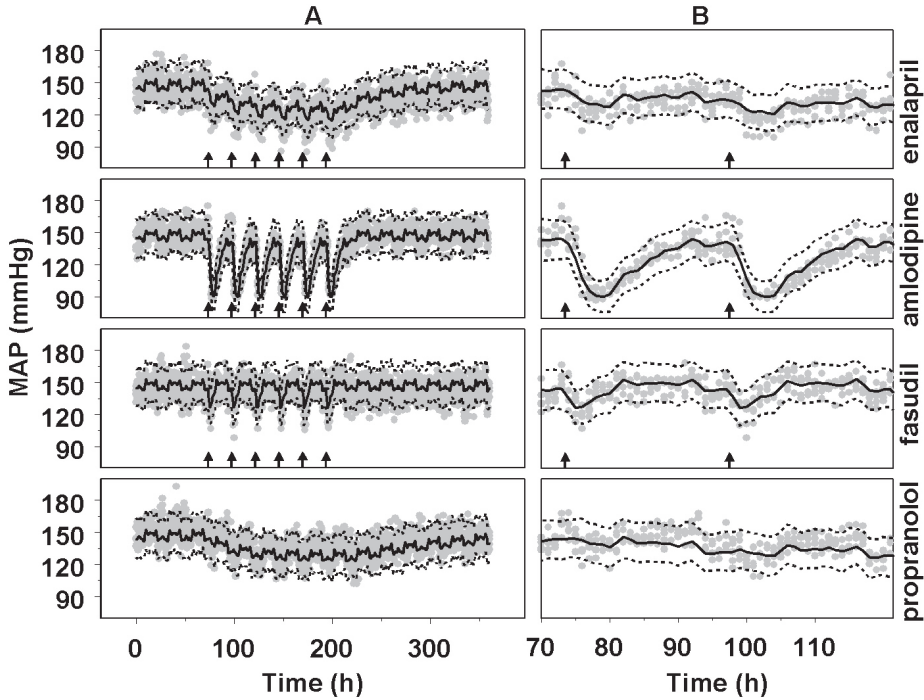


Figure 3: Visual predictive check of the description of the data from the repeated dosing Study 1 by the developed drug-independent CVS model. A) Full time scale; B) Expansion of the first two administrations of each drug. The grey dots represent the observations in SHR after administration of enalapril (30 mg/kg po) and amlodipine (10 mg/kg p.o.), fasudil (30 mg/kg p.o.) and propranolol (1 mg/mL in drinking water); $N=5$ SHR/drug. The continuous lines represent the predicted median and the dashed lines represent the predicted lower and upper limit of the 90% prediction interval. The arrows indicate the six daily administrations of each drug.

In general, the model adequately described the data (Figures 3 and 4). However, for HCTZ the effect of a dose of 1 mg/kg was under-predicted, but the effects of the higher and lower doses of HCTZ were adequately described (Figure 4b). This could indicate that the selected pharmacodynamic model, an E_{max} model with the value of E_{max} fixed to 1, was not optimal. However, this effect model could not be further optimized as the selected dose range was not sufficiently large to cover the complete range from no effect to maximal effect.

All system parameters could be estimated with good precision as all standard errors were less than 50% of the parameter estimates (Table 5). Fixing E_{max} to 1 for amlodipine, fasudil, enalapril and HCTZ did not have a significant influence on the estimates of the system parameters (results shown for amlodipine after fixing the E_{max} of amlodipine to

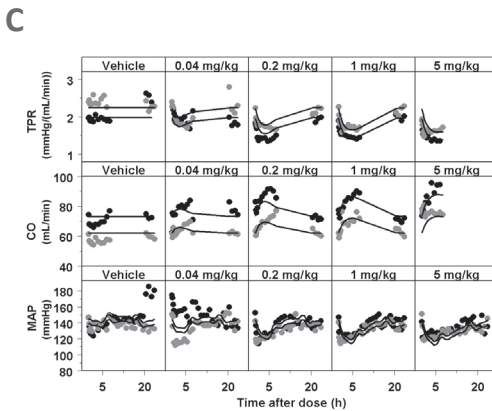
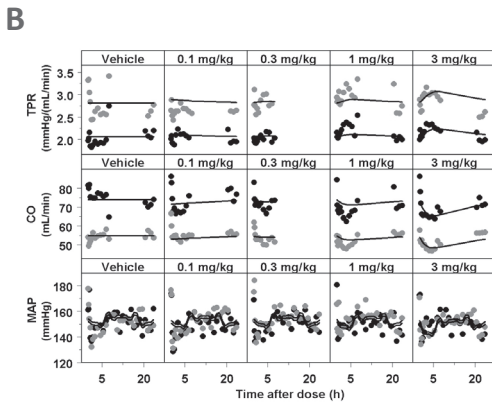
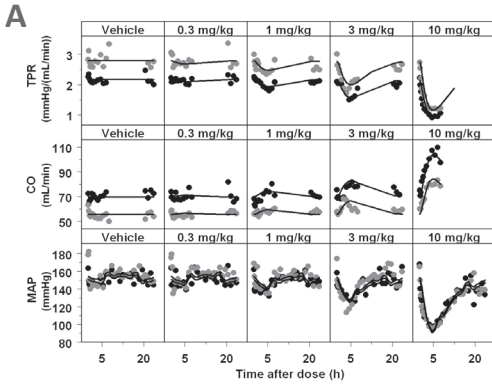


Figure 4: Description of the effects of amlodipine (plot A), HCTZ (plot B) and prazosin (plot C) on cardiac output (CO), total peripheral resistance (TPR) and mean arterial pressure (MAP) by the developed drug-independent CVS model. Data are from Study 2, in which vehicle and a different dose of amlodipine (0.3, 1, 3 and 10 mg/kg p.o.), HCTZ (0.1, 0.3, 1 and 3 mg/kg p.o.) or prazosin (0.04, 0.2, 1 and 5 mg/kg p.o.) was administered on separate days. *The grey and black dots represent the observations of two different rats. The continuous lines represent the individual prediction by the developed drug-independent CVS model after administering amlodipine.*

Table 5: The system parameter values from the drug-independent model to describe the CVS.

Parameter	Value	SE	CV	LLCI	ULCI	Value when E_{max} of amlodipine was fixed to 0.8 instead of 1
BSL_TPR (mmHG)/(mL/min)	2.32	0.132	5.69	2.06	2.58	2.32
BSL_MAP (mmHG)	147	1.38	0.939	144	150	147
kout_CO (1/h)	99 FIXED					
kout_TPR (1/h)	0.260	0.129	49.6	0.00716	0.513	0.308
SL1 (1/mmHG)	0.00378	0.000148	3.92	0.00349	0.00407	0.00382
SL2 (1/mmHG)	0.00492	0.00101	20.5	0.00294	0.00690	0.00468

SE: Standard error of parameter estimate

CV: Coefficient of variation

LLCI: Lower limit of 95 % confidence interval

ULCI: Upper limit of 95 % confidence interval

Table 6: The drug-dependent parameter values estimated by the drug-independent model to describe the CVS

Parameter	Value	SE	CV	LLCI	ULCI
Amlodipine					
E_{max}	1 fixed				
IC ₅₀ (ng/mL)	185	26.2	14.2	134	236
Fasudil					
E_{max}	1 fixed				
IC ₅₀ (ng/mL)	321	60.3	18.8	203	439
Propranolol					
E_{max}	0.335	0.0624	18.6	0.213	0.457
IC ₅₀ (ng/mL)	9.82	3.8	38.7	2.37	17.3
Enalapril					
E_{max}	1 fixed				
IC ₅₀ (ng/mL)	2410	373	15.5	1679	3141
HCTZ					
E_{max}	1 fixed				
IC ₅₀ (ng/mL)	12300	780	6.34	10771	13829
Prazosin					
E_{max}	0.213	0.0158	7.42	0.182	0.244
IC ₅₀ (ng/mL)	0.133	0.146	109.8	-0.15	0.4

SE: Standard error of parameter estimate

CV: Coefficient of variation

LLCI: Lower limit of 95 % confidence interval

ULCI: Upper limit of 95 % confidence interval

the arbitrarily selected value of 0.8 (instead of 1) in Table 5). In addition, all drug-specific parameters could be estimated with good precision, except for the EC_{50} of prazosin (CV: 110%) (Table 6). For this compound EC_{50} and E_{max} were estimated simultaneously. Fixing E_{max} to 1, as was done for four other compounds, resulted in a more precise estimate of the EC_{50} , but the goodness of fit was less good as indicated by a significant increase in the MVOF. All correlations between system-specific parameters were less than 0.95, except for the correlation between k_{out_TPR} and $FB2$ (-0.984).

Influence of the selection of compounds on the system-parameters

None of the parameters changed significantly when data of one of the six compounds were selectively omitted with the exception of the value of the parameter $FB1$, which was

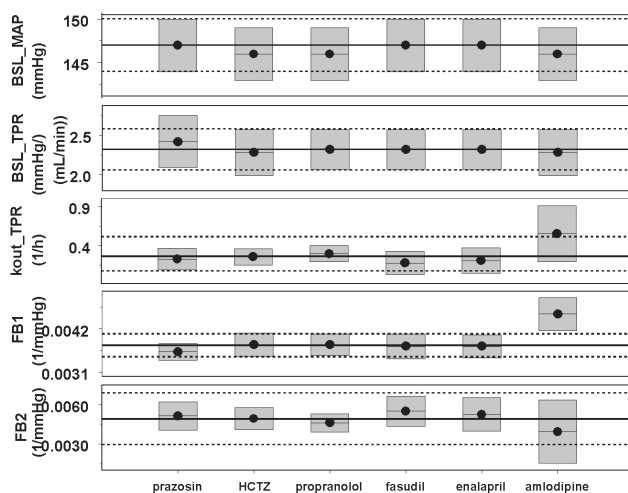


Figure 5: Evaluation of drug-independency of the developed CVS model

Six different compounds, prazosin, HCTZ, propranolol, fasudil, enalapril and amlodipine, were used to estimate the system parameters of the developed CVS model. To determine if the system parameters were truly drug-independent the model was re-evaluated omitting the different compounds one by one. *The continuous black lines represent the parameter estimates of the model including all compounds and the dashed lines represent the 90% confidence intervals around these parameter estimates. The black lines with a black dot and the grey boxes represent the parameter estimates and the 90% confidence intervals around these parameter estimates after omitting one of the compounds. When the grey boxes overlap with the area between the dotted lines, parameters are not significantly different and the model is independent of that compound. Therefore, the parameter estimate of $FB1$ is dependent on the presence of the amlodipine data.*

found to be dependent on the presence of the amlodipine data (Figure 5). *FB1* changed from 0.00379 (CI: 0.00348-0.00410) to 0.00454 (CI: 0.00418-0.00490) 1/mmHg.

System properties

Clear differences were found between the signature profiles of MAP, CO and TPR after simulating drug effects on CO and TPR. It was found that an increase in MAP can only be obtained by stimulating CO or TPR, and not by an overshoot of the feedback. Specifically, the simulation showed that inhibiting CO or TPR always results in a decrease in MAP, which demonstrates that feedback cannot be stronger than the primary effect (Figure 6).

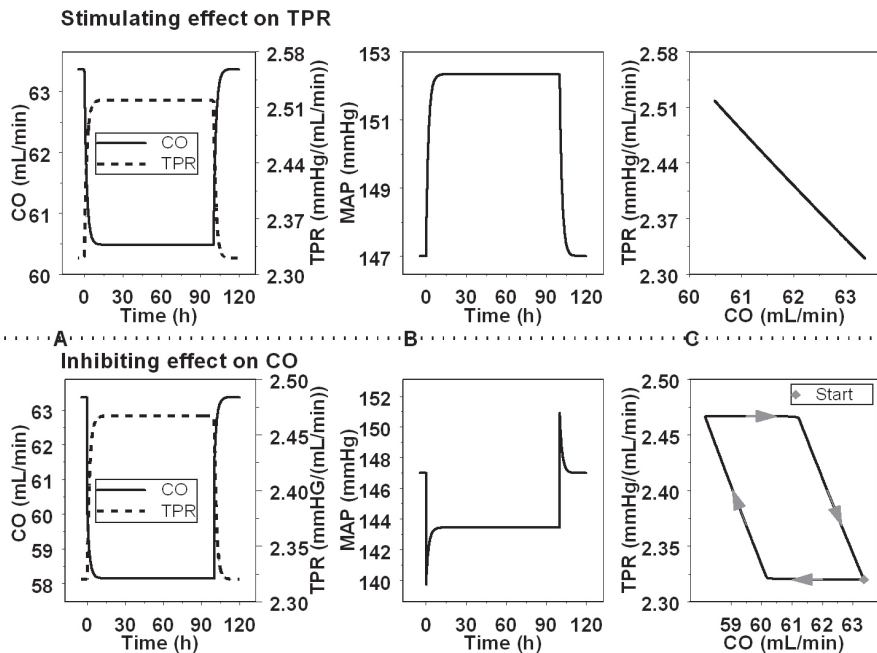


Figure 6: System properties of the CVS

The system properties of the CVS were investigated by simulating the response on CO, TPR and MAP after stimulating TPR (upper panel) or inhibiting CO (lower panel). Both perturbations result in visually comparable effects on CO and TPR (plot A). However, the response on MAP is in the opposite direction (plot B) indicating that the model can be used to identify the site of action. In addition, the hysteresis plot shows that an effect on TPR results in an immediate response on CO as a result of feedback, whereas, an effect on CO results in a delayed response on TPR as a result of feedback (plot C).

In addition, the delay in response was longer when the drug effect was on CO as compared to on TPR (Figure 6c).

Discussion

A mechanism-based PKPD model was developed to describe drug effects on the interrelationship between MAP, CO and TPR using data from preclinical experiments with a training set of six compounds with diverse effects on BP. Several models that describe the physiology of the CVS in great detail have been published, such as the Guyton and Coleman model (Guyton *et al.*, 1972), which has provided the basis for the understanding of long-term BP control (Montani and Van Vliet, 2009). However, to date no models exist that integrate a quantitative description of the physiology of the CVS and the effect of cardiovascular drugs on the relationship between MAP, CO and TPR except for a model that was postulated by Francheteau *et al.* (Francheteau *et al.*, 1993). This model provides a description of the effect of dihydropyridine drugs on the relationship between MAP, CO and TPR. As several key model parameters of the Francheteau model were not identifiable this is not a truly mechanism-based model in the sense that drug- and system-specific properties were indistinguishable. An important feature of a mechanism-based PKPD model is that both the drug-specific and the system-specific model parameters are identifiable and quantifiable on datasets from preclinical or clinical studies (Danhof *et al.*, 2007). This enables an adequate prediction of cardiovascular drug effects and becomes especially relevant when the interest is to also understand the variation between biological systems (i.e., between species) or between individuals (Danhof *et al.*, 2007). Therefore, the developed model is the first mechanism-based model that can be applied to describe the effect of cardiovascular drugs with different MoA's on the interrelationship between MAP, CO and TPR.

The developed model was based on a number of assumptions. One assumption was that only taking the primary/direct effects of the compounds on either CO or TPR into consideration was sufficient for identifying the system. For compounds like amlodipine and fasudil this assumption can be justified, since these compounds primarily influence TPR. The change in CO, which is observed after administration of these compounds, is thought to be a secondary effect, which is triggered by the feedback mechanisms of the CVS. For compounds like enalapril and propranolol, the MoA is less clear as these compounds influence both CO and TPR albeit with different magnitudes and on different timescales (Table 1). Since the aim of this research was to develop a drug-independent model to describe the functioning of CVS, an adequate description of the system, based on all drug effects,

was considered more important than the best possible description of the individual drug effects of the different compounds.

Another assumption was that all compounds influence the production rates rather than the dissipation rates of CO or TPR. This assumption was based on the MoA of the different compounds. The compounds that have a primary effect on TPR all influence smooth muscle cell contraction rather than causing relaxation. Therefore, assuming that contraction is equivalent to production, modeling of the drug effect on the production rather than the dissipation rate makes mechanistically sense. The two compounds that influence CO, HCTZ and propranolol, have quite different MoA's (Table 1). HCTZ, a diuretic, decreases ventricular stroke volume by decreasing cardiac filling. On the other hand, propranolol reduces sympathetically mediated stimulation of left ventricular contractility and heart rate. Therefore, from a mechanistic point of view, both compounds are thought to also influence the production rather than the dissipation rates. As the MoA of HCTZ and propranolol are quite different, it might be expected that the delay in response, as reflected by k_{out_CO} , would be different for these compounds. However, for both compounds, this delay was too short to quantify with good precision. Therefore, both the effects of HCTZ and propranolol could be adequately described by the model with k_{out_CO} fixed to a high value of 99 1/h. Although k_{out_CO} could not be quantified, the data did contain information about the rate of change in CO being high as fixing this parameter to a lower value resulted in bias in the description of the HCTZ and propranolol data (results not shown). The exact value of k_{out_CO} is only relevant when the interest is in the effect on shorter time scales than investigated in the current studies, i.e. seconds instead of minutes or hours. In addition, in theory, adding one or more compounds with an effect on the dissipation rate would provide additional information for identification of the system parameters. However, from a mechanistic point of view it is difficult to find compounds with an effect on the k_{out} of CO or TPR. For example, enalapril influences the k_{out} of angiotensin I as it inhibits angiotensin-I-converting enzyme. This effect however translates into an inhibition of the kin of angiotensin II which in turn leads to vasodilation. The current model therefore describes the effect of enalapril on the K_{in} of TPR. Moreover, from a data driven point of view including compounds with an effect on k_{out} will only add additional information for quantification of the system parameters when the selected dose range is large enough to reach the maximum effect (Sharma and Jusko, 1996; 1998). In *in vivo* investigations however attainment of the maximum drug effect is not always feasible for safety reasons. Moreover, in situations where rapid adaptation occurs, it may be impossible experimentally to reach the E_{max} (Porchet *et al.*, 1988). An interesting feature of the developed model is that it can be extended to more detailed levels without having to change the structure of the model. For example, the system can be described in more detail by parsing CO into

heart rate and stroke volume. In addition, including more information on the different feedback mechanisms could lead to a model that distinguishes the effects of different classes of antihypertensive drugs in more detail. The feedback mechanisms currently included in the model are likely to reflect the acute compensatory mechanisms (such as the baroreceptor reflex) better than the long term compensatory mechanisms (such as the renin-angiotensin-aldosterone system (RAAS)) as the baroreflex system is active within minutes to hours to days whereas the RAAS is active within hours to days/weeks. To evaluate if the model is predictive for long-term effects on the CVS long-term studies of days or weeks with CO measurements are required.

The assumptions made regarding the use of PK models derived from published results may have a large impact on the PK profiles. Therefore, the PK models were descriptive and the PK and drug-specific PD parameters may not represent “true” values. Therefore, these estimates should only be interpreted in the context of this model. This was considered acceptable as system-specific parameters, which are of primary interest in this research, are considerably less sensitive to changes in PK compared to drug-specific parameters. This is explained by the fact that drug-specific parameters are directly dependent on the PK of a specific drug, whereas the values of system-specific parameters are determined by the data of all compounds.

Beforehand it was hypothesized that two aspects of the experimental design were pivotal to successfully quantify the parameters of the CVS model: i) the selection of the training set of compounds to challenge the functioning of the CVS and ii) measuring both MAP and CO during the on- and offset phases of the drug effects. The correlations between some drug- and system-specific parameters were high (results not shown). However, evaluating if the model was indeed drug independent has demonstrated that the selected combination of compounds was adequate to develop a drug-independent model as only the parameter *FB1*, i.e. 1 of the 5 system-specific parameters, changed when the data of 1 of the 6 compounds (amlodipine) were omitted (Figure 5). To evaluate the importance of measuring both MAP and CO during the on- and offset phases of the drug effects, a retrospective sensitivity analysis was performed, using the parameter estimates of the developed model (Appendix). This sensitivity analysis demonstrated that measuring both MAP and CO during the on- and offset phase provided the pertinent information to quantify the system parameters. This is in agreement with the good precision of the estimates of all system-specific parameters. However, the values of $k_{out-TPR}$ and *FB2* were strongly correlated (-0.984) indicating that there was not enough information to estimate both parameters independently. This was confirmed by the sensitivity analysis, which showed that both parameters are most sensitive to the data collected during approximately the

same period after drug administration and during the offset phase of the drug effects for compounds influencing TPR (Appendix: Figure A). For compounds that influence CO these peaks are more distinct (results not shown), which indicates that the information to estimate these parameters independently was mainly provided by the compounds with an effect on CO. In the current research, only two compounds were included with a primary effect on CO, i.e., propranolol and HCTZ, and CO was measured only after administration of HCTZ. To distinguish these parameters, detailed MAP and CO measurements from more compounds with an influence on CO would be required. This should be taken into consideration when the model is applied for simulation purposes. Measuring CO provided insight into the magnitude of the counteracting effects on TPR and CO underlying the effect on BP. Since MAP is the primary regulated hemodynamic variable, drug effects on TPR and CO were disproportionately greater than those reflected by MAP alone. This indicates that a small observed pharmacologic effect on MAP may mask much larger therapeutic benefits or, conversely, an increased risk of cardiovascular disease. Based on estimates of the residual error, the model is qualified to distinguish changes in MAP, CO and TPR larger than 7.6 mmHg, 4.3 ml/min and 0.5 mmHg/(ml/min), respectively, from noise. This indicates that the model can be used to identify clinically relevant changes in BP. In conclusion, the rigorous experimental design was adequate to provide the data to describe the interrelationship between MAP, CO and TPR in a quantitative and mechanism-based manner.

The developed CVS model can be applied to estimate drug-specific parameters for new compounds, but this requires accurate and precise description of the pharmacokinetics. Recently, novel approaches have been proposed to accurately characterize pharmacokinetics without influencing the pharmacodynamics in pre-clinical PKPD investigations, e.g. the PK can be measured after completion of the pharmacodynamic part of the study (Bender *et al.*, 2009) or the PK and PD can be measured on different days during the study (Viberg *et al.*, 2012). In addition, the developed model can be applied to identify the site of action of new compounds influencing MAP through an unknown MoA, as it was shown in a simulation experiment that distinct differences exist between the signature profiles of compounds with an effect on CO or TPR (Figure 6). In this context, the developed model provides key insights to support drug development, i.e. to learn about the underlying MoA of compounds with desired or undesired effects on BP. The model can also be applied to test hypotheses, e.g., hypotheses on multiple sites of action can be evaluated by including drug-effects on multiple parameters in the model. It should be noted that the identified set of system parameters is specific for spontaneously hypertensive rats. Drug effects on MAP, CO and TPR may vary considerably in other (normotensive) rat strains due to physiological differences (Pinto *et al.*, 1998). Consequently, applications of the

developed model, using the identified set of system parameters, are limited to this rat strain. However, an advantage of a mechanism-based model is that it allows accurate extrapolation between different rat strains and from one species to another (Danhof *et al.*, 2008; Ploeger, 2009) as the structure of the model is expected to be the same in all species. Therefore, an ultimate application of the developed drug-independent model would be to facilitate the anticipation of the clinical response based on preclinical data for newly developed compounds. Before our model can be applied for that purpose, the predictability of long-term blood pressure effect should be evaluated and the model should be scaled to human and validated on human MAP and CO measurements.

References

- Anderson BJ, Holford NH (2009). "Mechanistic basis of using body size and maturation to predict clearance in humans." *Drug Metab Pharmacokinet.* 24(1): 25-36.
- Asdaq SM, Inamdar MN (2009). "The potential for interaction of hydrochlorothiazide with garlic inrats." *Chem Biol Interact.* 181(3): 472-479.
- Bender G, Gosset J, Florian J, Tan K, Field M, Marshall S *et al.* (2009). "Population pharmacokinetic model of the pregabalin-sildenafil interaction in rats: application of simulation to preclinical PK-PD study design." *Pharm Res.* 26(10):2259-69.
- Bazil MK, Krulan C, Webb RL (1993). "Telemetric monitoring of cardiovascular parameters in conscious spontaneously hypertensive rats." *J Cardiovasc Pharmacol.*, 22(6): 897-905
- Cleophas TJ (1998). "Mechanisms offsetting the beneficial effects of antihypertensive drugs: a problem increasingly considered but incompletely understood." *Am J Ther* 5(6):413-419.
- Danhof M, de Jongh J, De Lange EC, Della Pasqua O, Ploeger BA, Voskuyl RA (2007). "Mechanism-based pharmacokinetic-pharmacodynamic modeling: biophase distribution, receptor theory, and dynamical systems analysis." *Annu Rev Pharmacol Toxicol.* 47: 357-400.
- Danhof M, de Lange EC, Della Pasqua OE, Ploeger BA, Voskuyl RA (2008). "Mechanism-based pharmacokinetic-pharmacodynamic (PK-PD) modeling in translational drug research." *Trends Pharmacol Sci.* 29(4): 186-191.
- Dayneka NL, Garg V, Jusko WJ (1993). "Comparison of four basic models of indirect pharmacodynamic responses." *J Pharmacokinet Biopharm.* 21(4): 457-478.
- Doursout MF, Wouters P, Kashimoto S, Hartley CJ, Rabinovitz R, Chelly JE (2001). "Measurement of cardiac function in conscious rats." *Ultrasound Med Biol.* 27(2): 195-202.
- Brands MW, Fitzgerald SM, Hewitt WH, Hailman AE (2000). "Decreased cardiac output at the onset of diabetes: renal mechanisms and peripheral vasoconstriction." *Am J Physiol Endocrinol Metab.* 278(5): E917-924.
- Ebadi M (2008). *Desk Reference of Clinical Pharmacology.* Taylor & Francis Group: Boca Raton Florida.
- EMA (2004). "EMA guideline: note for guidance on clinical investigation of medicinal products in the treatment of hypertension." CPMP/EWP/238/95 Rev. 2.
- Francheteau P, Steimer JL, Merdjan H, Guerret M, Dubray C (1993). "A mathematical model for dynamics of cardiovascular drug action: application to intravenous dihydropyridines in healthy volunteers." *J Pharmacokinet Biopharm.* 21(5): 489-514.
- Frohlich ED (1989). Angiotensin converting enzyme inhibitors. Present and future. *Hypertension*, 13, 1125-30.
- Gabrielsson J, Weiner D. (2000). "Pharmacokinetic/Pharmacodynamic Data Analysis: Concepts and Applications", 3rd eds. Stockholm.
- Graham I, Atar D, Borch-Johnsen K, Boysen G, Burell G, Cifkova R *et al.* (2007). "European guidelines on cardiovascular disease prevention in clinical practice: executive summary." *Eur Heart J* 28: 2375-2414.
- Guyton AC, Coleman TG, Granger HJ (1972). "Circulation: overall regulation." *Ann Rev Physiol* 34: 13-46.
- Hamilton CA, Reid JL, Vincent J (1985). "Pharmacokinetic and pharmacodynamic studies with two alpha-adrenoceptor antagonists, doxazosin and prazosin in the rabbit." *Br J Pharmacol.* 86(1): 79-87.
- Ikegaki I., Hattori T., Yamaguchi T., Sasaki Y., Satoh S.I., Asano T *et al.* (2001). "Involvement of Rho-kinase in vascular remodeling caused by long-term inhibition of nitric oxide synthesis in rats." *Eur J Pharmacol.* 427(1): 69-75.
- Levick JR (2003). *An introduction to cardiovascular physiology.* Hodder Arnold Publishers: London (book)
- Lin JH, Chen IW, Ulm EH, Duggan DE (1988). "Differential renal handling of angiotensin-converting enzyme inhibitors enalaprilat and lisinopril in rats." *Drug Metab Dispos.* 16(3): 392-96.
- Masumoto A, Hirooka Y, Shimokawa H, Hironaga K, Setoguchi S, Takeshita A (2001). "Possible involvement of Rho-kinase in the pathogenesis of hypertension in humans." *Hypertension.* 38(6): 1307-1310.
- Michalewicz L, Messerli FH (1997). Cardiac effects of calcium antagonists in systemic hypertension. *Am J Cardiol.*, 79, 39-46; discussion 47-48.
- Montani JP, Van Vliet BN (2009). "Understanding the contribution of Guyton's large circulatory model to

- long-term control of arterial pressure." *Exp Physiol.* 94(4): 382-888.
- Perez-Reyes E, Van Deusen AL & Vitko I (2009). Molecular pharmacology of human Cav3.2 T-type Ca²⁺ channels: block by antihypertensives, antiarrhythmics, and their analogs. *J Pharmacol Exp Ther.*, 328, 621-627.
- Pinto YM, Paul M, Ganten D (1998). "Lessons from rat models of hypertension: from Goldblatt to genetic engineering." *Cardiovasc Res.* 39(1): 77-88
- Ploeger BA, van der Graaf PH, Danhof M (2009). "Incorporating receptor theory in mechanism-based pharmacokinetic-pharmacodynamic (PK-PD) modeling." *Drug Metab Pharmacokinet.* 24(1): 3-15.
- Porchet HC, Benowitz NL, Sheiner LB (1988). "Pharmacodynamic model of tolerance: application to nicotine." *J Pharmacol Exp Ther.* 244(1): 231-236.
- Ram CV, Anderson RJ, Hart GR, Crumpler CP (1981). "Alpha adrenergic blockade by prazosin in therapy of essential hypertension." *Clin Pharmacol Ther.* 29(6): 719-722.
- Reid JL, Elliott HL, Vincent J, Meredith PA (1987). Clinical pharmacology of selective alpha blockers. Hemodynamics and effects on lipid levels. *Am J Med.*, 82, 15-20.
- Sharma A, Jusko WJ (1996). "Characterization of four basic models of indirect pharmacodynamic responses." *J Pharmacokinetic Biopharm.* 24(6): 611-635.
- Sharma A, Jusko WJ (1998). "Characteristics of indirect pharmacodynamic models and applications to clinical drug responses." *Br J Clin Pharmacol.* 45(3):229-239.
- Stopher DA, Beresford AP, Macrae PV, Humphrey MJ, (1988). "The metabolism and pharmacokinetics of amlodipine in humans and animals." *J Cardiovasc Pharmacol.* 12 Suppl 7: S55-59.
- Van der Graaf PH, Van Schaick EA, Visser SA, De Greef HJ, Ijzerman AP, Danhof M. (1999). "Mechanism-based pharmacokinetic-pharmacodynamic modeling of antipolytic effects of adenosine A(1) receptor agonists in rats: prediction of tissue-dependent efficacy in vivo." *J Pharmacol Exp Ther.* 290(2): 702-709.
- Van Schaick EA, Mathot RA, Gubbens-Stibbe JM, Langemeijer MW, Roelen HC, Ijzerman AP *et al.* (1997). "8-Alkylamino-substituted analogs of N⁶-cyclopentyladenosine are partial agonists for the cardiovascular adenosine A1 receptors in vivo." *J Pharmacol Exp Ther.* 283(2): 800-808.
- Van Steeg TJ, Krekels EH, Freijer J, Danhof M, de Lange EC (2010). "Effect of altered AGP plasma binding on heart rate changes by S(-)-propranolol in rats using mechanism-based estimations of in vivo receptor affinity (K(B,vivo))." *J Pharm Sci.* 99(5): 2511-2520.
- Viberg A, Martino G, Lessard E, Laird JM (2012). "Evaluation of an innovative population pharmacokinetic-based design for behavioral pharmacodynamic endpoints." *AAPS J.* 14(4): 657-663.
- West GB, Brown JH, Enquist BJ (1999). "The fourth dimension of life: fractal geometry and allometric scaling of organisms." *Science.* 284(5420):1677-1679.
- Zuideveld KP, Maas HJ, Treijtel N, Hulshof J, van der Graaf PH, Peletier LA *et al.* (2001), "A set-point model with oscillatory behavior predicts the time course of 8-OH-DPAT-induced hypothermia." *Am J Physiol Regul Integr Comp Physiol.* 281(6): R2059-2071

Abbreviations

Amp	Amplitude
BP	Blood pressure
<i>BSL_CO</i>	Baseline value of cardiac output
<i>BSL_MAP</i>	Baseline value of mean arterial pressure
<i>BSL_TPR</i>	Baseline value of total peripheral resistance
C	drug concentration in plasma
CO	Cardiac output
CVS	Cardiovascular system
E_{max}	Maximum effect
EC_{50}	Concentration resulting in a half-maximal effect
<i>FB1</i>	negative feedback of mean arterial pressure on cardiac output
<i>FB2</i>	negative feedback of mean arterial pressure on total peripheral resistance
HCTZ	Hydrochlorothiazide
HOR	Horizontal displacement
IIV	Inter-individual variability
K_{in_CO}	Zero-order production rate constant of cardiac output
K_{in_TPR}	Zero-order production rate constant of total peripheral resistance
k_{out_CO}	First-order dissipation rate constant of cardiac output
k_{out_TPR}	First-order dissipation rate constant of total peripheral resistance
MAP	Mean arterial pressure
MC	Methylcellulose
MoA	Mechanisms of action
MVOF	Minimum value of the objective function
PD	Pharmacodynamics
PK	Pharmacokinetics
PKPD	Pharmacokinetic-pharmacodynamic
RAAS	Renin-angiotensin-aldosterone system
SHR	Spontaneously hypertensive rats
T	Time
TPR	Total peripheral resistance

Appendix: Sensitivity analysis, evaluation of the experimental design

An adequate experimental design was thought to be pivotal to distinguish drug- from system-specific parameters in this investigation. By showing how the dynamic behavior of the system responds to changes in parameter values, a sensitivity analysis enables identification of the part of the experimental protocol that provides the pertinent information to quantify the parameters and to distinguish one parameter from another. Using the parameter estimates of the developed model, a retrospective parameter sensitivity analysis was performed in Berkeley Madonna (version 8.3.5, Berkeley Madonna Inc., University of California) to determine how “sensitive” the developed model is to changes in the values of the parameters of the model.

First a simulation was performed with all system parameters fixed at their estimated values ($S(t, x_0)$), while assuming an inhibiting drug effect on TPR during a constant drug infusion of 100 h to ensure that the drug effect is in steady state. Subsequently, simulations were performed after 0.1% increments in the system parameters (0.1% is the standard in Berkeley Madonna) ($S(t, x)$). Finally, for each parameter, the sensitivity ($S(t)$) was calculated according to Equation A.1.

$$S(t) = x_0 \frac{\partial S(t, x)}{\partial x} \cong \frac{S(t, x) - S(t, x_0)}{(x - x_0)/x_0} = \frac{S(t, x) - S(t, x_0)}{0.1\%} \quad (\text{A.1})$$

The sensitivity ($S(t)$) in change from baseline for MAP, CO and TPR was evaluated for all system parameters (Figure A.1). This figure shows that the on- and offset phases of the drug effect contained complementary information as in both phases the peaks of the values of the different parameters of the pharmacodynamic system (BSL_TPR, BSL_MAP, $k_{\text{out_TPR}}$, FB1 and FB2) occurred at different time points relative to each other. In addition, the three biomarkers of the CVS, MAP, CO and TPR also contained complementary information regarding the dynamics of the system. For example, the peaks of the two feedback parameters FB1 and FB2 occurred almost simultaneously when examining the sensitivity in MAP, whereas when looking at the sensitivity in CO and TPR the peaks occurred relatively later. Therefore, measuring CO provided the pertinent information to distinguish these parameters.

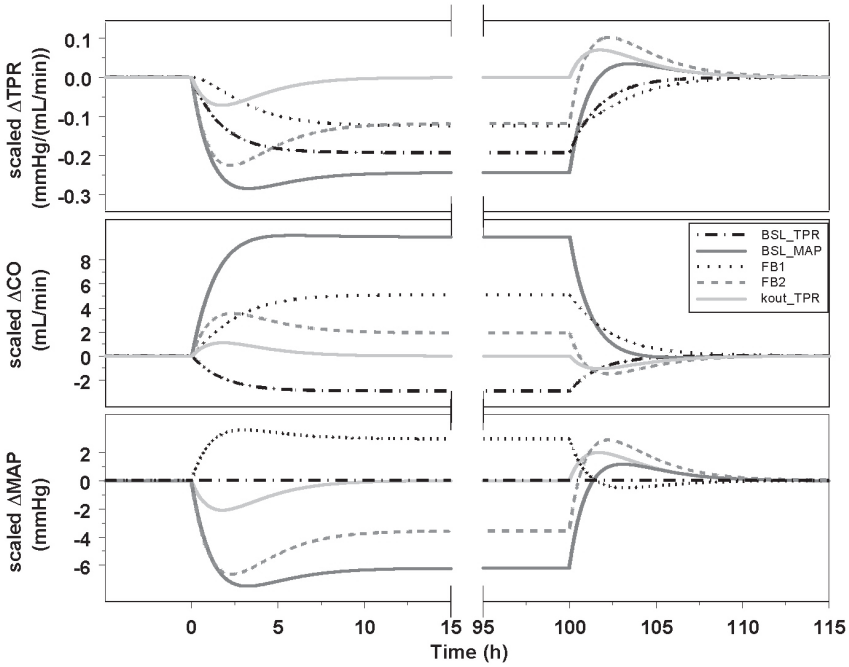
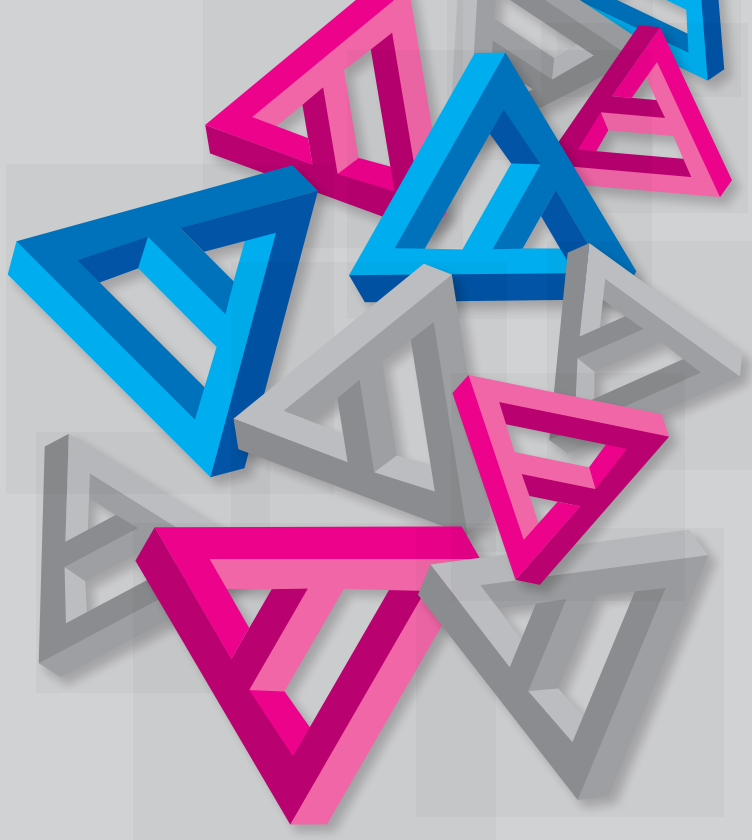


Figure A: Sensitivity analysis

Influence of a 0.1% increase in the values of the system parameters of the drug-independent model (BSL_TPR , BSL_MAP , k_{out_TPR} , $FB1$ and $FB2$) on the dynamic behavior of the CVS parameters MAP , CO and TPR . In this sensitivity analysis an inhibiting drug effect (an on/off response; constant infusion during 100 h) on TPR was simulated.



CHAPTER 4

Drug effects on the cardiovascular system in conscious rats – separating cardiac output into heart rate and stroke volume using PKPD modeling

N. Snelder, B.A. Ploeger, O. Luttringer, D.F. Rigel, F. Fu, M. Beil, D.R. Stanski and M. Danhof

British Journal of Pharmacology; Submitted

Summary

Background and purpose | Previously, a systems pharmacology model was developed characterizing drug effects on the interrelationship between mean arterial pressure (MAP), cardiac output (CO) and total peripheral resistance (TPR). The present investigation aims to 1) extend the previously developed model by parsing CO into heart rate (HR) and stroke volume (SV) and 2) to evaluate if the mechanism of action (MoA) of new compounds can be elucidated using HR and MAP measurements only.

Experimental approach | The cardiovascular effects of 8 drugs with diverse MoA's (amiloride, amlodipine, atropine, enalapril, fasudil, hydrochlorothiazide, prazosin and propranolol) were characterized in spontaneously hypertensive rats (SHR) and in normotensive Wistar-Kyoto (WKY) rats following single administrations of a range of different doses. The rats were instrumented with ascending aortic flow probes and aortic catheters/radiotransmitters for continuous recording of MAP, HR and CO for the full duration of the experiments. Data were analyzed in conjunction with independent information on the time course of the drug concentration following a mechanism-based pharmacokinetic-pharmacodynamic modeling approach.

Key results | The extended model, which quantifies the changes in TPR, HR and SV with negative feedback through MAP, adequately described the cardiovascular effects of the drugs while accounting for circadian variation and the influence of handling.

Conclusions and Implications | A systems pharmacology model characterizing the interrelationship between MAP, CO, HR, SV and TPR has been obtained in hypertensive and normotensive rats. The extended model can be used to quantify the dynamic changes in the CVS and elucidate the MoA for novel compounds, with one site of action, using HR and MAP measurements only. The questions whether the model can also be applied for compounds with a more complex mechanism of action remains to be established.

Introduction

Blood pressure (BP) and heart rate (HR) are important parameters in the safety evaluation of novel drugs for a wide variety of disorders (Sudano, 2012, Gasparyan, 2012; Cardinale, 2013; Guth, 2007). Although BP and HR are usually measured simultaneously, it is common practice to quantify drug effects on these hemodynamic parameters independently resulting in two separate dose/concentration-effect relationships. However, this approach disregards the interrelationship between BP and HR. As this interrelationship is complex due to the feedback mechanisms regulating the cardiovascular system (CVS), interpretation of the separate relationships can be challenging and ambiguous. With the physiology of the CVS being well understood, an integrated analysis could result in improved understanding of cardiovascular effects and the underlying mechanism of action (MoA). Moreover, it has the advantage that a single dose/concentration-effect relationship can be established. Previously, it has been demonstrated that drug effects on the interrelationship between mean arterial pressure (MAP), cardiac output (CO) and total peripheral resistance (TPR) can be quantified using a systems pharmacology model (Snelder *et al.*, 2013a). As CO equals the product of HR and stroke volume (SV) it is anticipated that this model can be extended to a more detailed level by parsing CO into HR and SV with the advantage that drug effects on MAP, CO, HR, SV and TPR can be characterized simultaneously. It has been demonstrated that the previously developed CVS model (basic CVS model) can be applied to elucidate the MoA of novel compounds (Snelder *et al.*, 2013a). This requires continuous recording of CO. However, measuring CO has not been integrated into daily practice due to the challenges associated with invasive instrumentation procedures (Doursout *et al.*, 2001). Therefore, it is of interest to investigate if the proposed extended CVS model can be applied to elucidate the MoA of new compounds using HR and MAP measurements only.

The basic CVS model is specific for spontaneously hypertensive rats (SHR). Thus modeling of the hemodynamic effects in normotensive rats has not been achieved. This is of interest since the prediction of hemodynamic side effects is also important for normotensive subjects. The normotensive Wistar-Kyoto (WKY) rat strain is generally accepted as the most appropriate control strain for SHR (Louis *et al.*, 1990). As there are pronounced differences in MAP regulation between hypertensive and normotensive rats (Pinto *et al.*, 1998) the magnitude of the effect of cardiovascular drugs on the different hemodynamic endpoints may vary considerably between strains. Therefore, the basic CVS model might not be directly applicable to data from normotensive rats. This is a major drawback especially for drug safety evaluations, which are usually conducted in normotensive rats. As the ultimate aim of the proposed quantitative pharmacology model is to predict clinical

responses to novel pharmacologic agents, it is pivotal that the CVS model is applicable to both normotensive and hypertensive rats.

In this investigation, we describe the extension of the basic CVS model to a more detailed level by 1) parsing CO into HR and SV and 2) quantifying differences in BP regulation between normotensive and hypertensive rats, with the aim to evaluate if the MoA of new compounds can be elucidated using HR and MAP measurements only. To this end, data from preclinical experiments in hypertensive and normotensive rats with a training set of eight cardiovascular drugs with diverse MoA's are used. Ultimately, this quantitative pharmacology model may be used to predict, in quantitative manner, clinical responses to novel pharmacologic agents.

Methods

Animals

For the investigations male, SHR (Taconic Farms, Germantown, NY, USA) and WKY rats (Taconic Farms, Germantown, NY, USA) were used. All experiments were conducted in accordance with Novartis Animal Care and Use Committee protocols. These protocols have been accredited and conform to international animal welfare standards and to the Guide for the Care and Use of Laboratory Animals. The ages of the rats ranged from 41-54 wk and 35-38 wk for SHR and WKY rats, respectively. The body weights were between 367-504 gram and between 499-600 gram for SHR and WKY rats, respectively. Rats were housed on a 12-h light/dark cycle (light: 0600–1800 h), kept at room temperature, 22°C, and were provided normal chow (Harlan Teklad 8604; Indianapolis, IN, USA) and water ad libitum. The studies were reported in accordance with the ARRIVE guidelines for the reporting of experiments involving animals (Kilkenny *et al.*, 2010; McGrath *et al.*, 2010).

Experimental Procedures

For continuous recording of BP, HR and CO rats were surgically instrumented with both an ascending aortic flow probe and a femoral arterial catheter/radiotransmitter as described by Snelder *et al.* (Snelder *et al.*, 2013a).

Experimental design

The effects of a training set of compounds were obtained in two studies. In Study 1, information on the effect on MAP, CO, HR, SV and TPR was obtained following a single oral administration of different doses of each drug (amiloride, amlodipine, enalapril, fasudil, HCTZ or prazosin) on separate days (Table 2a). The number of dose strengths investigated

Table 1: Selected compounds to challenge the CVS with the aim of distinguishing system- from drug-specific parameters and their mechanism of action.

Compound	Class	Mechanism of action	Effect
amiloride	diuretic	Diuretics cause blood volume contraction and lower venous pressure, which decreases cardiac filling and, by the Frank-Starling mechanism, decreases ventricular stroke volume (Levick, 2003).	SV
amlodipine	calcium channel blocker	Amlodipine is a dihydropyridine that blocks voltage gated calcium channels and selectively inhibits Ca^{2+} influx into vascular smooth muscle cells. Calcium antagonists act by decreasing total peripheral resistance to lower arterial pressure. As a consequence, reflex tachycardia, increased cardiac output, and increased plasma catecholamine and plasma renin activity are commonly seen, particularly with the initial dose and with short-acting dihydropyridines (Michalewicz <i>et al.</i> , 1997; Perez-Reyes <i>et al.</i> , 2009).	TPR
atropine	M2 receptor antagonist	Muscarinic (M2) receptor antagonist (MRA) is an agent that blocks the activity of the muscarinic acetylcholine receptor. It causes tachycardia by blocking vagal effects on the sinoatrial node. Acetylcholine hyperpolarizes the sinoatrial node which is overcome by MRA and thus increases the heart rate	HR
enalapril	angiotensin-converting enzyme (ACE) inhibitor	ACE inhibitors competitively inhibit angiotensin I-converting enzyme, preventing the conversion of angiotensin I to angiotensin II, a potent vasoconstrictor that also stimulates release of aldosterone. Decreased levels of angiotensin II lead to decreased total peripheral resistance that is unassociated with reflex stimulation of the heart (Frohlich, 1989). In addition, aldosterone acts on the distal tubules and collecting ducts of the nephron, the functional unit of the kidney. Decreased levels of aldosterone, cause the depletion of sodium, conservation of potassium, decreased water retention, and decreased blood pressure	TPR and SV
fasudil	rho-kinase inhibitor	Rho-kinase inhibits myosin light chain phosphatase activity and plays a key role in Ca^{2+} sensitization and hypercontraction of vascular smooth muscle cells. Rho-kinase inhibitors decrease total peripheral resistance (Masumoto <i>et al.</i> , 2001).	TPR
HCTZ	diuretic	See amiloride	SV
prazosin	selective α_1 adrenergic receptor blocker	Prazosin is a quinazoline derivative that is a specific and selective competitive antagonist of α_1 adrenoceptors on vascular smooth muscle cells. Prazosin reduces BP by reducing elevated peripheral resistance and has little effect on cardiac function (Reid <i>et al.</i> , 1987).	TPR
propranolol	β -adrenergic receptor blocker	Propranolol is a non-selective beta blocker. It antagonizes the action of norepinephrine and epinephrine at all β -adrenergic receptors. Propranolol decreases cardiac output and heart rate with a reflex rise in total peripheral resistance (Ebadi <i>et al.</i> , 2008).	HR

varied per drug in order to find an appropriate dose showing a clear effect, and therefore, the duration of the study also varied per drug. The MAP and CO measurements following the administration of amlodipine, prazosin and HCTZ (first occasion) in SHR were also used for the development of the previous CVS model (Snelder *et al.*, 2013a). As these data are also informative for the proposed extended CVS model they are included in this investigation as well. However, in the previous investigation, the maximum effect of HCTZ was not observed at the investigated dose range. Therefore, information on the influence of higher doses of HCTZ on the hemodynamic parameters was obtained in this study (second occasion) (Table 2a). In Study 2, the effects of atropine (10 mg/kg) and propranolol (30 mg/kg) on MAP, CO, HR, SV and TPR were measured following a single, sequential or combined oral administration of propranolol and/or atropine in 8 SHR (Table 2b). No WKY rats were included in this Study. In the rats repeated experiments were conducted over periods of up to 6 months. Sufficient washout between consecutive experiments was allowed. In Studies 1 and 2 together, 10 SHR and 2 WKY rats were used. Data from 1 SHR (Study 2) were omitted for model development as this rat learned how to disconnect its flow cable and responded much stronger than all other rats (Table 2). For practical reasons, the flow cables were disconnected from the flow probes between 5:00 pm and 7:00 am the following morning. On the experiment days baseline data were collected between 7:00 am and 10:00 am. Drug administration took place at 10:00 am and 13:00 am (Study 2 only). Data collection was continued until 5:00 pm. In the period between 5:00 pm and 7:00 am the following morning, only MAP and HR data were captured.

Compounds

Amiloride HCl hydrate (Sigma-Aldrich, St. Louis, MO, USA, A7410), enalapril maleate (Sigma-Aldrich, E6888), fasudil mono HCl (LC Laboratories, Woburn, MA, F-4660), atropine sulfate (Sigma-Aldrich, A0257) and propranolol HCl (Sigma-Aldrich, P0884) were dissolved in water. Amlodipine besylate (Lek Pharmaceuticals, Ljubljana, Slovenia) and prazosin HCl (Sigma-Aldrich, P7791) were homogenized in 0.5% methylcellulose (MC) (Fisher Scientific, Pittsburgh, PA). Hydrochlorothiazide (HCTZ, Sigma-Aldrich, H2910) was dissolved in NaOH and diluted with filtered water (vehicle was water adjusted to pH 11). All compounds were formulated for administration at 2 ml/kg by oral gavage.

Data analysis

The interrelationship between MAP, TPR, CO, HR and SV is expressed by the formulas 1) $MAP=CO*TPR$ and 2) $CO=HR*SV$ (Levick, 2003). Previously, we have developed a mechanism-based linked turnover model to describe the inter-relationship between MAP, CO and TPR (Snelder *et al.*, 2013a). This model consisted of two turnover equations, one for CO and one for TPR, which were linked by negative feedback through MAP represent-

Table 2a: Study overview Study 1

Study	Measures	Study designs	Compound	Dose (mg/kg)	Strain	Number of rats
1	MAP, HR and SV (CO and TPR)	Day 1: vehicle Following days: a different dose each day	amiloride amlodipine ^a enalapril fasudil HCTZ ^a HCTZ ^b prazosin ^a	10 0.3, 1, 3, 10 3, 10, 30 3, 10, 30 0.1, 0.3, 1, 3 10, 30 0.04, 0.2, 1, 5	SHR SHR WKY SHR SHR SHR WKY SHR SHR WKY	3 2 2 4 ^{**} 4 2 2 4 2 1

Table 2b: Study overview Study 2

Study	Measures	Study designs	Number of rats (SHR)
2	MAP, HR and SV (CO and TPR)	vehicle followed by vehicle 3h later atropine followed by propranolol 3h later propranolol followed by atropine 3h later combination of atropine and propranolol atropine followed by no dosing propranolol followed by no dosing	2 3 ^{**} 3 1 3 ^{**} 3

^a 1st occasion

^b 2nd occasion

*Data from SHR were previously use for the characterization of the CVS model (Snelder *et al.*, 2013a)

**Data from one rat were excluded for model development as this rat learned how to disconnect its flow cable and responded much stronger than all other rats resulting in a low MAP

ing homeostatic feedback mechanisms such as the baroreflex system (Cleophas, 1998) (Equation 1).

$$\begin{aligned} \frac{dCO}{dt} &= K_{in_CO} \cdot (1 - FB1 \cdot MAP) - k_{out_CO} \cdot CO \\ \frac{dTPR}{dt} &= K_{in_TPR} \cdot (1 - FB2 \cdot MAP) - k_{out_TPR} \cdot TPR \end{aligned} \quad (1)$$

$$MAP = CO \cdot TPR$$

In these equations, K_{in_CO} and K_{in_TPR} are the zero-order production rate constants and k_{out_CO} and k_{out_TPR} the first-order dissipation rate constants of CO and TPR respectively. These rate constants describe the time course of the effect on CO and TPR. $FB1$ and $FB2$ are constants characterizing the negative feedback of MAP on CO and TPR.

In the present study, this model was extended by parsing CO into HR and SV. More precisely, the turnover equation for CO was replaced by two turnover equations for HR and SV (Figure 1). Therefore, the extended CVS model consisted of three linked turnover equa-

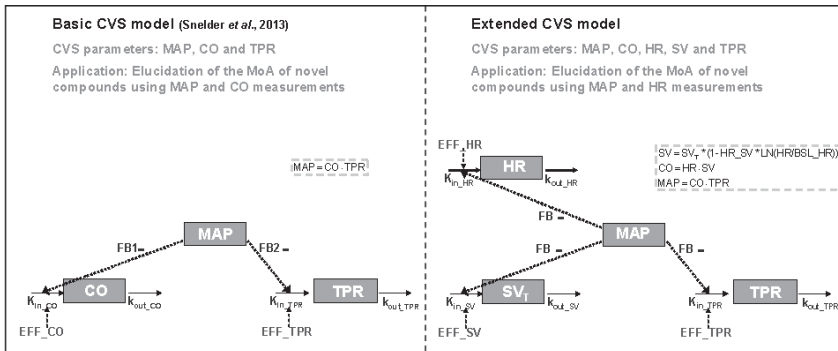


Figure 1: Comparison between the basic CVS model to characterize drug effects on the interrelationship between MAP, CO and TPR and the extended CVS model to characterize drug effects on the interrelationship between MAP, CO, HR, SV and TPR.

*Extended CVS model: Cardiac output (CO) equals the product of HR and SV (CO=HR*SV) and MAP equals the product of CO and TPR (MAP=CO*TPR). SV is influenced by indirect feedback through MAP (SV_i) and by HR through a direct inverse log-linear relationship, where HR_{SV} represents the magnitude of this direct effect. Effects on HR, SV and TPR are described by three linked turnover equations. In these equations K_{in_HR} , K_{in_SV} and K_{in_TPR} represent the zero-order production rate constants and k_{out_HR} , k_{out_SV} and k_{out_TPR} represent the first-order dissipation rate constants. When MAP increases as a result of a stimulating effect on HR, SV or TPR, the values of HR, SV and TPR will decrease as a result of the action of the different feedback mechanisms regulating the CVS. In this model the magnitude of feedback on HR, SV and TPR is represented by FB. System-specific parameters are indicated in black and drug-specific parameters are indicated in dark grey.*

tions involving TPR, HR and SV all linked by negative feedback through MAP (Equation 2). In addition, a direct inverse relationship between HR and SV was included in the model representing the relationship between the cardiac interval and left ventricular filling time (LVFT), i.e. when HR increases, the cardiac interval decreases, and therefore, LVFT decreases and SV decreases (Equation 2).

$$\begin{aligned}
 \frac{dHR}{dt} &= K_{in_HR} \cdot (1 - FB \cdot MAP) - k_{out_HR} \cdot HR \\
 \frac{dSV^*}{dt} &= K_{in_SV} \cdot (1 - FB \cdot MAP) - k_{out_SV} \cdot SV^* \\
 \frac{dTPR}{dt} &= K_{in_TPR} \cdot (1 - FB \cdot MAP) - k_{out_TPR} \cdot TPR
 \end{aligned}
 \tag{2}$$

$$\begin{aligned}
 SV &= SV^* \cdot (1 - HR_SV \cdot \ln(HR/BSL_HR)) \\
 CO &= HR \cdot SV \\
 MAP &= CO \cdot TPR
 \end{aligned}$$

In these equations, SV^* represents the SV influenced by the negative feedback of MAP, K_{in_HR} and K_{in_SV} represent the zero-order production rate constants and k_{out_HR} and k_{out_SV} and represent the first-order dissipation rate constants of HR, SV and TPR, respectively. These hypothetical production and dissipation rate constants reflect the rate of change in HR, SV and TPR. FB is a constant representing the magnitude of the negative feedback of MAP on HR, SV and TPR and HR_SV is a constant that represents the magnitude of the direct effect of HR and SV. Following the criteria for statistical significance as specified in the section “Computation”, a linear relationship between MAP and the production rate constants of HR, SV and TPR and a log-linear relationship between HR and SV were the most parsimonious relationships that adequately captured the feedback mechanism and the direct inverse relationship between HR and SV, respectively.

The circadian rhythm, which was observed in all 5 parameters of the CVS, was described by two cosine functions, one influencing K_{in_HR} and one influencing K_{in_TPR} (Equation 3). As a result of the feedback through MAP this model also describes the circadian rhythm in SV, CO and MAP in addition to that of HR and TPR.

$$CR_{HR} = amp_{HR} \cdot \cos\left(\frac{2\pi \cdot (t + hor_{HR})}{24}\right)$$

$$CR_{TPR} = amp_{TPR} \cdot \cos\left(\frac{2\pi \cdot (t + hor_{TPR})}{24}\right)$$

$$\frac{dHR}{dt} = K_{in_HR} \cdot (1 + CR_{HR}) \cdot (1 - FB \cdot MAP) - k_{out_HR} \cdot HR \quad (3)$$

$$\frac{dSV_T}{dt} = K_{in_SV} \cdot (1 - FB \cdot MAP) - k_{out_SV} \cdot SV_T$$

$$\frac{dTPR}{dt} = K_{in_TPR} \cdot (1 + CR_{TPR}) \cdot (1 - FB \cdot MAP) - k_{out_TPR} \cdot TPR$$

In these equations, the parameter amp is the amplitude, t is the time and hor is the horizontal displacement of the physiological variable over time.

Brief manual restraint and oral dose administration either directly or indirectly (i.e., sensed by a bystander rat in the same room) caused a temporary increase in HR, TPR, CO and MAP and decrease in SV that was independent of drug exposure. This handling effect was described by an empirical function HD (Visser *et al.*, 2006) influencing the K_{in_HR} and K_{in_TPR} (Equation 4).

$$HD_{HR} = P_{HR} \cdot \exp(-k_{HD} \cdot (t - t_{HD})) \text{ when } t > t_{HD}$$

$$HD_{TPR} = P_{TPR} \cdot \exp(-k_{HD} \cdot (t - t_{HD})) \text{ when } t > t_{HD}$$

$$\frac{dHR}{dt} = K_{in_HR} \cdot (1 + CR_{HR}) \cdot (1 - FB \cdot MAP) \cdot (1 + HD_{HR}) - k_{out_HR} \cdot HR \quad (4)$$

$$\frac{dSV_T}{dt} = K_{in_SV} \cdot (1 - FB \cdot MAP) - k_{out_SV} \cdot SV_T$$

$$\frac{dTPR}{dt} = K_{in_TPR} \cdot (1 + CR_{TPR}) \cdot (1 - FB \cdot MAP) \cdot (1 + HD_{TPR}) - k_{out_TPR} \cdot TPR$$

In this equation, P_{HR} and P_{TPR} determine the magnitudes of the handling effect on HR and TPR respectively, k_{HD} determines the rate of disappearance of the handling effect and t_{HD} equals the time of handling.

At baseline, before drug administration, the system is in oscillating steady state. This means that the values of the parameters oscillate around their baseline values. For turn-over models it is common practice to derive the steady-state conditions and to express K_{in}

in terms of BSL and k_{out} (Dayneka *et al.*, 1993). For this system the steady-state conditions for the oscillating steady state cannot be derived analytically. Therefore, K_{in} was expressed in terms of BSL and k_{out} without accounting for the circadian rhythm (Equation 5). To ensure that the system is in oscillating steady state at start of pharmacological intervention the observations were shifted two weeks (determined empirically), i.e. the system was initialized at time=0 h and the pharmacological interventions started at time=336 h.

$$K_{in_HR} = \frac{k_{out_HR} \cdot BSL_HR}{1 - FB \cdot BSL_MAP}$$

$$K_{in_SV} = \frac{k_{out_SV} \cdot BSL_SV}{1 - FB \cdot BSL_MAP} \quad (5)$$

$$K_{in_TPR} = \frac{k_{out_TPR} \cdot BSL_TPR}{1 - FB \cdot BSL_MAP}$$

In this equation, BSL_HR , BSL_SV and BSL_TPR represent the baseline values of HR, SV and TPR, respectively. In the experiments, SV and TPR were derived from the directly measured MAP, CO and HR. Therefore, in the modeling, the BSL_MAP and BSL_CO and BSL_HR were estimated and BSL_SV and BSL_TPR were derived from these parameters. To functionally characterize the system, eight different drugs with different mechanisms of action were administered. In the analysis of the data, it was assumed that the drugs (EFF) influence the production rates of HR, SV or TPR according to Equation 6.

$$\frac{dHR}{dt} = K_{in_HR} \cdot (1 + CR_{HR}) \cdot (1 - FB \cdot MAP) \cdot (1 + EFF + HD_{HR}) - k_{out_HR} \cdot HR$$

$$\frac{dSV_T}{dt} = K_{in_SV} \cdot (1 - FB \cdot MAP) \cdot (1 + EFF) - k_{out_SV} \cdot SV_T \quad (6)$$

$$\frac{dTPR}{dt} = K_{in_TPR} \cdot (1 + CR_{TPR}) \cdot (1 - FB \cdot MAP) \cdot (1 + EFF + HD_{TPR}) - k_{out_TPR} \cdot TPR$$

The time course of the drug plasma concentrations, i.e., the pharmacokinetics (PK), rather than the dose, was used as a predictor for the pharmacodynamics (PD). This enables an accurate description of the time course of the drug effect. For that purpose predicted plasma concentration *versus* time profiles were used, which were derived from the literature (Table 3). However, for atropine and prazosin the administration route was different in these literature studies (intravenous administration) as compared to the experiments described in this paper (oral administration). Therefore, for these compounds the ab-

Table 3: Specification of the PK models to describe the pharmacokinetics of the six selected compounds, enalapril, fasudil, amlodipine, prazosin, propranolol and HCTZ to challenge the CVS. The PK models were based on literature models. The adjustments required to account for the differences in experimental conditions and formulations in these literature studies as compared to the experiments described in this paper are described in the “Comments” column.

Compound	PK model	Literature model	Comments	Species
amiloride	2-compartmental model with liver compartment	(Segre <i>et al.</i> , 1998) 2-compartmental model with liver compartment	-	Wistar rats
amlodipine	1-compartmental model	(Stopher <i>et al.</i> , 1988): Non-compartmental analysis	Ka was derived from the reported half-life, Vd, F and T_{max} using Berkeley Madonna	Sprague-Dawley rats
atropine	2-compartmental model	(Perlstein <i>et al.</i> , 2002) 2-compartmental model	Ka was estimated simultaneously with PD	Sabra rats
enalapril	2-compartmental model with Michaelis-Menten elimination	(Lin <i>et al.</i> , 1988) and (Li <i>et al.</i> , 2007)	Data read out from the manuscripts and a 2-compartmental model with Michaelis-Menten elimination was optimized in NONMEM	Sprague-Dawley rats
fasudil	1-compartmental model	(Ikegaki <i>et al.</i> , 2001): Non-compartmental analysis	Ka and lag-time were derived from the reported half-life, AUC and C_{max} using Berkeley Madonna	Wistar-Kyoto rats
HCTZ	1-compartmental model	(Asdaq and Inamdar, 2009): 1-compartmental model	Reported: Ke, Ka, Vd, AUC -> F was calculated from these parameters	Wistar-Kyoto rats
prazosin	1-compartmental model	(Hamilton <i>et al.</i> , 1985): 1-compartmental model	CL, Vd; scaled to rat using allometric scaling. Ka was estimated	New Zealand white rabbits
propranolol	3-compartmental model	(van Steeg <i>et al.</i> , 2010) and (Belpaire <i>et al.</i> , 1990): 3-compartmental model	Distribution and elimination parameters were fixed to van Steeg <i>et al.</i> . Ka was estimated in NONMEM using data read out from Belpaire <i>et al.</i>	Wistar-Kyoto rats

CL: clearance

Vd: distribution volume

Ke: elimination rate

Ka: absorption rate

F: bioavailability

sorption rate was estimated based on the time course of the effect on BP in conjunction with the relevant information on the pharmacokinetics from the literature (Table 3). For atropine and prazosin, PK and PD parameters were estimated simultaneously. The concentration-effect relations for the drug effects on HR, SV and TPR were evaluated using linear, power, E_{max} or Sigmoid E_{max} pharmacodynamic models (Equation 7).

$$\begin{array}{ll}
 \text{Linear :} & \text{EFF} = SL \cdot C \\
 \text{Power :} & \text{EFF} = SL \cdot C^{\text{POW}} \\
 E_{\text{max}} : & \text{EFF} = \frac{E_{\text{max}} \cdot C}{EC_{50} + C} \\
 \text{Sigmoid } E_{\text{max}} : & \text{EFF} = \frac{E_{\text{max}} \cdot C^{\gamma}}{EC_{50}^{\gamma} + C^{\gamma}}
 \end{array} \quad (7)$$

In this equation, EFF represents the effect at concentration C. SL , E_{max} , EC_{50} and γ represent the slope of the linear relationship, the maximum effect, the concentration at which half of the maximum effect is achieved and the Hill coefficient (sigmoidicity parameter), respectively.

For the basic CVS model we have presented an equation to calculate TPR and CO at steady state during pharmacological intervention. For the extended CVS model there is no analytical solution for the steady-state values during pharmacological intervention. However, these values can be simulated from the final model by using the steady-state concentration C_{ss} .

The proposed model assumes that the time delay between concentration and effect (hysteresis) is the same for all classes of compounds influencing a certain effect site, i.e. HR, SV or TPR. To evaluate this assumption, for each compound it was investigated if there was an additional delay between concentration and effect by re-evaluating the proposed model with an extra hypothetical effect compartment (Equation 8).

$$\frac{dC_e}{dt} = k_{e0} \cdot (C - C_e) \quad (8)$$

In this equation, C and C_e represent the plasma concentration and the concentration in the hypothetical effect compartment, respectively, and k_{e0} represents the first order rate constant describing drug transport. This approach implies that at equilibrium C equals C_e .

A significant improvement of the goodness of fit after the addition of an effect compartment indicates that there is a difference in temporal delay between plasma concentration and effect between different classes of drugs influencing the same parameter (HR, SV or TPR).

The PK and PD models were based on the assumptions described in Table 4 and discussed by Snelder *et al.* (Snelder *et al.*, 2013a).

Table 4: Model assumptions

No.	Assumption	Clarification
1	All compounds influence the production rates of HR, SV or TPR rather than the dissipation rates.	This assumption is based on the MoA of the selected compounds (Table 1).
2	For compounds for which the maximum effect was not observed, complete inhibition (i.e., $E_{max} = 1$) was assumed at infinite concentrations to ensure identification of the EC_{50} parameter.	The validity of this assumption was evaluated for amlodipine using the basic CVS model (Snelder <i>et al.</i> , 2013a). The influence of different values of the E_{max} (i.e. $E_{max} = 0.8$) on the estimates of the system parameters was tested.
3	The PK do not differ between rat strains and can be scaled between rabbit and rat on the basis of an allometric function (West 1999; Anderson, 2009).	Although published information on the PK of all selected compounds was available, the PK was often evaluated in different rat strains and, for prazosin, even in a different species (rabbit).

SHR versus WKY rats

The difference in BP regulation between hypertensive SHR and normotensive WKY rats was investigated by evaluating the system parameters per strain under the assumption that the structural model was the same for SHR and WKY rats. In addition, as the level of baseline BP, which is known to differ between and within strains (Louis *et al.*, 1990), is continuously and proportionally related to cardiovascular risk (Pinto *et al.*, 1998), it was investigated if continuous relationships between BSL_MAP and the system parameters could be identified. Linear and power relationships were investigated.

System properties

To investigate if the profiles of the time-course of the drug effect on MAP, CO, HR, SV and TPR are different for compounds with a direct effect on HR, SV or TPR respectively, simulations were performed. The obtained simulated profiles of the time course of the change in MAP, CO, HR, SV and TPR are referred to as signature profiles. Distinct differences in the signature profiles for compounds with an effect on HR, SV or TPR indicate that the extended CVS model can be applied to identify the site of action (HR, SV or TPR) of novel compounds with an unknown MoA on BP. The time courses of the effects on MAP, CO, HR,

SV and TPR were simulated after triggering the model by inhibiting HR, SV or TPR with a hypothetical compound after a single oral dose.

HR and MAP measurements only

Previously, it was demonstrated that measuring CO is pivotal for characterizing the system (Snelder *et al.*, 2013a). However, at present, the measurement of CO is not common practice, due to the technical difficulties of these invasive instrumentation procedures (Doursout *et al.*, 2001). Therefore, the question arises if the extended CVS model, which was developed using MAP, HR and CO measurements, can be used to quantify the dynamic changes in the CVS and elucidate the MoA for novel compounds using HR and MAP measurements only. This was investigated using the data from the compounds from Table 2. These data were also used for model development and, therefore, for estimation of the system specific parameters. Hence it seems obvious that the drug effects of these compounds can be quantified using the extended CVS model. However, for model development, the site of action was assumed to be known (Table 1). Moreover, MAP, CO, HR, SV and TPR measurements were used to quantify the drug effects. Therefore, the question remains if the site of action and the drug effect of each compound on HR and MAP can be quantified using a limited amount of data (i.e., only HR and MAP measurements). For each compound, a model-based hypothesis testing procedure was followed using the extended CVS model with the system-specific parameters fixed to values from Table 5.

- 1) Different hypotheses of the site of action (i.e. HR, SV and TPR) and direction of the effect (i.e., inhibiting or stimulating) were formulated, resulting in 6 possible combinations of effects.
- 2) For each hypothesis, the model was fitted to the HR and MAP measurements.
- 3) It was evaluated which hypothesis resulted in the best description of the data as judged by the agreement between the observed and predicted direction and magnitude of effect and the lowest minimum value of the objective function (MVOF) as specified in the section "Computation".

Since not all compounds were investigated in WKY rat, only data from SHR were used.

Table 5: The system- and drug-specific parameter values from the extended drug-independent model to describe the CVS.

Parameter	Value	RSE	LLCI	ULCI
System-specific parameters				
BSL_HR_SHR (beats/min)	310	1.12	303	317
BSL_MAP_SHR (mmHg)	155	0.684	153	157
BSL_CO_SHR (mL/min)	69.0	4.17	63.4	74.6
BSL_HR_WKY (beats/min)	323	1.61	313	333
BSL_MAP_WKY (mmHg)	102	0.884	100	104
BSL_CO_WKY (mL/min)	129	1.47	125	133
k_{out_HR} (1/h)	11.6	19.1	7.27	15.9
k_{out_SV} (1/h)	0.126	30.7	0.0501	0.202
k_{out_TPR} (1/h)	3.58	29.1	1.54	5.62
FBO (1/mmHg)	0.00290	5.93	0.00256	0.00324
FBO_MAP	-1.98	10.6	-2.39	-1.57
HR_SV	0.312	15.6	0.216	0.408
k_{HD} (1/h)	4.70	8.19	3.95	5.45
P_{HR}	0.632	9.67	0.512	0.752
P_{TPR}	0.331	12.9	0.247	0.415
hor _{HR} (h)	8.73	3.10	8.20	9.26
amp _{HR}	0.0918	5.15	0.0825	0.101
hor _{TPR} (h)	19.3	1.92	18.6	20.0
amp _{TPR}	Fixed to amp _{HR}			
Drug-specific parameters				
<i>amiloride: E_{max} model with E_{max} fixed to 1</i>				
EC ₅₀ (ng/mL)	245	25.1	125	365
<i>amlodipine: E_{max} model with E_{max} fixed to 1</i>				
EC ₅₀ (ng/mL)	82.8	4.99	74.7	90.9
<i>atropine: linear model</i>				
SL (1/(ng/mL))	0.00149	32.3	0.000547	0.00243
Ka (1/h)	1.17	59.9	-0.204	2.54
<i>enalapril: E_{max} model with E_{max} fixed to 1</i>				
EC ₅₀ (ng/mL)	1200	4.03	1110	1290
ke0 (1/h)	0.163	5.07	0.147	0.179
<i>fasudil: E_{max} model with E_{max} fixed to 1</i>				
EC ₅₀ (ng/mL)	0.172	18.4	0.110	0.234
<i>HCTZ: E_{max} model with E_{max} fixed to 1</i>				
EC ₅₀ (ng/mL)	28900	7.65	24600	33200
<i>prazosin: power model</i>				
SL (1/(ng/mL))	0.328	5.58	0.292	0.364
POW	0.0910	6.05	0.0802	0.102
Inter-Individual variability				
BSL_HR (CV%)	6.1		4.36	7.47

Table 5 Continued

Parameter	Value	RSE	LLCI	ULCI
BSL_MAP (CV%)	3.7		2.67	4.49
BSL_CO (CV%)	22.7		18.09	26.57
Residual variability				
Prop. Res.Error _{HR} (CV%)	7.8		7.26	8.22
Prop. Res.Error _{MAP} (CV%)	6.0		5.44	6.57
Prop. Res.Error _{CO} (CV%)	6.9		5.72	7.83

RSE: Relative standard error of parameter estimate

CV: Coefficient of variation

LLCI: Lower limit of 95 % confidence interval

ULCI: Upper limit of 95 % confidence interval

Computation

The data from Studies 1 and 2 were simultaneously analyzed using a non-linear mixed-effects modeling approach implemented in NONMEM (version 7.2.0; Icon Development Solutions, Ellicott City, Maryland, USA). The models were compiled using Digital Fortran (version 6.6C3, Compaq Computer Corporation, Houston, Texas) and executed on a PC equipped with an AMD Athlon 64 processor 3200+ under Windows XP. The results from the NONMEM analysis were subsequently analyzed using the statistical software package S-Plus for Windows (version 8.0 Professional, Insightful Corp., Seattle, USA). Modeling techniques were detailed by Snelder et al. (Snelder *et al.*, 2013a). Goodness-of-fit was determined using the MVOF defined as minus twice the log-likelihood. For nested models, a decrease of 10.8 points in the MVOF (corresponding to $p < 0.001$ in a chi-squared distribution) by adding an additional parameter was considered significant. The goodness-of-fit was also investigated by visual inspection of the plots of individual predictions and the diagnostic plots of (weighted) residuals (Snelder *et al.*, 2013a).

Results

The extended CVS model as expressed by Equations 2 - 8 and as shown graphically in Figure 1 was used to simultaneously analyze the data from Studies 1 and 2. In the analysis, inter-individual variation in the baseline values of the parameters, *BSL_{HR}*, *BSL_{MAP}* and *BSL_{CO}*, was allowed (inter-individual variability (IIV)). The residual errors of HR, MAP and CO were best described by proportional residual error models. The residual errors of TPR and SV were derived from these parameters.

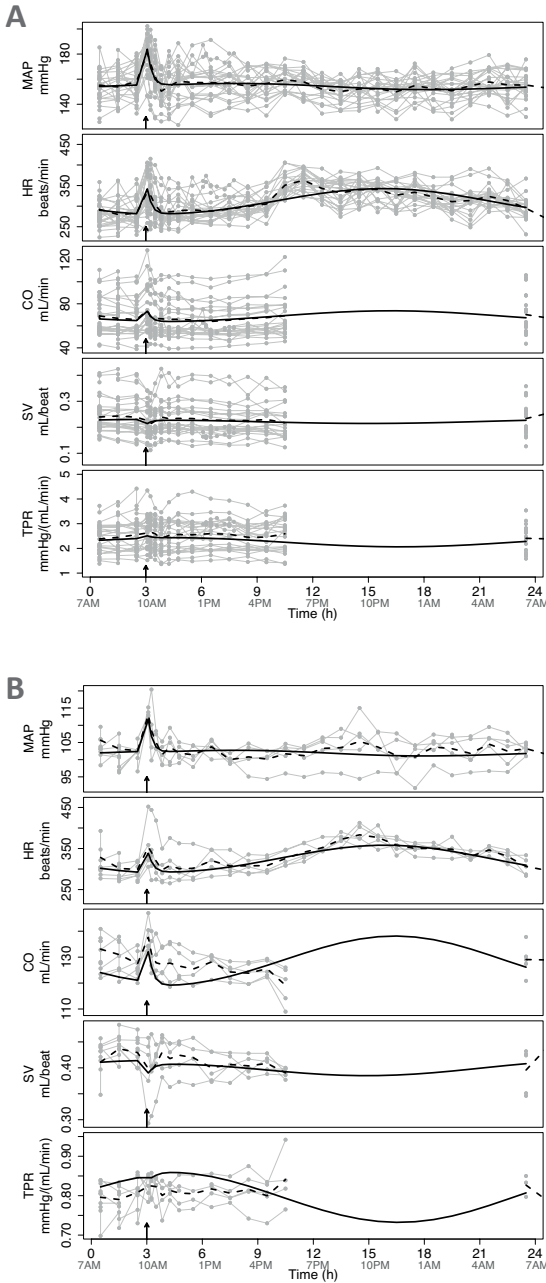


Figure 2: Description of the handling effect and circadian rhythm in MAP, HR, CO, SV and TPR in SHR (plot A) and WKY rats (plot B) after vehicle administration. Data are from Study 1 and Study 2 from all treatment groups.

Handling of the rats caused a temporary increase in HR, TPR, CO and MAP and decrease in SV that was independent of drug exposure. The handling effect is visible at 10 AM, i.e. when the rats were dosed with vehicle as indicated by the arrows. SHR were also dosed at 1PM (not indicated in the plot). The grey dots represent the observations, which are connected by the continuous grey lines, the dashed black lines represent the mean of the observations and the continuous black lines represent the population prediction by the developed extended CVS model.

SHR versus WKY rats

The baseline parameters were found to differ per strain with a higher BSL_MAP and a lower BSL_CO for SHR as compared to WKY rats, whereas BSL_HR did not significantly differ between the strains (Table 5). BSL_SV and BSL_TPR were derived from these parameters, resulting in a lower BSL_SV and a higher BSL_TPR for SHR as compared to WKY rats. In addition, for both SHR and WKY rats FB was found to decrease with BSL_MAP according to the following relationship (Equation 9):

$$FB = FB0 * \left(\frac{IBSL_MAP}{TVBSL_MAP_SHR} \right)^{FB0_MAP} \quad (9)$$

In this equation, $FB0$, $FB0_MAP$, $IBSL_MAP$ and $TVBSL_MAP_SHR$ represent the feedback for a typical SHR, the exponent of the power relationship, the individual baseline values of MAP and typical value of BSL_MAP in SHR, respectively. Overall, the feedback is about 2-fold higher in WKY rats as compared to SHR. Based on statistical grounds this model was preferred over a model with FB estimated per strain.

Vehicle response

The response in the p.o. vehicle groups is characterized by circadian variation and a handling effect. The handling effect, which is visible at 3 hours, was adequately described by Equation 4 (Figure 2). The circadian rhythm, which was observed in all 5 parameters of the CVS, was adequately described by two cosine functions influencing K_{in-HR} and K_{in-TPR} in both SHR (Figure 2A) and WKY rats (Figure 2B). However, on two out five occasions CO is under-predicted between 3 and 5 hours in WKY rats. In addition, in WKY rats CO is slightly under-predicted on a population level. As TPR is derived from MAP and CO , TPR is slightly over-predicted on a population level. The amplitudes of the 2 cosine functions, i.e. amp_{HR} and amp_{TPR} , could not be distinguished and were estimated to be 0.09 indicating that the variation in K_{in-HR} and K_{in-TPR} is maximally 9% during the day. The horizontal displacement parameters of the 2 cosine functions, i.e. hor_{HR} and hor_{TPR} , were significantly different, even if one of the cosines would have been replaced by a sine (i.e. a shift of 12 hours) (Table 5). In addition, omitting one of the cosine functions resulted in a decrease in the goodness of fit indicated by a significant increase in the MVOF.

Drug effects

For prazosin, the absorption rate parameter (Ka) was found to be very high and could not be estimated with good precision. Therefore, for this compound Ka was fixed to a high value (99 1/h) prior to estimating the other model parameters. Overall, fixing Ka re-

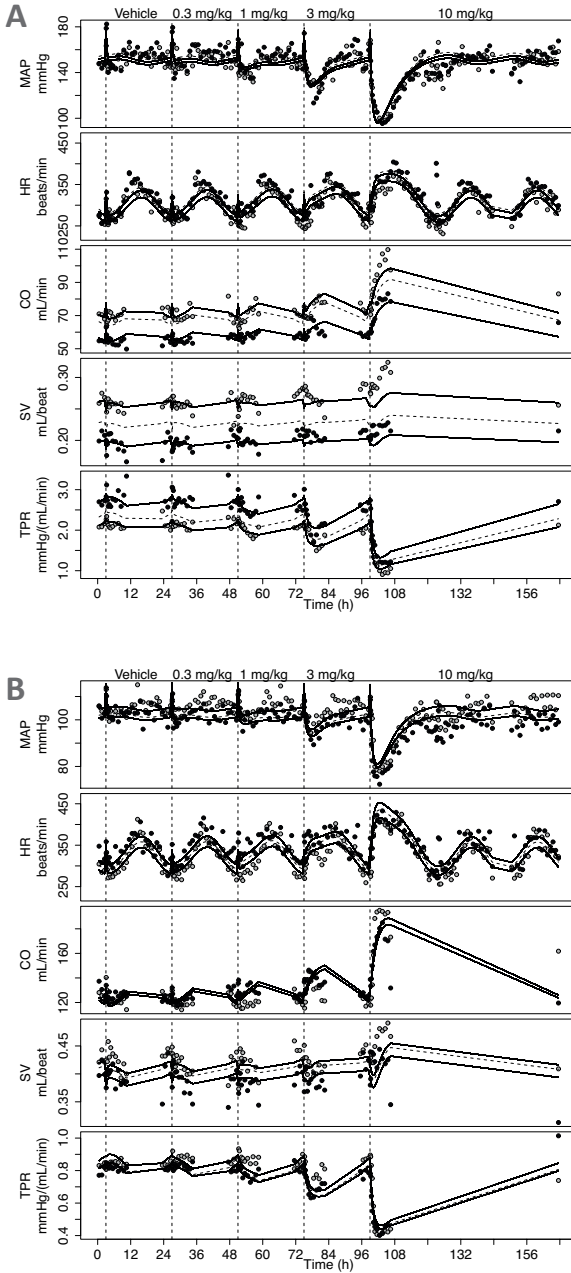


Figure 3: Description of the effects of amlodipine in SHR (plot A) and WKY rats (plot B). Data are from Study 1, in which vehicle and a different dose of amlodipine (0.3, 1, 3 and 10 mg/kg p.o.) were administered on separate days.

Amlodipine has an inhibiting effect on TPR. Therefore, TPR decreases after administration of amlodipine. As a result of the indirect feedback HR, SV and CO increase. In addition, the initial decrease SV is related to the direct inverse relationship between HR and SV. MAP changes in the same direction as the initial effect, i.e. MAP decreases. The grey and black dots represent the observations of two different rats. The continuous and dashed lines represent the individual and population prediction by the developed extended CVS model after administering amlodipine.

sulted in a reduction of runtimes as correlations between drug-specific parameters were removed. For atropine, K_a was estimated simultaneously with the PD. The poor precision of the estimate with a standard error of 59.9% (Table 5) was considered acceptable as system-specific parameters were not influenced by this parameter (results not shown). This was demonstrated by successively removing data from one of the compounds that were used for model development according to the methods as detailed by Snelder *et al.* (Snelder *et al.*, 2013a).

The concentration-effect relationships for amiloride, amlodipine, enalapril, fasudil and HCTZ were best described by E_{max} models. As described previously (Snelder *et al.*, 2013a), E_{max} was fixed to 1 for these compounds and EC_{50} was estimated. Enalapril was found to influence both TPR and SV with the same EC_{50} . Initially, different EC_{50} values were estimated. However, confidence intervals overlapped indicating that the EC_{50} values for the two effects could not be distinguished. In addition to the turnover equations (Equation 2), an effect compartment was used to describe the delay between change in enalapril plasma concentration and the effect on TPR and SV. The half-life of this additional delay was 4.3h. The effect of atropine was best described by a linear concentration-effect relationship. As atropine had a stimulating effect on K_{in_HR} applying a linear concentration-effect relationship did not result in problems with parameter optimization. The effect of prazosin was best described by a power model. The exponent of this relationship was low (0.0910) indicating that the maximum effect is not reached for the highest dose evaluated. Finally, the effect of propranolol was too small to be quantified.

In general, the data were adequately described by the model (Figure 3 and Supplemental Figures A and B). Except for the absorption rate of atropine, all system- and drug-specific parameters could be estimated with good precision as all standard errors were less than 50% of the parameter estimates (Table 5). In addition, all parameter correlations were below 0.85.

System properties

In the simulations, distinct differences between the signature profiles of MAP, CO, HR, SV and TPR were observed for direct drug effects on HR, SV and TPR, respectively. Specifically, in the simulations it was shown that inhibition of HR, SV or TPR always results in a decrease in MAP, demonstrating that homeostatic feedback cannot be stronger than the primary effect (Figure 4). Interestingly, the delay between the stimulus and the response on MAP was longer in case the drug effect was on SV as compared to TPR.

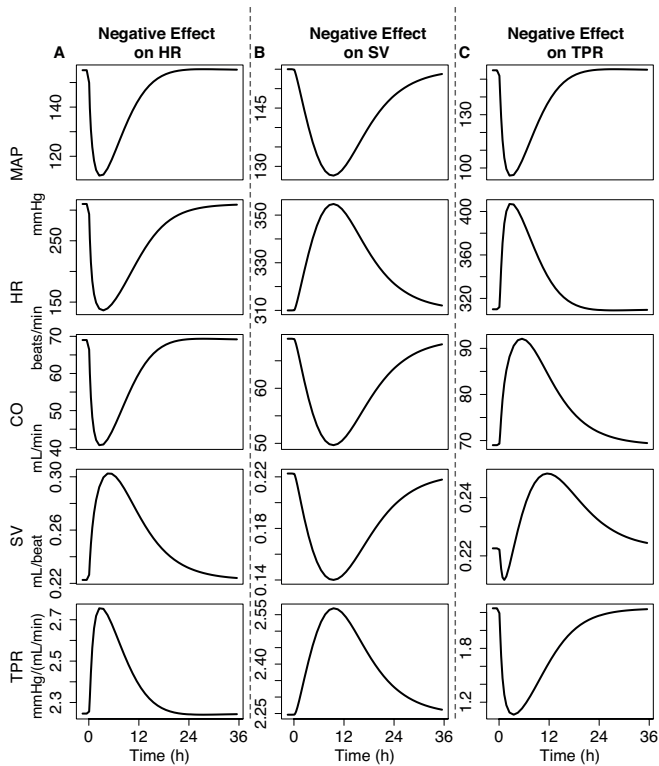


Figure 4: System properties of the CVS

The system properties of the CVS were investigated by simulating the response on MAP, CO, HR and TPR after inhibiting HR (A), SV (B) or TPR (C). Inhibiting HR, SV or TPR always results in a decrease in MAP, which demonstrates that feedback cannot be stronger than the primary effect. In addition, the delay in response on MAP was longer when the drug effect was on SV as compared to TPR.

HR and MAP measurements only

For each compound, it was investigated if the developed extended CVS model could be used to quantify the dynamic changes in the CVS and identify the site of action (HR, SV or TPR) using HR and MAP measurements only. Amlodipine was selected as a paradigm compound to illustrate the results of this analysis. Assuming a stimulating effect of amlodipine on HR resulted in an adequate description of the effect on HR. However, the description of the effect on MAP was inadequate as the directions of the observed and predicted effects were opposite (Figure 5). Assuming an inhibiting effect of amlodipine on SV resulted in an adequate description of the effect on HR and a reasonable description of the effect on MAP (Figure 5). However, the delay in effect on MAP was over-predicted. Finally, assuming an inhibiting effect of amlodipine on TPR resulted in an adequate description of the effect on HR and MAP (Figure 5). Overall, the effect of amlodipine on the CVS was best

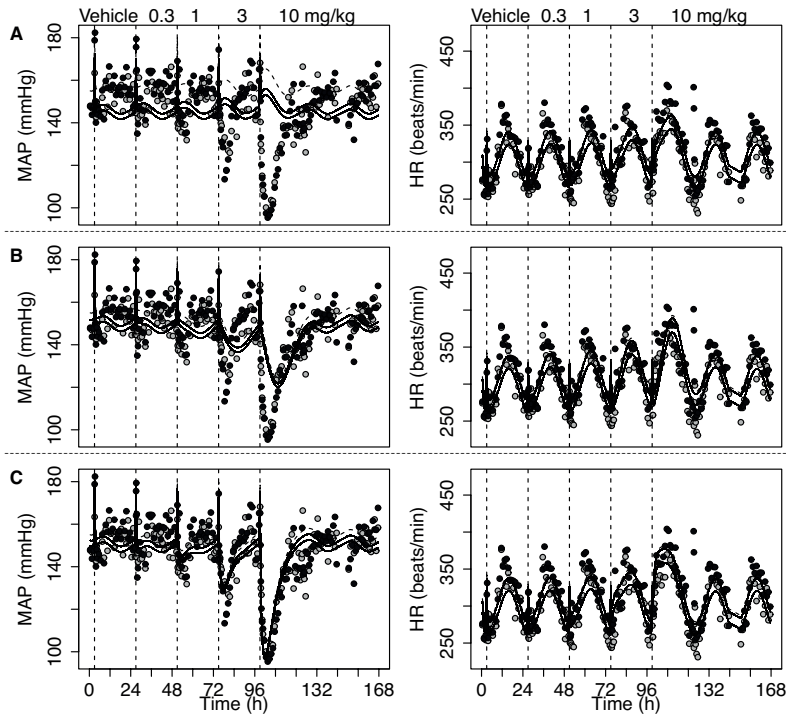


Figure 5: Description of the effects of amlodipine on MAP and HR using the extended CVS model with the system-specific parameters fixed to values from Table 5, while assuming a stimulating effect on HR (A), an inhibiting effect on SV (B) or an inhibiting effect on TPR (C). Data are from Study 1, in which vehicle and a different dose of amlodipine (0.3, 1, 3 and 10 mg/kg p.o.) were administered on separate days.

To evaluate if the site of action of amlodipine can be identified using MAP and HR measurements only, three hypotheses were evaluated. A) Hypothesizing a stimulating effect on HR resulted in an adequate description of the effect on HR. However, the description of the effect on MAP was inadequate as the directions of the observed and predicted effects were opposite. B) Hypothesizing an inhibiting effect of amlodipine on SV resulted in an adequate description of the effect on HR and a reasonable description of the effect on MAP. However, the delay in effect on MAP was over-predicted. C) Hypothesizing an inhibiting effect of amlodipine on TPR resulted in an adequate description of the effect on HR and MAP. In conclusion, model-based hypothesis testing indicated that it is most likely that the effect of amlodipine is on TPR, which is consistent with the available information from the literature. This indicated the MoA of a compound can be elucidated using MAP and HR measurements only. The grey and black dots represent the observations of two different rats. The continuous and dashed lines represent the individual and population prediction.

described assuming an inhibiting effect on TPR, which was confirmed by a significantly lower MVOF for the model with an effect on TPR as compared to the models with an effect on HR or SV. The estimated EC_{50} (84.9 [confidence interval (CI): 75.4–94.4] ng/mL) did not differ significantly from the estimated EC_{50} from the final extended CVS model (82.8 [CI: 74.7–90.9] ng/mL).

The effects of fasudil and prazosin on HR and MAP were best described assuming inhibition of TPR (results not shown). For amiloride, HCTZ and enalapril the effect on HR and MAP were best described following inhibition of SV (results not shown). Finally, the effect of atropine was best described by stimulating HR (results not shown). As the effect of propranolol was too small to be quantified, propranolol was omitted from this analysis. For all compounds the estimated drug-specific parameters did not differ significantly from the drug-specific parameters estimated by the final extended CVS model.

Discussion

Previously, a systems pharmacology model was developed that integrated a quantitative description of the physiology of the interrelationship between MAP, CO and TPR and the pharmacological effects of cardiovascular drugs in SHR (Snelder *et al.*, 2013a). This model can be applied for elucidation of the MoA of novel compounds, but this requires continuous recording of MAP and CO. Measuring CO has not been integrated into daily practice due to the challenges associated with invasive instrumentation procedures (Doursout *et al.*, 2001). Therefore, the aim of this research was to evaluate if the MoA of new compounds can be elucidated using HR and MAP measurements only.

First, the basic CVS model was extended by parsing CO into HR and SV. This extension was successfully established since 1) all drug-effects of compounds with different MoA's were adequately described, 2) all system-specific parameters were estimated with good precision and 3) drug- and system-specific parameters were not correlated. Distinguishing drug- from system-specific properties is essential for mechanism-based PKPD modeling (Danhof *et al.*, 2007; Ploeger *et al.*, 2009) and enables the prediction of treatment effects to later stages of development using a translational modeling approach (Danhof *et al.*, 2008), which is an ultimate application of the developed quantitative systems pharmacology model. The system-specific parameters of the extended CVS model were comparable to the system-specific parameters of the basic CVS model (Snelder *et al.*, 2013a) except for $k_{out-TPR}$ which was about 10 fold higher in the extended CVS model. This may be explained by the fact that in the basic CVS model $k_{out-TPR}$ and $FB2$ (feedback of MAP on TPR) were highly correlated (-0.984) indicating that these parameters could not be distinguished. In

the current model, the feedback parameters representing the magnitude of the feedback of MAP on HR, SV and TPR could not be distinguished. Therefore, only one feedback parameter could be estimated. As FB_2 was a little higher than FB this could well explain the difference in k_{out_TPR} between the two models.

SHR versus WKY rats

A secondary aim of this research was to quantify possible differences in BP regulation between hypertensive and normotensive rats. This is important as normotensive rats are often used for safety evaluation and are thought to be more predictive for the effects in human with normal BP than hypertensive rats. As expected, the baseline parameters were found to differ per strain with a higher BSL_MAP and a lower BSL_CO for SHR as compared to WKY rats (Table 5). In addition, FB decreased with higher BSL_MAP indicating impaired BP regulation in hypertensive rats. Similar findings were reported by Francheteau *et al.* regarding BP regulation in humans (Francheteau *et al.*, 1993). They hypothesized that the effect of dihydropyridine drugs in hypertensive patients can be adequately predicted by assuming different baselines and lower feedback relative to normotensive subjects.

The relationship between FB and BSL_MAP was described by a hyperbolic function. It should be noted that this function is purely descriptive and was based on data from only 10 SHR and 2 WKY rats. Therefore, further research is required to establish the precise relationship between FB and BSL_MAP .

Vehicle response

The under-prediction of CO between 3 and 5 hours in WKY rats is a result of a large and highly variable handling effect. Since including inter-occasion variability, which describes the variability of a parameter within a rat from one occasion to another, in the model did improve the description of the data on an individual level, but did not influence the estimates of the structural parameters this bias was accepted. In addition, the under-prediction of CO on a population level in WKY rats is a result of the fact that the population prediction is based on the observations from all rats, including the observations following active treatment, and the observed baselines of the rats following vehicle administration are in the tail of the overall baseline distribution, which is thought to be chance finding that is related to the low number of WKY rats included in the study.

Drug effects

As the PK was not measured in these experiments, predicted plasma concentration *versus* time profiles were derived from the literature (Table 3). As discussed previously (Snelder *et al.*, 2013a), the assumptions made regarding the use of PK models derived from published results may have a large impact on the PK profiles. Therefore, the PK models were

descriptive and the PK and drug-specific PD parameters should only be interpreted in the context of this model. The effects of all compounds were adequately described by the extended CVS model. However, the effect of propranolol was too small to be quantified. Therefore, propranolol did not contribute to the identification of the system-parameters. Enalapril was found to influence TPR and SV with the same EC_{50} . In our previous research less detailed information on the effect of enalapril on the CVS was available as CO was not measured at that stage (Snelder *et al.*, 2013a). Therefore, only the primary effect of enalapril on TPR was included in the model. Enalapril is an angiotensin-converting enzyme, which influences TPR and SV through the RAAS (see Table 1 for a description of the MoA). Therefore, the effect of this compound is delayed in comparison to the effect of calcium channel blockers or selective α_1 adrenergic receptor blockers, which directly influence vascular smooth muscle cell contraction. This additional delay was described adequately by an effect compartment. From a mechanistic point of view a turnover model might be better as it has been demonstrated that the RAAS can be described by a set of turnover equations (Hong *et al.*, 2008). However, as there was only one compound included in this research with an effect on the RAAS, the data did not contain enough information to characterize the RAAS in a mechanism-based manner.

System properties

Clear differences were found between the signature profiles of MAP, CO, HR, SV and TPR after simulating drug effects on HR, SV and TPR (Figure 4). From these simulations it can be concluded that, even if CO is not measured, it is likely that the extended CVS model can be used to elucidate the site of action of novel compounds with a simple MoA (i.e., one site of action). In summary, when the direction of the effect on HR and MAP is the same, the primary effect is on HR. When the direction of the effect on HR and MAP is opposite, the primary effect of the drug is on SV or TPR. Effects on SV and TPR can be distinguished by the delay between the perturbation and the effect on MAP, i.e. a long delay indicates that the primary effect is on SV and a short delay indicates that the primary effect is on TPR. These conclusions are based on data from eight different cardiovascular drugs. To further support these conclusions data from more compounds is required.

HR and MAP measurements only and system properties

To further evaluate if the extended CVS model can be applied to elucidate the MoA of novel compounds using HR and MAP measurements only, the effect of each compound was quantified using the extended CVS model, while assuming different sites of action and different directions of the effects. For all compounds, the identified site of action was consistent with the available information on the MoA of the compounds (Table 1). However, the effect of enalapril on HR and MAP was best described after inhibiting SV,

whereas according to information from the literature enalapril influences both TPR and SV (Table 1). Evaluating a model that is structurally comparable to the final extended CVS model, but with a combined delayed inhibiting effect on TPR and SV, improved the goodness of fit (results not shown). However, without any prior knowledge it is foreseen that it may be difficult to identify the site of action of novel compounds with unknown and more complex MoA's. Nevertheless, since the site of action of 6 out of 7 compounds was adequately characterized, and there are pronounced differences in signature profiles, it is anticipated that the extended CVS models can be applied to elucidate the MoA for novel compounds using HR and MAP measurements only. Before our model can be applied for that purpose, this conclusion should be validated using data from new compounds, i.e. compounds that were not used for model development, but with a known mechanism of action. Recently, the extended CVS model was applied to provide insights into the site of action of fingolimod (Snelder *et al.*, 2013b), which is effective in the treatment of multiple sclerosis (Cohen *et al.*, 2010), but is associated with cardiovascular effects (Kappos *et al.*, 2006; Kappos *et al.*, 2010). Results indicated that the active metabolite of fingolimod, fingolimod-phosphate (fingolimod-P), has an effect on TPR in rats, and it is likely that fingolimod-P also influences HR. This is in line with the available information on the mechanisms underlying the cardiovascular effects of fingolimod-P, which indicates that the model can also be applied to provide insights into the site of action of compounds with a more complex MoA. In addition, for all compounds, the estimated drug-specific parameters did not differ significantly from the estimated drug-specific parameters from the final extended CVS model. This implies that the model also can be used to predict the dynamics of the effects on CO, SV and TPR for novel compounds using HR and MAP measurements only.

In conclusion, the extended CVS model can be applied to elucidate the MoA and to quantify drug-specific parameters for new compounds with desired and undesired effects on the CVS using HR and MAP measurements only. Applications of the developed model, using the identified set of system parameters, are limited to SHR and WKY rats. However, since a mechanism-based modeling approach was applied, it is foreseen that accurate extrapolation between different rat strains and from one species to another is possible (Danhof *et al.*, 2008; Ploeger *et al.*, 2009). This requires the differences in the values of the systems specific parameters between the different species to be known. An ultimate application of the extended CVS model would be to predict the change in the hemodynamic parameters in humans based on preclinical data for newly developed compounds. However, before our model can be applied for that purpose, it is necessary to predict long-term blood pressure effects (Snelder *et al.*, 2013a). Moreover, the model should be scaled to humans and validated on human MAP, HR and CO measurements.

References

- Anderson B.J., Holford N.H., (2009). "Mechanistic basis of using body size and maturation to predict clearance in humans." *Drug Metab Pharmacokinet.* 24(1): 25-36.
- Asdaq SM, Inamdar MN (2009). The potential for interaction of hydrochlorothiazide with garlic in rats. *Chem Biol Interact* 181: 472-479.
- Belpaire FM, de Smet F, Vynckier LJ, Vermeulen AM, Rosseel MT, Bogaert MG *et al.* (1990). Effect of aging on the pharmacokinetics of atenolol, metoprolol and propranolol in the rat. *J Pharmacol Exp Ther* 254: 116-122.
- Cardinale D, Bacchiani G, Beggiato M, Colombo A, Cipolla CM (2013). Strategies to prevent and treat cardiovascular risk in cancer patients. *Semin Oncol* 40: 186-198.
- Cleophas TJ (1998). Mechanisms offsetting the beneficial effects of antihypertensive drugs: a problem increasingly considered but incompletely understood. *Am J Ther* 5: 413-419.
- Cohen JA, Barkhof F, Comi G, Hartung HP, Khatri BO, Montalban X *et al.* (2010). Oral fingolimod or intramuscular interferon for relapsing multiple sclerosis. *N Engl J Med.*, 362, 402-415.
- Danhof M, de Jongh J, De Lange EC, Della Pasqua O, Ploeger BA, Voskuyl RA (2007). Mechanism-based pharmacokinetic-pharmacodynamic modeling: biophase distribution, receptor theory, and dynamical systems analysis. *Annu Rev Pharmacol Toxicol* 47: 357-400.
- Danhof M, de Lange EC, Della Pasqua OE, Ploeger BA, Voskuyl RA (2008). Mechanism-based pharmacokinetic-pharmacodynamic (PK-PD) modeling in translational drug research. *Trends Pharmacol Sci* 29: 186-191.
- Dayneka NL, Garg V, Jusko WJ (1993). Comparison of four basic models of indirect pharmacodynamic responses. *J Pharmacokinet Biopharm* 21: 457-478.
- Doursout MF, Wouters P, Kashimoto S, Hartley CJ, Rabinovitz R, Chelly JE (2001). «Measurement of cardiac function in conscious rats.» *Ultrasound Med Biol.* 27(2): 195-202.
- Ebadi M (2008). *Desk Reference of Clinical Pharmacology.* Taylor, Francis Group: Boca Raton Florida (book).
- Francheteau P, Steimer JL, Merdjan H, Guerret M, Dubray C (1993). A mathematical model for dynamics of cardiovascular drug action: application to intravenous dihydropyridines in healthy volunteers. *J Pharmacokinet Biopharm* 21: 489-514.
- Frohlich ED (1989). Angiotensin converting enzyme inhibitors. Present and future. *Hypertension* 13: 1125-130.
- Gasparyan AY, Aivazyan L, Cocco G, Kitas GD (2012). Adverse cardiovascular effects of antirheumatic drugs: implications for clinical practice and research. *Curr Pharm Des* 18: 1543-1555.
- Guth BD (2007). Preclinical cardiovascular risk assessment in modern drug development. *Toxicol Sci* 97: 4-20.
- Hamilton CA, Reid JL, Vincent J (1985). Pharmacokinetic and pharmacodynamic studies with two alpha-adrenoceptor antagonists, doxazosin and prazosin in the rabbit. *Br J Pharmacol* 86: 79-87.
- Hong Y, Dingemans J, Mager DE (2008). Pharmacokinetic/pharmacodynamic modeling of renin biomarkers in subjects treated with the renin inhibitor aliskiren. *Clin Pharmacol Ther* 84: 136-143.
- Ikegaki I, Hattori T, Yamaguchi T, Sasaki Y, Satoh SI, Asano T *et al.* (2001). Involvement of Rho-kinase in vascular remodeling caused by long-term inhibition of nitric oxide synthesis in rats. *Eur J Pharmacol* 427: 69-75.
- Levick JR (2003). *An introduction to cardiovascular physiology.* Hodder Arnold Publishers: London (book).
- Li P, Callery PS, Gan LS, Balani SK (2007). Esterase inhibition attribute of grapefruit juice leading to a new drug interaction. *Drug Metab Dispos* 35: 1023-31.
- Lin JH, Chen IW, Ulm EH, Duggan DE (1988). Differential renal handling of angiotensin-converting enzyme inhibitors enalaprilat and lisinopril in rats. *Drug Metab Dispos* 16: 392-396.
- Louis WJ, Howes LG (1990). Genealogy of the spontaneously hypertensive rat and Wistar-Kyoto rat strains: implications for studies of inherited hypertension. *J Cardiovasc Pharmacol* 16: S1-5.
- Kappos L, Antel J, Comi G, Montalban X, O'Connor P, Polman CH *et al.* (2006). Oral fingolimod (FTY720) for relapsing multiple sclerosis. *N Engl J Med.*, 355, 1124-1140.

- Kappos L, Radue EW, O'Connor P, Polman C, Hohlfeld R, Calabresi P *et al.* (2010). A placebo-controlled trial of oral fingolimod in relapsing multiple sclerosis. *N Engl J Med.*, 362, 387-401.
- Kilkenny C, Browne W, Cuthill IC, Emerson M, Altman DG (2010). NC3Rs Reporting Guidelines Working Group. *Br J Pharmacol* 160: 1577-1579.
- Masumoto A, Hirooka Y, Shimokawa H, Hironaga K, Setoguchi S, Takeshita A (2001). Possible involvement of Rho-kinase in the pathogenesis of hypertension in humans. *Hypertension* 38: 1307-1310.
- McGrath J, Drummond G, McLachlan E, Kilkenny C, Wainwright C (2010). Guidelines for reporting experiments involving animals: the ARRIVE guidelines. *Br J Pharmacol* 160: 1573-1576.
- Michalewicz L, Messerli FH (1997). Cardiac effects of calcium antagonists in systemic hypertension. *Am J Cardiol* 79: 39-46.
- Perez-Reyes E, Van Deusen AL, Vitko I (2009). Molecular pharmacology of human Cav3.2 T-type Ca²⁺ channels: block by antihypertensives, antiarrhythmics, and their analogs. *J Pharmacol Exp Ther* 328: 621-627.
- Perlstein I, Stepanyk D, Krzyzanski W, Hoffman A (2002). A signal transduction pharmacodynamic model of the kinetics of the parasympathomimetic activity of low-dose scopolamine and atropine in rats. *J Pharm Sci* 91, 2500-10.
- Pinto YM, Paul M, Ganten D (1998). Lessons from rat models of hypertension: from Goldblatt to genetic engineering. *Cardiovasc Res* 39, 77-88.
- Ploeger BA, van der Graaf PH, Danhof M (2009). Incorporating receptor theory in mechanism-based pharmacokinetic-pharmacodynamic (PK-PD) modeling. *Drug Metab Pharmacokinet* 24: 3-15.
- Reid JL, Elliott HL, Vincent J, Meredith PA (1987). Clinical pharmacology of selective alpha blockers. Hemodynamics and effects on lipid levels. *Am J Med* 82: 15-20.
- Segre G, Cerretani D, Bruni G, Urso R, Giorgi G (1998). Amiloride pharmacokinetics in rat. *Eur J Drug Metab Pharmacokinet* 23: 218-22.
- Snelder N, Ploeger BA, Luttringer O, Rigel DF, Webb RL, Feldman D *et al.* (2013a). PKPD modeling of the interrelationship between mean arterial blood pressure, cardiac output and total peripheral resistance in conscious rats. *Br J Pharmacol*, 169, 1510-1524.
- Snelder N, Ploeger BA, Luttringer O, Rigel DF, Webb RL, Feldman D *et al.* (2013b). PAGE 22, Abstr 2686 [www.page-meeting.org/?abstract=2686]
- Stopher DA, Beresford AP, Macrae PV, Humphrey MJ (1988). The metabolism and pharmacokinetics of amlodipine in humans and animals. *J Cardiovasc Pharmacol* 12: S55-59.
- Sudano I, Flammer AJ, Roas S, Enseleit F, Noll G, Ruschitzka F (2012). Nonsteroidal antiinflammatory drugs, acetaminophen, and hypertension. *Curr Hypertens Rep* 14: 304-309.
- van Steeg TJ, Krekels EH, Freijer J, Danhof M, de Lange EC (2010). Effect of altered AGP plasma binding on heart rate changes by S(-)-propranolol in rats using mechanism-based estimations of in vivo receptor affinity (K(B,vivo)). *J Pharm Sci* 99: 2511-2520.
- Veerman DP, Imholz BP, Wieling W, Wesseling KH, van Montfrans GA (1995). Circadian profile of systemic hemodynamics. *Hypertension* 26: 55-59.
- Visser SA, Sallstrom B, Forsberg T, Peletier LA, Gabrielsson J (2006). Modeling drug-and system-related changes in body temperature: application to clomethiazole-induced hypothermia, long-lasting tolerance development, and circadian rhythm in rats. *J Pharmacol Exp Ther* 317, 209-219.
- West GB, Brown JH, Enquist BJ (1999). "The fourth dimension of life: fractal geometry and allometric scaling of organisms." *Science*. 284(5420):1677-1679.

Abbreviations

Amp	Amplitude
BP	Blood pressure
<i>BSL_CO</i>	Baseline value of cardiac output
<i>BSL_HR</i>	Baseline value of heart rate
<i>BSL_MAP</i>	Baseline value of mean arterial pressure
<i>BSL_SV</i>	Baseline value of stroke volume
<i>BSL_TPR</i>	Baseline value of total peripheral resistance
C	drug concentration in plasma
CO	Cardiac output
CVS	Cardiovascular system
Emax	Maximum effect
EC50	Concentration resulting in a half-maximal effect
FB	Negative feedback of mean arterial pressure
<i>FBO</i>	Feedback of a typical subject
<i>FBO_MAP</i>	Exponent of the power relationship between FB and the individual <i>BSL_MAP</i>
HCTZ	Hydrochlorothiazide
<i>hor</i>	Horizontal displacement
HR	Heart rate
IIV	Inter-individual variability
K_{in_HR}	Zero-order production rate constant of heart rate
K_{in_SV}	Zero-order production rate constant of stroke volume
K_{in_TPR}	Zero-order production rate constant of total peripheral resistance
k_{out_HR}	First-order dissipation rate constant of heart rate
k_{out_SV}	First-order dissipation rate constant of stroke volume
k_{out_TPR}	First-order dissipation rate constant of total peripheral resistance
LVFT	Left ventricular filling time
MAP	Mean arterial pressure
MC	Methylcellulose
MoA	Mechanisms of action
MVOF	Minimum value of the objective function
PD	Pharmacodynamics
PK	Pharmacokinetics
PKPD	Pharmacokinetic-pharmacodynamic
RAAS	Renin-angiotensin-aldosterone system
SHR	Spontaneously hypertensive rats
SV	Stroke volume
T	Time

TPR Total peripheral resistance
WKY Wistar Kyoto rats

Appendix

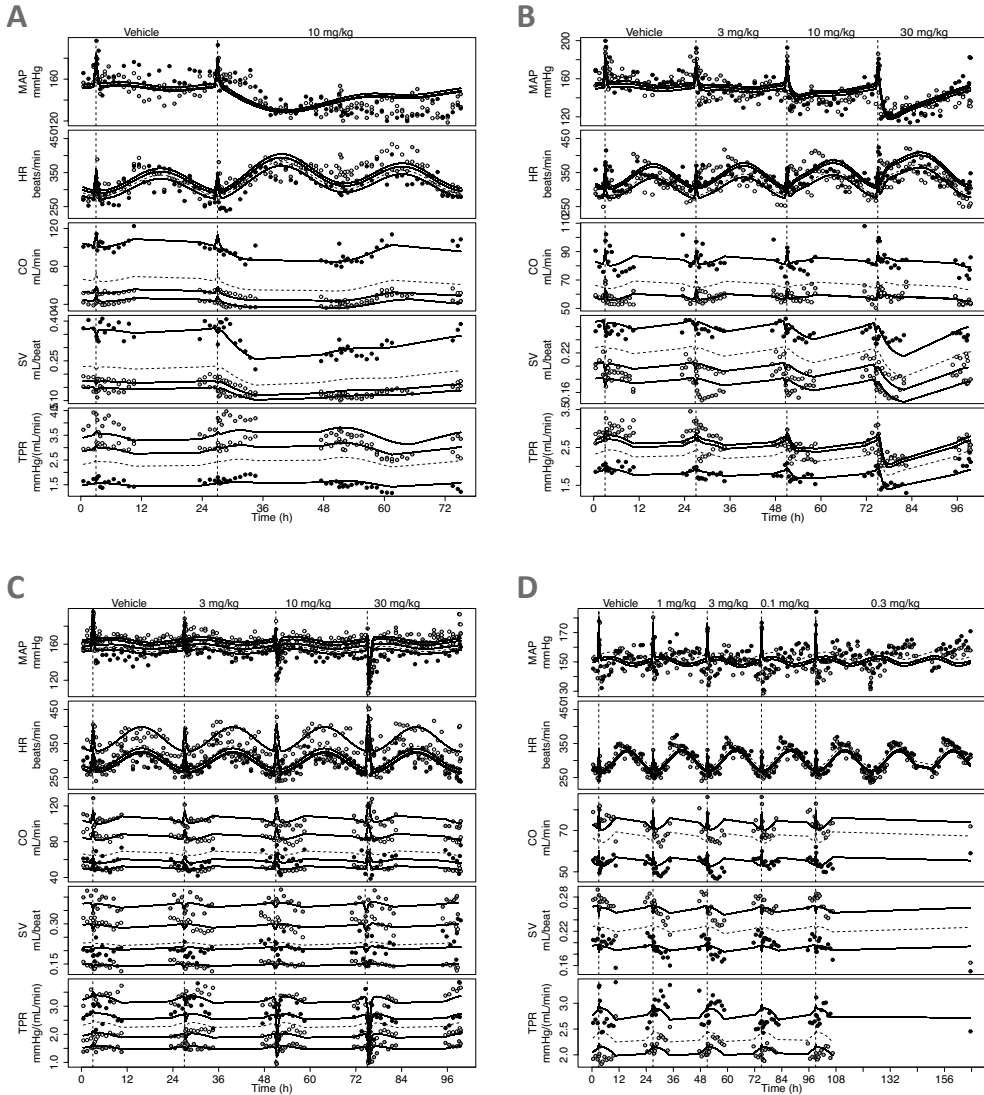
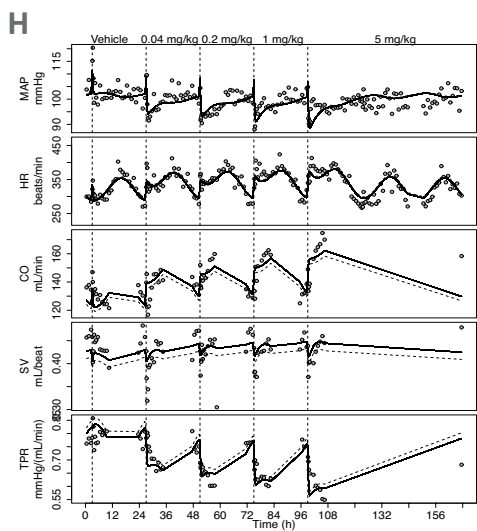
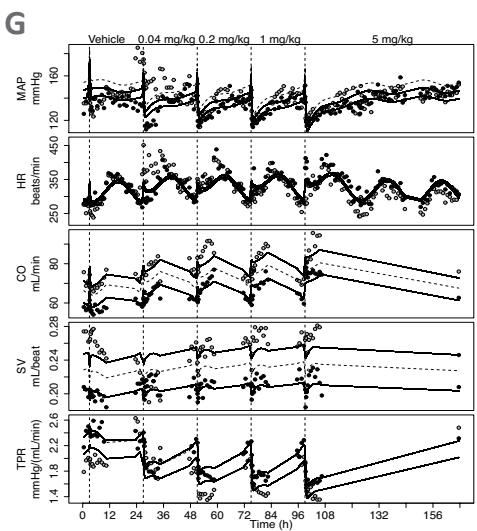
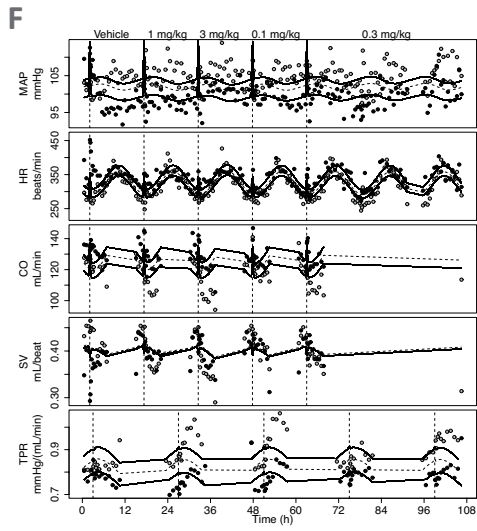
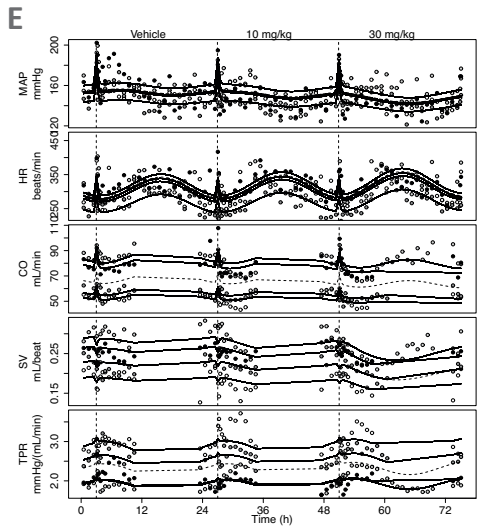


Figure A: Description of the effects of amiloride in SHR (plot A), enalapril in SHR (plot B), fasudil in SHR (plot C), HCTZ part a in SHR (plot D), HCTZ part b in SHR (plot E), HCTZ part a in WKY rats (plot F), prazosin in SHR (plot G) and prazosin in WKY rats (plot H). Data are from Study 1, in which vehicle and a different dose of amiloride (10 mg/kg p.o.), enalapril (3, 10 and 30 mg/kg p.o.), fasudil (3, 10 and 30 mg/kg p.o.), HCTZ (part a: 1, 3, 0.1 and 0.3 mg/kg p.o; part b: 10 and 30 mg/kg p.o.) or prazosin (0.04, 0.2, 1 and 5 mg/kg p.o.) were administered on separate days. *Fasudil and prazosin have an inhibiting effect on TPR. Therefore, TPR decreases after administration of these compounds. As a result of the indirect feedback HR and CO increase. SV first decreases due to the direct inverse relationship between HR and SV. Subsequently, this decrease is reversed by the indirect feedback. Enalapril inhibits TRP.*



Therefore, the influence on the parameters of the CVS is similar to the influence of fasudil and prazosin. However, as enalapril also has an inhibiting effect on SV the initial decrease in SV is not reversed by the indirect feedback. Amiloride and HCTZ have an inhibiting effect on SV. Therefore, SV and, consequently, CO, decrease after administration of these compounds. As a result of the indirect feedback HR and TPR increase. MAP changes in the same direction as the initial effect for all compounds. The dots represent the observations of different rats (colored in different shades of grey by rat). The continuous and dashed lines represent the individual and population predictions by the developed extended CVS model after administering amiloride, enalapril, fasudil, HCTZ or prazosin.

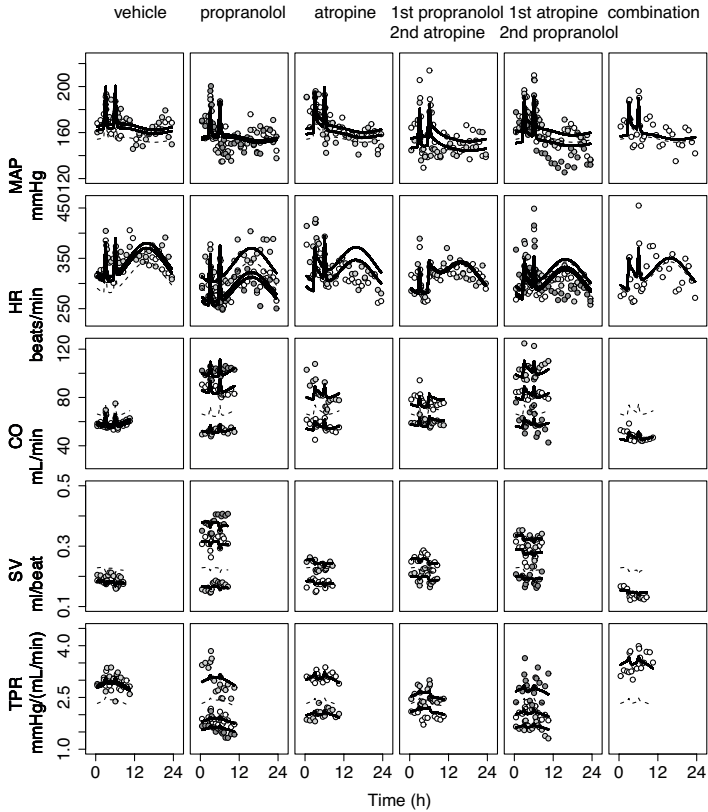
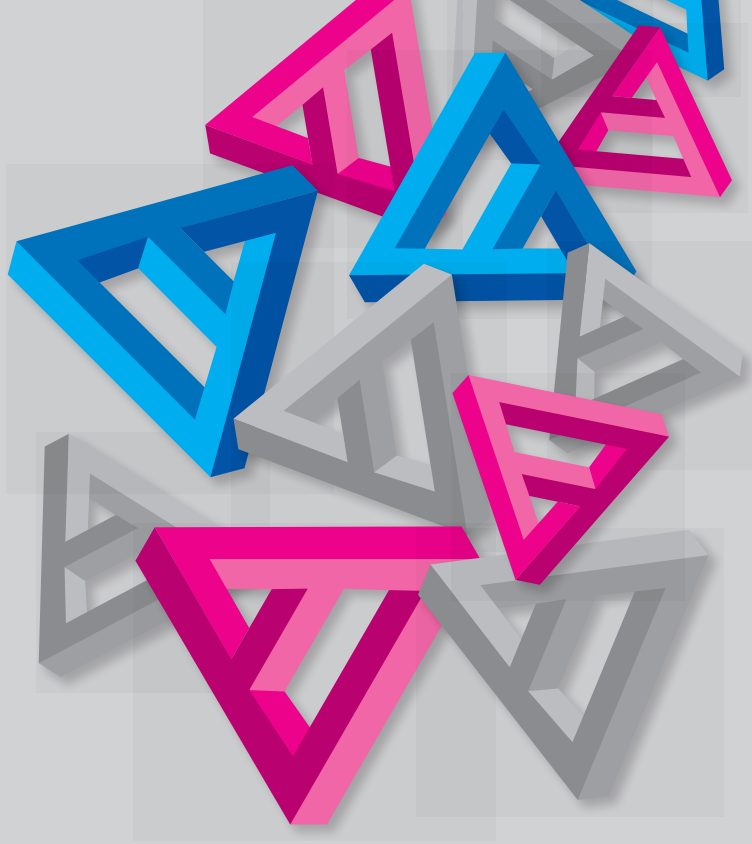


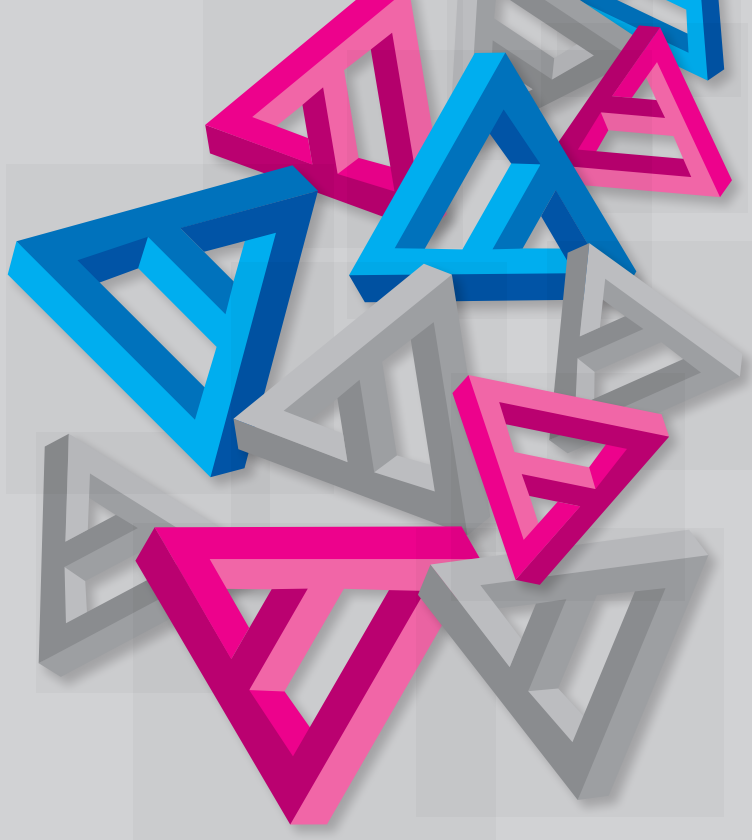
Figure B: Description of the effects of atropine and propranolol. Data are from Study 2, in which atropine (10 mg/kg) and/or propranolol (30 mg/kg) were administered alone, sequentially with a 3 hour interval or simultaneously on separate days.

Atropine has a stimulating effect on HR. Therefore, HR and, consequently, CO, increase after administration of atropine. As a result of the indirect feedback SV and TPR decrease. MAP changes in the same direction as the initial effect. The effect of propranolol was too small to be quantified. The dots represent the observations of different rats (colored in different shades of grey by rat). The continuous and dashed lines represent the individual and population predictions by the developed extended CVS model.



SECTION III

Application of the developed systems pharmacology model to S1P receptor agonists



CHAPTER 5

Translational pharmacokinetic modeling of fingolimod as a paradigm compound subject to sphingosine kinase-mediated phosphorylation

N. Snelder, B.A. Ploeger, O. Luttringer, D.R. Stanski and M. Danhof

Drug Metabolism and Disposition; Submitted

Summary

A complicating factor in the translational pharmacology of sphingosine 1-phosphate (S1P) agonists is that they exert their pharmacological effect through their respective phosphate metabolites, which are formed by the enzyme sphingosine kinase (S1PHK). In this investigation, we present a semi-mechanistic pharmacokinetic model for the inter-conversion of S1PHK substrates and their respective phosphates in rats and humans with the aim of investigating whether characterization of the rate of phosphorylation in blood platelets constitutes a basis for interspecies scaling using fingolimod as a paradigm compound. Data on the time course of fingolimod and fingolimod-phosphate (fingolimod-P) blood concentrations following intravenous and oral administration of fingolimod and/or fingolimod-P in rats and following oral administration of fingolimod in doses of 0.5, 1.25 and 5 mg once daily in healthy volunteers were analyzed in conjunction with data on the *ex vivo* inter-conversion and blood-plasma distribution in rat and human blood, respectively. Integrating the data from the *ex vivo* and *in vivo* studies enabled prediction of fingolimod and fingolimod-P concentrations in plasma rather than blood, which are more relevant for predicting drug effects. Large interspecies differences in the rate of phosphorylation between rats and humans were quantified. In human, phosphorylation of fingolimod in the platelets was 4 times slower compared to rat, whereas the de-phosphorylation rates were comparable in both species. This partly explained the 12-fold over-prediction of fingolimod-P exposure in human when applying an allometric scaling approach on the developed rat model. Additionally, differences in pre-systemic phosphorylation should also be taken into account.

Introduction

Fingolimod is a sphingosine 1-phosphate (S1P) receptor modulator, which is effective in the treatment of multiple sclerosis (Cohen *et al.*, 2010). The active metabolite of fingolimod, fingolimod-phosphate (fingolimod-P) binds to 4 of the 5 subtypes of the S1P receptor (S1P₁ and S1P₃₋₅) with high affinity (0.3-3.1nM) (Mandala *et al.*, 2002; Brinkmann, 2007; Brinkmann *et al.*, 2004; Chun and Hartung, 2010). In contrast, the affinity of fingolimod for all S1P receptors is low (Hale *et al.*, 2004; Albert *et al.*, 2005). The phosphorylation of fingolimod is therefore a critical step in its pharmacological effect. With the discovery of fingolimod and the elucidation of its mechanism of action, the search for other S1P agonists with different pharmacokinetic (PK)-pharmacodynamic (PD) properties has been propelled. Currently available S1P agonists can be categorized into two classes: amino alcohol pro-drugs and second-generation direct agonists (Cusack and Stoffel, 2010). The first class of compounds, to which fingolimod belongs, owes its biological activity to phosphorylation by the enzyme sphingosine kinase (S1PHK) (Billich *et al.*, 2003; Kihara and Igarashi, 2008; Kharel *et al.*, 2005). There are important inter-species differences in the expression and function of S1PHK. In the rat, S1PHK is predominately expressed in the kidney, spleen and liver tissue (Olivera *et al.*, 1998). In humans, S1PHK1, which is one of the two S1PHK isoforms, is mainly expressed in lung and spleen, whereas the other isoform, S1PHK2, is predominantly expressed in liver and heart tissue (Liu *et al.*, 2000; Paugh *et al.*, 2003). These large inter-species differences complicate the prediction of exposure to phosphorylated S1P pro-drugs in humans using *in vivo* animal data. Therefore, an allometric scaling approach, which does not consider inter-species differences in enzyme tissue distribution or enzyme activity, will not be applicable to S1P pro-drugs. Since an adequate characterization of the exposure in rat and human may be important for translational modeling (Danhof *et al.*, 2008) a qualitative and quantitative understanding of differences in the PK of S1PHK substrates between rat and human must be considered.

Fingolimod is an interesting paradigm compound to investigate the pharmacokinetics of S1PHK substrates since the inter-conversion between fingolimod and its phosphate has been well investigated in several *in vitro*, *in vivo* and *ex vivo* studies (Albert *et al.*, 2005; Billich *et al.*, 2003; Kihara and Igarashi, 2008; Olivera *et al.*, 1998; Liu *et al.*, 2000; Kovarik *et al.*, 2007). From *ex vivo* studies it is known that fingolimod is phosphorylated in the blood platelets (Albert *et al.*, 2005; Kihara and Igarashi, 2008; Anada *et al.*, 2007). We hypothesize that characterization of the inter-conversion between fingolimod and fingolimod-P in blood platelets may constitute a basis for the scaling of the PK between rats and humans. To date, no PK models have been published that describe the time course of the fingolimod and fingolimod-P concentrations simultaneously. Since the conversion between fingolimod and its phosphate is a reversible and dynamic process it

is anticipated that the PK of fingolimod-P is closely linked to the PK of fingolimod. Therefore, a simultaneous analysis of the *in vivo* concentration-time course of fingolimod and fingolimod-P and the *ex vivo* inter-conversion, and blood-plasma distribution will yield an understanding of the dynamics of the overall inter-conversion and the relevance of the inter-conversion in blood platelets. Moreover, characterizing the blood to plasma distribution allows the prediction of the fingolimod-P plasma concentrations rather than whole blood concentrations, which are the relevant concentrations for the modeling of pharmacodynamic effects in future pharmacokinetic pharmacodynamic investigations.

In this investigation, we present a semi-mechanistic population PK model for the inter-conversion of S1PHK substrates and their respective phosphates using fingolimod as a paradigm compound with the aim a) to investigate whether characterization of the inter-conversion in blood (platelets) constitutes a basis for the scaling of the PK between rats and humans and b) to predict the time course of plasma (rather than whole blood) concentrations of phosphate metabolites.

Materials and Methods

An overview of the studies used to characterize the PK of fingolimod(-P) in rat and human can be found in Table 1.

Ex vivo studies

Three *ex vivo* experiments were performed in isolated blood from male albino rats of strain Hanover Wistar and human blood obtained from healthy male volunteers (Blutspendezentrum SRK, Basel, Switzerland). Experiment A was an inter-conversion experiment in which (rat and human) blood samples (~ 6 mL) were spiked with a fingolimod or fingolimod-P spiking solution (20 µg/mL; solvent: ethanol abs: 1 M HCl (95:5, w:w)) to achieve final concentrations of 100 ng/mL fingolimod and fingolimod-P. In total, 11 samples were incubated at 37°C with gentle agitation. 0.8 mL aliquots were taken after 0, 1, 2, 4, 7, 24 and 48 h of incubation, immediately frozen on dry ice and stored at – 80°C. Fingolimod and fingolimod-P blood concentrations were determined by LC/MS/MS after liquid/liquid extraction. The lower limits of quantification (LOQ) were 1.08 and 2.5 ng/mL for fingolimod and fingolimod-P, respectively. Experiments B and C investigated the blood/plasma distribution of fingolimod-P. In experiment B the time dependency of blood/plasma distribution (time points: 0.25, 0.5, 1, 2 and 4 h) was studied for a concentration of 30 ng/mL [¹⁴C]fingolimod-P in rat blood and at 30 and 300 ng/mL [¹⁴C]fingolimod-P in human blood. Experiment C investigated the fingolimod-P blood/plasma distribution for the nominal concentrations of 3, 30, 300 and 3000 ng/mL [¹⁴C]fingolimod-P in trip-

licate (in addition at 1 and 0.3 ng/mL for human). Samples were incubated for 120 min at 37°C with constant agitation on an orbital shaker. In experiments B and C separation of cells and plasma was achieved by centrifugation (1500 g, 10 min, 37°C). Samples for quantification of total radioactivity were taken before and after (plasma fraction only) centrifugation. The radioactivity in the biological samples was measured by LSC with Irga-Safe Plus (Packard) as Scintillator. Radiometry was performed in TriCarb 2500 TR and 2700 TR Liquid Scintillation Systems (Packard Instr. Co., Meriden, CT, USA). Concentrations of radiolabeled substances in plasma and blood were determined in weighed samples. Data were converted from dpm/g to ng/mL assuming a density of 1.00 g/mL for all samples and using the specific radioactivity.

Studies in rat

The studies in rats were conducted in accordance with the Guide for the Care and Use of Laboratory Animals as adopted and promulgated by the U.S. National Institutes of Health. Study 1, was a single dose PK-PD study in which fingolimod and fingolimod-P concentrations were measured following intravenous (iv) and oral administration of fingolimod, in male, Lewis rats. Rats were provided normal chow and water *ad libitum*. Study 2, was a study on the PK of fingolimod and fingolimod-P after single iv administration of fingolimod or fingolimod-P, in male Sprague Dawley rats (Charles River, France). At the time of study, body weights ranged from 296-318 gram. Rats were provided normal chow (NAFAG pellets No. 890, ECOSAN Eberle NAFAG AG, Gossau, Switzerland) and tap water *ad libitum*. In these pharmacokinetic investigations the vena femoralis was cannulated for compound administration and the arteria femoralis for blood sample collection. Following cannulation, a recovery period of 72 h was observed. Meloxicam was used for post-surgery analgesia (1-2 mg/kg, subcutaneously). Cannulae were filled with aqueous heparin solution. During the recovery time, the functional capability of the cannulae was regularly tested.

Studies in healthy volunteers

The studies in healthy volunteer were conducted in accordance with the Declaration of Helsinki. The protocols for studies 2105, 2213 and 2215 were approved by local medical ethics committees and written informed consent was obtained from all subjects. Subjects were judged eligible for the studies if they were aged between 19 and 50 years or between 18 and 45 years for studies 2105 and 2213/2215, respectively. In addition, all subjects were in good health as determined by past medical history, physical examination, vital signs, electrocardiogram, and laboratory tests at screening.

Table 1: Study overview

Rat					
Study	Description	Dosing regimen	Route	Blood sample collection	Measured
1	Single dose PKPD study in Lewis rat	Single iv fingolimod dose: 1 mg/kg or single oral fingolimod dose: 0.1, 0.3, 1 or 3 mg/kg (n=3, per group)	iv and oral	iv: 0, 0.25, 0.5, 1, 2, 6, 24 and 48 h after dose oral: 0, 1, 2, 6, 24, 48, 96, 168, 216, 264 and 336 h after dose	fingolimod and fingolimod-P
2	Pharmacokinetics of fingolimod and fingolimod-P in male Sprague Dawley rats after single intravenous administration of fingolimod or fingolimod-P	Single iv fingolimod dose: 1 mg/kg or single iv fingolimod-P dose: 0.1 mg/kg (n=3, per group)	iv	0.0083, 0.0167, 0.025, 0.033, 0.0833, 0.1667, 0.5 and 1 h after dose	fingolimod and fingolimod-P
Human					
Study	Description	Dosing regimen	Route	Sampling scheme	Measured
2105	randomized, double-blind, placebo-controlled, multiple dose study in healthy subjects	Once-daily dosing of 0.5 mg fingolimod (n=12), 1.25 mg fingolimod (n=12), or placebo (n=12) for 14 days	oral	Day 1: predose, 1, 2, 6, 8, 12, 16, 20 and 24 h after dose. Days 3 and 7: predose (trough). Days 28 and 42: any time	fingolimod and fingolimod-P
2213	randomized, double-blind, placebo-controlled, multiple dose study in healthy subjects (Kovarik, 2004)	Once-daily dosing of 1.25 mg fingolimod (n=20), 5 mg fingolimod (n=20), or placebo (n=20) for 7 days	oral	Days 1 and 7: predose, 1, 2, 6, 8, 12, 16, 20 and 24 h after dose. Days 2 to 6: before (trough) and 6-8 h (peak) after the daily dose	fingolimod
2215	randomized, single-blind, placebo-controlled, time-lagged, ascending single dose study in healthy subjects	Single dose of 5, 7.5, 10, 15, 25 or 40 mg fingolimod (n=6, per group) or placebo (n=2, per group)	oral	predose, 0.25, 0.5, 1, 1.5, 2, 3, 4, 6, 8, 12, 24, 36, 48, 72, 96, (120), 168, 264, 600 and 936 h after the first dose	fingolimod and fingolimod-P

Bioanalytics

Venous blood samples were collected according to the sampling schemes described in Table 1. Blood concentrations were determined by a validated liquid chromatography method with mass spectrometry detection. Samples were analyzed following liquid-liquid extraction (Kovarik *et al.*, 2004). In the studies in rats, the LOQ's were 0.250 and 1 ng/mL for fingolimod and fingolimod-P, respectively. In the clinical studies the LOQ was 0.080 ng/mL for fingolimod. For fingolimod-P, the LOQ's were and 0.1 and 1 ng/mL in studies 2105 and 2215, respectively. Assay accuracy ranged from 97.5% to 108.7% and precision coefficients of variation from -2.5% to 8.7%.

Population PK modeling strategy

Two PK models were developed, i.e. one model to characterize the PK of fingolimod and fingolimod-P in rat and one model to characterize the PK of fingolimod and fingolimod-P in human. The rat PK model was developed using data from studies 1 and 2 and the *ex vivo* studies in rat blood. The human PK model was developed using data from studies 2105 and 2213 and the *ex vivo* studies in human blood. Data from study 2215 were used for (external) evaluation of the predictive value of the model.

Only physiologically plausible models were evaluated, i.e. all evaluated models were based on the knowledge from published *in vitro*, *in vivo* and *ex vivo* studies. Briefly, the following is known about the inter-conversion between fingolimod and its phosphate.

- i) Fingolimod is phosphorylated peripherally (Olivera *et al.*, 1998; Liu *et al.*, 2000), in the platelets in blood (Albert *et al.*, 2005), and pre-systemically during first-pass in the liver upon oral administration (Kovarik *et al.*, 2007).
- ii) Fingolimod-P is dephosphorylated back to fingolimod before it is eliminated from the body (Zollinger *et al.*, 2011).
- iii) Dephosphorylation occurs only in the plasma. Fingolimod-P is dephosphorylated by the enzyme lipid phosphatase type 3 (LLP3) (Kihara and Igarashi, 2008), which is expressed in the plasma membrane on cells exposed to plasma such as vascular endothelial cells and blood cells (Kihara and Igarashi, 2008).

One-, two- and three-compartmental models were evaluated to describe the disposition of fingolimod and fingolimod-P. Furthermore, it was investigated if the absorption from the gastrointestinal-tract (dose compartment) to the blood (central compartment) could be described with first- or zero-order processes. In addition, an exploratory graphical analysis of the dose-normalized raw fingolimod and fingolimod-P blood concentrations indicated that absorption, distribution and/or inter-conversion might be non-linear with

dose/concentration. Therefore, it was evaluated if the description of the data could be improved by describing the absorption, distribution or inter-conversion by saturable processes, i.e. by Michaelis-Menten like processes (Equation 1) or by saturable binding to plasma proteins (Equation. 2).

$$\text{SPK} = A(x) * \frac{Vm}{Km + C(x)} \quad (1)$$

In this equation $A(x)$ is the amount in compartment x , $C(x)$ is the concentration in compartment x , Vm is the maximum rate of biotransformation and Km is the concentration at which the half maximal rate of biotransformation is reached. The term SPK is used to represent saturation of a certain mechanism, e.g. a saturable distribution or saturable inter-conversion. It results in a sigmoid relationship approaching a maximum at infinitely high concentration.

$$\text{phi} = \frac{(C - B_{\max} - Kd) + \sqrt{(C - B_{\max} - Kd)^2 + 4 * Kd * C}}{2 * C} \quad (2)$$

In case of saturable binding, in this equation, phi is the free fraction, C is the total concentration in the plasma and B_{\max} and Kd are the binding capacity and binding affinity, respectively.

Allometric scaling

The PK of fingolimod and fingolimod-P in human was also predicted from the rat model using an allometric scaling approach (West *et al.*, 1999). This approach describes how biological properties vary with body mass. As the fingolimod and fingolimod-P plasma protein binding is comparable for rat and human, predictions were not corrected for differences in the unbound fraction. Mean body weights of human and rat were assumed to be 70 and 0.3 kg, respectively. All rate constants were scaled with an allometric exponent of - 0.25 and an exponent of 1 was used for scaling the volume of distribution. The absorption was not scaled, according to the assumption that the bioavailability ($F1$) and absorption rate constant (ka) equal the average $F1$ and ka of the values in different preclinical species as determined in compartmental PK models (Vuppugalla *et al.*, 2011). As we described the PK of fingolimod and fingolimod-P only in rat, this yields the situation where the values of $F1$ and ka are the same in rat and human.

Computation

Data from the *in vivo* and *ex vivo* studies were analyzed simultaneously using the non-linear mixed-effects modeling approach implemented in NONMEM (version 7.1.0; Icon Development Solutions, Ellicott City, Maryland, USA). The models were compiled using Digital Fortran (version 6.6C3, Compaq Computer Corporation, Houston, Texas) and executed on a PC equipped with an AMD Athlon 64 processor 3200+ under Windows XP. The results were analyzed using the statistical software package S-Plus for Windows (version 6.2 Professional, Insightful Corp., Seattle, USA). Parameters were estimated using the first order conditional estimation method with interaction between the two levels of stochastic effects (FOCE interaction). Random effects were included as exponential terms reflecting lognormal distributions of model parameters. The residual variability was explored with proportional and additive error models. Goodness-of-fit was determined using the minimum value of the objective function defined as minus twice the log-likelihood. For nested models, a decrease of 10.8 points in the minimum value of the objective function (MVOF) (corresponding to $p < 0.001$ in a chi-squared distribution) by adding an additional parameter was considered significant. The goodness-of fit was also investigated by visual inspection of the plots of individual predictions and the diagnostic plots of (weighted) residuals. To evaluate the predictive value of the human pharmacokinetic model a visual predictive check (VPC) was performed in which the median and the 90% inter-quantile range of data simulated with the developed model were plotted together with the observations. In addition, the predictive value of the human pharmacokinetic model was externally validated with data from study 2215 using the same VPC technique.

Results

Rat PK model

The data from the rat *ex* and *in vivo* studies (studies 1 and 2) were described by the model depicted in Figure 1, (Rat). The phosphorylation of fingolimod was described by the combination of a first-order process in the platelets (k_{67}) and a first-order phosphorylation process in plasma (k_{34}), which is only relevant *in vivo*. *In vivo* dephosphorylation was found to be faster than the *ex vivo* dephosphorylation. This was accounted for by estimating an extra rate constant (k_{43b}), which is only relevant *in vivo*. The disposition of fingolimod and fingolimod-P were characterized by three-compartmental models with saturable distribution from the plasma to one of the peripheral compartments for fingolimod and fingolimod-P. The absorption and elimination of fingolimod were described by first-order processes (k_a and k_{30}). Fingolimod was also pre-systemically phosphorylated. As calculated from the absorption rates, 82% of the total fingolimod dose was converted

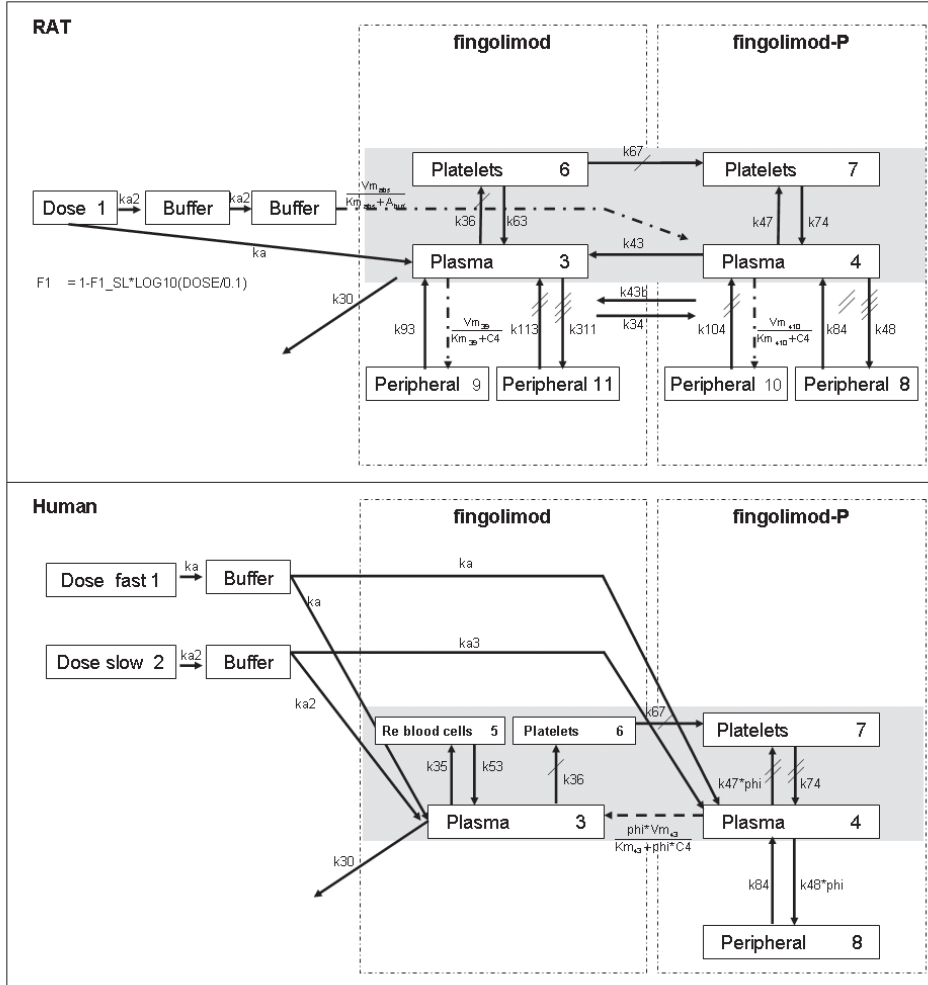


Figure 1: Pharmacokinetic models to describe the time course of the fingolimod and fingolimod-P blood concentration in rat and human. The grey area describes the inter-conversion and blood/plasma distribution in isolated blood. k_{xy} represent the first-order distribution and elimination rate constants. Arrows with an equal number of slashes indicate that these rates are the same. In addition, the dashed lines represent saturable processes.

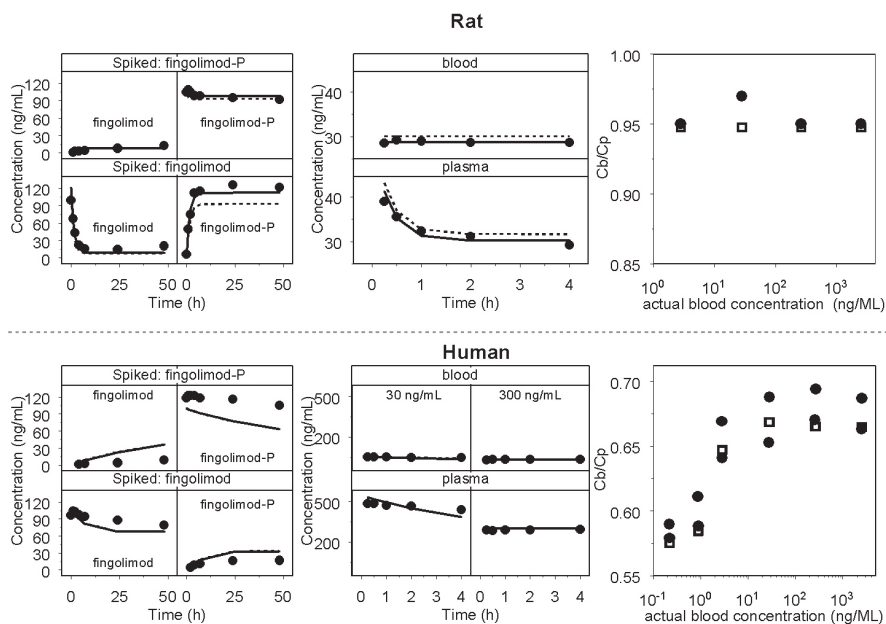


Figure 2: Description of the data from the *ex vivo* inter-conversion (A) and blood/plasma distribution (B and C) studies in isolated blood from rat (upper half) and human (lower half). The dots represent the observations and the continuous lines (A and B) and squares (C) represent the individual predictions. The dashed lines represent the population predictions.

to fingolimod-P before entering the blood. The absorption of the pre-systemically formed fingolimod-P was characterized by two transit compartments to describe observed delay in absorption. In addition, the absorption from the last transit compartment to the central compartment was described by a saturable Michaelis-Menten like process. The bioavailability was found to decrease from 1, for a dose of 0.1 mg/kg, to 0.36, for the highest orally administered dose, i.e. 3 mg/kg, according to a descriptive log-dose equation (Table 2), which is only valid in the observed dose range between 0.1 and 3 mg/kg. The *ex-vivo* blood volume ($V_{ex\ vivo}$) and *in vivo* central volume of distribution ($V_{in\ vivo}$) were allowed to vary between experiments and between individual rats (IIV). The residual errors for the *ex* and *in vivo* were best described by proportional residual error models with an extra additive residual error for *ex vivo* experiment A.

The developed model adequately described the inter-conversion between fingolimod and fingolimod-P as well as the blood-plasma distribution as can be seen in the description

Table 2: The parameter values from the PK models to describe the time course of the fingolimod and fingolimod(-P) blood concentrations in rat and human

Parameter	Rat				Human			
	Value	RSE	LLCI	ULCI	Value	RSE	LLCI	ULCI
blood								
k67 (1/h)	2.61	19.1	1.63	3.59	0.151	17.0	0.101	0.201
k43 (1/h)	0.0870	14.4	0.0625	0.112	—	—	—	—
VM ₄₃ (ng/(mL* <i>h</i>))	—	—	—	—	2.48	32.7	0.89	4.07
k36 (1/h)	fixed to k67	—	—	—	fixed to k67	—	—	—
k63 (1/h)	5.90	45.8	0.608	11.2	—	—	—	—
k35 (1/h)	—	—	—	—	0.195	21.2	0.114	0.276
k53 (1/h)	—	—	—	—	0.0328	12.7	0.0246	0.0410
k74 (1/h)	1.70	10.9	1.34	2.06	0.106	16.7	0.0713	0.141
k47 (fraction of k74)	0.773	1.68	0.748	0.798	1 fixed	—	—	—
KM ₄₃ (ng/mL)	—	—	—	—	0.729	27.4	0.337	1.12
B _{max} (ng/mL)	—	—	—	—	3.79	16.8	2.54	5.04
Kd (ng/mL)	—	—	—	—	0.0795	23.0	0.0436	0.115
V _{ex-vivo} (L)	1 fixed	—	—	—	1 fixed	—	—	—
1-hematocrit	0.535 fixed	—	—	—	0.55 fixed	—	—	—
disposition								
k30 (1/h)	3.67	12.2	2.79	4.55	0.104	12.6	0.0783	0.1297
V _{ex-vivo} (human: L; rat: L/kg)	0.211	11.0	0.166	0.256	475	8.44	396	554
k311 (1/h)	21.6	18.2	13.9	29.3	—	—	—	—
k113 (1/h)	1.75	9.43	1.43	2.07	—	—	—	—
k48 (1/h)	fixed to k311	—	—	—	fixed to VM ₄₃	—	—	—
k84 (1/h)	fixed to k113	—	—	—	0.0158	18.4	0.0101	0.0215
VM ₃₉ (ng/(mL* <i>h</i>))	3170	23.6	1706	4634	—	—	—	—
k93 (1/h)	26.6	21.4	15.4	37.8	—	—	—	—
KM ₃₉ (ng/mL)	43.0	30.0	17.7	68.3	—	—	—	—
VM ₄₁₀ (ng/(mL* <i>h</i>))	fixed to VM39	—	—	—	—	—	—	—
k104 (1/h)	fixed to k113	—	—	—	—	—	—	—
k34std1 (1/h)	16.4	10.3	13.1	19.7	—	—	—	—
k34std2 (1/h)	2.68	9.33	2.19	3.17	—	—	—	—
k43b (1/h)	4.82	8.57	4.01	5.63	—	—	—	—

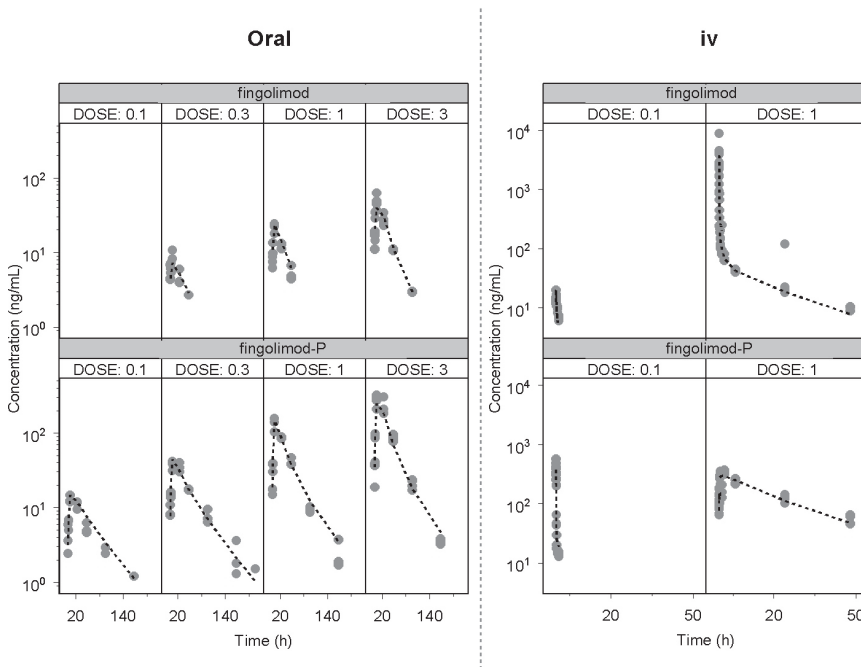


Figure 3: Description of the fingolimod and fingolimod-P blood concentrations from studies 1 and 2 after oral fingolimod (dose: 0.1, 0.3, 1, or 3 mg/kg) or intravenous administration of fingolimod (dose: 1 mg/kg) or fingolimod-P (dose: 0.1 mg/kg)

The grey dots represent the observations and the dashed lines represent the population predictions.

of the data from the *ex vivo* experiments (Figure 2, Rat). The *in vivo* time course of the fingolimod(-P) blood concentrations was also adequately described after both iv and oral administration of fingolimod (Figure 3). All parameters could be estimated with good precision as all standard errors were less than 50% of the parameter estimates (Table 2). The estimated clearance of 0.774 L/h/kg does not differ from the systemic clearance of 0.748 L/h/kg derived from a published physiologically based pharmacokinetic (PBPK) model (Meno-Tetang *et al.*, 2006).

Allometric scaling

The predicted PK of fingolimod and fingolimod-P in human after allometric scaling demonstrated that the fingolimod exposure was adequately predicted, but the fingolimod-P exposure was 12-fold over-predicted (Figure 4). Hence, an allometric scaling approach seems not applicable for predicting fingolimod-P exposure in human.

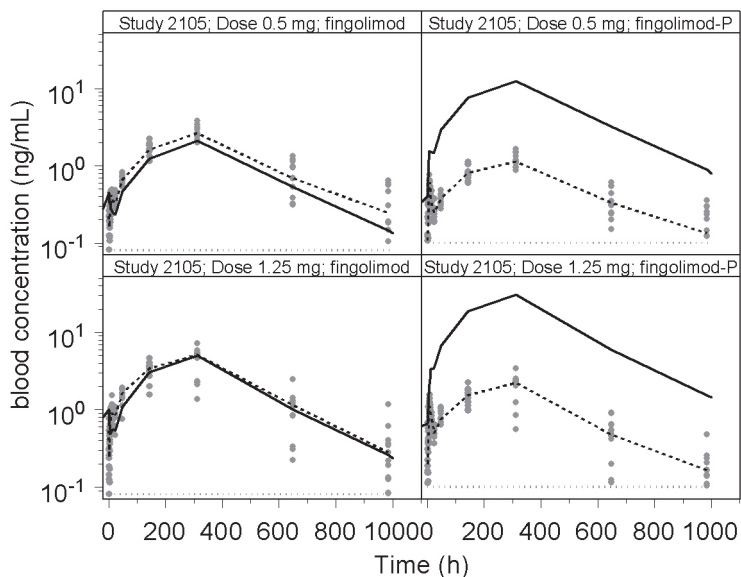


Figure 4: Prediction of the fingolimod and fingolimod-P blood concentrations from multiple dose studies 2105 in health volunteers using the allometrically scaled rat model

The grey dots represent the observations after administration of fingolimod (0.5 or 1.25 mg po) and the dashed lines represent the observed median. The continuous lines represent the predicted median.

Human PK model

The model to describe the data from the human *ex* and *in vivo* studies (studies 2213 and 2105) was comparable to the model to describe the rat data (Figure 1, Human). However, several differences are noticeable between the rat and human models. i) Only one peripheral compartment could be quantified to describe the distribution of fingolimod-P. ii) The phosphorylation and dephosphorylation processes in plasma, which were identified in rat, could not be quantified in human. Instead, the dephosphorylation in plasma was described by a saturable, Michaelis-Menten like process (Equation 1). iii) In human, two peaks were observed during the absorption phase. This was described by two dose compartments with a lag time for the absorption from the second dose compartment. iv) The distribution of fingolimod into the red blood cells could be quantified in human, whereas this process could not be quantified in rat. v) The distribution of fingolimod-P into the platelets and the peripheral compartment was found to be faster for higher concentrations. This was described by a saturable binding process (Equation 2) resulting in a higher blood/plasma

ratio for higher concentrations (Figure 2C, human). k_{30} and the $V_{in\ vivo}$ were allowed to vary between individual subjects. The residual errors for the *ex* and *in vivo* studies were best described by proportional residual error models.

In general, the developed model adequately described the data from the *ex vivo* studies (Figure 2, Human). In addition, the time course of the *in vivo* fingolimod and fingolimod-P blood concentrations was adequately described as the continuous lines, which represent the predicted median, closely resemble the observed median (dashed lines) (Figure 5). However, the observations from the 1.25 mg dose group in study 2105 were slightly over-predicted. For study 2213, the variability was adequately predicted as about 90% of the observations are within the 90% prediction interval (grey area) (Figure 5). For study 2105, the variability was slightly over-predicted. All parameters could be estimated with good precision as all standard errors were less than 50% of the parameter estimates (Table 2).

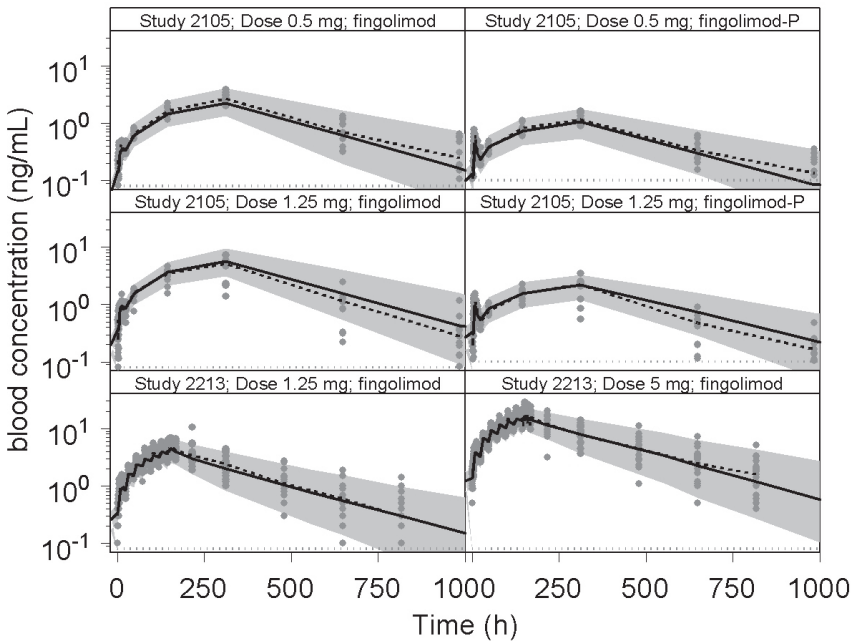


Figure 5: Visual predictive check of the description of the fingolimod and fingolimod-P blood concentrations from multiple dose studies 2105 and 2213 in health volunteers

The grey dots represent the observations after administration of fingolimod (0.5, 1.25 or 5 mg po) and the dashed lines represent the observed median. The continuous lines represent the predicted median and the grey area represents the 90% prediction interval.

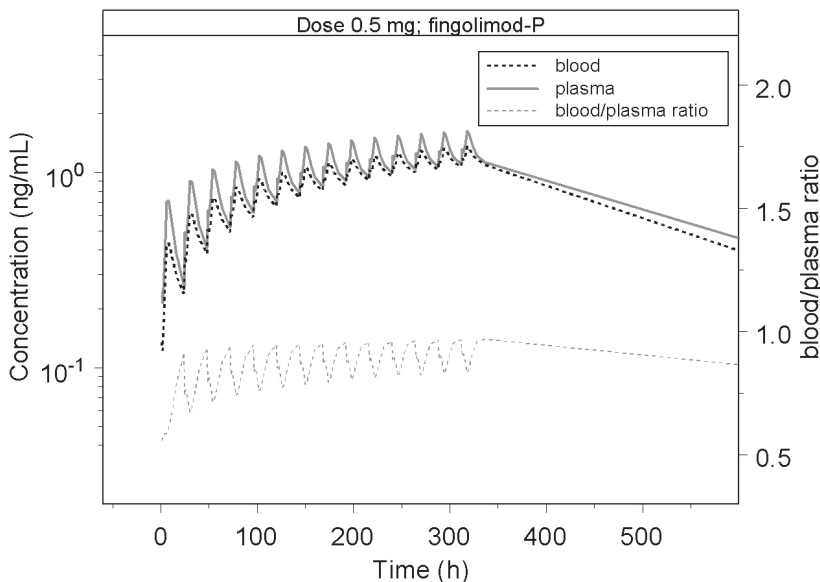


Figure 6: Predicted fingolimod-P blood and plasma concentrations and blood/plasma ratio after once daily administration of fingolimod during 14 days

The grey line represents the predicted fingolimod-P plasma concentration and the dashed lines black represents the predicted fingolimod-P blood concentration after administration of fingolimod (0.5 mg po). The dashed grey line represents the predicted blood/plasma ratio.

About 69% of the total fingolimod dose was converted to fingolimod-P before entering the blood. A comparison of the time course of the predicted fingolimod-P blood and plasma concentrations demonstrates that for a dose of 0.5 mg/day the fingolimod-P blood/plasma concentration ratio varies between 0.8 and 0.95 within a day at steady state. The difference between blood and plasma concentrations is the largest around t_{\max} (Figure 6). The developed model could, in general, adequately predict both the trend and the variability in the data from the external (i.e. study not used for model development) study 2215 (Figure 7). However, fingolimod and fingolimod-P concentrations observed in the 10 mg dose-group were slightly over-predicted. On the other hand the concentrations of 5 out of 6 subjects included in this treatment-group fall within the prediction interval. Therefore, this might be a chance observation, which is due to the low number of subjects. The observed concentrations of the 6th subject of this treatment are much lower than predicted, but also much lower than the observed concentrations in the lowest dose group. In addition, the maximum fingolimod-P concentrations are slightly under-predicted for the higher dose groups. This indicates that there might be another non-linear process involved that becomes relevant after administration of doses higher than 10 mg.

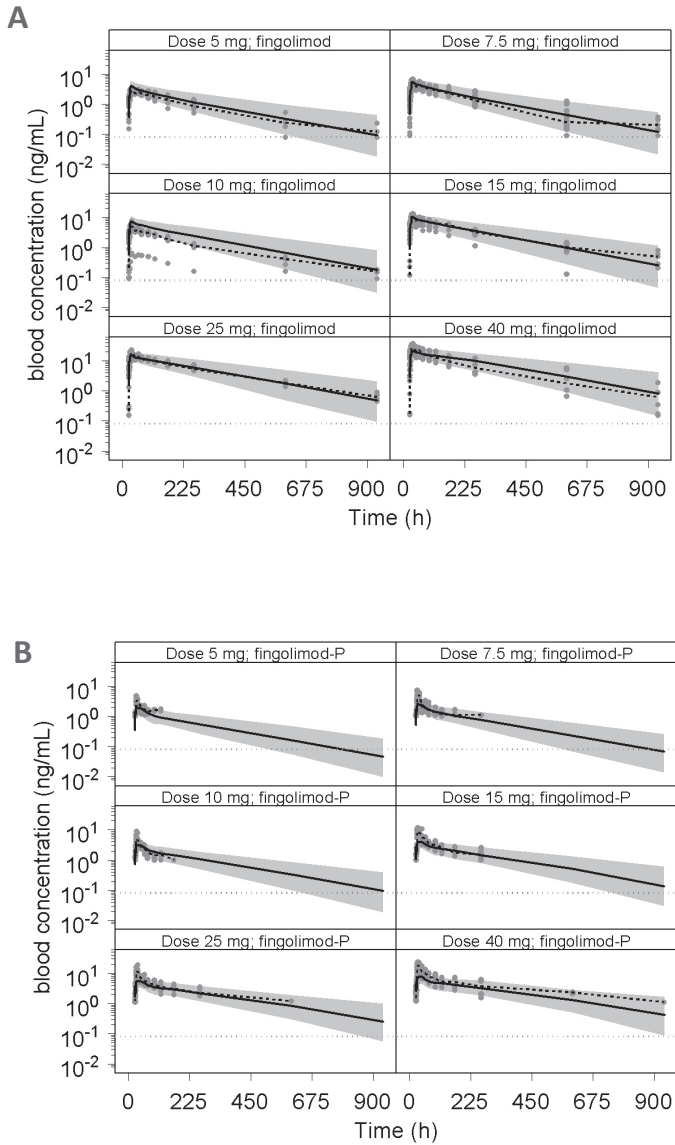


Figure 7: Prediction of the fingolimod and fingolimod-P blood concentrations from single dose study 2215 in health volunteers

The grey dots represent the observations after administration of fingolimod (5-40 mg po) and the dashed lines represent the observed median. The continuous lines represent the predicted median and the grey area represents the 90% prediction interval.

Comparison of exposure between rat and human

A comparison between the predicted steady-state fingolimod-P exposure in rat and human demonstrated that fingolimod-P exposure was about 10-12 fold lower in human as compared to rat for equivalent doses when following a dose-by-factor approach, which is commonly applied to scale the 'no-observed adverse effect level' (Figure 8)(Sharma and McNeill, 2009; FDA, 2010). This approach uses allometric scaling on the basis of body surface area. Generally, an exponent of 0.67 or 0.75 is used. For example, in rat a dose of 0.1 mg/kg results in an exposure of 1005 ng*h/mL. The human-equivalent dose after applying the dose-by-factor approach with an exponent of 0.75 equals 1.8 mg ($0.1 \cdot 70 \cdot (70/0.3)^{0.25}$). The "observed" exposure as predicted by the developed PK model for human was 95 ng*h/mL. As a result, there was an 11 (1005/95) fold difference in exposure between rat and human.

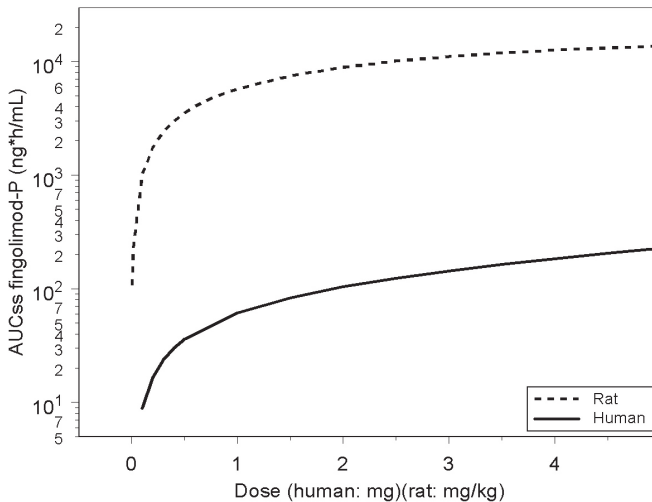


Figure 8: Comparison of the predicted steady state fingolimod-P exposures in blood after oral administration of fingolimod in doses of 0.1-5 mg/kg in rat and 0.1-5 mg in human.

The dashed and continuous lines represent the exposure in rat and human, respectively.

Discussion

With the aim of 1) of investigating whether characterization of the phosphorylation in blood platelets constitutes a basis for pharmacokinetic scaling and 2) predicting plasma rather than whole blood concentrations of fingolimod phosphate, PK models were de-

veloped to quantify the exposure of the prototypical S1PHK substrate fingolimod and its active metabolite, fingolimod-P, in rat and human. Previously, the time course of the blood concentrations of the parent compound but not the phosphorylated metabolite has been described by a physiologically-based pharmacokinetic model (Meno-Tetang *et al.*, 2006). In addition, the time course of the fingolimod-P blood concentrations has been described by a descriptive population PK model (Wu *et al.*, 2011). However, to date, no pharmacokinetic models have been published that describe the time course of the fingolimod and fingolimod-P concentrations simultaneously.

The developed models, i.e. the rat model and the human model, consisted of three parts to describe the phosphorylation and the dephosphorylation in blood, the distribution and elimination from the systemic circulations and the absorption, respectively. Although both models were structurally related, several differences are noticeable between the rat and human models. First of all, not all peripheral compartments that were identified in the rat model could be identified in the human model. This is explained by the fact that fingolimod(-P) concentrations were not measured following intravenous administration of fingolimod in human, and therefore, less detailed information was available about the distribution. Another important difference between the rat and human model is that saturable binding to a high affinity/low capacity binding site on a protein in the plasma was identified in humans, whereas this could not be identified in rats. As a result, the fingolimod-P blood/plasma exposure ratio was constant over the observed dose range (the ratio was about 1) in rats, whereas this ratio increased with higher doses from 0.95 for a dose of 0.5 mg to 1.9 for a dose of 5 mg at steady state in human. Therefore, the human plasma concentrations may be a little higher than anticipated after administration of doses below 0.5 mg/day. In addition, for a dose of 0.5 mg/day the blood/plasma concentration ratio varied between 0.8 and 0.95 within a day at steady state (Figure 6). The difference between blood and plasma concentrations is the largest around t_{max} . This is relevant since the fingolimod-P plasma concentrations are likely to be more predictive for pharmacodynamic effects than blood concentrations. Finally, in both species, the *in vivo* dephosphorylation was found to be much faster than the dephosphorylation in isolated blood. Fingolimod-P is dephosphorylated by LLP3, which is expressed on cells exposed to plasma such as vascular endothelial cells, which are not present in the isolated blood used for the *ex vivo* studies. In humans, dephosphorylation is best described by a Michaelis-Menten process, whereas in rats no capacity limited (Michaelis-Menten) kinetics could be identified, due to the limited concentration range that has been studied. The developed models are valid in the evaluated dose range of 0.1 to 3 mg/kg following oral administration in rat and 0.5 to 5 mg following oral once daily administration to humans. In general, the data from the studies in rat and human were adequately described. However, in study

2105 the observations from the 1.25 mg dose group were slightly over-predicted. This is thought to be due to non-compliance for some subjects in this treatment group. In addition, for this study, the variability was slightly over-predicted. As there were only 12 subjects per treatment-group included in this study the observed variability may not be representative for the variability in a larger population. An external validation of the human model using data from a single-dose study with doses between 5 and 40 mg demonstrated that the model can also be used to predict fingolimod(-P) blood concentrations following doses up to 10 mg, which is a dose well above the therapeutic dose of 0.5 mg once daily. The developed models can be applied to evaluate possible covariate influences or to predict the time course of the fingolimod and fingolimod-P plasma concentrations. Moreover, the model can be applied to characterize the time course of pharmacodynamic effects of fingolimod-P by linking the time course of the fingolimod-P plasma or blood concentrations to pharmacodynamic observations.

Besides describing the PK of fingolimod and fingolimod-P in human by a compartmental model, the PK in human were predicted from rat data using an allometric scaling approach. Various dose extrapolation techniques have been described ranging from empirical allometric scaling to semi-mechanistic methodologies, which attempt to account for species difference in physiology, and further to the mechanistic whole-body PBPK modeling approach, which relies on physicochemical properties of the drug and knowledge of human physiology (tissue composition)(Jones et al, 2011). Allometric scaling of the PK parameters from rat resulted in an adequate prediction of the PK of fingolimod. However, the exposure of fingolimod-P was 12-fold over-predicted. When examining the inter-conversion rate parameters in both species it is noticeable that the phosphorylation of fingolimod in the platelets is 4-fold faster in rats as compared to humans after allometric scaling (Table 1, K67). As in rats, an extra phosphorylation rate was estimated in the plasma, the overall phosphorylation was 9-fold faster in rats as compared to humans. This extra phosphorylation could represent rapid phosphorylation in other tissues, but this rate was not quantifiable in human. This could possibly be due to differences in the S1PHK2 enzyme tissue distribution, which may also explain the inadequate allometric prediction of the volume of distribution as inter-species differences in inter-conversion are not accounted for in a general allometric scaling approach. Overall, the 4-fold difference in phosphorylation rate quantified from the *ex vivo* experiments is indicative for differences in exposure between rat and human, but does not exclusively elucidate this difference. This is explained by the minor contribution of phosphorylation in the platelets as compared to the 82% and 69% pre-systemic phosphorylation seen in rats and humans, respectively. More mechanistic approaches are required to integrate the differences in pre-systemic

phosphorylation and enzyme tissue distribution in the translational pharmacokinetics of fingolimod and fingolimod-P and other S1PHK substrates.

In conclusion, large interspecies differences in the rate of phosphorylation between rats and humans were demonstrated, using fingolimod as a paradigm compound, which cannot be accounted for by allometric scaling. A semi-mechanistic PK model is proposed that constitutes a basis for the prediction of the concentrations of S1PHK substrates and their phosphorylated metabolites in plasma. In this model, differences in the rate of phosphorylation in blood, estimated from *ex vivo* inter-conversion measurements in platelets, partly explain the differences in exposure between rats and humans. However, differences in pre-systemic phosphorylation should also be taken into account.

References

- Albert R, Hinterding K, Brinkmann V, Guerin D, Muller-Hartwig C, Knecht H, et al. (2005). Novel immunomodulator FTY720 is phosphorylated in rats and humans to form a single stereoisomer. Identification, chemical proof, and biological characterization of the biologically active species and its enantiomer. *J Med Chem.*, 48, 5373-5377.
- Anada Y, Igarashi Y & Kihara A (2007). The immunomodulator FTY720 is phosphorylated and released from platelets. *Eur J Pharmacol.*, 568, 106-111.
- Billich A, Bornancin F, Devay P, Mechtcheriakova D, Urtz N & Baumruker T (2003). Phosphorylation of the immunomodulatory drug FTY720 by sphingosine kinases. *J Biol Chem.*, 278, 47408-47415.
- Brinkmann V (2007). Sphingosine 1-phosphate receptors in health and disease: mechanistic insights from gene deletion studies and reverse pharmacology. *Pharmacol Ther.*, 115, 84-105.
- Brinkmann V, Cyster JG & Hla T (2004). FTY720: sphingosine 1-phosphate receptor-1 in the control of lymphocyte egress and endothelial barrier function. *Am J Transplant.*, 4, 1019-1025.
- Chun J & Hartung HP (2010). Mechanism of action of oral fingolimod (FTY720) in multiple sclerosis. *Clin Neuropharmacol.*, 33, 91-101.
- Cohen JA, Barkhof F, Comi G, Hartung HP, Khatri BO, Montalban X, et al. (2010). Oral fingolimod or intramuscular interferon for relapsing multiple sclerosis. *N Engl J Med.*, 362, 402-415.
- Cusack KP & Stoffel RH (2010). S1P(1) receptor agonists: Assessment of selectivity and current clinical activity. *Curr Opin Drug Discov Devel.*, 13, 481-488.
- Danhof M, de Lange EC, Della Pasqua OE, Ploeger BA & Voskuyl RA (2008). Mechanism-based pharmacokinetic-pharmacodynamic (PK-PD) modeling in translational drug research. *Trends Pharmacol Sci.*, 29, 186-191.
- FDA press release on approval of Gilenya (2010). Available at: <http://www.fda.gov/NewsEvents/Newsroom/PressAnnouncements/ucm226755.htm> (Accessed: 30 September 2012).
- Hale JJ, Yan L, Neway WE, Hajdu R, Bergstrom JD, Milligan JA, et al. (2004). Synthesis, stereochemical determination and biochemical characterization of the enantiomeric phosphate esters of the novel immunosuppressive agent FTY720. *Bioorg Med Chem.*, 12, 4803-4807.
- Jones RD, Jones HM, Rowland M, Gibson CR, Yates JW, Chien JY, et al. (2011). PhRMA CPCDC initiative on predictive models of human pharmacokinetics, part 2: Comparative assessment of prediction methods of human volume of distribution. *J Pharm Sci*, 30, 22553.
- Kharel Y, Lee S, Snyder AH, Sheasley-O'neill S L, Morris MA, Setiady Y, et al. (2005). Sphingosine kinase 2 is required for modulation of lymphocyte traffic by FTY720. *J Biol Chem.*, 280, 36865-36872.
- Kihara A & Igarashi Y (2008). Production and release of sphingosine 1-phosphate and the phosphorylated form of the immunomodulator FTY720. *Biochim Biophys Acta.*, 1781, 496-502.
- Kovarik JM, Hartmann S, Bartlett M, Riviere GJ, Neddermann D, Wang Y, et al. (2007). Oral-intravenous crossover study of fingolimod pharmacokinetics, lymphocyte responses and cardiac effects. *Biopharm Drug Dispos.*, 28, 97-104.
- Kovarik JM, Schmouder R, Barilla D, Wang Y & Kraus G (2004). Single-dose FTY720 pharmacokinetics, food effect, and pharmacological responses in healthy subjects. *Br J Clin Pharmacol.*, 57, 586-591.
- Liu H, Sugiura M, Nava VE, Edsall LC, Kono K, Poulton S, et al. (2000). Molecular cloning and functional characterization of a novel mammalian sphingosine kinase type 2 isoform. *J Biol Chem.*, 275, 19513-19520.
- Mandala S, Hajdu R, Bergstrom J, Quackenbush E, Xie J, Milligan J, et al. (2002). Alteration of lymphocyte trafficking by sphingosine-1-phosphate receptor agonists. *Science.*, 296, 346-349.
- Meno-Tetang GM, Li H, Mis S, Pyszczynski N, Heining P, Lowe P & Jusko WJ (2006). Physiologically based pharmacokinetic modeling of FTY720 (2-amino-2-[2-(4-octylphenyl)ethyl]propane-1,3-diol hydrochloride) in rats after oral and intravenous doses. *Drug Metab Dispos.*, 34, 1480-1487.
- Olivera A, Kohama T, Tu Z, Milstien S & Spiegel S (1998). Purification and characterization of rat kidney sphingosine kinase. *J Biol Chem.*, 273, 12576-12583.
- Paugh SW, Payne SG, Barbour SE, Milstien S & Spiegel S (2003). The immunosuppressant FTY720 is

phosphorylated by sphingosine kinase type 2. *FEBS Lett.*, 554, 189-193.

Sharma V & McNeill JH (2009). To scale or not to scale: the principles of dose extrapolation. *Br J Pharmacol.*, 157, 907-921.

Vuppugalla R, Marathe P, He H, Jones RD, Yates JW, Jones HM, et al. (2011). PhRMA CPCDC initiative on predictive models of human pharmacokinetics, part 4: Prediction of plasma concentration-time profiles in human from in vivo preclinical data by using the Wajima approach. *J Pharm Sci*, 7, 22551.

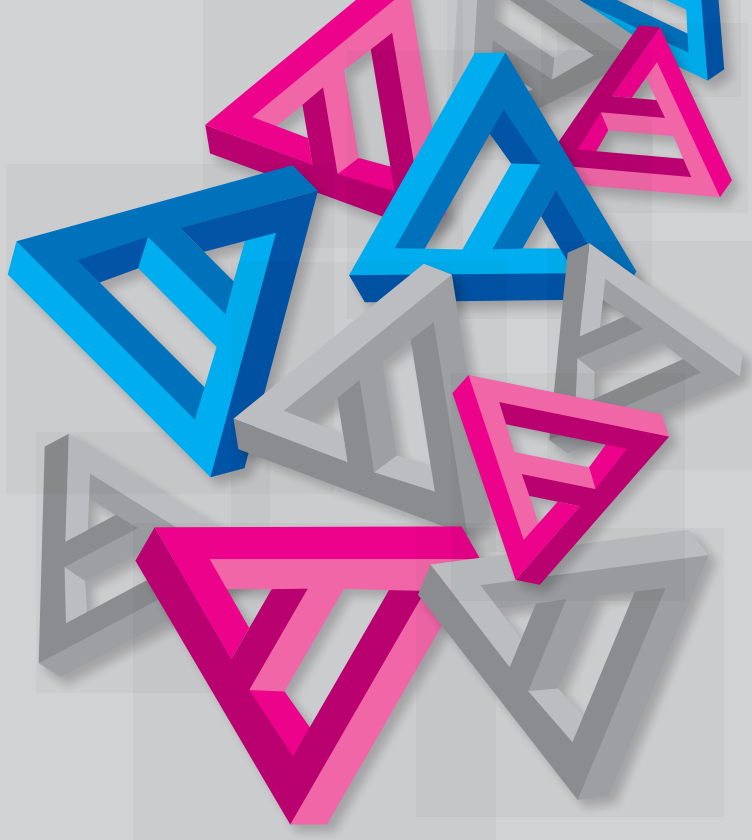
West GB, Brown JH & Enquist BJ (1999). The fourth dimension of life: fractal geometry and allometric scaling of organisms. *Science.*, 284, 1677-1679.

Wu K, Mercier F, David OJ, Schmouder RL & Looby M (2011). Population Pharmacokinetics of Fingolimod Phosphate in Healthy Participants. *J Clin Pharmacol*, 22, 22.

Zollinger M, Gschwind HP, Jin Y, Sayer C, Zecri F & Hartmann S (2011). Absorption and disposition of the sphingosine 1-phosphate receptor modulator fingolimod (FTY720) in healthy volunteers: a case of xenobiotic biotransformation following endogenous metabolic pathways. *Drug Metab Dispos.*, 39, 199-207.

Abbreviations

B_{max}	Binding capacity
$F1$	Bioavailability
fingolimod-P	Fingolimod-phosphate
IIV	Inter-individual variability
iv	Intravenous
ka	Absorption rate constant
Kd	Binding affinity
Km	Concentration at which the half maximal rate of biotransformation is reached
kxx	First order rate constant
LLP3	Lipid phosphatase type 3
LOQ	Lower limits of quantification
MVOF	Minimum value of the objective function
PBPK	Physiologically based pharmacokinetic
PD	Pharmacodynamic
PK	Pharmacokinetic
S1P	Sphingosine 1-phosphate
S1PHK	Sphingosine kinase
$V_{ex vivo}$	<i>Ex-vivo</i> blood volume
$V_{in vivo}$	<i>In-vivo</i> blood volume
Vm	Maximum rate of biotransformation
VPC	Visual predictive check



CHAPTER 6

Characterization and prediction of cardiovascular effects of fingolimod and siponimod using a systems pharmacology modeling approach

N. Snelder, B.A. Ploeger, O. Luttringer, D.F. Rigel, R.L. Webb, D. Feldman, F. Fu, M. Beil, L. Jin, D.R. Stanski and M. Danhof

Summary

Background and purpose | Fingolimod and siponimod are sphingosine 1-phosphate (S1P) receptor agonists which are effective in treating multiple sclerosis, but are associated with cardiovascular effects in humans. This investigation aimed to characterize these effects, in a quantitative manner, using a recently developed systems cardiovascular pharmacology (CVS) model for drug effects on the interrelationship between mean arterial pressure (MAP), cardiac output (CO), heart rate (HR), stroke volume (SV) and total peripheral resistance (TPR).

Experimental approach | The cardiovascular effects of fingolimod-phosphate (fingolimod-P), and siponimod were characterized in spontaneously hypertensive and Wistar-Kyoto rats following once daily administration of 0, 0.1, 0.3, 1, 3 and 10 mg/kg and 3 and 15 mg/kg, respectively. The rats were chronically instrumented with ascending aortic flow probes and/or aortic catheters/radiotransmitters for continuous recording of CO, MAP and HR.

Key results | The effect of fingolimod-P on MAP, CO, HR, SV and TPR was adequately characterized by the CVS model combined with a receptor binding model, a receptor down-regulation model and a sensitization model with direct inhibiting and stimulating drug effects on HR and TPR, respectively. The effect of siponimod on MAP and HR in rats was adequately predicted on the basis of constants derived from *in vitro* assays.

Conclusions and Implications | The proposed CVS model can be applied to predict the cardiovascular effects of S1P receptor agonists with different selectivity profiles in rats and, ultimately, it may constitute a basis for prediction of cardiovascular effects of S1P receptor agonists in humans.

Introduction

Fingolimod and siponimod are sphingosine 1-phosphate (S1P) receptor agonists with different subtype selectivity profiles, which are effective in the treatment of multiple sclerosis (Cohen *et al.*, 2010; Gergely *et al.*, 2012). Fingolimod, and more specifically, the active metabolite of fingolimod, fingolimod-phosphate (fingolimod-P) binds to 4 of the 5 subtypes of the S1P receptor (S1P₁ and S1P_{3,5}) with high affinity (0.3-3.1 nM) (Mandala *et al.*, 2002; Brinkmann, 2007; Brinkmann *et al.*, 2004), whereas siponimod binds only to 2 of the 5 subtypes (S1P₁ and S1P₅) with high affinity, while the affinity for the S1P₃ receptor is low (Gergely *et al.*, 2012). In humans, S1P receptor ligands have been associated with cardiovascular side effects. Briefly, following the administration of fingolimod and siponimod a dose-dependent decrease in HR was observed on the first day of treatment with a gradual return to baseline with continued treatment (Kappos *et al.*, 2006; Kappos *et al.*, 2010; Selmaj *et al.*, 2013; Gergely *et al.*, 2012). In addition, after administration of fingolimod a small increase of 1 – 2 mm Hg in mean arterial pressure (MAP) was observed at a dose of 0.5 mg and MAP was mildly increased by 4-6 mmHg after 2 months at doses of 1.25 and 5 mg (Kappos *et al.*, 2006; Kappos *et al.*, 2010). No information has been published on potential effects of siponimod on MAP. The immunosuppressant, as well as the cardiovascular effects of fingolimod-P and siponimod are believed to be mediated through various S1P receptor subtypes, which complicates the search for novel S1P receptor agonists that are devoid of cardiovascular side effects. A mechanistic and quantitative understanding of the hemodynamic effects of S1P receptor agonists is important as it may constitute a basis for 1) the prediction, in a strictly quantitative manner, of the cardiovascular effects of novel S1P receptor agonists with different receptor selectivity profiles and 2) the extrapolation of cardiovascular effects to humans based on information from preclinical investigations.

Recently, a systems cardiovascular pharmacology (CVS) model was developed to characterize drug effects on the interrelationship between mean arterial pressure (MAP), cardiac output (CO), heart rate (HR), stroke volume (SV) and total peripheral resistance (TPR) using hemodynamic data from rats (Snelder *et al.*, 2013a; submitted (a)). The parameters of the CVS model were quantified by challenging the CVS with a prototype set of compounds with different, but well known, mechanisms of action (MoA). It was demonstrated that the CVS model is system-specific by showing that successively removing data from one of the compounds that were used for model development does not affect the estimates of the system parameters. Furthermore by the analysis of hemodynamic profiles, it was demonstrated that the site of action of new compounds can be identified by a model-based analysis of the time course of the change in the hemodynamic variables. Therefore, this model is uniquely suited to provide a quantitative understanding of the mechanisms

underlying the cardiovascular effects of S1P receptor agonists. A potential application of this model is the prediction of the cardiovascular effects of novel compounds. This requires the interfacing of the CVS model with a receptor binding and activation model. Ultimately this quantitative pharmacology model could be a basis for the prediction of cardiovascular effects in man based on preclinical data (Danhof et al., 2008).

In this investigation, the recently proposed systems cardiovascular pharmacology model was combined with 1) a target binding-activation model and 2) a receptor down-regulation and sensitization model, to describe the cardiovascular effects of fingolimod-P in rat. Subsequently, the developed model was used to predict the cardiovascular effects of siponimod in rats on the basis of dissociation constants derived from *in vitro* assays.

Methods

Animals

Experiments were conducted on male, spontaneously hypertensive rats (SHR) (Taconic Farms, Germantown, NY, USA), Wistar-Kyoto (WKY) rats (Taconic Farms, Germantown, NY, USA) and Lewis rats in accordance with approved Novartis Animal Care and Use Committee protocols (which have been accredited and conform to international animal welfare standards) and the Guide for the Care and Use of Laboratory Animals (National Research Council, 2011). At the time of study, rats' ages (body weights) ranged from 24-50 (331-504), 24-36 (477-781) wk (g) for SHR, and WKY rats, respectively. Rats were housed on a 12-h light/dark cycle (light: 0600–1800 h), kept at room temperature, 22°C, and were provided normal chow (Harlan Teklad 8604; Indianapolis, IN, USA) and water *ad libitum*. All studies involving animals are reported in accordance with the ARRIVE guidelines for reporting experiments involving animals (Kilkenny *et al.*, 2010; McGrath *et al.*, 2010).

Experimental Procedures

The effect of fingolimod-P on the CVS after repeated dosing was evaluated in two studies (Table 1). In Study 1, MAP, HR and CO were measured. In Study 2, only MAP and HR were measured. In the second study, in addition to the effect of fingolimod-P, the effects of the new ligand siponimod were studied. For continuous recording of CO and/or MAP and HR rats were surgically instrumented with an ascending aortic flow probe and/or a femoral arterial catheter/radiotransmitter as described by Snelder *et al.* (Snelder *et al.*, 2013a). After 5 weeks of washout in this study, carotid arterial catheters were implanted for conducting a single-dosing pharmacokinetics (PK) study one week later. In Study 3, the PK of siponimod were investigated in Lewis rats, which were instrumented 72 h earlier

Table 1: Study overview

Study	Measures	Study designs	Experiment	Dose (mg/kg)	Rats
1	CO multiple dosing study to investigate the cardiovascular effects of fingolimod-P (p.o. once daily)	Days -4 - 0 : baseline Days 1 - 7 : active treatment Days 8 -16 : washout	1	Vehicle 0.1 0.3 1 3 10	SHR: n=2 SHR: n=2 SHR: n=2 SHR: n=3 SHR: n=3 SHR: n=3
2	MAP, HR and CO (TPR and SV)	Days -6 - 0 : baseline Days 1 - 14 : active treatment Days 15 - 28 : washout	2	Vehicle 10	SHR: n=1 WKY rat: n=2 SHR: n=5 WKY rat: n=5
3	MAP and HR	Days -5 - 0 : baseline Days 1 - 28 : active treatment Days 29 - 44* : washout	3	Vehicle 10	SHR: n=2 WKY rat: n=2 SHR: n=3 WKY rat: n=3
2	Telemetry multiple dosing study to investigate the effect of fingolimod-P and siponimod on MAP and HR (p.o. once daily)	Days -6 - 0 : baseline (SHR) Days -4 - 0 : baseline (WKY rat) Days 1 - 56 : active treatment Days 57 - 83 : washout	4	Vehicle fingolimod 0.1, 0.3, 1, 3 and 10 Siponimod 3 and 15	SHR: n=5 WKY rat: n=5 per treatment group
3	PK siponimod	Day 100 : PK (only in SHR) Single i.v. or p.o. siponimod dose. Measurements at: i.v.: 0.25, 1, 2, 4, 8, 24 and 48 h p.o.: 0, 0.5, 1, 2, 4, 8, 24, 48 and 72h	5	1	Lewis: n=3 per treatment group

* The duration of washout measurements varied per rat and was at least 16 days. In several rats, washout data was collected during a longer period, with a maximum duration of 53 days.

with a femoral venous and arterial cannula for compound administration and for blood sample collection, respectively.

Experimental design

In Study 1, baseline measurements were recorded during 5-7 days prior to active treatment with fingolimod, which was administered once daily for 1, 2 or 4 weeks, at doses of 0, 0.1, 0.3, 1, 3 and 10 mg/kg p.o. Thereafter, washout data were collected during at least 9 days. In several rats, washout data was collected during a longer period (maximal 53 days) to investigate if the hemodynamic variables returned to baseline. In total, 21 SHR and 11 WKY rats were included in this study. One SHR and 2 WKY rats died during the washout period. Flow cables were connected to the flow probes by 7:00 am and disconnected after 5:00 pm. Rats were dosed at 10:00 am and all data were continued to be collected until 5:00 pm. Thereafter, only MAP and HR data were captured until the flow probes were reconnected the next morning. For each variable, hourly averages of the observations were calculated using the continuously recorded CO, MAP and HR measurements. Subsequently, only one observation every 4 hours was included in the dataset for model development to reduce run times.

In Study 2, baseline measurements were recorded for 5 days. Thereafter, fingolimod (0, 0.1, 0.3, 1, 3 and 10 mg/kg p.o.) or siponimod (3 and 10 mg/kg p.o.) was administered once daily for 8 weeks. Subsequently, washout data was collected during 3 weeks. In addition, after 6 weeks of washout from the repeated-dosing study the PK of fingolimod and its active metabolite fingolimod-P were investigated following a single oral administration of fingolimod (0.1, 0.3, 1, 3 and 10 mg/kg) in SHR. Blood samples were collected at pre-dosing and at 2, 4, 8, and 24 hrs post-dosing.

In Study 3, siponimod blood concentrations were measured following intravenous (iv) and oral administration of 1 mg/kg of siponimod, in male, Lewis rats. Rats for the oral experiment were fasted from approximately 8 h prior to and 2 h post drug administration. For each route 3 rats were used. After intravenous administration, blood samples were taken at 0.25, 1, 2, 4, 8, 24, 48h and after oral administration at 0.5, 1, 2, 4, 8, 24, 48, 72 h post administration.

Compounds

In Studies 1 and 2, fingolimod (synthesized at Novartis, Basel, Switzerland, PKF117-812-AA) and siponimod (synthesized at Novartis, Basel, Switzerland, NVP-BAF312-NX) were dissolved in water or 1% carboxymethylcellulose and formulated for administration at 5

ml/kg by oral gavage. In Study 3, siponimod (NVP-BAF312-AA) was dissolved in PEG200/ glucose/water (pH-adjusted to 3-4) for administration at 1 ml/kg i.v. and 4 ml/kg p.o..

Data analysis

Pharmacokinetics of fingolimod-P

Recently, a PK model was developed to characterize the PK of fingolimod and fingolimod-P in male Lewis and Sprague Dawley rats in blood (Snelder *et al.*, submitted (b)). This model was valid in the evaluated dose range of 0.1 to 3 mg/kg (Snelder *et al.*, submitted (b)). As this excludes the 10 mg/kg dose, which was administered in the current studies, the predictive value of the model to describe the PK data from the 10 mg/kg dose group in Study 2 was assessed. Therefore, the PK model was optimized using the fingolimod-P PK measurements from this dose group by changing the parameters one by one using the NWPRI prior option in NONMEM® (Gisleskog *et al.*, 2002). Generally, this option serves to obtain stable parameter estimates, even with insufficient data, by constraining the values of these parameter estimates using *prior* knowledge from the previously developed PK model. When optimizing the parameter Vm_{obs} , which represents the maximum rate of absorption of pre-systemically formed fingolimod-P for the 10 mg/kg dose group only, the data from this dose group were adequately described and the model-predicted PK profiles could be used for pharmacokinetic pharmacodynamic (PKPD) model development as specified in the section “Results”.

Systems pharmacology model for the interrelationships between hemodynamic variables

The interrelationships between MAP, TPR, CO, HR and SV are expressed by the formulas 1) $MAP=CO*TPR$ and 2) $CO=HR*SV$ (Levick, 2003). Recently, a systems cardiovascular pharmacology model was developed to describe drug effects on the inter-relationship between MAP, CO, HR, SV and TPR (Snelder *et al.*, 2013a; Snelder *et al.*, submitted (a)). This “CVS model” consists of three differential equations, for HR, SV and TPR respectively, which are linked by negative feedback through MAP (Figure 1, Equation 1). The circadian rhythm, which was observed in all 5 parameters of the CVS, is described by two cosine functions, one influencing the production rate of HR (K_{in_HR}) and one influencing the production rate of TPR (K_{in_TPR}).

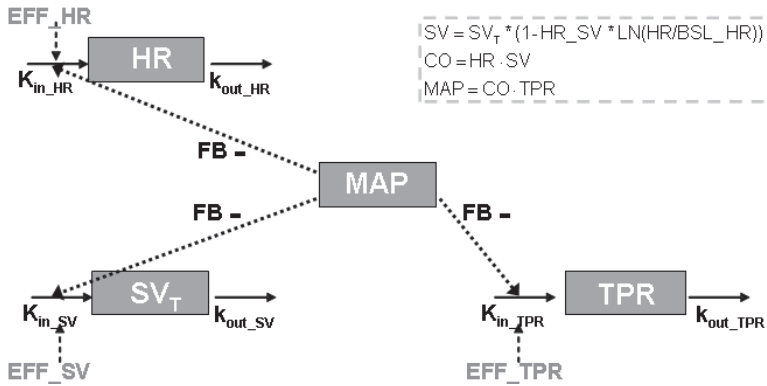


Figure 1: CVS model to characterize drug effects on the interrelationship between MAP, CO, HR, SV and TPR. (Copied from Snelder (Snelder *et al.* with permission, submitted).

Cardiac output (CO) equals the product of HR and SV ($CO=HR \cdot SV$) and MAP equals the product of CO and TPR ($MAP=CO \cdot TPR$). SV influenced by indirect feedback through MAP (SVT) and by HR through a direct inverse log-linear relationship, where HR_{SV} represents the magnitude of this direct effect. Effects on HR, SV and TPR are described by three linked turnover equations. In these equations K_{in_HR} , K_{in_SV} and K_{in_TPR} represent the zero-order production rate constants and k_{out_HR} , k_{out_SV} and k_{out_TPR} represent the first-order dissipation rate constants. When MAP increases as a result of a stimulating effect on HR, SV or TPR, the values of HR, SV and TPR will decrease as a result of the action of the different feedback mechanisms regulating the CVS. In this model the magnitude of feedback on HR, SV and TPR is represented by FB. System-specific parameters are indicated in black and drug-specific parameters are indicated in dark grey.

$$CR_{HR} = amp_{HR} \cdot \cos\left(\frac{2\pi \cdot (t + hor_{HR})}{24}\right)$$

$$CR_{TPR} = amp_{TPR} \cdot \cos\left(\frac{2\pi \cdot (t + hor_{TPR})}{24}\right)$$

$$\frac{dHR}{dt} = K_{in_HR} \cdot (1 + CR_{HR}) \cdot (1 - FB \cdot MAP) - k_{out_HR} \cdot HR$$

$$\frac{dSV_T}{dt} = K_{in_SV} \cdot (1 - FB \cdot MAP) - k_{out_SV} \cdot SV_T$$

$$\frac{dTPR}{dt} = K_{in_TPR} \cdot (1 + CR_{TPR}) \cdot (1 - FB \cdot MAP) - k_{out_TPR} \cdot TPR$$

(1)

$$SV = SV_T \cdot (1 - HR_{SV} \cdot \ln(HR/BSL_HR))$$

$$CO = HR \cdot SV$$

$$MAP = CO \cdot TPR$$

In these equations, SV^* represents the SV influenced by the negative feedback of MAP, K_{in_SV} represents the zero-order production rate constant and k_{out_HR} , k_{out_SV} and k_{out_TPR} represent the first-order dissipation rate constants of HR, SV and TPR, respectively. In addition, amp represents the amplitude of the circadian rhythms, t the time and hor the horizontal displacement over time.

The CVS model was applied to characterize the time course of the effect of fingolimod-P on the hemodynamic variables. All system-specific parameters were fixed to values reported by Snelder *et al.* (Snelder *et al.*, submitted (a)). However, the parameters of the circadian rhythm were optimized as the circadian rhythm varied between studies. The handling effect, i.e. the influence of a short manual restraint and oral dose administration, was excluded from the model as only 1 observation every 4 hours was included in the dataset for model development and the handling effect is only relevant on a much shorter time scale. Previously, inter-individual variability was identified on the baseline values of MAP, CO and HR (BSL_MAP , BSL_CO and BSL_HR). In contrast, in this analysis the observed baseline values, calculated as the mean of all observations before active treatment, were used to reduce runtimes. The residual errors of MAP, CO and HR were optimized on the available data. In addition, an exploratory graphical analysis revealed that, in the vehicle-treated groups, within the time frame of these studies, HR decreases over time in both SHR and WKY rats and that TPR decreases over time in WKY rats only. Therefore, exponentially decreasing functions, linear, power and E_{max} models were evaluated to describe the change over time of K_{in_HR} and K_{in_TPR} (Equation 2).

$$\begin{aligned}
 \text{Exponential:} & \quad K_{in} = K_{in_0} \cdot \exp(-k \cdot T) \\
 \text{Linear:} & \quad K_{in} = K_{in_0} \cdot (1 - SL \cdot T) \\
 \text{Power:} & \quad K = K_{in_0} \cdot (1 - SL \cdot T^{POW}) \\
 E_{max}: & \quad K_{in} = K_{in_0} \cdot \left(1 - \frac{E_{max} \cdot T}{ET_{50} + T} \right)
 \end{aligned} \tag{2}$$

In this equation, k , SL , POW , E_{max} and ET_{50} represent the first-order rate constants for decrease, the slope of the linear relationship, the power parameter in the power relationship, the maximum effect and the time at which half of the maximum effect is achieved in the E_{max} relationship, respectively.

Target activation and transduction model for fingolimod-P

Data on the blood concentrations of fingolimod-P and the changes in various hemodynamic variables were analyzed using the CVS model without changing the system-specific

parameters. In a first step, a model-based hypothesis testing procedure (Snelder *et al.*, submitted (a)) was followed to obtain insights in the site of action of fingolimod-P and the hemodynamics of its cardiovascular effects.

- 1) Different hypotheses of the site of action (i.e. HR, SV and TPR) and direction of the effect (i.e., inhibiting or stimulating) were formulated, resulting in 6 possible combinations of effects.
- 2) For each hypothesis, the model was fitted to the MAP, CO, HR, SV and TPR measurements.
- 3) It was evaluated which hypothesis resulted in the best description of the data as judged by the agreement between the observed and predicted direction and magnitude of effect and the lowest minimum value of the objective function (MVOF) as specified in the section “Model selection and evaluation”.

The hypothesis that fingolimod-P has a stimulating effect on TPR resulted in the best description of the data. Briefly, the effects on MAP, CO, TPR and SV were adequately predicted, albeit that the magnitude of the effect on SV was under-predicted (Table 2). In addition, although the nature of the response on HR, i.e. an increase or decrease in HR, was predicted adequately, the transient nature of this effect was not captured indicating that fingolimod-P might have an additional effect on HR. Overall, it was found that the effect of fingolimod-P on all variables of the CVS could be described adequately while assuming multiple sites of action, i.e. TPR and HR (Snelder *et al.*, 2013b). In total, three different

Table 2: Investigation of the site of action of fingolimod-P

Site of action	Direction of effect	Result
HR	Stimulating	Adequate prediction of the effect on MAP and SV; Inadequate prediction of the direction of the effect on TPR, CO and HR
HR	Inhibiting	Adequate prediction of the effect on TPR and CO; Inadequate prediction of the direction of the effect on MAP and SV; Transient nature of the effect on HR not captured
TPR	Stimulating	Adequate prediction of the effect on MAP, TPR and CO; Reasonable prediction of the effect on SV (magnitude of effect underestimated); Transient nature of the effect on HR not captured
TPR	Inhibiting	Inadequate prediction of the direction of the effect on MAP, CO, HR, SV and TPR
SV	Stimulating	Adequate prediction of the effect on MAP; Inadequate prediction of the direction of the effect on CO, TPR and SV; Transient nature of the effect on HR not captured
SV	Inhibiting	Adequate prediction of the effect on SV and CO; Reasonable prediction of the effect on TPR (magnitude of effect underestimated); Inadequate prediction of the direction of the effect on MAP and HR

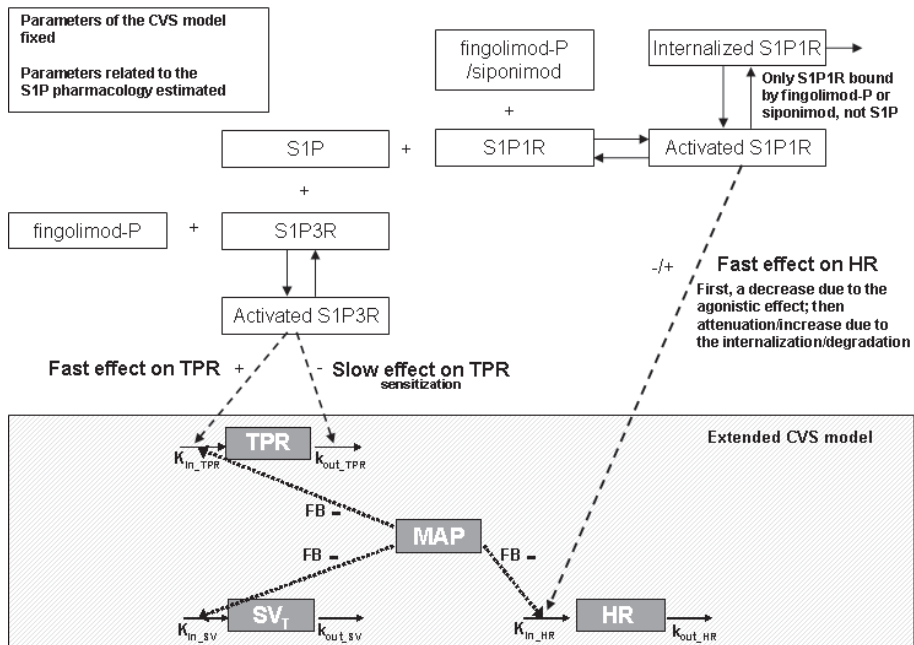


Figure 2: Target binding and activation model to describe the cardiovascular effects of fingolimod-P and siponimod integrated with the CVS model.

Effect of S1P agonists on HR: The effect of S1P agonists on HR is thought to be mediated through the S1P1 receptor (S1P1R). Fingolimod-P and siponimod bind with high affinity to the S1P1R. The effect of siponimod was considered negligible and, therefore, not included in this figure. Fingolimod and siponimod first act as full S1PR agonists causing a decrease in HR, and thereafter function as an S1PR antagonist, following the internalization and degradation of bound S1P1Rs.

Effect of S1P agonists on TPR: The effect of S1P agonists on TPR is thought to be mediated through the S1P3 receptor (S1P3R). Fingolimod-P and siponimod bind with high and low affinity to the S1P3R, respectively. The effect of siponimod was considered negligible and, therefore, not included in this figure. The effect of fingolimod-P on TPR is a combination of a fast stimulating effect and a slowly occurring stimulating effect (sensitization).

effects were quantified: 1) a fast stimulating effect on TPR, 2) a slow sustained stimulating effect on TPR which is only relevant in hypertensive rats following doses higher than 1 mg/kg and 3) a transient inhibiting effect on HR, which could be described by a standard feedback model (type I) (Gabrielsson and Weiner, 2000). In this first step, the changes in the hemodynamic variables were described by empirical models. This provided information on the most plausible site of action of fingolimod-P, but it also demonstrated that the CVS model can be applied to quantify the hemodynamics of the effect of fingolimod-P on five different variables, i.e. MAP, CO, HR, SV and TPR, while assuming only two sites of action. The obtained information on the site of action of fingolimod-P was in line with independent information on the mechanism of action underlying the effect of fingolimod-P as

discussed in detail in the section “Discussion”. Therefore, in a next step, receptor theory concepts for the characterization of target binding and target activation processes were incorporated in the model (Figure 2), to enable the prediction of the effects of follow-up compounds on the basis of information from *in vitro* assays (Danhof *et al.*, 2007; Ploeger *et al.*, 2009). The different components of the proposed target binding and activation model are detailed below.

Effect of fingolimod-P on heart rate

As fingolimod-P is an agonist for the S1P receptor, a competitive interaction between the endogenous agonist, S1P, and fingolimod-P was taken into account. This is especially important for the effect on HR since this effect is transient, which may be a result of internalization of the S1P receptor through binding of fingolimod-P (agonistic effects) and, thereby, reducing the bound S1P concentration resulting in an opposite effect (functional antagonism), i.e. an increase in HR.

It is assumed that the effect on HR is driven by the concentration of receptors activated (R_{AC}) by S1P or fingolimod-P (excluding the number of internalized receptors). At baseline the activated concentration of receptors (R_{AC_0}) is given by Equation 3.

$$R_{AC_0} = F_{RAC_0} \cdot R_{T_0} \tag{3}$$

$$F_{RAC_0} = \left(\frac{S1P}{1 + S1P} \right)$$

In these equations, RT_0 represents the apparent concentration of receptors at baseline, which has been set to 1 to enable calculation of the fractional receptor occupancy. In addition, $FRAC_0$ represents the fraction of activated receptors at baseline.

In the presence of fingolimod-P the activated receptor concentration is given by the equation for reversible competitive interaction between two agonists (Ariëns and Simonis, 1964; Romero *et al.*, 2012)(Equation 4).

$$R_{AC} = F_{RAC} \cdot R_T$$

$$F_{RAC} = \left(\frac{S1P + \frac{C_B}{K_d}}{1 + S1P + \frac{C_B}{K_d}} \right) \quad (4)$$

In these equations, R_T reflects the concentration of total receptors, K_d represents the receptor equilibrium dissociation constant for the effect of fingolimod-P on HR, C_b equals the fingolimod-P blood concentration as predicted by the PK model and $S1P$ represents the ratio between the unknown S1P concentration and its dissociation constant for binding to the S1P receptor. As the S1P concentration is unknown, this ratio is combined into one parameter that was estimated.

A turnover equation was used to describe the internalization of the S1P receptor (Romero *et al.*, 2012)(Equation 5). Turnover models are also called indirect response models and can be used to describe hysteresis, i.e. the delay between a perturbation and a response (Dayneka, 1993).

$$\frac{dR_T}{dt} = K_{in_R} - k_{out_R} \cdot R_T \quad (5)$$

In this equation, K_{in_R} represents the zero-order receptor synthesis rate constant and k_{out_R} represents the first-order degradation rate constant. As mentioned previously, R_{T_0} was assumed equal to 1 and, therefore, before pharmacological intervention $K_{in_R} = k_{out_R}$.

During pharmacological intervention, the receptor is internalized and degraded, which may explain the observed tolerance in the effect of fingolimod-P on HR (Horga *et al.*, 2010; Mullershausen *et al.*, 2009) (Equation 6).

$$\begin{aligned} \frac{dR_T}{dt} &= K_{in_R} \cdot I_R - k_{out_R} \cdot R_T \\ I_R &= \frac{I_{R_{50}}}{IR_{50} + F_{RAC} - F_{RAC_0}} \\ \frac{dk_{out_R}}{dt} &= DEGR \cdot (F_{RAC} - F_{RAC_0}) \cdot k_{out_R} \end{aligned} \quad (6)$$

In these equations, I_R represents the internalized receptor concentration, which is driven by the difference between F_{RAC} and F_{RAC_0} . IR_{50} represents the value of the difference between F_{RAC} and F_{RAC_0} that elicits a half maximal reduction in K_{in_R} and $DEGR$ represents the rate of receptor degradation. At baseline ($F_{RAC}=F_{RAC_0}$ and $R_T=R_{T_0}=1$), I_R equals 1. An increase in F_{RAC} caused by the binding of fingolimod-P to the receptor is associated with a decrease in I_R and, consequently, with a reduction in the synthesis of R_T representing internalization. In addition, an increase in F_{RAC} is associated with a sustained increase in K_{out_R} representing receptor degradation.

Effect of fingolimod-P on TPR

The receptor activation underlying the effect of fingolimod-P on TPR was described using the same equations as were used for the effect on HR (Equations 3 and 4). In addition, an exploratory graphical analysis provided evidence of sensitization as reflected in an increase in the values of TPR and MAP. Here, a complex pattern was observed. Specifically the values of both variables increased rapidly after the first administration of fingolimod in both SHR and WKY rat. Subsequently, a more gradual increase over time in TPR and MAP was observed during the whole active treatment period. This gradual increase was more apparent in SHR as compared to WKY rats. For some of the rats the effect on TPR and MAP did not return to baseline after the termination of treatment. Therefore, models including an irreversible receptor sensitization were evaluated for the effect of fingolimod-P on TPR according to Equation 7.

$$\frac{dk_{out_TPR}}{dt} = -SENS \cdot (F_{RAC} - F_{RAC_0}) \cdot k_{out_TPR} \quad (7)$$

In this equation, $SENS$ represents the first-order rate of the receptor sensitization. The change over time of k_{out_TPR} is driven by the difference between F_{RAC} and F_{RAC_0} . The baseline value of k_{out_TPR} is fixed to the value from the CVS model. At baseline F_{RAC} equals F_{RAC_0} and therefore, k_{out_TPR} does not change over time. An increase in F_{RAC} caused by the binding of fingolimod-P to the receptor is associated with a decrease in k_{out_TPR} and consequently with a sustained increase in TPR. As it was observed that the change over time was dependent on the baseline mean arterial blood pressure (BMAP), BMAP was evaluated as a continuous covariate on $SENS$ using linear, power, E_{max} and sigmoid E_{max} relationships (Equation 8). In the linear and power relationships, the effect of BMAP on $SENS$ was evaluated relative to the population median of BMAP.

$$\begin{aligned}
\text{Linear :} & \quad \text{SENS} = \text{TVSENS} \cdot (1 + \text{SENS}_{\text{SL}} \cdot (\text{BMAP} - 148.55)) \\
\text{Power :} & \quad \text{SENS} = \text{TVSENS} \cdot \left(\frac{\text{BMAP}}{148.55} \right)^{\text{SENS}_{\text{POW}}} \\
\text{E}_{\text{MAX}} : & \quad \text{SENS} = \text{SENS}_{\text{EMAX}} \cdot \frac{\text{BMAP}}{\text{SENS}_{\text{EC50}} + \text{BMAP}} \\
\text{Sigmoid E}_{\text{MAX}} : & \quad \text{SENS} = \text{SENS}_{\text{EMAX}} \cdot \frac{\text{BMAP}^{\text{SENS}_{\text{NH}}}}{\text{SENS}_{\text{EC50}}^{\text{SENS}_{\text{NH}}} + \text{BMAP}^{\text{SENS}_{\text{NH}}}}
\end{aligned} \tag{8}$$

In these equations, TVSENS represents the value of SENS for a typical subject, SENS_{SL} , SENS_{POW} , $\text{SENS}_{\text{EMAX}}$, $\text{SENS}_{\text{EC50}}$ and SENS_{NH} represent the slope of the linear relationship, the power coefficient in the power relationship, the maximum effect and the BMAP at which half of the maximum effect is achieved in the E_{max} relationship, respectively.

Overall, the activated concentration of TPR and HR receptors ($R_{\text{AC_TPR}}$ and $R_{\text{AC_HR}}$) was assumed to influence the production rates of TPR and HR according to Equation 9 (Figure 2).

$$\begin{aligned}
\text{CR}_{\text{HR}} &= \text{amp}_{\text{HR}} \cdot \cos\left(\frac{2\pi \cdot (t + \text{hor}_{\text{HR}})}{24}\right) \\
\text{CR}_{\text{TPR}} &= \text{amp}_{\text{TPR}} \cdot \cos\left(\frac{2\pi \cdot (t + \text{hor}_{\text{TPR}})}{24}\right)
\end{aligned} \tag{9}$$

$$\begin{aligned}
\frac{d\text{HR}}{dt} &= K_{\text{in_HR}} \cdot (1 + \text{CR}_{\text{HR}}) \cdot (1 - \text{FB} \cdot \text{MAP}) \cdot (1 - R_{\text{AC_HR}}) - k_{\text{out_HR}} \cdot \text{HR} \\
\frac{d\text{SV}_T}{dt} &= K_{\text{in_SV}} \cdot (1 - \text{FB} \cdot \text{MAP}) - k_{\text{out_SV}} \cdot \text{SV}_T \\
\frac{d\text{TPR}}{dt} &= K_{\text{in_TPR}} \cdot (1 + \text{CR}_{\text{TPR}}) \cdot (1 - \text{FB} \cdot \text{MAP}) \cdot R_{\text{AC_TPR}} - k_{\text{out_TPR}} \cdot \text{TPR} \\
\frac{dk_{\text{out_TPR}}}{dt} &= -\text{SENS} \cdot (F_{\text{RAC}} - F_{\text{RAC}_0}) \cdot k_{\text{out_TPR}}
\end{aligned}$$

External model evaluation

The developed model was externally evaluated using data from Study 2. As the amplitude of the circadian rhythm and the change in $K_{\text{in_HR}}$ and $K_{\text{in_TPR}}$ over time may vary between experiments due to different stress levels and differences in age and body weight, respectively, first the parameters of the circadian rhythms and the change of $K_{\text{in_HR}}$ and $K_{\text{in_TPR}}$ over time were estimated on the data from the vehicle groups. Subsequently, the effect of fingolimod-P on MAP and HR was predicted using the developed model and the predictions were compared with the actual data.

Prediction of the effect of siponimod

The CVS model, integrated with the developed receptor binding, down-regulation and sensitization model, was used to predict the effect of siponimod on MAP and HR, on the basis of information from *in vitro* assays. First the PK of siponimod was characterized using data from Study 3. One-, two- and three-compartmental models were evaluated to describe the disposition of siponimod. Furthermore, it was investigated if the absorption from the gastrointestinal-tract (dose compartment) to the blood (central compartment) could be described with first- or zero-order processes. In addition, an exploratory graphical analysis of the raw data indicated that there are two peaks in the absorption phase. Therefore, it was evaluated if the description of the data could be improved by including two dose compartments in the model from which siponimod was absorbed into the blood. Subsequently, the developed PK model for siponimod and the CVS model combined with the developed receptor binding and transduction model for fingolimod-P were used to predict the effect of siponimod on MAP and HR. The K_d 's of fingolimod-P for the effects on HR and TPR were adjusted for siponimod by correcting them for the molecular weights (MW) (MW fingolimod-P: 387.46 g/mol; MW siponimod: 516.61 g/mol), the unbound fractions (fingolimod-P: 1-1.6%; siponimod: 0.03%) and the ratio of the potencies derived from *in vitro* binding assays. It was assumed that fingolimod-P influences HR through binding to the S1P₁ receptor (Koyrakh *et al.*, 2005). The potencies of fingolimod-P and siponimod for binding to the S1P₁ receptor as derived from a GTPγS assay were 2 and 0.2 nM (Lukas *et al.*, 2013), respectively. The efficacy was the same for both compounds, i.e. 0.91-0.92 (Brinkman *et al.*, 2002; Gergely *et al.*, 2012). Overall, the estimated K_d for the effect on HR of fingolimod-P (total blood concentrations) was multiplied with 4.44 $((0.2 \cdot 516.61 / 0.0003) / (2 \cdot 387.46 / 0.01))$ to obtain the K_d for siponimod (total blood concentrations). In addition, Sykes *et al.* indicated that β-arrestin recruitment could play a role in the persistent internalization of the S1P₁ receptor, which might explain the observed tolerance in the effect on HR (Sykes *et al.*, submitted). Since the potencies derived from β-arrestin recruitment assays differ between fingolimod-P and siponimod, i.e. the EC₅₀'s for β-arrestin recruitment are 0.4 nM for fingolimod-P and 2.5 nM siponimod (Sykes *et al.*, submitted), it was investigated whether the estimated IR_{50} and/or $k_{out,R}$ should be corrected for this by multiplying the IR_{50} by 6.25 (2.5/0.4) and/or the $k_{out,R}$ by 0.16 (0.4/2.5). Furthermore, it was assumed that fingolimod-P influences TPR through binding to the S1P₃ receptor (Peters and Alewijnse, 2007; Coussin *et al.*, 2002; Fryer *et al.*, 2012). The potencies of fingolimod-P and siponimod for binding to the S1P₃ receptor were 3.98 nM (Brinkmann *et al.*, 2002) and >1000 nM (Gergely *et al.*, 2012), respectively. Due to its marginal affinity to the S1P₃ receptor compared to fingolimod-P, it is unlikely that siponimod changes TPR through S1P₃ binding. Hence the effect of siponimod on TPR was omitted from the model.

Computation

The data from Studies 1 and 2 were simultaneously analyzed using the non-linear mixed-effects modeling approach implemented in NONMEM (version 7.2.0; Icon Development Solutions, Ellicott City, Maryland, USA). The models were compiled using Digital Fortran (version 6.6C3, Compaq Computer Corporation, Houston, Texas) and executed on a PC equipped with an AMD Athlon 64 processor 3200+ under Windows XP. The results from the NONMEM analysis were subsequently analyzed using the statistical software package S-Plus for Windows (version 8.0 Professional, Insightful Corp., Seattle, USA). Modeling techniques were detailed by Snelder *et al.* (Snelder *et al.*, 2013a; Snelder *et al.*, submitted (a)). In addition, the NWPRI subroutine in NONMEM was used to optimize the PK model for the 10 mg/kg dose. This allowed a penalty function based on a frequency prior to be specified and added to the $-2\log$ likelihood function (Gisleskog *et al.*, 2002). It computes a function based on a frequency prior that has a multivariate normal form for THETA and an inverse Wishart form for OMEGA.

Model selection and evaluation

Models were developed and selected based on the ability to answer the research question and pre-defined statistical criteria. For nested models, a decrease of 10.8 points (corresponding to $p < 0.001$ in a χ^2 -distribution) in the MVOF, which is defined as minus 2 log likelihood, after adding an additional parameter was considered statistically significant. In addition, standard errors of a parameter estimate should be less than 50% of the estimated parameter value and correlations between parameter estimates should lie between -0.95 and 0.95. Overall, the simplest model that met the objectives of this investigation and the pre-defined statistical criteria was preferred in the process of model development. Model evaluation was detailed by Snelder *et al.* (Snelder *et al.*, 2013a).

Results

Pharmacokinetics of fingolimod-P

In the previously developed PK model for fingolimod-P in rats the bioavailability was found to decrease with increasing dose according to a log-dose equation (Snelder *et al.*, submitted (b)). According to this equation the bioavailability of the 10 mg/kg dose would be very low, i.e. 14%. When using this PK model, and assuming the bioavailability of the 10 mg/kg dose equals 14%, the PK of fingolimod-P in Study 2 was predicted adequately for the doses of 0.1-3 mg/kg. However, fingolimod-P blood concentrations following a dose of 10 mg/kg were under-predicted (results not shown). Assuming that the bioavailability does not decrease further for doses higher than 3 mg/kg or, more specifically, assuming

that bioavailability of the 10 mg/kg dose equals the value of the 3 mg/kg dose, significantly improved the goodness of fit. In addition, after optimizing Vm_{obs} (for the 10 mg/kg dose group only), the data from the 10 mg/kg dose group were adequately described (results not shown). The estimated Vm_{obs} (254 [confidence interval (CI): 162–346] ng/h) was significantly higher than the estimated Vm_{obs} from the previously developed PK model (105 [CI: 70.7–139] ng/h (Snelder *et al.*, submitted (b))).

Systems pharmacology model for the interrelationships between hemodynamic variables

The CVS model as expressed by Equation 1 and graphically represented in Figure 1 was applied to characterize the hemodynamics of the effect of fingolimod-P on the CVS. All system-specific parameters were fixed to values reported by Snelder *et al.* (Snelder *et al.*, submitted (a)). However, the parameters of the circadian rhythm were optimized. The amplitude (0.0726 [CI: 0.0663–0.0789]) was significantly lower than the amplitude from the previous investigation (0.0918 [CI: 0.825–1.01] (Snelder *et al.*, submitted (a))). The change in K_{in_HR} and K_{in_TPR} over time was best described by an E_{max} model as expressed by Equation 2 with E_{max} fixed to 1. In SHR, only K_{in_HR} was found to change over time, whereas in WKY rats K_{in_HR} and K_{in_TPR} changed over time with the same ET_{50} .

Target activation and transduction model for fingolimod-P

The model as expressed by equations 1 - 9 was used to analyze the data from Study 1. The response on HR was characterized by a rapid decrease, which attenuated within 1-2 days. This transient effect was described by a fast inhibiting effect on K_{in_HR} (receptor binding), which was followed by stimulation of HR due to tolerance development (presumably receptor internalization and degradation). In addition, the change in TPR was described by a combination of a fast (receptor binding) and slow sustained (receptor sensitization) effect on TPR. The fast effect resulted in a rapid increase in TPR during active treatment. Due to the different feedback mechanisms between TPR, HR and SV (Snelder *et al.*, submitted (a)) the effect of fingolimod-P on TPR was expected to translate into differential effects on MAP, CO, HR, SV. This was indeed observed in the data and adequately described by model. The slow effect was best described by permanent modulation of k_{out_TPR} resulting in a gradual increase in TPR during active treatment. As a result of the modulation of k_{out_TPR} TPR did not return to baseline after stopping treatment. Because of the negative feedback, MAP was increased and CO, HR and SV were decreased after stopping treatment. Consequently, the sustained increase in HR, which was mediated through the effect of fingolimod-P on HR, was partially reversed. $SENS$ was found to increase with BMAP according to a sigmoid E_{max} relationship as expressed by Equation 8 and $SENS$ was 126.3% higher in SHR (typical BMAP: 153.62 mmHg) as compared to WKY rats (typical BMAP:

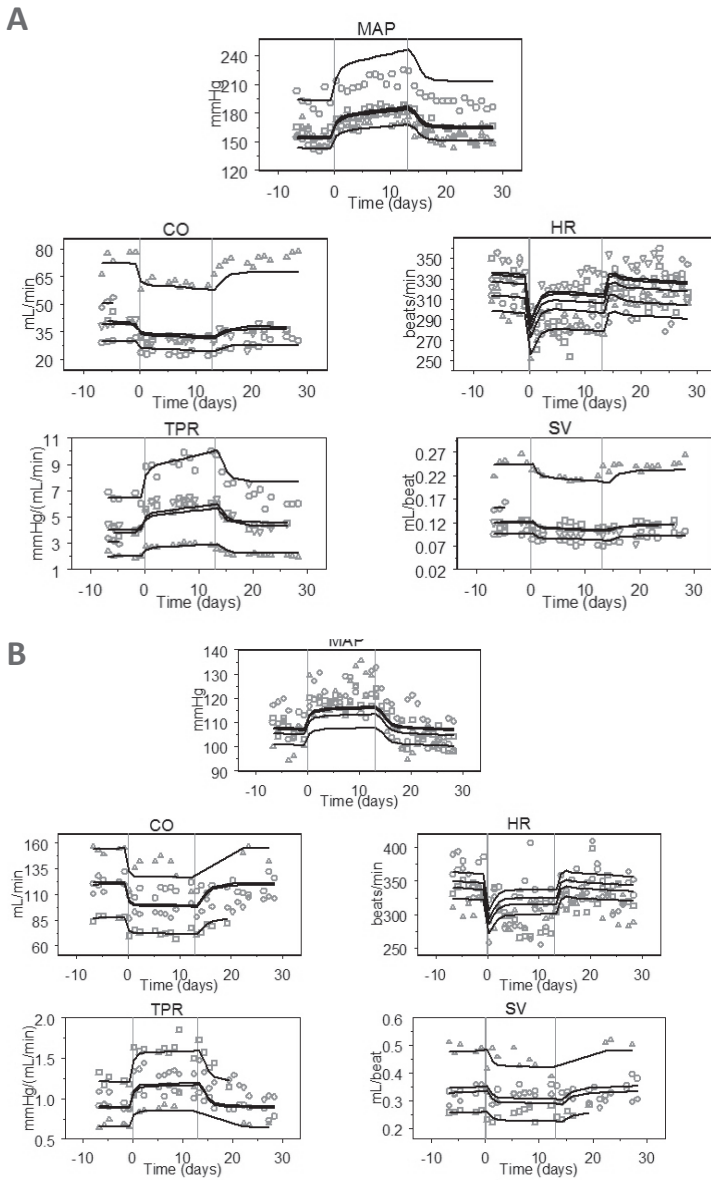
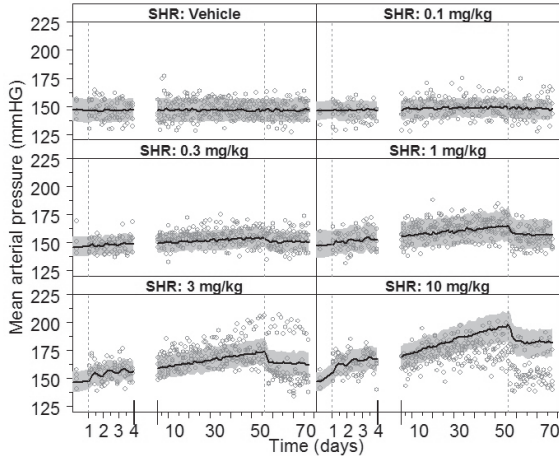


Figure 3: Prediction of the effect of fingolimod-P on MAP, CO, HR, SV and TPR in SHR (A) and WKY rats (B) after oral administration of fingolimod at a dose of 10 mg/kg once daily at 10:00 for 14 days using data from Study 1, experiment 2.

The dots represent the observations (symbols varied per rat) and the continuous lines represent the individual predictions. Start and stop of active treatment are indicated by the vertical grey lines. For clarity, only one observation per day was plotted (hourly average of 16:00-17:00).

A



B

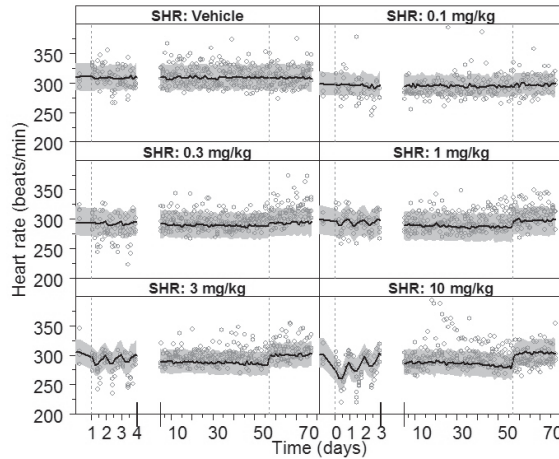
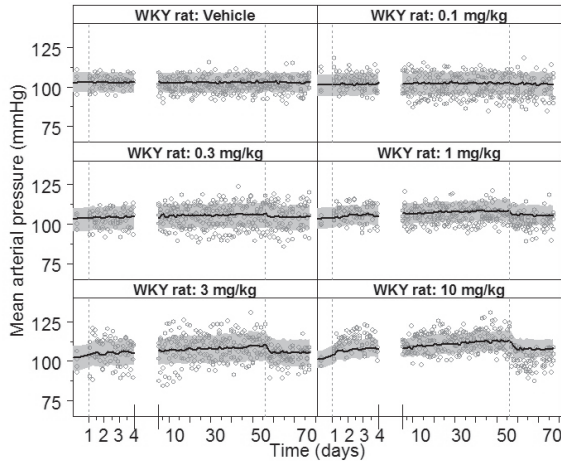
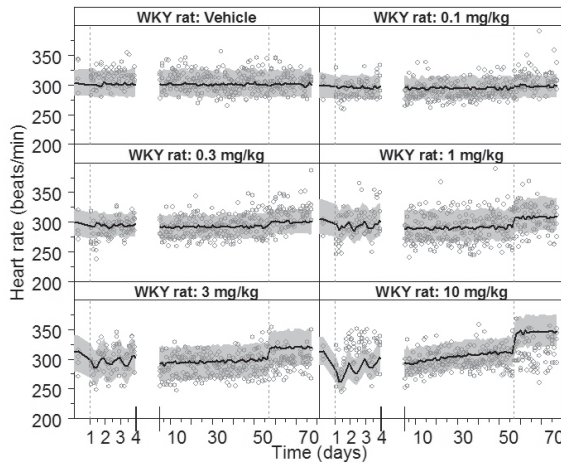


Figure 4: Prediction of the effect of fingolimod-P on MAP and HR in SHR (A and B) and WKY rats (C and D) after oral administration of fingolimod at a dose of 0, 0.1, 0.3, 1, 3 or 10 mg/kg once daily for 8 weeks using data from Study 2 (external model evaluation).

C



D



The grey dots represent the observations after administration of fingolimod. The continuous lines represent the predicted median and the grey area represents the 90% prediction interval. The observations and predictions were corrected for the circadian rhythm and drug-independent change over time as characterized in the vehicle group. For clarity, only six (hourly average, one every 4 hours) and one (hourly average of 16:00-17:00) observations per day were plotted for days 0-3 and 5-75, respectively. Start and stop of treatment are indicated by vertical grey dashed lines.

105.31 mmHg). Within SHR, *SENS* of a rat with a BMAP of 162.14 mmHg (95th percentile of the BMAP distribution) was 21.5 % higher as compared to a rat with a BMAP 139.11 mmHg (5th percentile of the BMAP distribution). The baseline values, *BSL_HR*, *BSL_MAP* and *BSL_CO*, were fixed to the individually observed values as specified in the section “System-specific model”.

In general, the model adequately described the effect of fingolimod-P on MAP, CO, HR, SV and TPR in SHR (Figures 3A and A (appendix)). However, the effect of fingolimod-P on MAP of one rat was over-predicted (Figure 3A). Nonetheless, an external model evaluation using the data from Study 2 demonstrated that the model adequately predicts the

Table 3: Parameter values for the final PKPD model for the effect of fingolimod on the CVS

<i>Parameters</i>	<i>Value</i>	<i>RSE (%)</i>	<i>LLCI</i>	<i>ULCI</i>
Kd_{HR}^* (ng/mL)	3740	24.4	1950	5530
$IR_{50_{fr}}^{***}$ (mL/ng)	1080	19.4	668	1490
$k_{out,R}$ (1/h)	0.0720	14.7	0.0512	0.0928
DEGR (1/h)	0.00286	28.0	0.00129	0.00443
Kd_{TPR}^* (ng/mL)	500	40.2	106	894
$SENS_{EMAX}$ (1/h)	0.00267	44.2	0.000357	0.00498
$SENS_{EC50}$ (mmHG)	122	25.6	60.8	183
$SENS_{NH}$	4.87	44.8	0.597	9.14
S1P	1.17	19.2	0.729	1.61
hor_{HR} (h)	11.1	2.05	10.7	11.5
amp_{HR}	0.0726	4.52	0.0662	0.0790
hor_{TPR} (h)	22.8	1.61	22.1	23.5
amp_{TPR}	Fixed to amp_{HR}			
$ET_{50_{SHR}}$	16300	15	11500	21100
$ET_{50_{WKY rats}}$	7360	18.1	4750	9970
Residual variability				
Prop. Res.Error _{HR} (CV%)	7.4		6.70	7.98
Prop. Res.Error _{MAP} (CV%)	5.7		4.88	6.41
Prop. Res.Error _{CO} (CV%)	8.2		6.60	9.55
RSE: Relative Standard Error				
LLCI: Lower limit of 95 % confidence interval				
ULCI: Upper limit of 95 % confidence interval				
CV: Coefficient of variation				
Blood-plasma ratio: 0.95				
Molecular weight: 387.46 g/mol				
Unbound fraction: 1.3%				

* Kd_{HR} based free plasma concentrations: $3740 \cdot 0.013 \cdot 1000 / (387.46 \cdot 0.95) = 132$ nM

** Kd_{TPR} based free plasma concentrations: $500 \cdot 0.013 \cdot 1000 / (387.46 \cdot 0.95) = 17.7$ nM

*** $IR_{50} = IR_{50_{fr}} / Kd_{HR}$

effect of fingolimod-P on MAP and HR (Figure 4A). In addition, the effect of fingolimod-P on CO, HR, SV and TPR in WKY rats was also adequately described (Figure 3B). The effect on MAP was slightly under-predicted for 4 out of 7 WKY rats (Figure 3B). On the other hand, an external model evaluation using the data from Study 2 demonstrated that the model adequately predicts the effect of fingolimod-P on MAP and HR in WKY rats for doses of 0.1-10 mg/kg (Figure 4B). All parameters could be estimated with good precision (Table 3). Residual errors were small and comparable to the values from the previously developed CVS model (Snelder *et al.*, submitted (a)). In addition, all correlations between structural parameters were less than 0.95.

Prediction of the effect of siponimod

The PK of siponimod in the rats from Study 3 was described adequately by a two-compartmental model with first-order elimination (results not shown). The absorption, which was characterized by two peaks, was described by first-order absorption from two dose compartments. The absorption from the second dose compartment was delayed with a lag-time ($Alag_2$). All parameters could be estimated with good precision, except for the absorption rates from the two dose compartments (k_{a1} and k_{a2}) (Table 4). 67.7 % of the dose was absorbed via the first dose compartment.

The effect of siponimod on MAP and HR in SHR and WKY rats was predicted adequately (Figure 5) using the target activation and transduction model that was developed for fingolimod-P and replacing Kd_{HR} and k_{out_R} (Figure 2). More specifically, the K_d for binding of fingolimod-P to the S1P₁ receptor was replaced with the K_d for binding of siponimod to the S1P₁ receptor. In addition, the k_{out_R} for fingolimod-P induced receptor internalization was replaced with the k_{out_R} for siponimod induced receptor internalization from *in vitro* assays. Overall, the effect of siponimod on HR was characterized by a small transient decrease in HR followed by a small increase in HR. The effect of siponimod on MAP was negligible.

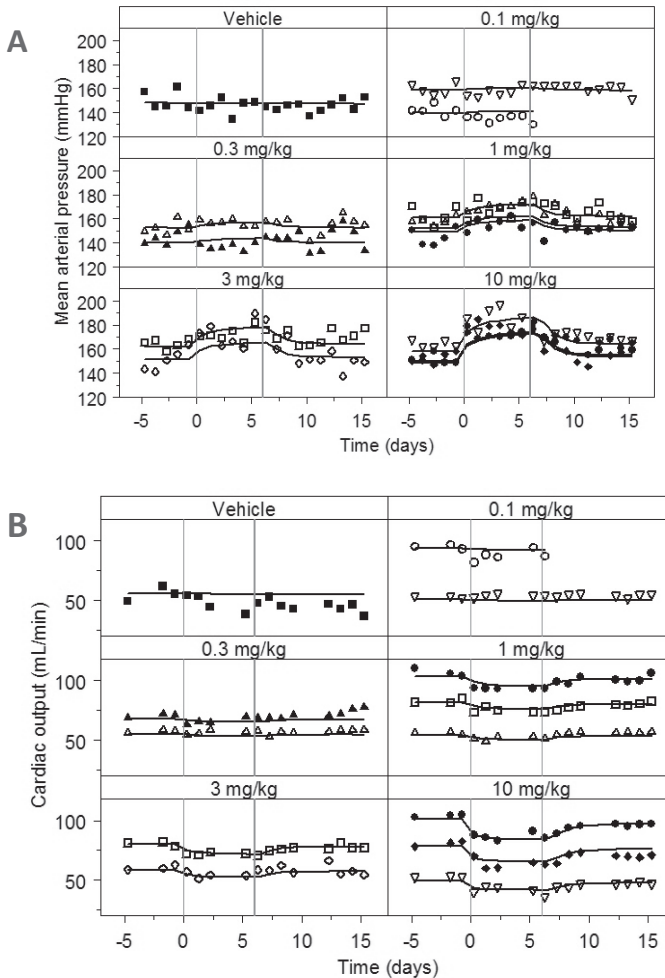


Figure 5: Prediction of the effect of siponimod on MAP (A) and HR (B) in SHR and WKY rats after oral administration of siponimod at a dose of 3 or 15 mg/kg once daily for 8 weeks using data from Study 2.

The grey dots represent the observations after administration of siponimod (3 or 15 mg po). The continuous lines represent the predicted median and the grey area represents the 90% prediction interval. The observations and predictions were corrected for the circadian rhythm and drug-independent change over time as characterized in the vehicle group. For clarity, only six (hourly average, one every 4 hours) and one (hourly average of 16:00-17:00) observations per day were plotted for days 0-3 and 5-75, respectively. Start and stop of treatment are indicated by vertical grey dashed lines.

Table 4: Parameter values for the final PK model for siponimod

Parameter	Value	RSE (%)	LLCI	ULCI
Structural parameters				
k_e (1/h)	0.389	11.3	0.303	0.475
V_c (L)	1.50	16.5	1.01	1.99
k_{a1} (1/h)	0.112	55.4	-0.00952	0.234
k_{23} (1/h)	0.676	40.2	0.143	1.21
k_{32} (1/h)	0.845	24.4	0.441	1.25
k_{24} (1/h)	0.0673	24.2	0.0354	0.0992
k_{42} (1/h)	0.0846	19.6	0.0521	0.117
F_r^*	0.738	44.6	0.0932	1.38
k_{a2} (1/h)	0.431	100	-0.414	1.28
$Alag_2$	7.13	28.2	3.19	11.1
Inter-Individual variability				
F_r (additive) (CV%)	123.3	43.0	39.6	211.5
Residual variability				
Prop. Res.Error _{HR} (CV%)	21.8		17.77	25.23

RSE: Relative Standard Error

LLCI: Lower limit of 95 % confidence interval

ULCI: Upper limit of 95 % confidence interval

CV: Coefficient of variation

*: F_1 (Relative bioavailability dose compartment 1) = $EXP(F_r)/(1+EXP(F_r))$

F_5 (Relative bioavailability dose compartment 2) = $1- EXP(F_r)/(1+EXP(F_r))$

Discussion

In humans, S1P receptor agonists, which are effective in the treatment of multiple sclerosis (Cohen *et al.*, 2010; Gergely *et al.*, 2012), are associated with cardiovascular effects. The immunosuppressant effects, as well as the cardiovascular effects, of these compounds are believed to be mediated through the S1P receptor, which complicates the search for novel S1P receptor agonists that are devoid of cardiovascular effects. A quantitative understanding of the hemodynamics of these effects is important to select new compounds with an improved safety profile. Moreover, it may provide insights in how to pharmacologically prevent and reverse these effects for new S1P receptor agonists (Kovarik *et al.*, 2008), or to design dose titration schemes to attenuate these effects (Legangneux *et al.*, 2013). Recently, a CVS model was developed to characterize drug effects on the CVS (Snelder *et al.*, 2013a; Snelder *et al.*, submitted (a)). As a systems pharmacology model it characterizes the interactions between different components of a complex system (Kohl *et al.*, 2010) and can be applied to characterize drug effects. A potential application of this model is the prediction of the cardiovascular effects of novel compounds. To facilitate the prediction of cardiovascular effects *in vivo* using parameters derived from *in vitro*

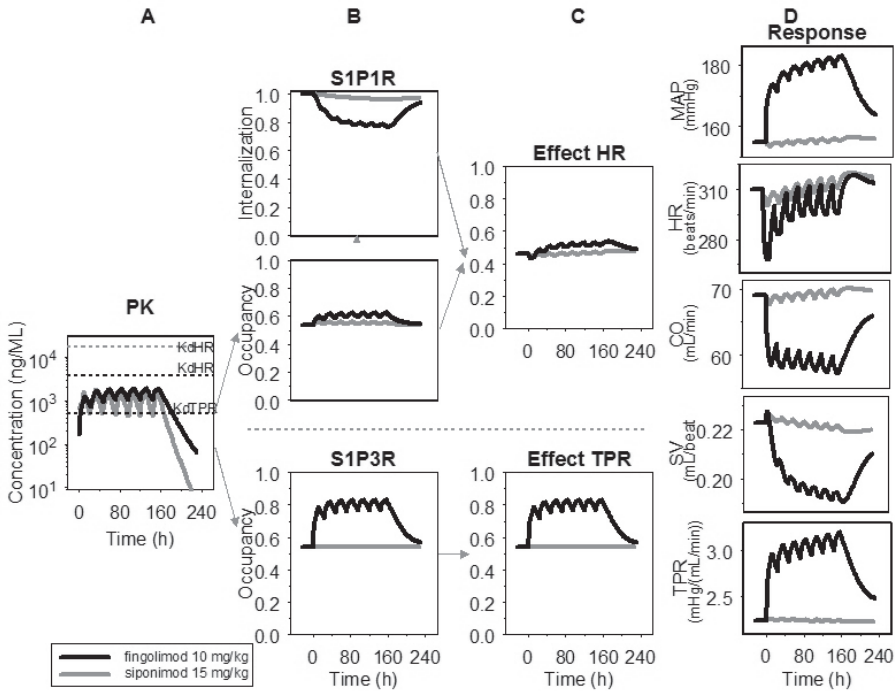


Figure 6: Illustration of the change over time in the pharmacokinetics of fingolimod or siponimod (A), receptor binding kinetics (B), receptor activation (C) and response (D) in SHR after administration of 7 daily doses of fingolimod (10 mg/kg; black lines) or siponimod (15 mg/kg; grey lines) as predicted by the CVS model integrated with expression for receptor binding kinetics.

For fingolimod the estimated Kd_{TPR} is in the same range as the total blood concentrations, whereas the Kd_{HR} is above estimated total blood concentrations resulting in a larger change in receptor occupancy and a larger relative effect at the $S1P_3$ receptor ($S1P3R$) than at the $S1P_1$ receptor ($S1P1R$). For siponimod the assumed Kd_{HR} is higher than the Kd_{HR} for fingolimod, whereas the concentrations are in the same range. Therefore, the relative effect of siponimod on HR is smaller than the effect of fingolimod. The overall responses on MAP, HR, CO, SV and TPR result from the combined effects on HR and TPR. Receptor sensitization was omitted. The predicted maximum decrease in HR is approximately 42 beats/min after administration of fingolimod (10 mg/kg), of which ~15 and 27 beats/min result from the effects on HR and TPR respectively, and 10 beats/min after administration of siponimod (15 mg/kg). The nadir is reached at approximately 8 and 3 hours after the first dose for fingolimod and siponimod, respectively

experiments this requires the interfacing of the CVS model with a target receptor binding and activation model. In this investigation the systems cardiovascular pharmacology CVS model was successfully applied to characterize and predict the hemodynamics of the cardiovascular effects of S1P receptor agonists in rats, using fingolimod-P and siponimod as paradigm compounds.

First the effect of fingolimod-P on the CVS was characterized. The CVS model was combined with a receptor binding, down-regulation and sensitization model to describe the effect of fingolimod-P on HR and TPR (Figure 2). More specifically, the transient effect on HR was described by a fast inhibiting effect depending on the degree of receptor binding, which was followed by stimulation of HR due to tolerance development presumably as a result of receptor internalization and degradation. Furthermore, the effect of fingolimod-P on TPR was described by a combination of a fast and a slow sustained effect. As a next step, the effect of siponimod on MAP and HR was predicted. The effect of siponimod on MAP was negligible and the effect on HR was characterized by a small transient decrease in HR followed by a small increase in HR. In general, these effects were adequately predicted in SHR and WKY rats (Figure 5), which indicates that the developed model may be applied to predict the effect of other S1P agonists on the CVS in rat. The simulated changes over time in all components leading to the overall response on MAP, CO, HR, SV and TPR are illustrated in Figure 6 following once daily administration of fingolimod or siponimod at doses of 10 and 15 mg/kg, respectively.

The identified drug effects of fingolimod-P and siponimod are in line with the available information on the mechanisms underlying the cardiovascular effects of fingolimod-P and siponimod, which increases the confidence in the applied systems pharmacology modeling approach and the predictive power of the model. Briefly, the current understanding on the mechanisms underlying the cardiovascular effects of fingolimod-P and siponimod are as follows. Fingolimod, and more specifically, fingolimod-P binds to 4 of the 5 subtypes of the S1P receptor ($S1P_1$ and $S1P_{3-5}$) with high affinity (0.3-3.1 nM) (Mandala *et al.*, 2002; Brinkmann, 2007; Brinkmann *et al.*, 2004), whereas siponimod binds to only 2 of the 5 subtypes ($S1P_1$ and $S1P_5$) with high affinity, while the affinity for the $S1P_3$ receptor is low (Gergely *et al.*, 2012). $S1P_1$ is thought to be the relevant receptor subtype involved in the modulation of HR (Horga *et al.*, 2010; Gergely *et al.*, 2012). The atrial muscarinic-gated potassium channel IKACH is activated (Koyrakh *et al.*, 2005), which results in a negative chronotropic effect. Therefore, fingolimod-P first acts as a full agonist at the $S1P_1$ receptor (Horga *et al.*, 2010; Mullershausen *et al.*, 2009). The transient nature of the effect on HR is related to receptor internalization and degradation (Horga *et al.*, 2010; Mullershausen *et al.*, 2009). As a result fingolimod-P acts a functional antagonist. The exact mechanism

underlying the effect of fingolimod-P on TPR, and thus MAP, is under debate. Three different mechanisms have been proposed.

- i) Fingolimod-P influences TPR through binding to the S1P₃ receptor (Peters and Alewijnse, 2007; Coussin *et al.*, 2002).
- ii) Fingolimod-P influences TPR via a shift in the balanced S1P-S1P₁/S1P₂/S1P₃-signaling resulting from fingolimod-P induced S1P₁ receptor internalization (Bigaud *et al.*, 2013).
- iii) Fingolimod (not fingolimod-P) induces TPR via inhibition of S1PHK1 (Spijkers *et al.*, 2012).

In humans, the first hypothesis is thought to be unlikely as the blood concentrations of S1P as well as the affinities of S1P for the S1P₃ receptor are considerably higher compared to fingolimod-P (Sykes *et al.*, submitted; Bigaud *et al.*, 2013). However, for several reasons it is possible that this hypothesis is valid in rat. For instance, 1) the exact free S1P concentration in different tissues is unknown (Bigaud *et al.*, 2013), 2) large inter-species differences may exist in S1P concentration (Gräler *et al.*, 2004) and 3) receptor binding kinetics may vary considerably between rat and human. The second hypothesis represents the current understanding on the small slow, increase in MAP following therapeutic dosing regimen in humans. As siponimod leads to internalization of the S1P₁ receptors this assumption implies that siponimod would have an effect on MAP, whereas such an effect has not been reported in man and was not observed in rats. It cannot be excluded, however, that this was not observed in rats due to a limited experimental design, e.g. a low number of rats or too low siponimod doses. Finally, the third hypothesis seems implausible as inhibiting S1P synthesis would influence the whole S1P biology. Overall, it seems most likely that the fast effect of fingolimod-P on TPR, which was observed in rats, is mediated through the S1P₃ receptor. Furthermore, the slow effect on TPR may be a result of receptor sensitization. More precisely, the major trigger for smooth muscle cell contraction is a rise in intracellular calcium concentration. Whereas the calcium-dependent phase of smooth muscle cell contraction is rapid and relatively transient, calcium sensitization produced by agonist stimulation results in a sustained contraction of vascular smooth muscle cells (Watterson *et al.*, 2005), and thus, in a sustained increase in TPR. However, other mechanisms underlying the slow effect on TPR, including a shift in the balanced S1P- S1P₁/S1P₂/S1P₃-signaling as proposed by Bigaud *et al.* (Bigaud *et al.*, 2013), may not be excluded as it is not possible to distinguish between different hypotheses following a data driven modeling approach when the expected effect is comparable.

In general, the effect of fingolimod-P on MAP, CO, HR, SV and TPR in SHR and WKY rats was adequately described by the model (Figure 3, 4 and A (appendix)). However, the effect on MAP in WKY rats was slightly under-predicted for 4 out of 7 WKY rats. This could indicate

that the feedback, which was fixed to the value from the CVS model, was too strong for WKY rats. In the CVS model, the efficiency of the feedback was found to decrease with higher BSL_MAP values, indicating a decrease in the efficiency of blood pressure regulation in hypertensive subjects. Since the characterization of the feedback relationship was based on data from a limited number of rats, i.e. 10 SHR and 2 WKY rats, the accuracy of the estimation of feedback might be low for WKY rats. In addition, it should be noted that in Study 1 the effect of fingolimod-P on the CVS was investigated for a dose of 10 mg/kg only. As the external model evaluation demonstrated that the data from Study 2 could be adequately predicted for all doses in both SHR and WKY rats, the small under-prediction of the effect of fingolimod-P on MAP in WKY rats in Study 1 was accepted. The inter-individual variability in the response was large and originated mostly from variability in baselines and receptor sensitization. Therefore, in the final model the variability in baselines was accounted for by using the observed baseline values of MAP, CO and HR (BSL_MAP , BSL_CO and BSL_HR), rather than the model predictions. Quantification of the covariate effect of BMAP on $SENS$ largely explained the observed variability in sensitization. However, after accounting for these inter-individual differences, the effect of fingolimod-P on MAP in 1 SHR was over-predicted indicating that not all variability between rats was explained (Figure 3A). As, in general, the data from Study 1 were adequately described by the model, and an external model evaluation demonstrated that the data from Study 2 could be adequately predicted, the random structure of the model was not further optimized. Kd_{TPR} and Kd_{HR} were estimated to be 17.7 [CI: 3.74–31.6] and 132 [CI: 68.9–195] nM based on free plasma concentrations, respectively (Table 3). In addition, $S1P$, which represents the ratio of the S1P concentration and the Kd of S1P for binding to the S1P receptor, was estimated to be 1.17 [CI: 0.729-1.61] (Table 3). This indicates that the free S1P plasma concentration, which is probably the best predictor for the effect of S1P on the CVS, is in the same order of magnitude as the Kd .

Finally, it should be noted that the identified receptor (target) binding and activation parameters are estimated on the basis of hemodynamic data. Therefore, a comparison with parameters derived from *in vitro* binding assays using the rat S1P receptor is required in order to investigate whether the receptor binding and activation are reflected adequately. However, to date no quantitative information has been published on the receptor binding kinetics of S1P agonists in rats. Therefore, these estimates should only be interpreted in the context of this model. For the same reason, the modeling results do not provide definite conclusions on the plausibility of the different hypothesized mechanisms underlying the effect of fingolimod-P on TPR, and thus MAP.

In conclusion, a previously developed system-specific model to characterize drug effects on the CVS was combined with a receptor binding model with drug-specific parameters, and down-regulation and sensitization models with class-specific parameters. This model was applied to quantify the cardiovascular effects of fingolimod-P in rat and provided a quantitative understanding of the hemodynamics of the cardiovascular effects following the administration of fingolimod-P. In addition, the effect of siponimod on the CVS was predicted adequately by multiplying the estimated *in vivo* dissociation constants of fingolimod-P for binding to the S1P receptors with the ratio of the potencies of fingolimod-P and siponimod derived from *in vitro* binding assays. Therefore, it is anticipated that the developed model can be applied to predict the effect of other S1P receptor agonists on the CVS in rat. Ultimately, this quantitative pharmacology model may be used to predict the clinical response of fingolimod-P and follow-up compounds on the CVS based on preclinical data. Before our model can be applied for that purpose, the model should be scaled to human and validated on human MAP, CO and HR measurements (Snelder *et al.*, 2013a). In addition, inter-species differences in plasma protein binding, blood-plasma distribution (Snelder *et al.*, submitted (b)) and receptor function and expression should be taken into account.

References

- Ariëns EJ & Simonis AM (1964). A Molecular Basis for Drug Action. The Interaction of One or More Drugs with Different Receptors. *J Pharm Pharmacol.*, 16, 289-312.
- Bigaud M, Guerini D, Billich A, Bassilana F & Brinkmann V (2013). Second generation S1P pathway modulators: Research strategies and clinical developments. *Biochim Biophys Acta*, 12, 00243-00246.
- Brinkmann V, Davis MD, Heise CE, Albert R, Cottens S, Hof R, et al. (2002). The immune modulator FTY720 targets sphingosine 1-phosphate receptors. *J Biol Chem.*, 277, 21453-21457.
- Brinkmann V, Cyster JG & Hla T (2004). FTY720: sphingosine 1-phosphate receptor-1 in the control of lymphocyte egress and endothelial barrier function. *Am J Transplant.*, 4, 1019-1025.
- Brinkmann V (2007). Sphingosine 1-phosphate receptors in health and disease: mechanistic insights from gene deletion studies and reverse pharmacology. *Pharmacol Ther.*, 115, 84-105.
- Cohen JA, Barkhof F, Comi G, Hartung HP, Khatri BO, Montalban X, et al. (2010). Oral fingolimod or intramuscular interferon for relapsing multiple sclerosis. *N Engl J Med.*, 362, 402-415.
- Coussin F, Scott RH, Wise A & Nixon GF (2002). Comparison of sphingosine 1-phosphate-induced intracellular signaling pathways in vascular smooth muscles: differential role in vasoconstriction. *Circ Res.*, 91, 151-157.
- Danhof M, de Jongh J, De Lange EC, Della Pasqua O, Ploeger BA & Voskuyl RA (2007). Mechanism-based pharmacokinetic-pharmacodynamic modeling: biophase distribution, receptor theory, and dynamical systems analysis. *Annu Rev Pharmacol Toxicol.*, 47, 357-400.
- Danhof M, de Lange EC, Della Pasqua OE, Ploeger BA & Voskuyl RA (2008). Mechanism-based pharmacokinetic-pharmacodynamic (PK-PD) modeling in translational drug research. *Trends Pharmacol Sci.*, 29, 186-191.
- Dayneka NL, Garg V & Jusko WJ (1993). Comparison of four basic models of indirect pharmacodynamic responses. *J Pharmacokinetic Biopharm.*, 21, 457-478.
- Fryer RM, Muthukumarana A, Harrison PC, Nodop Mazurek S, Chen RR, Harrington KE, et al. (2012). The clinically-tested S1P receptor agonists, FTY720 and BAF312, demonstrate subtype-specific bradycardia (S1P(1)) and hypertension (S1P(3)) in rat. *PLoS One.*, 7, e52985.
- Gabrielsson J. and Weiner D. (2000) Pharmacokinetic and pharmacodynamic data analysis: concepts and applications. Swedish Pharmaceutical Press: Stockholm (book)
- Gergely P, Nuesslein-Hildesheim B, Guerini D, Brinkmann V, Traebers M, Bruns C, et al. (2012). The selective sphingosine 1-phosphate receptor modulator BAF312 redirects lymphocyte distribution and has species-specific effects on heart rate. *Br J Pharmacol.*, 167, 1035-1047.
- Gisleskog PO, Karlsson MO & Beal SL (2002). Use of prior information to stabilize a population data analysis. *J Pharmacokinetic Pharmacodyn.*, 29, 473-505.
- Graler MH & Goetzl EJ (2004). The immunosuppressant FTY720 down-regulates sphingosine 1-phosphate G-protein-coupled receptors. *Faseb J.*, 18, 551-553.
- Horga A, Castillo J & Montalban X (2010). Fingolimod for relapsing multiple sclerosis: an update. *Expert Opin Pharmacother.*, 11, 1183-1196.
- Kappos L, Antel J, Comi G, Montalban X, O'Connor P, Polman CH, et al. (2006). Oral fingolimod (FTY720) for relapsing multiple sclerosis. *N Engl J Med.*, 355, 1124-1140.
- Kappos L, Radue EW, O'Connor P, Polman C, Hohlfeld R, Calabresi P, et al. (2010). A placebo-controlled trial of oral fingolimod in relapsing multiple sclerosis. *N Engl J Med.*, 362, 387-401.
- Kilkenny C, Browne W, Cuthill IC, Emerson M, Altman DG (2010). NC3Rs Reporting Guidelines Working Group. *Br J Pharmacol* 160: 1577–1579.
- Kohl P, Crampin EJ, Quinn TA & Noble D (2010). Systems biology: an approach. *Clin Pharmacol Ther.*, 88, 25-33.
- Kovarik JM, Slade A, Riviere GJ, Neddermann D, Maton S, Hunt TL & Schmouder RL (2008). The ability of atropine to prevent and reverse the negative chronotropic effect of fingolimod in healthy subjects. *Br J Clin Pharmacol.*, 66, 199-206.
- Koyrakh L, Roman MI, Brinkmann V & Wickman K (2005). The heart rate decrease caused by acute FTY720 administration is mediated by the G

protein-gated potassium channel I. *Am J Transplant.*, 5, 529-536.

Legangneux E, Gardin A & Johns D (2013). Dose titration of BAF312 attenuates the initial heart rate reducing effect in healthy subjects. *Br J Clin Pharmacol.*, 75, 831-841.

Levick JR (2003). *An introduction to cardiovascular physiology*. Hodder Arnold Publishers: London (book).

Lukas S, Patnaude L, Haxhinasto S, Slavin A, Hill-Drzewi M, Horan J & Modis LK (2013). No Differences Observed among Multiple Clinical S1P1 Receptor Agonists (Functional Antagonists) in S1P1 Receptor Down-regulation and Degradation. *J Biomol Screen*, 3, 3.

Mandala S, Hajdu R, Bergstrom J, Quackenbush E, Xie J, Milligan J, et al. (2002). Alteration of lymphocyte trafficking by sphingosine-1-phosphate receptor agonists. *Science.*, 296, 346-349.

McGrath J, Drummond G, McLachlan E, Kilkenny C, Wainwright C (2010). Guidelines for reporting experiments involving animals: the ARRIVE guidelines. *Br J Pharmacol* 160: 1573-1576.

Mullershausen F, Zecri F, Cetin C, Billich A, Guerini D & Seuwen K (2009). Persistent signaling induced by FTY720-phosphate is mediated by internalized S1P1 receptors. *Nat Chem Biol.*, 5, 428-434.

National Research Council (2011). *Guide for the Care and Use of Laboratory Animals*. National Academies Press, 8th edition.

Peters SL & Alewijnse AE (2007). Sphingosine-1-phosphate signaling in the cardiovascular system. *Curr Opin Pharmacol.*, 7, 186-192.

Ploeger BA, van der Graaf PH & Danhof M (2009). Incorporating receptor theory in mechanism-based pharmacokinetic-pharmacodynamic (PK-PD) modeling. *Drug Metab Pharmacokinet.*, 24, 3-15.

Romero E, Velez de Mendizabal N, Cendros JM, Peraire C, Bascompta E, Obach R, et al. (2012). Pharmacokinetic/pharmacodynamic model of the testosterone effects of triptorelin administered in sustained release formulations in patients with prostate cancer. *J Pharmacol Exp Ther.*, 342, 788-798.

Selmaj K, Li DK, Hartung HP, Hemmer B, Kappos L, Freedman MS, et al. (2013). Siponimod for patients with relapsing-remitting multiple sclerosis (BOLD): an

adaptive, dose-ranging, randomised, phase 2 study. *Lancet Neurol.*, 12, 756-767.

Snelder N, Ploeger BA, Luttringer O, Rigel DF, Webb RL, Feldman D, et al. (2013a). PKPD modeling of the interrelationship between mean arterial blood pressure, cardiac output and total peripheral resistance in conscious rats. *Br J Pharmacol*, 169, 1510-1524.

Snelder N, Ploeger BA, Luttringer O, Rigel DF, Webb RL, Feldman D, et al. (2013b). PAGE 22, Abstr 2686 [www.page-meeting.org/?abstract=2686]

Snelder N, Ploeger BA, Luttringer O, Rigel DF, Fu F, Beil M, et al. (Submitted (a)). PKPD modeling of drug effects on the cardiovascular system in conscious rats – parsing cardiac output into heart rate and stroke volume.

Snelder N, Ploeger BA, Luttringer O, Stanski D & Danhof M (Submitted (b)). Translational pharmacokinetic modeling of fingolimod (FTY720) as a paradigm compound subject to sphingosine kinase-mediated phosphorylation.

Spijkers LJ, Alewijnse AE & Peters SL (2012). FTY720 (fingolimod) increases vascular tone and blood pressure in spontaneously hypertensive rats via inhibition of sphingosine kinase. *Br J Pharmacol.*, 166, 1411-1418.

Sykes DA, Riddy D, Stamp C, Bradley M, McGuinness N, Guerini D, et al. (Submitted). Investigating the molecular mechanisms through which FTY720-P causes persistent S1P1 receptor internalisation.

Watterson KR, Ratz PH & Spiegel S (2005). The role of sphingosine-1-phosphate in smooth muscle contraction. *Cell Signal.*, 17, 289-298.

Abbreviations

Amp	Amplitude
BMAP	Observed baseline value of mean arterial pressure (covariate)
<i>BSL_CO</i>	Baseline value of cardiac output
<i>BSL_HR</i>	Baseline value of heart rate
<i>BSL_MAP</i>	Baseline value of mean arterial pressure (parameter)
<i>BSL_SV</i>	Baseline value of stroke volume
<i>BSL_TPR</i>	Baseline value of total peripheral resistance
C	drug concentration in plasma
CO	Cardiac output
CVS	Cardiovascular system
Emax	Maximum effect
EC50	Concentration resulting in a half-maximal effect
FB	Negative feedback of mean arterial pressure
fingolimod-P	Fingolimod-phosphate
HCTZ	Hydrochlorothiazide
HOR	Horizontal displacement
HR	Heart rate
IIV	Inter-individual variability
K_{in_HR}	Zero-order production rate constant of heart rate
K_{in_SV}	Zero-order production rate constant of stroke volume
K_{in_TPR}	Zero-order production rate constant of total peripheral resistance
k_{out_HR}	First-order dissipation rate constant of heart rate
k_{out_SV}	First-order dissipation rate constant of stroke volume
k_{out_TPR}	First-order dissipation rate constant of total peripheral resistance
LVFT	Left ventricular filling time
MAP	Mean arterial pressure
MC	Methylcellulose
MoA	Mechanisms of action
MVOF	Minimum value of the objective function
PD	Pharmacodynamics
PK	Pharmacokinetics
PKPD	Pharmacokinetic-pharmacodynamic
RAAS	Renin-angiotensin-aldosterone system
SHR	Spontaneously hypertensive rats
SV	Stroke volume
S1P	sphingosine 1-phosphate
S1PHK1	Sphingosine kinase

S1P1R	sphingosine 1-phosphate receptor, subtype 1
S1P3R	sphingosine 1-phosphate receptor, subtype 1
T	Time
TPR	Total peripheral resistance
WKY	Wistar Kyoto rats

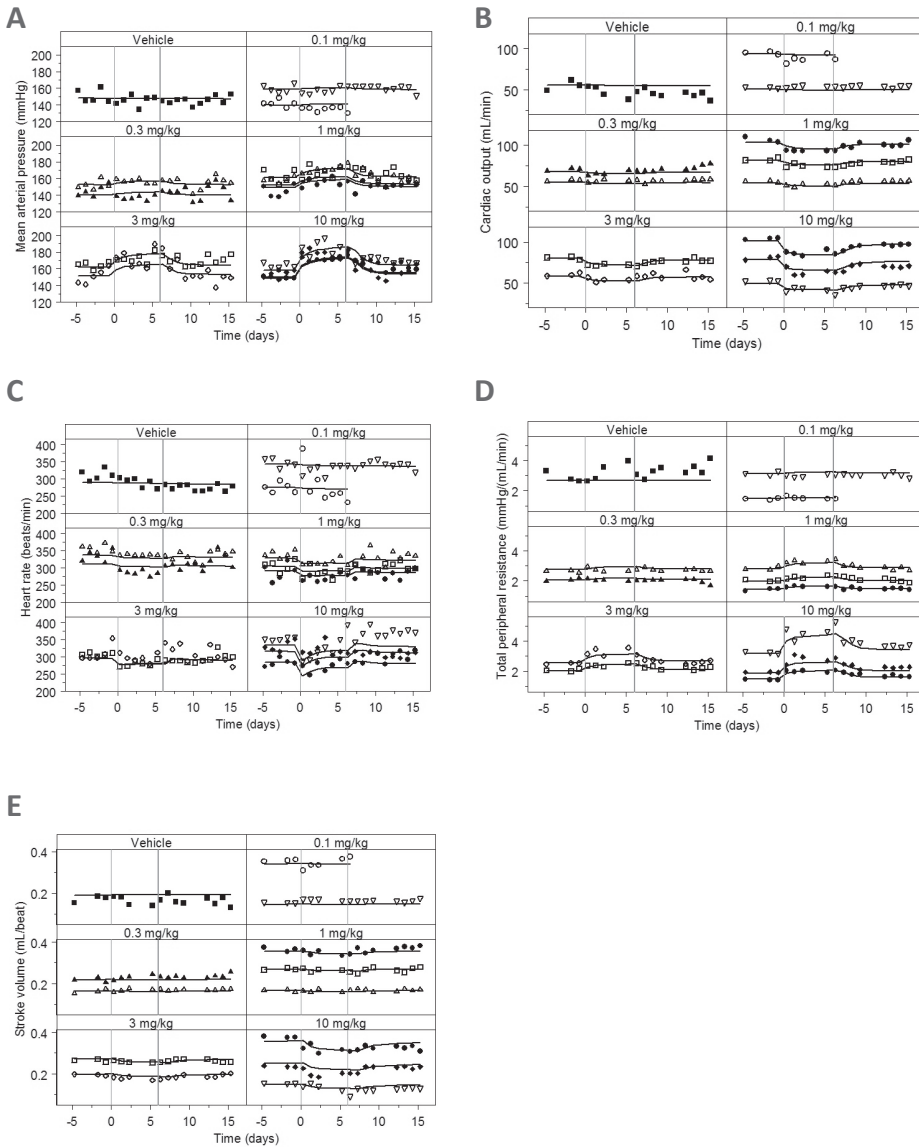
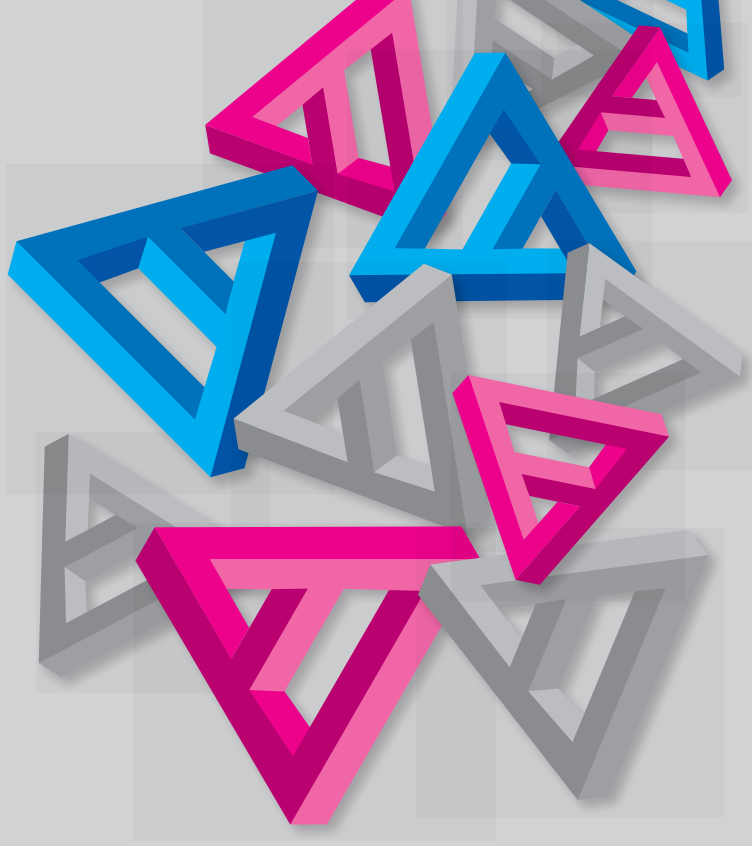


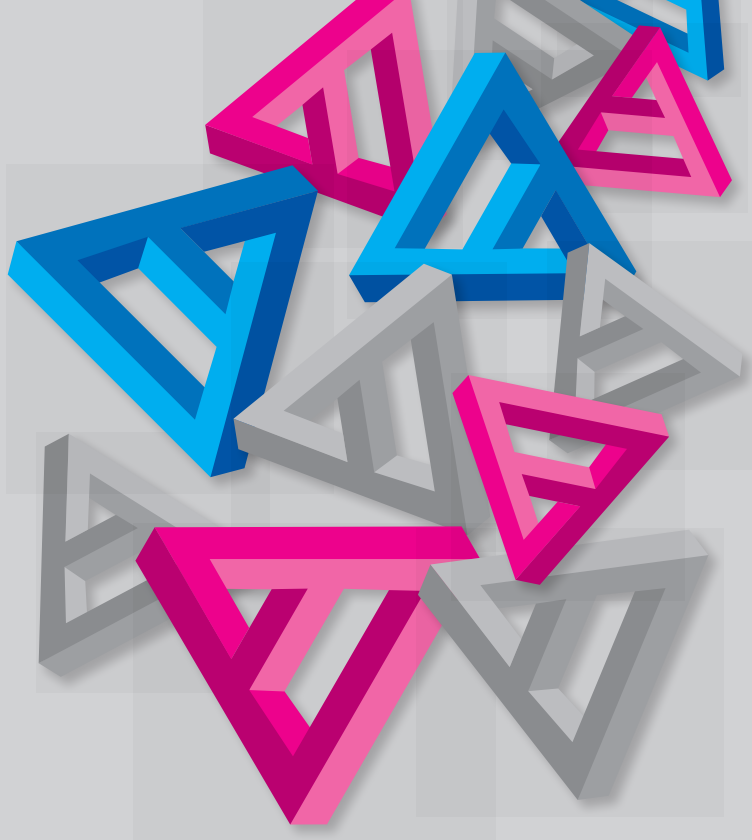
Figure A: Prediction of the effect of fingolimod-P on MAP (A), CO (B), HR (C), SV (D) and TPR (E) in SHR after once daily administration of fingolimod (dose: vehicle, 0.1, 0.3, 1, 3 or 10 mg/kg p.o.) using data from Study 1, experiment 1.

The dots represent the observations (symbols varied per rat) and the continuous lines represent the individual predictions. Start and stop of active treatment are indicated by the vertical grey lines. For clarity, only one observation per day was plotted (hourly average of 16:00-17:00).



SECTION IV

Summary, conclusions & perspectives



CHAPTER 7

A systems pharmacology approach to the prediction of cardiovascular side effects in man - Summary, conclusions & perspectives

Introduction and objectives

Cardiovascular safety issues related to changes in blood pressure, arise frequently in drug development. In this thesis, a systems pharmacology model is described which allows predicting hemodynamic changes in man on the basis of information from pre-clinical studies. The proposed model is based on well-established principles of the regulation of blood-pressure. It is well-known that mean arterial pressure (MAP) equals the product of cardiac output (CO) and total peripheral resistance (TPR) and that CO equals the product of HR and stroke volume (SV). However, the effects of drugs on this interrelationship have not been analyzed in a mechanism-based and quantitative manner. A pertinent feature of mechanism-based pharmacokinetic-pharmacodynamic (PKPD) models is the distinction between drug and biological-system specific properties for the characterization of *in vivo* drug effects (Danhof *et al.*, 2007; Ploeger *et al.*, 2009). In this regard, drug-specific parameters describe the interaction between the drug and the biological system in terms of target affinity and target activation, whereas system-specific parameters describe the dynamics of the biological system. This separation enables prediction and extrapolation of treatment effects to biological systems other than the systems that have been studied (e.g. the translation from laboratory animals to humans) (Danhof *et al.*, 2007). Typically, mechanism-based and mechanistic PKPD models are based on an analysis of the causal path between drug exposure and response. More recently the concept of systems pharmacology has been introduced. With systems pharmacology models the complexity is increased by focusing on networks and the interactions between different components of the network. A systems pharmacology modeling approach is uniquely suited to quantify drug effects on the interrelationship between MAP, CO, HR, SV and TPR (**Chapter 1**).

The objectives of the investigations described in this thesis were 1) to establish a systems pharmacology model to characterize the effects of drugs with different mechanisms of action (MoA's) on the interrelationship between MAP, CO, HR, SV and TPR in a quantitative manner and 2) to apply the model to the quantification of the cardiovascular effects of the sphingosine 1-phosphate (S1P) receptor modulator fingolimod. In this chapter, the results of the investigations described in this thesis are reviewed and the perspectives and conclusions are presented.

Development of a systems pharmacology model to characterize the CVS

In **Chapter 3**, a systems pharmacology model was proposed to characterize the CVS in hypertensive rats. This system pharmacology model is based on the interrelationship between MAP, CO and TPR. The effects of a prototype set of cardiovascular compounds

with different mechanisms of action were characterized in chronically instrumented spontaneously hypertensive rats (SHR). Beforehand it was hypothesized that two aspects of the experimental design were pivotal to successfully quantify the parameters of the basic CVS model: i) the selection of the prototype set of compounds affecting the functioning of the CVS and ii) measuring both MAP and CO during the on- and offset phases of the drug effects. By selecting a range of cardiovascular drugs with well described, but different target sites and with different profiles of the time courses of the effects, all parameters of the systems pharmacology model could be estimated with good precision. Moreover, system-specific parameters could be distinguished from drug-specific parameters indicating that the developed model is drug-independent. The measurement of CO, was pivotal to identify all parameters of the basic systems pharmacology model as this provide the information to distinguish between changes in CO and TPR. To be able to measure drug effects on MAP and CO, rats were surgically instrumented with both an ascending aortic flow

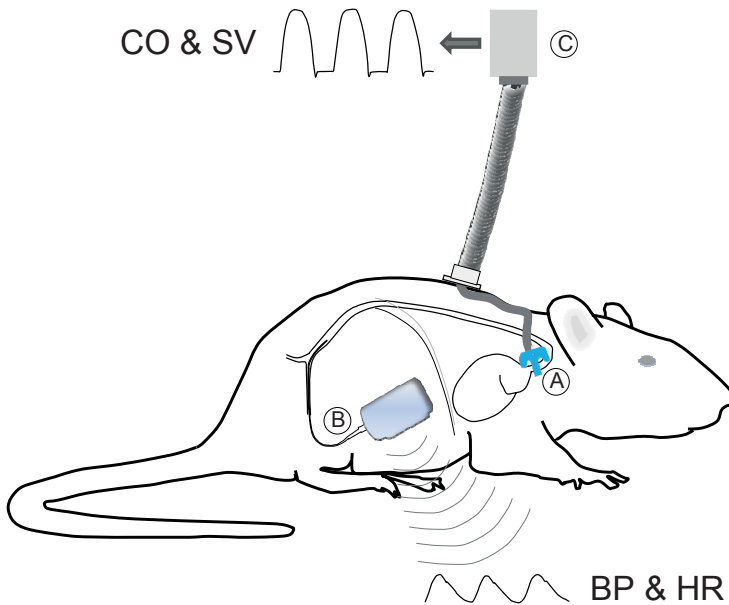


Figure 1: Experimental animal instrumentation. Rats were surgically instrumented with both an ascending aortic flow probe (A) and a femoral arterial catheter/radiotransmitter (B). CO was measured by connecting the flow probe to the flow meter via a cable and electrical swivel (C), which allowed the animal to remain fully ambulatory. MAP, HR, SV, CO, and TPR were derived for all beats averaged over consecutive 2-min intervals.

probe and a femoral arterial catheter/radiotracer (Figure 1). Overall, the rigorous experimental design provided the data to describe the interrelationship between MAP, CO and TPR in a quantitative and mechanism-based manner. The basic CVS model can be applied to elucidate the site of action of new compounds which affect MAP through a still unknown MoA.

A limitation of this model is that measuring CO has not been integrated into daily practice due to the challenges associated with the implantation of aortic flow probes. Therefore, in **Chapter 4** the basic CVS model was extended by parsing CO into HR and SV (Figure

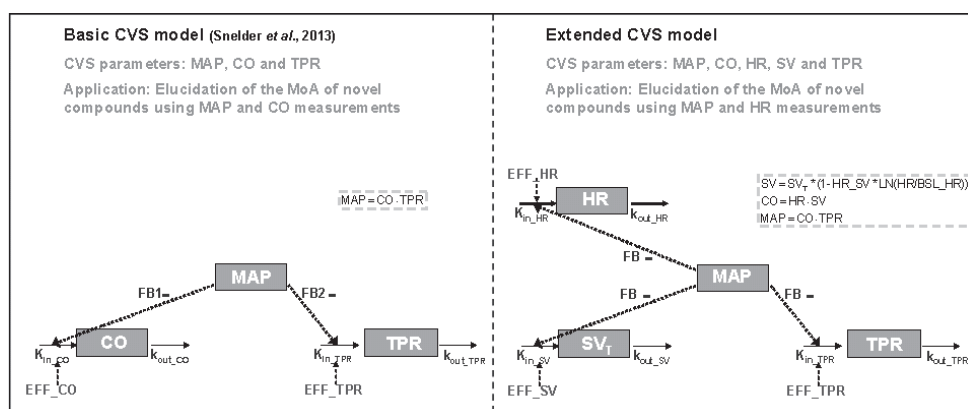


Figure 2: Comparison between the basic CVS model to characterize drug effects on the interrelationship between MAP, CO and TPR and the extended CVS model to characterize drug effects on the interrelationship between MAP, CO, HR, SV and TPR

Basic CVS model (Chapter 3): MAP equals the product of CO and TPR ($MAP=CO*TPR$). Effects on CO and TPR are described by two linked turnover equations. When MAP increases as a result of a stimulating effect on CO or TPR, the values of CO and TPR will decrease as a result of the action of the different feedback mechanisms regulating the CVS. The magnitude of feedback on CO and TPR is represented by FB1 and FB2.

Extended CVS model (Chapter 4): MAP equals the product of CO and TPR ($MAP=CO*TPR$) and CO equals the product of HR and SV ($CO=HR*SV$). SV is influenced by indirect feedback through MAP ($SV_{,}$) and by HR through a direct inverse log-linear relationship, where HR_SV represents the magnitude of this direct effect. Effects on HR, SV and TPR are described by three linked turnover equations. When MAP increases as a result of a stimulating effect on HR, SV or TPR, the values of HR, SV and TPR will decrease as a result of the action of the different feedback mechanisms regulating the CVS. The magnitude of feedback on HR, SV and TPR is represented by FB. Kin_{CO} , Kin_{HR} , Kin_{SV} and Kin_{TPR} represent the zero-order production rate constants and $kout_{CO}$, $kout_{HR}$, $kout_{SV}$ and $kout_{TPR}$ represent the first-order dissipation rate constants

2) with the aim to 1) characterize drug effects on the interrelationship between HR and MAP, which are both important variables in the safety evaluation of novel drugs and 2) investigate if the MoA of new compounds can be elucidated using HR and MAP measurements only.

The behavior of the extended CVS model was evaluated by simulating the changes in MAP, CO, HR, SV and TPR after triggering the model by inhibiting HR, SV or TPR with a hypothetical compound after a single oral dose (Figure 3). The characteristic profiles of the time-course of the drug effect on MAP, CO, HR, SV and TPR are referred to as signature profiles. For the different variables distinctly different profiles were observed. From these simulations it can be concluded that, even if CO is not measured, it is likely that the extended CVS model can be used to elucidate the site of action of novel compounds with a single MoA (i.e., one site of action). In summary, when the nature (i.e. an increase or decrease) of the drug induced change in HR and MAP is the same, it is likely that the primary effect is on HR. When HR and MAP change in opposite directions, i.e. an increase in HR and a decrease in MAP or *vice versa*, the primary effect of the drug is expected to be on SV or TPR. Effects on SV and TPR can be distinguished by the delay between the perturbation and the effect on MAP, i.e. a long delay indicates that the primary effect is on SV and a short delay indicates that the primary effect is on TPR. Next to MAP, HR is an important parameter in the safety evaluation of novel drugs for a wide variety of disorders (Sudano *et al.*, 2012; Gasparyan *et al.*, 2012; Cardinale *et al.*, 2013; Guth, 2007). Although MAP and HR are usually measured simultaneously, it is common practice to quantify drug effects on these hemodynamic parameters independently resulting in two separate dose/concentration-effect relationships. However, this approach disregards the interrelationship between MAP and HR. Therefore, an additional advantage of extending the basic CVS model by parsing CO into HR and SV is that drug effects on MAP, CO, HR, SV and TPR can be characterized simultaneously yielding a single unique set of parameter estimates. Furthermore, the basic CVS model was extended to a more detailed level by quantifying differences in blood pressure regulation between normotensive and hypertensive rats. As there are pronounced differences in MAP regulation between hypertensive and normotensive rats (Pinto *et al.*, 1998) the magnitude of the effect of cardiovascular drugs on the different hemodynamic endpoints varies considerably between strains. Therefore, the basic CVS model is not directly applicable to data from normotensive rats. This is a major drawback especially for drug safety evaluations, which are usually conducted in normotensive rats. As the ultimate aim of the proposed quantitative pharmacology model is to predict clinical responses to novel pharmacologic agents, it is pivotal that the CVS model is applicable to both normotensive and hypertensive rats. The baseline parameters were found to differ per strain with a higher baseline value of MAP and a lower baseline value

of CO for hypertensive as compared to normotensive rats, whereas the baseline value for HR did not significantly differ between the strains. The baseline values of SV and TPR were derived from these parameters, resulting in a lower baseline value of SV and a higher baseline value of TPR for hypertensive as compared to normotensive rats. In addition, feedback was found to decrease with the individual value of the baseline of MAP. Overall, the feedback was about 2-fold higher in normotensive rats as compared to hypertensive rats indicating impaired blood pressure regulation in hypertensive rats. In conclusion, a systems pharmacology model, characterizing the interrelationship between MAP, CO,

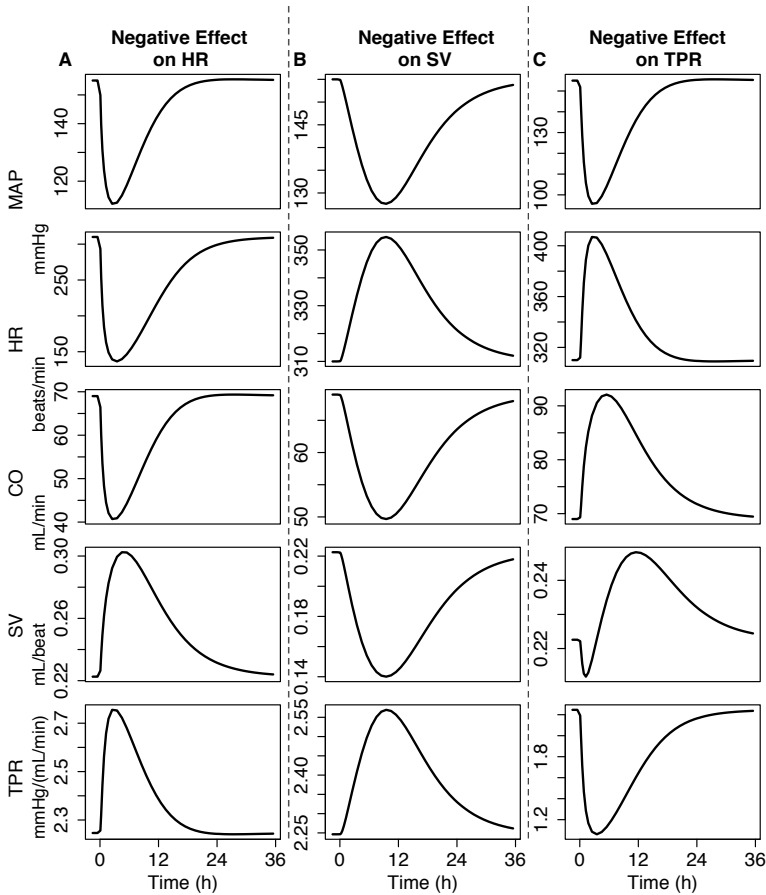


Figure 3: System properties of the CVS

The system properties of the CVS were investigated by simulating the response on MAP, CO, HR and TPR after inhibiting HR (A), SV (B) or TPR (C). Inhibiting HR, SV or TPR always results in a decrease in MAP, which demonstrates that feedback cannot be stronger than the primary effect. In addition, the delay in response on MAP was longer when the drug effect was on SV as compared to TPR.

HR, SV and TPR, was obtained in hypertensive and normotensive rats. The extended CVS model can be used to quantify the dynamic changes in the CVS and elucidate the MoA for novel compounds using HR and MAP measurements only. The model can also be applied to test hypotheses, e.g., hypotheses on multiple sites of action can be evaluated by including drug-effects on multiple parameters in the model. An ultimate application of the extended CVS model would be to facilitate the anticipation of the clinical response based on preclinical data for newly developed compounds. Before the extended CVS model can be applied for that purpose, the system-specific parameters of the model should be scaled to human and validated on human MAP, HR and CO measurements as detailed in the section “Towards characterization and prediction of cardiovascular drug effects in humans”.

Application of the systems pharmacology model to S1P receptor agonists

In humans, S1P receptor modulators, which are effective in the treatment of multiple sclerosis (Cohen *et al.*, 2010; Gergely *et al.*, 2012), are associated with cardiovascular side effects. More specifically, at the therapeutic dose of 0.5 mg, a transient decrease in HR (8 beats per minute with attenuation after 6 hours) and a small increase in MAP (1-2 mmHg after 2 months) were observed after administration of fingolimod (Kappos *et al.*, 2010). In addition, at the supra-therapeutic doses of 1.25 and 5 mg, HR was reduced within 6 hours by a mean of 13.8 and 16.6 beats per minute, respectively, returning towards the baseline value with continued treatment. At these doses, MAP was mildly increased by 5-6 mmHg following continuous treatment (Kappos *et al.*, 2006).

The immunosuppressant effects, as well as the cardiovascular side effects, of these compounds are believed to be mediated through the S1P receptor, which complicates the search for novel S1P receptor modulators, which are devoid of cardiovascular side effects. A quantitative understanding of the hemodynamics of these effects is important as it may constitute a basis for the selection of new compounds with an improved safety profile. Moreover, it may provide insights in the possibility to prevent and reverse these effects for new S1P receptor modulators by co-administration of other drugs (Kovarik *et al.*, 2008), or to design dose titration schemes to attenuate these effects (Legangneux *et al.*, 2013). The extended CVS model is uniquely suited to provide a quantitative understanding of these effects as the structure of the model and the values of the parameters describing the model are independent of the drugs that were used to create it and, therefore, the model can be used to quantify the dynamic changes in the CVS for other compounds and thus for fingolimod. A potential application of this model is the prediction of the cardiovascular effects of novel compounds. This requires interfacing the CVS model with a target

binding-activation model. Moreover, the proposed systems pharmacology model may allow prediction of cardiovascular effects of S1P receptor modulators in humans based on preclinical evaluations. A complicating factor in the translational pharmacology of fingolimod and, in general S1P receptor modulators, is that they exert their pharmacological effect through their respective phosphate metabolites, which are formed by the enzyme sphingosine kinase (S1PHK). At first, the pharmacokinetics (PK) of fingolimod and its active metabolite fingolimod-phosphate (fingolimod-P) were characterized in rats and humans. Since large inter-species differences exist in the S1PHK enzyme tissue distribution and enzyme activity, it is anticipated that the PK of S1PHK substrates in rats may not be scalable to humans using a standard allometric scaling approach. In **Chapter 5**, a semi-mechanistic PK model for the inter-conversion of S1PHK substrates and their respective phosphates in rats and humans was proposed. A specific aim was to determine whether species specific differences in the *ex vivo* rate of phosphorylation in blood platelets are representative for the differences in the phosphorylation in general and might therefore constitute a basis for pharmacokinetic scaling. To explore this, data on the time course of fingolimod and fingolimod-P blood concentrations in rats following intravenous administration of fingolimod and fingolimod-P as well as following oral administration of fingolimod were analyzed in conjunction with data on the *ex vivo* inter-conversion and blood-plasma distribution in rat blood. Separately, data from two healthy volunteer studies, in which fingolimod was administered orally in doses of 0.5, 1.25 and 5 mg once daily, were simultaneously analyzed with data on the *ex vivo* inter-conversion and blood-plasma distribution in human blood. Overall, the PK of fingolimod and fingolimod-P in rats and humans was adequately characterized by a semi-mechanistic model in which phosphorylation of fingolimod occurred pre-systemically during first-pass in the liver and in the platelets (Figure 4). In addition, dephosphorylation occurred in the plasma. Integrating data from the *ex vivo* and *in vivo* studies enabled prediction of fingolimod and fingolimod-P concentrations in plasma rather than blood. This is important because plasma concentrations are more relevant for predicting drug effects as, according to the free drug hypothesis, only drug present in plasma is able to bind to its target. Moreover, inter-species differences in the rate of phosphorylation could be quantified. In humans, phosphorylation of fingolimod in the platelets was 4 times slower compared to rats, whereas the de-phosphorylation rates were comparable in both species. In conclusion, using fingolimod as a paradigm compound, large interspecies differences in the rate of phosphorylation between rats and humans were demonstrated, which cannot be accounted for by allometric scaling. Although, this only partly explained the 12-fold over-prediction of fingolimod-P exposure in humans when applying an allometric scaling approach on the developed rat model, the developed semi-mechanistic PK model constitutes a basis for the prediction of the

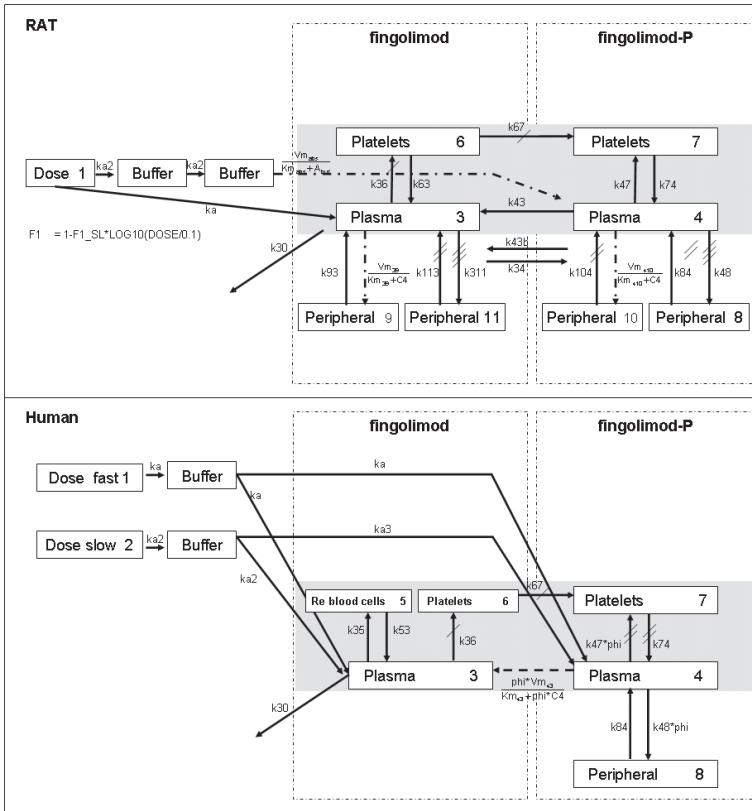


Figure 4: Pharmacokinetic models to describe the time course of the fingolimod and fingolimod-P blood concentration in rats and humans. The grey area describes the inter-conversion and blood/plasma distribution in isolated blood. k_{xy} represent the first-order distribution and elimination rate constants. Arrows with an equal number of slashes indicate that these rates are the same. In addition, the dashed lines represent saturable processes.

concentrations of S1PHK substrates and their phosphorylated metabolites in plasma. However, differences in pre-systemic phosphorylation should also be taken into account. In **Chapter 6**, the extended CVS model and semi-mechanistic PK model for fingolimod and fingolimod-P in rats were applied to characterize the cardiovascular effects following the administration of fingolimod in normotensive and hypertensive rats. Briefly, data on the concentrations of fingolimod-P and the changes in various hemodynamic variables were analyzed on the basis of the extended CVS model. In a first step, a model-based

hypothesis testing procedure was followed using the extended CVS model without changing the system-specific parameters.

- 1) Different hypotheses of the site of action (i.e. HR, SV and TPR) and direction of the effect (i.e., inhibiting or stimulating) were formulated, resulting in 6 possible combinations of effects.
- 2) For each hypothesis, the model was fitted to the MAP, CO, HR, SV and TPR measurements.
- 3) It was evaluated which hypothesis resulted in the best description of the data.

It was found that effect of fingolimod-P on the CVS could be described while assuming multiple sites of action, i.e. TPR and HR (Snelder *et al.*, 2013). Overall three different effects were quantified: 1) a fast stimulating effect on TPR, 2) a slow sustained stimulating effect on TPR which is only relevant in hypertensive rats following doses higher than 1 mg/kg and 3) a transient inhibiting effect on HR. In this first step, drug effects were described by empirical models. This provided information on the most plausible sites of action of fingolimod-P, but it also demonstrated that extended CVS model can be applied to quantify the hemodynamics of the effect of fingolimod-P on five different parameters, i.e. MAP, CO, HR, SV and TPR, while assuming only two different sites of action. In a next step, the obtained information on the site of action of fingolimod-P was compared with the available information on the mechanism of action of fingolimod-P. Briefly, at the time of the analysis the following was known about the MoA underlying the effect of fingolimod-P on the CVS.

- i. Fingolimod-P influences HR through to binding to the $S1P_1$ receptor. The arterial muscarinic-gated potassium channel IKACH is activated (Koyrakh *et al.*, 2005), which results in a negative chronotropic effect.
- ii. Fingolimod-P induces internalization and degradation of the $S1P_1$ receptor (Horga *et al.*, 2010; Mullershausen *et al.*, 2009). As a result fingolimod-P acts a functional antagonist.
- iii. Fingolimod-P influences TPR through binding to the $S1P_3$ receptor (Peters and Alewijnse, 2007; Coussin *et al.* 2002). The $S1P_3$ receptor is expressed in vascular smooth muscle cells and regulates the contractility of these cells. As a result fingolimod-P increases peripheral resistance and thus blood pressure.
- iv. The major trigger for smooth muscle cell contraction is a rise in intracellular calcium concentration. Whereas the calcium-dependent phase smooth muscle cell contraction is rapid and relatively transient, calcium sensitization produced by agonist stimulation results in as sustained contraction of vascular smooth muscle cells (Watterson *et al.*, 2005), and thus, in a sustained increase in TPR.

Since this information is in line with the elucidated site of action of fingolimod-P the empirical drug-effect models were replaced by models based on receptor theory concepts

for the characterization of target binding and target activation processes, which improved the properties for extrapolation to humans and the prediction of the effects of follow-up compounds (Danhof *et al.*, 2007; Ploeger *et al.*, 2009). As fingolimod-P is an agonist for the S1P receptor competitive interaction between the endogenous agonist, S1P, and fingolimod-P was taken into account for both the effects on HR and TPR. The developed model existed of expressions to describe 1) competitive receptor binding kinetics to the S1P₁ receptor (fast effect on HR), 2) S1P₁ receptor internalization and degradation (transient nature of the fast effect on HR), 3) competitive receptor binding kinetics to the S1P₃ receptor (fast effect on TPR), and 4) S1P₃ receptor sensitization (slow effect on TPR) (Figure 5). By characterizing drug effects on HR and TPR, the effects of fingolimod-P on MAP, CO, HR, SV and TPR were adequately described in hypertensive and normotensive rats. The dissociation constants for the effects on TPR (Kd_{TPR} ; binding to the S1P₃ receptor) and HR (Kd_{HR} ; binding to the S1P₁ receptor) were estimated to be 17.7 [confidence interval (CI): 3.74–31.6] and 132 [CI: 68.9–195] nM based on free plasma concentrations, respectively. The Kd_{TPR} is in the same order of magnitude as the *in vitro* binding dissociation constant for binding of fingolimod-P to the human S1P₃ receptor reported by Mandala *et al.* of 3.15 ± 1.7 nM (Mandala *et al.*, 2002; calculated using the Cheng-Prusoff equation (Cheng and Prusoff, 1973)). However, the estimated Kd_{HR} differs from the reported *in vitro* dissociation constants for the binding of fingolimod-P to the human S1P₁ receptor of 0.17 ± 0.14 nM (Mandala *et al.*, 2002; calculated using the Cheng-Prusoff equation (Cheng and Prusoff, 1973)). It should be noted that, *in vivo*, the S1P₁ receptor is internalized and degraded. This could confound the estimation of the dissociation constant. Moreover, it should be noted that the reported dissociation constants reflect binding to human S1P₁ and S1P₃ receptors. Dissociation constants for binding to rat S1P₁ and S1P₃ receptors are not reported and it is known that large interspecies differences may exist.

Since the developed model was based on receptor theory concepts for the characterization of target binding the model could readily be applied to predict the effect of siponimod, a S1P receptor agonist with different receptor subtype selectivity, on the CVS by correcting the estimated dissociation for fingolimod-P for the molecular weights, the unbound fractions and the ratio of the potencies derived from *in vitro* binding assays. Overall, the effect of siponimod on MAP and HR in rats was adequately predicted by the model (using its *in vitro* receptor binding constants), which indicates that the developed model can be applied to predict the effect of other S1P modulators on the CVS in rats. Ultimately, the proposed system pharmacology model may allow prediction of cardiovascular effects of S1P receptor modulators in humans based on preclinical evaluations of drug effects. However, this requires several steps, which are described in the next section.

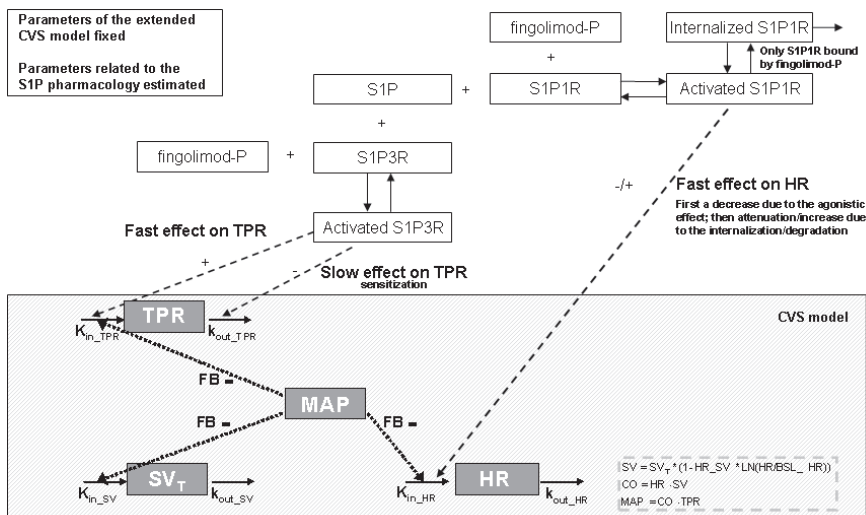


Figure 5: Cardiovascular model to describe drug effects on the interrelationship between mean arterial pressure (MAP), cardiac output (CO), heart rate (HR), stroke volume (SV) and total peripheral resistance (TPR) after administration of fingolimod.

Extended CVS model: Cardiac output (CO) equals the product of HR and SV ($CO=HR \cdot SV$) and MAP equals the product of CO and TPR ($MAP=CO \cdot TPR$). SV influenced by indirect feedback through MAP (SV_T) and by HR through a direct inverse log-linear relationship, where HR_{SV} represents the magnitude of this direct effect. Effects on HR, SV and TPR are described by three linked turnover equations. In these equations K_{in_HR} , K_{in_SV} and K_{in_TPR} represent the zero-order production rate constants and k_{out_HR} , k_{out_SV} and k_{out_TPR} represent the first-order dissipation rate constants. When MAP increases as a result of a stimulating effect on HR, SV or TPR, the values of HR, SV and TPR will decrease as a result of the action of the different feedback mechanisms regulating the CVS. In this model the magnitude of feedback on HR, SV and TPR is represented by FB.

Effect of fingolimod-P: The primary effect of fingolimod-P is on TPR. The effect on TPR is a combination of a fast stimulating effect and a slowly occurring stimulating effect (sensitization). The effect on HR is initially an inhibiting effect. However, as a result of the receptor internalization this effect rapidly attenuates.

Perspectives - Towards characterization and prediction of cardiovascular drug effects in humans

An ultimate application of the developed systems pharmacology model is to predict cardiovascular effects in man on the basis of information from pre-clinical studies for newly developed compounds and, more specifically, for S1P receptor agonists, i.e. follow-up compounds of fingolimod. In this section, first, the inter-species translation of the system-specific CVS model is discussed. Thereafter, the inter-species translation of the effect of S1P receptor agonists is addressed.

Translation of the system-specific CVS model

The extended CVS model consisted of three turnover equations, for HR, SV and TPR respectively, which were linked by negative feedback through MAP (Equation 1).

$$\begin{aligned}
 \frac{dHR}{dt} &= K_{in_HR} \cdot (1 + CR_{HR}) \cdot (1 - FB \cdot MAP) - k_{out_HR} \cdot HR \\
 \frac{dSV_T}{dt} &= K_{in_SV} \cdot (1 - FB \cdot MAP) - k_{out_SV} \cdot SV_T \\
 \frac{dTPR}{dt} &= K_{in_TPR} \cdot (1 + CR_{TPR}) \cdot (1 - FB \cdot MAP) - k_{out_TPR} \cdot TPR
 \end{aligned} \tag{1}$$

$$SV = SV^* \cdot (1 - HR_{SV} \cdot \ln(HR/BSL_HR))$$

$$CO = HR \cdot SV$$

$$MAP = CO \cdot TPR$$

$$FB = FB0 \cdot \left(\frac{IBSL_MAP}{TVBSL_MAP_SHR} \right)^{FB0_MAP}$$

In these equations, SV^* represents the SV influenced by the negative feedback of MAP, K_{in_HR} , K_{in_SV} and K_{in_TPR} represents the zero-order production rate constants and k_{out_HR} , k_{out_SV} and k_{out_TPR} represent the first-order dissipation rate constants of HR, SV and TPR, respectively. In addition, $FB0_MAP$, $IBSL_MAP$ and $TVBSL_MAP_SHR$ represent the exponent of the power relationship, the individual baseline values of MAP and typical value of BSL_MAP in SHR, respectively. The basic expectations in pharmacodynamics are that physiological turnover rate constants of most general structures and functions should be predictable among species based on allometric principles (Mager *et al.*, 2009; West *et al.*, 1999). Therefore, to extrapolate the extended CVS model to the human situation allometric scaling principles were applied to scale the first order rate constants k_{out_HR} , k_{out_SV} and k_{out_TPR} for humans. As allometric models often use an exponent value of 0.75 for clearance and 1 for volume of distribution, the corresponding first order rate constants will have an allometric exponent of -0.25 (Equation 2; Stevens *et al.*, 2012).

$$k_{\text{out_human}} = k_{\text{out_rat}} \cdot \left(\frac{BW_{\text{human}}}{BW_{\text{rat}}} \right)^{-0.25} \quad (2)$$

In this equation, $k_{\text{out_human}}$ and $k_{\text{out_rat}}$ represent the first-order dissipation rate constant of HR, SV or TPR in humans and rats, respectively. The principles of mass-balance define the zero-order rate constants (Equation 3).

$$K_{\text{in_HR}} = \frac{k_{\text{out_HR}} \cdot BSL_{\text{HR}}}{1 - FB \cdot BSL_{\text{MAP}}}$$

$$K_{\text{in_SV}} = \frac{k_{\text{out_SV}} \cdot BSL_{\text{SV}}}{1 - FB \cdot BSL_{\text{MAP}}} \quad (3)$$

$$K_{\text{in_TPR}} = \frac{k_{\text{out_TPR}} \cdot BSL_{\text{TPR}}}{1 - FB \cdot BSL_{\text{MAP}}}$$

In this equation, BSL_{MAP} , BSL_{HR} , BSL_{SV} and BSL_{TPR} represent the baseline values of MAP, HR, SV and TPR, respectively. This means that the zero-order human production rate constants are intrinsically scaled. Furthermore, Schmidt-Nielsen described how the baseline values of MAP, HR and CO (BSL_{CO}) should be scaled, i.e. BSL_{MAP} , BSL_{HR} and BSL_{CO} should be scaled with an allometric exponent of 0, -0.25 and 0.75, respectively (Schmit-Nielsen, 1995). Since $\text{MAP} = \text{CO} \cdot \text{TPR}$ and $\text{CO} = \text{HR} \cdot \text{SV}$ the allometric exponents for scaling BSL_{SV} and BSL_{TPR} follow directly from the allometric exponents for BSL_{MAP} , BSL_{HR} and BSL_{CO} and are 1 and -0.75, respectively. Concerning the extrapolation of the feedback parameter, FB was found to be dependent on BSL_{MAP} , which is this same in all species. Therefore, FB was assumed to be the same in all species too.

To evaluate the hypothesis that the extended CVS model can be extrapolated to the human situation by applying allometric scaling principles to scale the first order rate constants $k_{\text{out_HR}}$, $k_{\text{out_SV}}$ and $k_{\text{out_TPR}}$ from rats to humans, ideally, the experiments, which were performed to characterize the extended CVS model in rats should be repeated in humans, i.e. the effects of eight drugs with diverse MoA's (amiloride, amlodipine, atropine, enalapril, fasudil, hydrochlorothiazide, prazosin and propranolol) on MAP, HR and CO should be measured in humans. However, performing such a study in humans is outside the scope of this research. As for none of these compounds data on the time course of the effect on all three parameters, i.e. MAP, HR and CO, were published a literature search was

performed to obtain data on the time course of the effect of MAP, HR and/or CO following the administration of cardiovascular drugs. Francheteau *et al.* published data on the effect of nicardipine on MAP and CO following two types of nicardipine infusion (Francheteau *et al.*, 1993); data were digitized using TechDig® version 2.0). Although no HR data was published on the time course of the effect of nicardipine on HR, these data were selected to evaluate if the extended CVS model can be extrapolated to human.

To scale the extended CVS model from rat to human the following assumptions were made (Scenario 1_CVS_model).

- i. The dissipation rates can be allometrically scaled with an allometric exponent of -0.25. The body weights of rats and humans were assumed to be 0.3 and 72 kg, respectively.
- ii. In rats, feedback (*FB*) was found to decrease with the baseline MAP according to Equation 1. It was assumed that this equation is applicable in humans too.
- iii. The observed baselines can be used. These were slightly different from the allometrically scaled baselines, which may be due to inter-individual variability.
- iv. The drug specific parameters can be fixed to values from Francheteau *et al.* (Francheteau *et al.*, 1993; Table 1).

Following these assumptions the extent of the effects of nicardipine on CO and MAP were under-predicted (Figure 6, dashed lines). This could indicate that the feedback is slightly lower in man as compared to rats. In addition, the time course of the effects on MAP and CO was not captured as the observed time lag was much shorter than the predicted time lag indicating that men respond faster than rats. Several hypotheses can be postulated as to why the time course and the extent of the cardiovascular effects are not predicted adequately. First of all, the dissipation rates of HR, SV and TPR do not represent actual degradation rates as for proteins and enzymes. Instead they represent parameters for the delay in response at an organ level and represent several lumped processes as partly reflected by the Guyton model (Guyton *et al.*, 1972). Another hypothesis is that the differences between rats and humans may not be related solely to differences in size. The most obvious difference between rats and humans is that rats crawl, whereas men walk. This could influence both the delay in response and the feedback. To evaluate this last hypothesis, the extended CVS model was extrapolated from rats to humans according to the following assumptions (Scenario 2_CVS_model).

- i. The dissipation rates should be multiplied with an unknown factor (this factor was estimated).
- ii. In rats, *FB* was found to decrease with the baseline MAP according to Equation 1. It was assumed that this equation is applicable in humans.
- iii. The observed baselines can be used. These were slightly different from the allometrically scaled baselines, which may be due to inter-individual variability.

Table 1: Parameters values from the extended CVS model

Scenario 1_CVS_model: dissipation rates are allometrically scaled with an allometric exponent of -0.25

Scenario 2_CVS_model: dissipation rates are multiplied with an estimated factor of 23.4

Scenario 3_CVS_model: dissipation rates are multiplied with an estimated factor of 46.7 and FB is estimated

Parameter	human			
	rat	Scenario 1	Scenario 2	Scenario 3
System-specific parameters				
k_{out_HR} (1/h)	11.6	2.95 (11.6*(72/0.3)^(-0.25))	271 (11.6*23.4)	309 (11.6*46.7)
k_{out_SV} (1/h)	0.126	0.032 (0.126*(72/0.3)^(-0.25))	2.95 (0.126*23.4)	2.36 (11.6*46.7)
k_{out_TPR} (1/h)	3.58	0.91 (3.58*(72/0.3)^(-0.25))	83.7 (11.6*23.4)	95.6 (11.6*46.7)
FB (1/mmHg)	0.00664*	0.00664*	0.00664*	0.00817
Drug-specific parameters (nicardipine)				
E_{max}	0.27**	0.27**	0.27**	0.27
EC_{50} (ng/mL)	29.1	29.1	29.1	29.1
hill coefficient	4.52	4.52	4.52	4.52

* FB = 0.00290*(102/155)^(-1.98)=0.00664

** Emax=(TPReq-TPRmin)/TPReq; TPRReq=75/(6.08-12.33 mmHg/(L/min)); TPRmin=8.96 mmHg/(L/min); Emax=0.27

iv. The drug specific parameters can be fixed to values from Francheteau *et al.* (Francheteau *et al.*, 1993; Table 1).

Following these assumptions the time course and extent of the effect of nicardipine on CO was described adequately, whereas the time course and extent of the effect of nicardipine on MAP were not captured (Figure 6, dotted lines). The multiplication factor was estimated to be 23.4 (Table 1). Although MAP is assumed to be a non-scalable parameter, albeit in the same order of magnitude, the observed *BSL_MAP* in humans (75 mmHg) is actually lower than in rats (102 mmHg). This means that, when applying Equation 1 to calculate *FB*, an extrapolation was made beyond the observed *BSL_MAP* range. Therefore, the second assumption to extrapolate the extended CVS model from rats to humans was changed (Scenario 3_CVS_model).

- i. The dissipation rates should be multiplied with an unknown factor (this factor was estimated).
- ii. In rats, *FB* was found to decrease with the baseline MAP according to Equation 1. It was assumed that this equation is not valid in subjects with a *BSL_MAP* lower than 102 mmHg (*BSL_MAP* in normotensive rats). To test this hypothesis *FB* was estimated.
- iii. The observed baselines can be used. These were slightly different from the allometrically scaled baselines, which may be due to inter-individual variability.
- iv. The drug specific parameters can be fixed to values from Francheteau *et al.* (Francheteau *et al.*, 1993; Table 1).

Following these assumptions the time course and extent of the effect of nicardipine on CO and MAP were described adequately (Figure 6, continuous lines). The estimated *FB* (0.00817 [CI: 0.00740-0.00894] 1/mmHg) (Table 1) was slightly lower than the calculated *FB* from Equation 1 (0.0122 [CI: 0.0108-0.0136] 1/mmHg). Notably, the estimated *FB* does not differ significantly from the value from normotensive rats (0.00664 [CI: 0.00586-0.00742] 1/mmHg). This indicates that it is likely that *FB* does depend on *BSL_MAP*, but not according to a hyperbolic function as *FB* may reach a maximum. In addition, the multiplication factor was 46.7 indicating that the response in humans is very fast, i.e. the half-life's of the effect on HR, SV and TPR are 0.00128, 0.118 and 0.00415 h, respectively. In conclusion, the extended CVS model can be extrapolated from rat to human, but the extrapolation is not solely depended on size and other factors, such as the fact that men are standing whereas rats are crawling, seem to play an important role. By multiplying the dissipation rates with a certain factor (a high value which results in a very short delay in response in humans), and estimating the feedback, the effect of nicardipine on MAP and CO could be described adequately. As the extrapolation of the extended CVS model was based on data from one compound (nicardipine) it is not certain if the obtained system parameters are drug-independent. Therefore, further research is required to obtain a truly system specific CVS model in humans. Ideally, a study should be performed were the

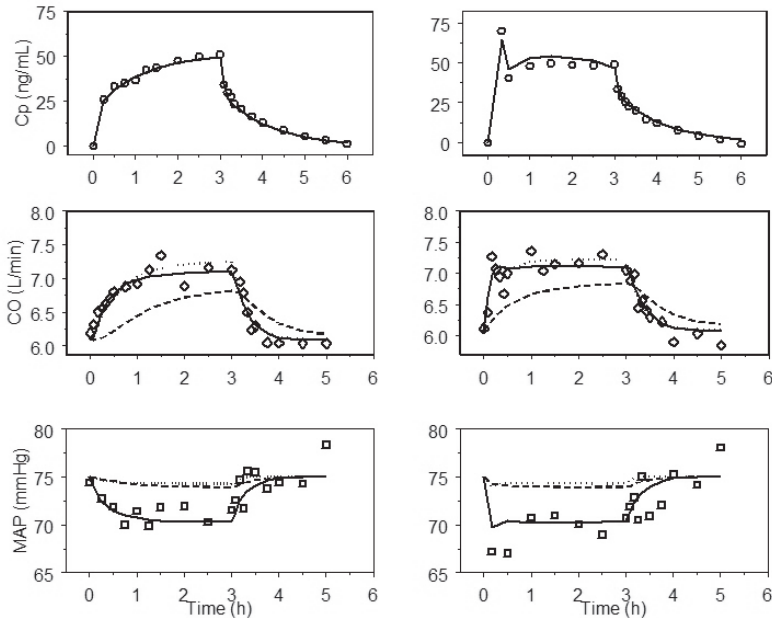


Figure 6: Observed (Francheteau *et al.*, 1993) and predicted curves of the extended CVS model to mean plasma concentrations of nicardipine (\circ), cardiac output data (\diamond) and mean arterial pressure data (\square) following two types of nicardipine infusion.

Left panel: constant rate infusion; Right panel: variable rate infusion

Scenario 1_CVS_model: Dissipation rates were allometrically scaled with an allometric exponent of -0.25 (dashed lines)

Scenario 2_CVS_model: Dissipation rates are multiplied with an estimated factor of 23.4 (dotted lines)

Scenario 3_CVS_model: Dissipation rates are multiplied with an estimated factor of 46.7 and FB is estimated (continuous lines)

time course of the effect of different cardiovascular compounds with different MoA's on MAP, HR and CO is measured.

Translation of the class/drug-specific target binding and activation model for S1P agonists

In a next step, it was investigated if the human CVS model, with the parameter estimates fixed, can be applied to the characterization and prediction of the cardiovascular effects of S1P agonists in humans (data on file). To this end, it is discussed how the rat target binding and activation model for fingolimod-P and siponimod may be scaled to man (Supplement).

General summary, discussion and applications

The objectives of the investigations described in this thesis were 1) to establish a systems pharmacology model to characterize the effects of drugs with different MoA's on the interrelationship between MAP, CO, HR, SV and TPR in a quantitative manner and 2) to apply the model to the quantification of the cardiovascular effects of the S1P receptor modulator fingolimod. A systems pharmacology modeling approach was applied, which allows predicting hemodynamic changes in man on the basis of information from pre-clinical studies. In this section, the development and translation of the system-specific CVS model is summarized and discussed first. Thereafter, the development of the target binding and activation model for S1P agonists is discussed. Finally, a strategy is presented to obtain a quantitative understanding of the *in vitro* to rat to human translation of the cardiovascular effects of S1P agonists.

First, a system-specific CVS model was developed to characterize drug effects on the interrelationship between MAP, CO, HR, SV and TPR in rats. This model can be applied to quantify the hemodynamics of novel cardiovascular compounds. Moreover, it can be applied to elucidate the site of action of novel compounds. In a first step towards the development of a translational system-specific CVS model, the parameters of the rat model were scaled to humans following an unconventional (not based on the allometric scaling principles), but physiologically plausible, scaling approach. The fact that parameters of the rat CVS model were not scaled according to the allometric scaling principles does not imply that cardiovascular effects cannot be scaled from rat to human. Instead, this implies that differences in cardiovascular responses between rats and humans do not solely depend on size, but other factors are also of importance, such as the fact that humans are standing whereas rats are crawling and this should be accounted for. As the translation of the CVS model was based on data from one compound (nicardipine) it is not certain if the obtained system parameters are drug-independent. Therefore, further research is required to obtain a truly system specific and drug independent CVS model in man. Once the human CVS model has been validated, it can be applied to the characterization and prediction of cardiovascular effects of novel compounds in humans.

In a next step, the rat CVS model, with the system-specific parameter estimates fixed, was integrated with a target binding and activation model to quantify the cardiovascular effects S1P agonists in rats, using fingolimod-P as a paradigm compound. This model provided a quantitative understanding of the mechanisms underlying the cardiovascular effects of fingolimod-P. In addition, the effect of siponimod on the CVS was predicted adequately by multiplying the estimated *in vivo* dissociation constants of fingolimod-P for binding to the S1P receptors with the ratio of the potencies of fingolimod-P and siponimod derived from

in vitro binding assays. Therefore, it is anticipated that the developed model can be applied to predict the effect of other S1P receptor agonists on the CVS in rats. Subsequently, hypotheses were generated on the rat to human translation of the cardiovascular effects of S1P agonists. Overall, the human CVS model, integrated with the target binding and activation model for S1P agonists from rat, was successfully applied to characterize the magnitude and dynamics of the effect of fingolimod-P and siponimod on HR (data on file).

However, this required several assumptions on the parameter values (Supplement). To date, no ‘gold’ standard approach exists for the inter-species translation of cardiovascular effects. In practice, the selected translational approach is often driven by the available data. Here, an approach is presented to obtain a mechanistic and quantitative understanding of the *in vitro* to rat to human translation of the cardiovascular effects of S1P agonists (Figure 7). First, a relationship between *in vitro* binding constants derived from saturation binding experiments using the rat S1P receptor and the apparent *in vivo* rat dissociation constants should be established. Possible differences between these parameters may result from processes that occur solely *in vivo* such as signal transduction. For fingolimod, it was demonstrated that valuable information on the mechanisms underlying its cardiovascular effects can be derived from rat experiments. More precisely, the model structure to characterize the interrelationship between the cardiovascular effects of S1P agonists can be derived from rat experiments and applied to the prediction of

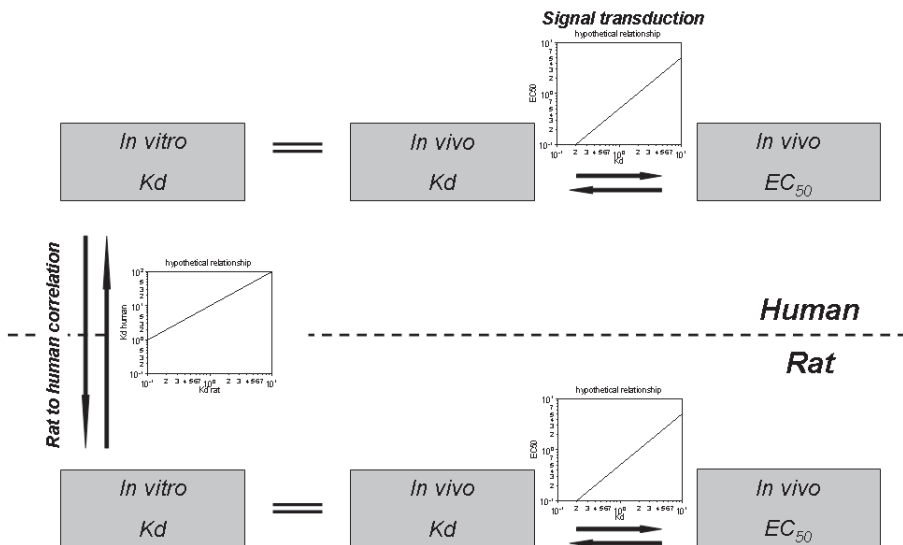


Figure 7: Schematic map for the translation of cardiovascular effects of S1P agonists.

cardiovascular effects in humans (Supplement), indicating that the physiological processes are qualitatively comparable between rats and humans. Subsequently, relationships between the *in vitro* dissociation constant for rats and humans and between the *in vitro* and apparent *in vivo* dissociation constants in humans should be established. This requires information on 1) the effects of multiple S1P receptor agonists on MAP, HR and CO in rats and humans and on 2) the corresponding dissociation constants for binding to the rat and human S1P receptors. When these relationships are established, it is foreseen that the magnitude and hemodynamics of the cardiovascular effects of novel S1P agonists, i.e. S1P agonists that were not included in model development, can be predicted directly using parameters estimates obtained from *in vitro* experiments and no further experiments in rats are required. If the proposed approach results in an adequate translational model for the cardiovascular effects of S1P agonists, this would demonstrate that preclinical experiments are predictive for clinical effects, but a quantitative understanding of the processes in the causal chain between drug administration and the change in response over time, including the pharmacokinetics of a drug, target site distribution and receptor binding kinetics, receptor activation and transduction (Ploeger *et al.*, 2009) in rats and humans is required.

References

- Brinkmann V, Davis MD, Heise CE, Albert R, Cottens S, Hof R *et al.* (2002). The immune modulator FTY720 targets sphingosine 1-phosphate receptors. *J Biol Chem.*, 277, 21453-21457.
- Cardinale D, Bacchiani G, Beggiato M, Colombo A, Cipolla CM (2013). Strategies to prevent and treat cardiovascular risk in cancer patients. *Semin Oncol.*, 40, 186-198.
- Cheng Y, Prusoff WH (1973). Relationship between the inhibition constant (K1) and the concentration of inhibitor which causes 50 per cent inhibition (I50) of an enzymatic reaction. *Biochem Pharmacol.*, 22, 3099-3108.
- Cohen JA, Barkhof F, Comi G, Hartung HP, Khatri BO, Montalban X *et al.* (2010). Oral fingolimod or intramuscular interferon for relapsing multiple sclerosis. *N Engl J Med.*, 362, 402-415.
- Coussin F, Scott RH, Wise A, Nixon GF (2002). Comparison of sphingosine 1-phosphate-induced intracellular signaling pathways in vascular smooth muscles: differential role in vasoconstriction. *Circ Res.*, 91, 151-157
- Danhof M, de Jongh J, De Lange EC, Della Pasqua O, Ploeger BA, Voskuyl RA (2007). Mechanism-based pharmacokinetic-pharmacodynamic modeling: biophase distribution, receptor theory, and dynamical systems analysis. *Annu Rev Pharmacol Toxicol.*, 47, 357-400.
- Francheteau P, Steimer JL, Merdjan H, Guerret M, Dubray C (1993). A mathematical model for dynamics of cardiovascular drug action: application to intravenous dihydropyridines in healthy volunteers. *J Pharmacokinet Biopharm.*, 21, 489-514.
- Gasparyan AY, Aivazyan L, Cocco G, Kitas GD (2012). Adverse cardiovascular effects of antirheumatic drugs: implications for clinical practice and research. *Curr Pharm Des.*, 18, 1543-55.
- Gergely P, Nuesslein-Hildesheim B, Guerini D, Brinkmann V, Traeber M, Bruns C *et al.* (2012). The selective sphingosine 1-phosphate receptor modulator BAF312 redirects lymphocyte distribution and has species-specific effects on heart rate. *Br J Pharmacol.*, 167, 1035-1047.
- Guth BD (2007). Preclinical cardiovascular risk assessment in modern drug development. *Toxicol Sci.*, 97, 4-20.
- Guyton AC, Coleman TG, Granger HJ (1972). Circulation: overall regulation. *Annu Rev Physiol.*, 34, 13-46.
- Horga A, Castillo J, Montalban X (2010). Fingolimod for relapsing multiple sclerosis: an update. *Expert Opin Pharmacother.*, 11, 1183-1196.
- Kappos L, Antel J, Comi G, Montalban X, O'Connor P, Polman CH *et al.* (2006). Oral fingolimod (FTY720) for relapsing multiple sclerosis. *N Engl J Med.*, 355, 1124-1140.
- Kappos L, Radue EW, O'Connor P, Polman C, Hohlfeld R, Calabresi P *et al.* (2010). A placebo-controlled trial of oral fingolimod in relapsing multiple sclerosis. *N Engl J Med.*, 362, 387-401
- Kovarik JM, Slade A, Riviere GJ, Neddermann D, Maton S, Hunt TL *et al.* (2008). The ability of atropine to prevent and reverse the negative chronotropic effect of fingolimod in healthy subjects. *Br J Clin Pharmacol.*, 66, 199-206.
- Koyrakh L, Roman MI, Brinkmann V, Wickman K (2005). The heart rate decrease caused by acute FTY720 administration is mediated by the G protein-gated potassium channel I. *Am J Transplant.*, 5, 529-536.
- Legangneux E, Gardin A, Johns D (2013). Dose titration of BAF312 attenuates the initial heart rate reducing effect in healthy subjects. *Br J Clin Pharmacol.*, 75, 831-841.
- Mager DE, Woo S, Jusko WJ (2009). Scaling pharmacodynamics from in vitro and preclinical animal studies to humans. *Drug Metab Pharmacokinet.*, 24, 16-24.
- Mandala S, Hajdu R, Bergstrom J, Quackenbush E, Xie J, Milligan J *et al.* (2002). Alteration of lymphocyte trafficking by sphingosine-1-phosphate receptor agonists. *Science.*, 296, 346-349.
- Mullershausen F, Zecri F, Cetin C, Billich A, Guerini D, Seuwen K (2009). Persistent signaling induced by FTY720-phosphate is mediated by internalized S1P1 receptors. *Nat Chem Biol.*, 5, 428-434.
- Peters SL, Alewijnse AE (2007). Sphingosine-1-phosphate signaling in the cardiovascular system. *Curr Opin Pharmacol.*, 7, 186-192.
- Pinto YM, Paul M, Ganten D (1998). Lessons from rat models of hypertension: from Goldblatt to genetic engineering. *Cardiovasc Res* 39, 77-88.

Ploeger BA, van der Graaf PH, Danhof M (2009). Incorporating receptor theory in mechanism-based pharmacokinetic-pharmacodynamic (PK-PD) modeling. *Drug Metab Pharmacokinet.*, 24, 3-15.

Schmidt-Nielsen K (1995). *Why is animal size so important?*, Cambridge.

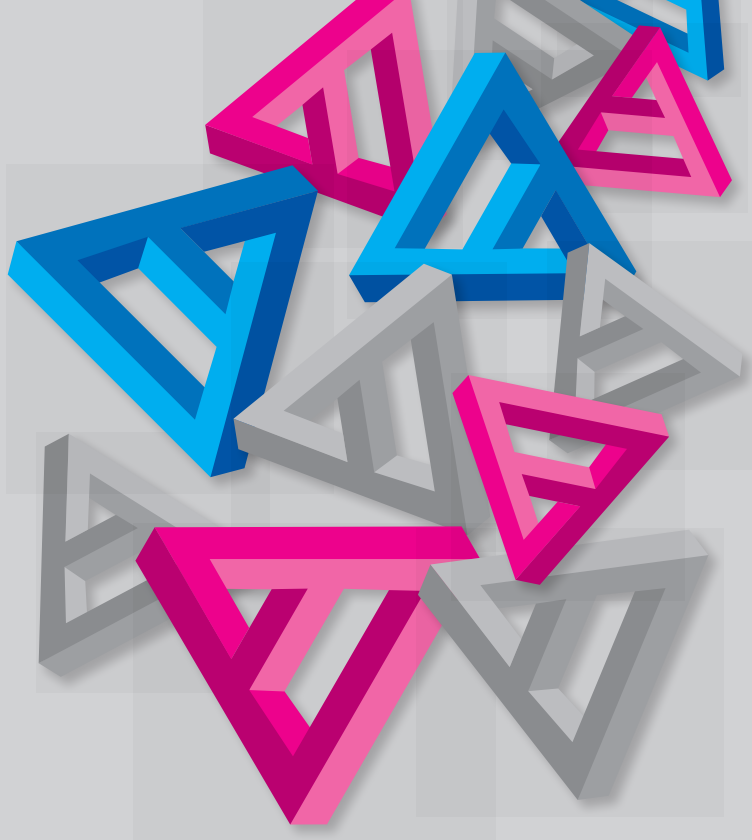
Snelder N, Ploeger BA, Luttringer O, Rigel DF, Webb RL, Feldman D *et al.* (2013). PAGE 22, Abstr 2686 [www.page-meeting.org/?abstract=2686]

Stevens J, Ploeger BA, Hammarlund-Udenaes M, Osswald G, van der Graaf PH, Danhof M *et al.* (2012). Mechanism-based PK-PD model for the prolactin biological system response following an acute dopamine inhibition challenge: quantitative extrapolation to humans. *J Pharmacokinet Pharmacodyn.*, 39, 463-477.

Sudano I, Flammer AJ, Roas S, Enseleit F, Noll G, Ruschitzka F (2012). Nonsteroidal antiinflammatory drugs, acetaminophen, and hypertension. *Curr Hypertens Rep.*, 14, 304-309.

Watterson KR, Ratz PH, Spiegel S (2005). The role of sphingosine-1-phosphate in smooth muscle contraction. *Cell Signal.*, 17, 289-298.

West GB, Brown JH, Enquist BJ (1999). The fourth dimension of life: fractal geometry and allometric scaling of organisms. *Science.*, 284, 1677-1679.



Samenvatting in het Nederlands

Algemene inleiding en doel van het onderzoek

Nieuwe geneesmiddelen hebben vaak cardiovasculaire bijwerkingen die gerelateerd zijn aan veranderingen in bloeddruk. Een voorbeeld van een geneesmiddel met ongewenste effecten op de bloeddruk is finglimod, dat het onlangs geregistreerd is voor de behandeling van multiple sclerose (MS). Dit middel werkt op de zogenaamde sphingosine-1-fosfaatreceptor (S1P) welke naast de gewenste verbetering van de MS symptomen ook voor een (kleine) verhoging van de bloeddruk en een (kortstondige) verlaging van de hartslag zorgt. Deze stof is in dit onderzoek als voorbeeld stof gebruikt om de ongewenste effecten op de bloeddruk te begrijpen. Dit proefschrift beschrijft de ontwikkeling van een systeemfarmacologiemodel dat gebruikt kan worden om de verandering in bloeddruk (en andere hemodynamische variabelen) in mensen te voorspellen, op basis van informatie verkregen uit preklinisch, reageerbuis (*in vitro*) en dierexperimenteel onderzoek. Dit model is gebaseerd op de algemeen bekende principes van de bloeddrukregulatie. Dat wil zeggen, het gemiddelde van de arteriële bloeddruk (*'mean arterial pressure (MAP)'*) is gelijk aan het product van het hartminuutvolume (*'cardiac output (CO)'*) en de perifere weerstand (*'total peripheral resistance (TPR)'*). Vervolgens, is CO gelijk aan het product van de hartslag (*'heart rate (HR)'*) en het slagvolume (*'stroke volume (SV)'*). Hoewel deze relaties algemeen bekend zijn, zijn de effecten van geneesmiddelen op deze relaties nog niet op een mechanistische en kwantitatieve manier onderzocht.

Het onderzoek is ook gebaseerd op de principes van farmacokinetisch-farmacodynamisch modeleren (*'pharmacokinetic-pharmacodynamic (PKPD) modelling'*). Bij PKPD modeleren wordt de relatie tussen de verandering in de geneesmiddelconcentratie (farmacokinetiek) en verandering in het geneesmiddeffect (farmacodynamiek) over tijd gekwantificeerd. Mechanistische PKPD modellen karakteriseren, op een kwantitatieve manier, het causale verband tussen de toediening van het geneesmiddel en het uiteindelijke effect. Eén van de eigenschappen van een mechanistisch PKPD model is de strikte scheiding tussen de eigenschappen van het geneesmiddel en die van het biologische systeem. Stofspecifieke parameters beschrijven de interactie tussen het geneesmiddel en het biologische systeem met binding- en activeringconstanten, terwijl de systeemspecifieke parameters de dynamiek van het biologische systeem beschrijven. Dit onderscheid maakt het voorspellen van de geneesmiddeffecten in andere biologische systemen mogelijk (bijvoorbeeld de voorspelling van geneesmiddeffecten in mensen op basis van een mechanistisch model dat ontwikkeld is voor ratten). Recent is het concept van de systeemfarmacologie geïntroduceerd. Systeemfarmacologiemodellen zijn complexer dan mechanistische PKPD modellen, omdat deze zijn gebaseerd op de relaties tussen verschillende componenten van een biologisch/farmacologisch systeem of netwerk. Om deze redenen is een systeem-

farmacologiemodel uitermate geschikt om de effecten van geneesmiddelen op de relatie tussen MAP, CO, HR, SV en TPR te kwantificeren (**Hoofdstuk 1**)

De doelen van het onderzoek dat beschreven is in dit proefschrift waren 1) het ontwikkelen van een systeemfarmacologiemodel om de effecten van geneesmiddelen met verschillende werkingsmechanismen op de relatie tussen MAP, CO, HR, SV en TPR op een kwantitatieve manier te karakteriseren en 2) het kwantificeren van de cardiovasculaire effecten van de S1P modulator fingolimod met dit model.

Ontwikkeling van een systeemfarmacologiemodel om het cardiovasculaire systeem (CVS) te karakteriseren

In **Hoofdstuk 3** is een systeemfarmacologiemodel ontwikkeld om geneesmiddeleffecten op het CVS te karakteriseren in spontaan hypertensieve ratten (SHR). Dit model is gebaseerd op de wisselwerking tussen MAP, CO en TPR en wordt hier het '*Basic CVS model*' genoemd. De effecten van een groep geneesmiddelen die op verschillende manieren de bloeddruk veranderen werden gekarakteriseerd in SHR's. Deze ratten waren langdurig geïnstrumenteerd met sondes die de stroming van het bloed in de aortawortel (CO), HR en MAP continue registreren. De veronderstelling was dat twee aspecten van de studieopzet essentieel zijn om de parameters van het '*Basic CVS model*' succesvol te karakteriseren: i) de selectie van de groep van geneesmiddelen met een werking op het cardiovasculaire systeem en ii) de continue meting van de waarden van zowel MAP als CO, voor, tijdens en na toedienen van het geneesmiddel. Door het selecteren van een aantal cardiovasculaire geneesmiddelen met bekende, maar verschillende werkingsmechanismes, was het mogelijk alle systeemspecifieke parameters van het '*Basic CVS model*' met goede precisie te schatten. Bovendien kon er een onderscheid gemaakt worden tussen systeemspecifieke en stofspecifieke parameters. Dit geeft aan dat het model inderdaad stofonafhankelijk is. Het model kan daarom, in principe, ook toegepast worden om de cardiovasculaire effecten van nieuwe stoffen (geneesmiddelen die niet voor dit onderzoek gebruikt zijn) te voorspellen. Het meten van CO was essentieel om alle parameters van het '*Basic CVS model*' te kunnen identificeren, omdat dit resulteerde in de informatie die nodig is om een onderscheid te kunnen maken tussen hemodynamische veranderingen in CO en TPR. De conclusie was dat de onderzoeksopzet heeft geresulteerd in de data om de wisselwerking tussen MAP, CO en TPR op een kwantitatieve en mechanistisch manier te identificeren. Het model kan worden toegepast om het werkingsmechanisme (het aangrijpingspunt) van nieuwe geneesmiddelen die de bloeddruk veranderen te identificeren.

Een beperking van dit model is dat in de praktijk CO niet vaak gemeten wordt vanwege het complexe en invasieve karakter van de bijbehorende procedure. Om deze reden, is het 'Basic CVS model' uitgebreid door CO te splitsen in HR en SV (**Hoofdstuk 4; 'Extended CVS model'**) met als doel 1) het karakteriseren van de werking van geneesmiddelen op de relatie tussen HR en MAP, welke beide belangrijke variabelen zijn voor de veiligheid van nieuwe geneesmiddelen, en 2) te onderzoeken of het werkingsmechanisme en het aangrijpingspunt van nieuwe geneesmiddelen vastgesteld kan worden op basis van alleen HR en MAP metingen.

Het gedrag van het 'Extended CVS model' is geëvalueerd door de verandering in MAP, CO, HR, SV en TPR te simuleren na het inhiberen van HR, SV of TPR met een fictief (hypothetisch) geneesmiddel. De karakteristieke profielen van het tijdsverloop van het geneesmiddeleffect op MA, CO, HR, SV en TPR worden ook wel 'signature profiles' genoemd. Er waren duidelijke verschillen zichtbaar na het inhiberen van HR, SV of TPR. Hieruit kan geconcludeerd worden dat, zelfs als CO niet wordt gemeten, het waarschijnlijk is dat 'Extended CVS model' gebruikt kan worden om het aangrijpingspunt van nieuwe geneesmiddelen te identificeren. De volgende wetmatigheden werden waargenomen bij de ontwikkeling van het model: i) Als de richting van het geneesmiddeleffect op HR en MAP hetzelfde is (een verhoging van HR en MAP of een daling van HR en MAP) is het waarschijnlijk dat het geneesmiddel primair HR beïnvloedt. ii) Als de richting van geneesmiddeleffect op HR en MAP tegengesteld is (een verhoging van HR en een daling in MAP of *vice versa*) is het waarschijnlijk dat het geneesmiddel een primair effect op SV of TPR heeft. Vervolgens kan er een onderscheid gemaakt worden tussen een primair effect op SV of TPR, op basis van de vertraging tussen het moment toedienen van het geneesmiddel en het optreden van het effect op MAP. Een grotere vertraging duidt op een primair effect op SV en een kleine vertraging duidt op een primair effect op TPR. Zowel MAP als HR zijn belangrijke variabelen in het onderzoek naar veiligheid van nieuwe geneesmiddelen.

Ondanks het feit dat in de praktijk vaak de verandering in MAP en HR simultaan gemeten wordt, worden er in het algemeen in het geneesmiddelonderzoek twee onafhankelijke relaties tussen de blootstelling aan het geneesmiddel en het effect op MAP en HR bepaald. Op deze manier wordt er geen rekening gehouden met de relatie tussen MAP en HR. Het 'Extended CVS model' heeft daarom als bijkomend voordeel dat geneesmiddeleffecten op MAP en HR simultaan geanalyseerd kunnen worden. Dit resulteert in één set van parameters en daarmee één schatting van de dosering/concentratie die nodig is om 50% van het maximale effect (' EC_{50} ') te bereiken. Hierdoor kunnen eenduidige conclusies over de cardiovasculaire effecten van nieuwe geneesmiddelen getrokken worden en dit komt de selectie van nieuwe geneesmiddelen ten goede.

Het *'Basic CVS model'* is verder uitgebreid door de invloed van verschillen in bloed-drukregulatie tussen normotensieve en hypertensieve ratten te kwantificeren. Omdat er duidelijke verschillen in bloeddrukregulatie zijn tussen normotensieve en hypertensieve ratten, kan de grootte van het geneesmiddeleffect op de verschillende hemodynamische eindpunten sterk variëren tussen verschillende rat stammen. Om deze reden zijn de uitkomsten die zijn verkregen met het *'Basic CVS model'* niet direct toepasbaar op normotensieve ratten. Dit is een nadeel, omdat de veiligheid van nieuwe geneesmiddelen initieel vaak in normotensieve ratten onderzocht wordt. Om het systeemfarmacologie model uiteindelijk te kunnen toepassen om de cardiovasculaire effecten van nieuwe geneesmiddelen in gezonde vrijwilligers en in patiënten met hoge bloeddruk te voorspellen, is het essentieel dat het model voor zowel normotensieve als hypertensieve ratten toepasbaar is. In vergelijking met normotensieve ratten hebben hypertensieve ratten een hogere uitgangswaarde voor MAP en lagere uitgangswaarde voor CO, terwijl de uitgangswaarde voor HR niet significant verschillend is. Uit de hemodynamische wetten ($MAP=CO \times TPR$ en $CO=HR \times SV$) volgt dan dat hypertensieve ratten een lagere uitgangswaarde voor SV en een hogere uitgangswaarde voor TPR hebben dan normotensieve ratten. Bovendien is er op individueel niveau een relatie vastgesteld tussen de sterkte van bloeddrukregulatie (*'feedback'*) en de uitgangswaarde van MAP wat resulteert in een 2-keer sterkere feedback van MAP (bloeddrukregulatie) in een typische normotensieve rat in vergelijking met een typische hypertensieve rat. Dit duidt op verminderde bloeddrukregulatie in hypertensieve ratten.

Toepassing van het systeemfarmacologiemodel op S1P receptor agonisten

Fingolimod is een S1P receptor agonist die wordt gebruikt in de behandeling van multiple sclerose. In mensen wordt het gebruik van S1P receptor agonisten geassocieerd met cardiovasculaire bijwerkingen. Er kan een kortstondige verlaging van hartslag (gemiddeld 8 bpm, 6 uur na de eerste toediening) en een kleine verhoging van MAP (gemiddeld 1-2 mmHg na 2 maanden) optreden na toediening van een therapeutische dosering van 0.5 mg fingolimod. Bovendien zijn er bij hogere doseringen van 1.25 en 5 mg gemiddelde verlagingen in HR van respectievelijk 13.8 en 16.6 bpm waargenomen, waarbij het minimum 6 uur na de eerste toediening bereikt werd. Na langdurige toediening verdween het effect en keerde HR terug naar de uitgangswaarde. Bij de hogere doseringen werd een milde verhoging in MAP waargenomen van ongeveer 5-6 mmHg. Zowel het immunosuppressieve effect, als de cardiovasculaire effecten, van deze stoffen worden veroorzaakt door binding aan de S1P receptor. Dit bemoeilijkt de zoektocht naar nieuwe S1P receptor

agonisten welke effectief zijn in de behandeling van multiple sclerose, maar geen cardio-vasculaire bijwerkingen hebben. Een kwantitatief begrip van de hemodynamica van deze effecten zou de basis kunnen vormen voor de selectie van nieuwe geneesmiddelen met een verbeterd bijwerkingenprofiel. Bovendien zou dit inzicht geven in de mogelijkheden om deze effecten voor bestaande en nieuwe S1P agonisten te voorkomen of te verminderen door gelijktijdige toediening van andere geneesmiddelen met een tegengesteld effect of door het ontwikkelen van titratieschema's, waarbij de dosering langzaam wordt verhoogd om het lichaam de tijd te geven de (geringe) verandering in de bloeddruk te compenseren voordat de volgende, hogere, dosering wordt gegeven. Het '*Extended CVS model*' kan gebruikt worden om een kwantitatief begrip van deze effecten te verkrijgen, omdat de modelstructuur en de bijbehorende parameterschattingen onafhankelijk zijn van de geneesmiddelen die gebruikt zijn om het model te ontwikkelen. Daarom kan het model in principe ook voor nieuwe geneesmiddelen gebruikt worden en zodoende ook voor fingolimod. Het effect van fingolimod wordt bewerkstelligd door binding aan de S1P receptor. In het algemeen, wordt receptorbinding gekarakteriseerd door de evenwichtsconstante (dissociatieconstante), welke de concentratie weergeeft waarbij 50% van de receptoren bezet is. Dissociatieconstanten kunnen met *in vitro* experimenten bepaald worden. Door het '*Extended CVS model*' met een receptorbinding- en activatiemodel te integreren kan het model niet alleen voor fingolimod, maar ook voor nieuwe S1P agonisten gebruikt worden (door de dissociatieconstante van fingolimod te vervangen door de dissociatieconstante van de nieuwe S1P agonist). Bovendien kan het model hierdoor gebruikt worden om de cardio-vasculaire effecten van fingolimod en nieuwe S1P agonisten in mensen te voorspellen.

De translatie van de farmacologie van fingolimod en andere S1P agonisten van ratten naar mensen wordt bemoeilijkt door het feit dat niet de stof zelf, maar de fosfaatmetabolieten, welke gevormd worden door afbraak (metabolisme) van het geneesmiddel, farmacologisch actief zijn. De eerste stap in de ontwikkeling van een translationeel model voor S1P agonisten was het karakteriseren van de PK van fingolimod en de actieve metaboliet fingolimod-fosfaat ('*fingolimod-phosphate (fingolimod-P)*') in ratten en mensen. Omdat er tussen ratten en mensen grote verschillen bestaan in weefseldistributie en activiteit van het enzym sphingosine kinase (S1PHK) dat de omzetting van fingolimod in fingolimod-P katalyseert, kan de PK van fingolimod-P in mensen niet eenvoudig voorspeld worden met behulp van schaling op basis van het verschil in het gewicht tussen ratten en mensen (allometrische schaling). In **Hoofdstuk 5** is daarom een semi-mechanistisch PK model ontwikkeld voor de inter-conversie van S1PHK substraten en de gevormde fosfaten in ratten en mensen. Een specifiek doel was het onderzoeken of de snelheid van de fosforylering

in de bloedplaatjes (welke *ex vivo* bepaald kan worden) een voorspellende waarde heeft voor de verschillen in farmacokinetiek tussen ratten en mensen.

In deze studies is het tijdsverloop van de fingolimod en fingolimod-P bloedconcentraties in ratten, na intraveneuze en orale toediening, simultaan geanalyseerd met gegevens over de snelheid van de inter-conversie in *ex vivo* experimenten en *ex vivo* gegevens over de verdeling tussen bloed en plasma. Daarnaast zijn data van twee studies in gezonde vrijwilligers, die oraal fingolimod kregen in dosering van 0.5, 1.25 en 5 mg, simultaan geanalyseerd met data van *ex vivo* inter-conversie en bloed-plasma verdelings experimenten in humaan bloed. De farmacokinetiek van fingolimod en fingolimod-P in de rat en in de mens kon goed worden beschreven met een semi-mechanistisch PK model met 1) een term (parameter) voor de pre-systemische fosforylering van fingolimod tijdens de eerste leverpassage, 2) een parameter voor de fosforylering in de bloedplaatjes en 3) een parameter voor de defosforylering in het plasma. Het integreren van *ex vivo* en *in vivo* data maakt de voorspelling van het de fingolimod en fingolimod-P concentraties in zowel plasma als bloed (in plaats van alleen in bloed) mogelijk. Dit is belangrijk omdat volgens de '*free drug hypothesis*' geneesmiddeleffecten gedreven worden door vrije plasmaconcentraties. Bovendien heeft het integreren van data van *ex vivo* en *in vivo* experimenten het mogelijk gemaakt verschillen in de fosforyleringssnelheid te kwantificeren. In mensen wordt fingolimod in bloedplaatjes vier keer langzamer gefosforyleerd dan in ratten, terwijl de defosforyleringssnelheid vergelijkbaar is tussen ratten en mensen.

Er kan geconcludeerd worden dat er grote verschillen bestaan in de fosforyleringssnelheid van fingolimod tussen ratten en mensen welke niet verklaard kunnen worden met allometrische schaling. Hoewel het verschil in fosforylering in de bloedplaatjes de twaalfvoudige overschatting van de fingolimod-P blootstelling in mensen slechts gedeeltelijk verklaart, vormt het ontwikkelde PK model een basis voor het voorspellen van het verloop van de plasmaconcentraties van S1PHK substraten en de bijbehorend fosfaatmetabolieten. Verschillen in de pre-systemische fosforylering moeten daarbij worden meegenomen.

In **Hoofdstuk 6**, zijn de cardiovasculaire effecten van fingolimod in normotensieve en hypertensieve ratten gekarakteriseerd op basis van het '*Extended CVS model*' in combinatie met het semimechanistische farmacokinetische model voor fingolimod. De eerste stap, in deze analyse, was de evaluatie van verschillende hypothesen over het werkingsmechanisme van fingolimod. Daartoe werden simulaties uitgevoerd, zonder daarbij de systeemspecifieke parameters van het '*Extended CVS model*' te veranderen.

- 1) Er werden verschillende hypothesen geformuleerd met betrekking tot het aangrijpingspunt (HR, SV of TPR) en de richting van het effect (positief of negatief). Dit resulteerde in 6 mogelijke combinaties van effecten.
- 2) Voor elke hypothese werden simulaties uitgevoerd voor de effecten op de MAP, CO, HR, SV en TPR.
- 3) Er werd geëvalueerd welke hypothese resulteerde in beste beschrijving van de experimentele data.

De conclusie was dat het effect van fingolimod-P op het CVS alleen beschreven kon worden als fingolimod-P op meerdere plaatsen het CVS beïnvloedt. Uiteindelijk zijn er 3 verschillende effecten geïdentificeerd: 1) een snel optredend positief effect op TPR, 2) een langzaam optredend (en blijvend) positief effect op TPR en 3) een kortstondig (en van tijdelijke aard) negatief effect op HR. In deze eerste stap werden empirische modellen gebruikt om het effect van fingolimod-P te beschrijven. Met deze modellen kon de meest waarschijnlijke werkingsplaats geïdentificeerd worden. Bovendien werd aangetoond dat het *'Extended CVS model'* toegepast kan worden om de hemodynamische veranderingen in vijf verschillende parameters (MAP, CO, HR, SV en TPR) te beschrijven, onder de aanname dat fingolimod-P het CVS op twee plaatsen beïnvloedt. Vervolgens werd de op deze manier verkregen informatie over het werkingsmechanisme van fingolimod-P vergeleken met informatie uit de literatuur. De volgende samengevatte informatie over het werkingsmechanisme van fingolimod-P was beschikbaar ten tijde van de analyse.

- i. Fingolimod-P beïnvloedt HR via binding aan de $S1P_1$ receptor. Hierdoor wordt het kaliumkanaal IKACH geactiveerd wat resulteert in een negatief chronotroop effect.
- ii. Fingolimod-P induceert internalisatie en degradatie van de $S1P_1$ receptor, waardoor deze niet meer functioneel is. Hierdoor gedraagt fingolimod-P zich als een functionele antagonist (een geneesmiddel dat de werking van een lichaamseigen stof opheft).
- iii. Fingolimod-P bindt aan de $S1P_3$ receptor en heeft hierdoor een effect op TPR.
- iv. Samentrekken van het gladde spierweefsel in de bloedvaten wordt geïnduceerd door een verhoging van de intracellulaire calciumconcentratie. De calciumafhankelijke fase van samentrekken van het gladde spierweefsel verloopt snel en is van korte duur, maar calcium sensitiviteit als resultaat van stimulatie door een agonist is van blijvende aard en resulteert in een blijvende verhoging van TPR

Deze informatie komt overeen met het op basis van het model geïdentificeerde werkingsmechanisme van fingolimod-P. In een volgende stap werd daarom het empirische model voor het effect van het geneesmiddel vervangen door een model dat is gebaseerd op de receptortheorie. In dit model wordt onderscheid gemaakt tussen receptorbinding en activatie processen. Hierdoor heeft het model een grotere voorspellende waarde voor het effect van fingolimod-P in mensen en voor het effect van andere $S1P$ agonisten in ratten en mensen. Omdat fingolimod-P een agonist voor de $S1P$ receptor is, is het van belang om

rekening te houden met de competitieve interactie tussen de endogene agonist, S1P, en fingolimod-P voor zowel het effect op HR als het effect op TPR. Het ontwikkelde model bestond uit vergelijkingen voor de beschrijving van 1) de kinetiek van competitieve binding aan de S1P₁ receptor (snel effect op HR), 2) de snelheid van S1P₁ receptor internalisatie en degradatie (kortstondig effect op HR), 3) de competitieve binding aan de S1P₃ receptor (snel effect op TPR) en 4) de sensibilisatie van de S1P₃ receptor (langzaam en blijvend effect op TPR).

Door het karakteriseren van de effecten op HR en TPR kon de door fingolimod-P geïnduceerde verandering in MAP, CO, HR, SV en TPR in normotensieve en hypertensieve ratten goed beschreven worden. De dissociatieconstanten voor de effecten op TPR (Kd_{TPR}) en HR (Kd_{HR}) werden geschat op respectievelijk 17.7 [betrouwbaarheidsinterval ('*confidence interval* (CI)'): 3.74 – 31.6] en 132 [CI: 68.9 – 195] nM op basis van de vrije plasmaconcentratie. De Kd_{TPR} is in dezelfde orde van grootte als de in de literatuur gerapporteerde *in vitro* dissociatieconstanten voor binding van fingolimod-P aan de humane S1P₃ receptor van 3.15 ± 1.7 nM. Echter, de geschatte waarde voor Kd_{HR} is ongeveer 1000 keer groter dan de in de literatuur gerapporteerde waarde van 0.17 ± 0.14 nM. Hierbij is het belangrijk om op te merken dat de S1P₁ receptor *in vivo* geïnternaliseerd en gedegradeerd wordt. Dit kan de schatting van dissociatieconstanten beïnvloeden. Bovendien refereren de waarden uit de literatuur naar experimenten met de humane S1P₁ en S1P₃ receptoren en zijn er geen dissociatieconstanten voor ratten gerapporteerd. Dit is belangrijk omdat er bekend is dat er grote verschillen in receptorbinding tussen ratten en mensen kunnen bestaan. Dit is een complicerende factor in de interpretatie van het eerder genoemde duizendvoudig verschil tussen de geschatte *in vivo* Kd_{HR} en de gerapporteerde *in vitro* Kd_{HR} .

Omdat het ontwikkelde model gebaseerd is op concepten uit de receptortheorie kon het model gebruikt worden om het effect van siponimod (een nieuwe S1P receptor agonist met een ander selectiviteitsprofiel) op CVS te voorspellen. Hiertoe werden de voor fingolimod-P geschatte dissociatieconstanten gecorrigeerd voor het moleculairgewicht, de vrije fractie en de ratio van de EC_{50} 's uit *in vitro* bindingsexperimenten. Dit resulteerde in een goede voorspelling van het effect van siponimod op MAP en HR in ratten. Dit impliceert dat het model in principe gebruikt kan worden om het effect van andere S1P agonisten op het CVS in ratten te voorspellen.

Prospect

Een uiteindelijke toepassing van het ontwikkelde systeemfarmacologiemodel is het voorspellen van de effecten van nieuwe geneesmiddelen, en specifiek S1P agonisten, op het

cardiovasculaire systeem in mensen op basis informatie uit preklinische experimenten. In de **Hoofdstuk 7** werd besproken welke stappen hiervoor nodig zijn en welke aannames hiervoor gedaan moeten worden.

Het is de verwachting dat het *'Extended CVS model'* van ratten naar mensen geëxtrapoleerd kan worden, maar deze extrapolatie zal niet alleen gebaseerd zijn op lichaamsgrootte en andere factoren. Deze verwachting is gebaseerd op de voorspelling de cardiovasculaire effecten van nicardipine (een calciumantagonist) als modelstof. Na het vermenigvuldigen van de dissipatiesnelheden (k_{out}) met een bepaalde factor (een hoge waarde wat resulteert in een erg kleine vertraging in respons in mensen) en het schatten van de *'feedback'* kon het effect van nicardipine op MAP en CO goed voorspeld worden. Deze extrapolatie is gebaseerd op data van slechts één voorbeeld stof, met een werkingsmechanisme dat identiek is aan dat van een de stoffen in de trainingset (amlodipine). Daarom is het niet zeker of de verkregen systeempparameters stofonafhankelijk zijn. Verder onderzoek is nodig om het effect van verschillende cardiovasculaire geneesmiddelen met verschillende werkingsmechanismes op MAP, CO en HR te voorspellen.

Als laatste werd onderzocht of het humane CVS model (dat ontwikkeld is voor nicardipine) gebruikt kan worden om het effect van S1P agonisten te karakteriseren en te voorspellen. In het supplement van dit proefschrift is beschreven welke stappen en aannames hiervoor nodig zijn.

Conclusies

Het onderzoek beschreven in dit proefschrift heeft geleid tot een systeemspecifiek model dat gebruikt kan worden om de effecten van nieuwe geneesmiddelen (die niet gebruikt zijn om het model te ontwikkelen) op de relatie tussen MAP, CO, HR, SV en TPR te kwantificeren. Bovendien kan dit model gebruikt worden om het aangrijpingspunt van nieuwe geneesmiddelen te identificeren op basis van alleen MAP en HR metingen. Een ultieme toepassing van het *'Extended CVS model'* is de voorspelling van cardiovasculaire effecten in mensen op basis van informatie uit preklinische experimenten. Voordat het ontwikkelde model hiervoor gebruikt kan worden, moeten de systeemspecifieke parameters naar mensen geschaald worden en moet het model gevalideerd worden met behulp dat MAP, HR en CO metingen na toediening van verschillende stoffen met een werking op het cardiovasculaire systeem.

Daarnaast heeft het onderzoek geleid tot een systeemfarmacologiemodel dat gebruikt kan worden om de cardiovasculaire effecten van fingolimod-P en andere S1P agonisten in

ratten te kwantificeren en voorspellen. Dit systeemfarmacologiemodel is een combinatie van het 'Extended CVS model' en receptorbinding en activatie modellen om het effect van fingolimod-P (en andere S1P agonisten) op HR en TPR te kwantificeren. Het ontwikkelde model geeft een kwantitatief begrip van het werkingsmechanisme onderliggend aan de cardiovasculaire effecten van fingolimod-P. Bovendien kon het model gebruikt worden om de cardiovasculaire effecten van een nieuwe stof, siponimod te voorspellen. Hiertoe werden de voor fingolimod-P geschatte dissociatieconstanten gecorrigeerd voor het moleculairgewicht, de vrije fractie en de ratio van de EC_{50} 's uit *in vitro* bindingsexperimenten. Op grond hiervan kan worden geconcludeerd dat het model gebruikt kan worden om het effect van andere S1P agonisten op het CVS in ratten te voorspellen. De verwachting is dat dit model ook gebruikt kan worden om de cardiovasculaire effecten van fingolimod-P en andere S1P agonisten in mensen te voorspellen. De aannames, beschreven in het supplement van dit proefschrift, dienen gevalideerd te worden middels verder onderzoek.

Nawoord

De afgelopen zes jaar heb ik, naast mijn werk bij LAP&P, met veel plezier aan mijn promotieonderzoek gewerkt. Klaar! Natuurlijk heb ik dit niet alleen gedaan en zijn er een aantal mensen die, een bijdrage hebben geleverd aan het tot stand komen van dit proefschrift. Ik zou het kort kunnen houden: "Iedereen bedankt!", maar dat zou geen recht doen aan alle hulp en steun, die ik heb gekregen.

Allereerst, wil ik het "Leiden-Novartis Collaboration Team" bedanken. Ik heb het geluk gehad om met dit kundige team te mogen werken. In het bijzonder, wil ik Bart, Meindert, Don, Olivier, Dean en Randy noemen. Bart, jij hebt mij, eerst vanuit Leiden en later vanuit verschillende andere Europese steden, uitgedaagd om steeds één, twee of drie stappen verder te gaan en mijn werk naar een hoger niveau te tillen. Bedankt voor alle interessante discussies en de prettige samenwerking. Meindert and Don, you were great tutors in many aspects and taught me how to present my work in a scientifically correct, but perhaps more important, in an understandable and attractive way. Olivier, thank you very much for all your support from within Novartis during this project. There were many challenges and you helped me to manage them. Dean and Randy, thank you very much for providing me with your extreme high quality data and giving me the opportunity to help designing the experiments.

Daarnaast bedank ik al mijn collega's bij LAP&P voor jullie oprechte interesse in mijn onderzoek. In het bijzonder wil ik Henk-Jan bedanken voor de tijd en ruimte die ik heb gekregen om aan mijn promotie te kunnen werken en Diana voor haar bijdrage aan het datamanagement. Via LAP&P heb ik ook met Bert Peletier mogen werken. Bert, bedankt voor onze discussies over de wiskundige aspecten van mijn modellen. Dit heeft zeker nieuwe inzichten opgeleverd.

De keuze voor mijn paranimfen was snel gemaakt. Tamara, mijn kamergenoot, we hebben talloze inhoudelijk discussies gehad over agonisten, antagonist, potencies, dissociatieconstanten, *in vitro* experimenten etc. etc., maar ook vele discussies over de randfactoren van promoveren Bedankt voor je hulp en steun op heel veel verschillende gebieden. Sanne, inmiddels geroutineerd paranimf. Met jou als paranimf weet ik zeker dat mijn promotie een feestje wordt.

Mama, het is nu echt zover. Maaïke, jij hebt het voorgedaan. Papa, Sanne en G, mijn cardiovasculaire gewetens. En last, but not least, Martin, jij bent er altijd voor mij en hebt ervoor gezorgd dat ik niet mijn promotieonderzoek was samen uit eten, samen op vakantie en samen heel veel andere leuke dingen doen. Nog even volhouden en je mag

|

me eindelijk officieel doctor ingenieur noemen. Bedankt voor jullie onvoorwaardelijke liefde en steun.

Nelleke

List of Publications

Snelder N, Ploeger BA, Luttringer O, Rigel DF, Webb RL, Feldman D, Fu F, Beil

M, Jin L, Stanski DR, Danhof M. Characterization and prediction of cardiovascular effects of fingolimod and siponimod using a systems pharmacology modeling approach. *Submitted*

Snelder N, Ploeger BA, Luttringer O, Rigel DF, Fu F, Beil M, Stanski D, Danhof M. PKPD modeling of drug effects on the cardiovascular system in conscious rats – parsing cardiac output into heart rate and stroke volume. *Submitted*

Snelder N, Ploeger BA, Luttringer O, Stanski D, Danhof M. Translational pharmacokinetic modeling of fingolimod (FTY720) as a paradigm compound subject to sphingosine kinase-mediated phosphorylation. *Submitted*

van Rijn-Bikker PC, **Snelder N**, Ackaert O, van Hest RM, Ploeger BA, van Montfrans GA, Koopmans RP, Mathôt RA. Nonlinear mixed effects modeling of the diurnal blood pressure profile in a multiracial population. *Am J Hypertens*. 2013 Sep;26(9): 1103-1113.

Snelder N, Ploeger BA, Luttringer O, Rigel DF, Webb RL, Feldman D, Fu F, Beil M, Jin L, Stanski DR, Danhof M. PKPD modelling of the interrelationship between mean arterial BP, cardiac output and total peripheral resistance in conscious rats. *Br J Pharmacol*. 2013 Aug;169(7):1510-1524.

van Rijn-Bikker PC, Ackaert O, **Snelder N**, van Hest RM, Ploeger BA, Koopmans RP, Mathôt RA. Pharmacokinetic-pharmacodynamic modeling of the antihypertensive effect of eprosartan in Black and White hypertensive patients. *Clin Pharmacokinet*. 2013 Sep;52(9):793-803.

Reif S, **Snelder N**, Blode H. Characterisation of the pharmacokinetics of ethinylestradiol and drospirenone in extended-cycle regimens: population pharmacokinetic analysis from a randomised Phase III study. *J Fam Plann Reprod Health Care*. 2013 Apr; 39(2):e1

Benson N, **Snelder N**, Ploeger B, Napier C, Sale H, Birdsall NJ, Butt RP, van der Graaf PH. Estimation of binding rate constants using a simultaneous mixed-effects method: application to monoamine transporter reuptake inhibitor reboxetine. *Br J Pharmacol*. 2010 May; 160(2):389-398.

Maas HJ, **Snelder N**, Danhof M, Della Pasqua O. Prediction of attack frequency in migraine treatment. *Cephalalgia*. 2008 Aug;28(8):847-855.

Curriculum Vitae

Nelleke Snelder werd op 28 augustus 1980 geboren te Rotterdam. Na het behalen van het diploma VWO in 1998 aan het Caland Lyceum te Rotterdam begon zij in datzelfde jaar aan de studie Technische Wiskunde aan de Technische Universiteit Delft. In 1999 maakte zij de overstap naar de studie Life Science & Technology aan de Universiteit Leiden en Technische Universiteit Delft. In de master fase heeft ze haar hoofdstage gedaan bij de afdeling Farmacologie van de Universiteit Leiden onder begeleiding van Dr. H. Maas en Dr. O. E. Della Pasqua. In 2004 behaalde zij haar Master en startte zij als consultant bij LAP&P Consultants BV in Leiden. Naast het consultancy werk, begon zij haar promotieonderzoek in 2008 onder begeleiding van Prof. Dr. M. Danhof (promotor) en Dr. B.A. Ploeger (co-promotor). In 2013 werd zij uitgenodigd om haar werk te presenteren in de *Lewis Sheiner Student Session* van het PAGE congres in Glasgow. In 2014 werd zij uitgenodigd haar werk te presenteren op het *7th Noordwijkerhout Symposium on Pharmacokinetics, Pharmacodynamics and Systems Pharmacology*. Op dit moment is zij werkzaam als senior consultant bij LAP&P Consultants BV in Leiden.

